Model-based estimation and control methods for batch cooling crystallizers

Model-based estimation and control methods for batch cooling crystallizers

PROEFSCHRIFT

ter verkrijging van de graad van doctor aan de
Technische Universiteit Eindhoven, op gezag van de
Rector Magnificus, prof.dr.ir. C.J. van Duijn, voor een
commissie aangewezen door het College voor
Promoties in het openbaar te verdedigen
op dinsdag 16 oktober 2012 om 16.00 uur

door

Jochem Adrianus Wilhelmus Vissers

geboren te Bergen op Zoom

Dit proefschrift is goedgekeurd door de promotoren:

prof.dr.ir. A.C.P.M. Backx
en
prof.dr. S. Weiland

Commissieleden:

prof.dr.ir O.H. Bosgra
dr.ir. P.J. Daudey
prof.dr.ir. P.M.J. Van den Hof
dr.ir. H.J. Kramer
prof.dr. H.J. Zwart

This research is supported by the Institute for Sustainable Process Technology (ISPT) under the project "Intelligent Observer and Control for Pharmaceutical Batch Crystallization" with number PH-00-04.

This dissertation has been completed in fulfillment of the requirements
of the Dutch Institute of Systems and Control DISC.

A catalogue record is available from the Eindhoven University of Technology Library.

Model-based estimation and control methods for batch cooling crystallizers
by J.A.W. Vissers. – Eindhoven : Technische Universiteit Eindhoven, 2012
Proefschrift. – ISBN: 978-90-386-3235-3

This thesis was prepared with the LaTeX documentation system.
Cover Design: Verspaget & Bruinink
Reproduction: Printservice, Eindhoven University of Technology.

Contents

Summary

Model-based estimation and control methods for batch cooling crystallizers

Crystallization processes are of key importance for the separation of chemical components in the chemical process industry and pharmaceutical industry. The quality of the materials produced by crystallization processes has a large impact on efficiency of the subsequent (downstream) processes.

This thesis describes research on the development of measurement and control technology to enable reproducible and predictable operation of industrial batch cooling crystallization processes. The goal of the research is to reduce sensitivity of the process to disturbances and to enable reproducible operation of the process. As such, these methods enable to produce crystalline products with high purity and quality at low costs.

The ability to infer information on the process states is of major importance when one desires to develop control methods for process. Therefore, the observability properties of the batch cooling crystallization processes equipped with concentration sensors and sensors for the crystal size have been analyzed in this thesis. Moreover, the controllability properties of the process have been analyzed.

In order to enable automatic control of batch cooling crystallization processes a control algorithm based on state feedback linearization has been developed. The method enables to use a relatively straight forward control strategy for crystallization processes where tracking of an a priori defined super saturation trajectory is desired. Since the method of feedback linearization is known to be sensitive to measurement noise and model uncertainties, considerable effort has been put in quantification the effect of both disturbance sources on the performance and robustness of the controlled system. The effectiveness of the control strategy has been demonstrated during a experimental campaign in an industrial environment.

Moreover, attention has been paid to the development of algorithms for state estimation based on available dynamic models of the crystallization processes. The research contributes to the development of a methodology for the design of estimators for infinite dimensional systems in general. The relation between control and estimation problems

for infinite dimensional system has been analyzed. The developed methodology is applied to design a state estimator for the batch crystallization processes under study.

The results on the method for estimator design for infinite dimensional systems provide insight in the optimal performance which can be achieved by the estimators. The research shows that optimal estimators for infinite dimensional system are also infinite dimensional systems themselves, which is a large hurdle for implementation. Based on the developed insight on estimators, known results on the approximation of control systems for infinite dimensional systems by discretization method have be used to analyze the effect of approximation of the estimators by discretization. This analysis has been used to support decisions on discretization methods which have to be made for implementation of the estimators.

The developed method enables to derive properties of the approximated estimators for the batch cooling crystallization process, which is in contrast to existing heuristic methods. The developed method enables to design estimators for crystallization processes where effects like non-uniform growth, crystal attrition or crystal dissolution are present. This is not possible with current state of the art methods based on the methods of moments. The developed algorithm has been tested by simulation for a representative test system such as a diffusion problem and representative simulations have been implemented for an industrial batch crystallization process.

Notational conventions

List of symbols

Notation	Explanation
Σ	General System
Σ_p	Process
Σ_g	Generalized plant
Σ_e	Estimator
$S(t)$	Semigroup operator
$\mathcal{T}(t)$	Semigroup operator
x	State of system
A	Infinitesimal generator of semigroup
G	State disturbance operator
S	Sensor distrubance operator
C	Output operator for measurements
H	Output operator for to-be-estimated variables
Π	Solution to Riccati equation
P	Solution to Riccati equation
N	Approximation Order

Physical quantities

Notation	Explanation	Unit
T	Reactor temperature	$^{\circ}\mathrm{C}$
T_j	Jacket temperature	$^{\circ}\mathrm{C}$
c	Concentration	kg/kg
n	Number density distribution	$1/\mathrm{m}^4$
m_s	Solvent mass	kg
m_l	Solute mass	kg
m_c	Solid mass	kg
μ_i	i-th moment	$\mathrm{m}^{\mathrm{i}}/\mathrm{m}^3$
t	Time	s
ℓ	Particle length	m
$\bar{\ell}$	Maximum particle length	m
S_a	Absolute supersaturation	kg/kg
S_r	Relative supersaturation	$-$
G	Growth rate	m/s
D	Dissolution rate	m/s
B	Birth rate	$1/\mathrm{s}$
k_g	Growth rate coefficient	m/s
g	Growth rate exponent	$-$
k_b	Birth rate coefficient	$1/\mathrm{s}$
b	Birth rate exponent	m/s
ΔH	Heat of crystallization	$\mathrm{J/kgm}^3$
E_T	Enthalpy	J
h	Heat transfer coefficient	$\mathrm{J/s}^{\circ}\mathrm{C}$
C_p	Heat capacity	$\mathrm{J}/^{\circ}\mathrm{C}$
c_p	Specific heat capacity	$\mathrm{J}/^{\circ}\mathrm{Ckg}$
ρ_c	Density of crystal	$\mathrm{kg/m}^3$
ρ	Density of slurry	$\mathrm{kg/m}^3$
α_0	Thermal time constant	$1/\mathrm{s}$
α_j	Thermal time constant	$1/\mathrm{s}$
R	Rate of crystallization	kg/s
V	Crystal volume fraction	$\mathrm{m}^3/\mathrm{m}^3$
V_r	Reactor volume	m^3

Mathematical notation

Notation	Explanation
col	Column operator
$\dim(X)$	Dimension of X
$*$	Hilbert adjoint
$\top$	Transpose

Spaces and sets

Notation	Explanation
L_1	Class of absolutely integrable functions
L_2	Class of quadratically integrable functions
$\mathcal{L}(X, Y)$	Class of linear operators from X to X
U	Input space, finite dimensional Euclidean space
X	State space, Hilbert space
Y	Output space, finite dimensional Euclidean space
Z	Output space, finite dimensional Euclidean space
$\mathcal{D}_1$	Finite dimensional Euclidean space
$\mathcal{D}_2$	Finite dimensional Euclidean space
$\mathbb{N}$	Natural numbers
$\mathbb{N}^+$	Positive natural numbers
$\mathbb{R}$	Real numbers
$\mathbb{R}^+$	Positive real numbers

The Cartesian product, denoted by $X \times Y$, of two sets X and Y is defined by:

$$X \times Y = \{(x, y) | x \in X, y \in Y\}.$$

CHAPTER 1

Introduction

Abstract

This thesis contains results of research that was carried out during four years on methods to improve the predictability and reproducibility of the behavior of industrial crystallization processes. In this chapter an introduction to the work described in this thesis is given. The first part of this chapter sets the scene. An introduction to the crystallization process as it is used in industry is given, after which the current issues in operation of these processes in an industrial environment are discussed. The second part of the chapter introduces the research objectives which have been formulated and explains how these objectives result in the desired improvement in the operation of these processes. Finally the outline of the thesis is given.

Separation of chemical components is one of the most important operations in modern process industry. Separation technology is of importance to extract and purify valuable components from a mixed component stream. It also plays a major role in analysis methods, waste treatment and recycling and is of key importance in production processes. At the pharmaceutical company Du Pont it has been estimated in 1988 that for 70% of their products crystallization is involved in the production process [Larsen et al., 2006]. The worldwide market for pharmaceutical products in 2009 was estimated to be 597 Billion Euro ex-factory prices and the Dutch pharmaceutical industry produced in 2009 products with a combined worth of 5.7 Billion Euro [EFPIA, 2011]. In general, separation processes are large energy consumers, since one has to apply a force to initiate and continue the separation of components. After distillation, crystallization is the second

largest method for purification and separation in process industry. In the production of fine chemicals and pharmaceutical active components separation by crystalllization is considered to be the major work horse. With this in mind, it is clear that crystallization processes have large economic significance.

Given the enormous scope that crystallization processes have, there is a large demand to operate these processes in a reliable and reproducible manner. Unfortunately, industrial crystallization processes are known to behave irreproducible and to be very sensitive to changes in operating procedures. On the other hand, small improvements of the efficiency of crystallization processes may result in large economic and environmental benefits.

This thesis contains results of research with the goal to develop methods to improve the predictability and reproducibility of crystallization processes in industrial environments. The conducted research has been focused on the operation of batch crystallization processes in the process industry and especially in the pharmaceutical industry. The study and analysis of operation methods and technology to improve the predictability and reproducibility of industrial batch crystallization processes is the primary goal of the research. Although it is an interesting research area, the research has not as its primary goal to study the physics and mechanisms of crystal growth itself.

In this chapter an overview of the crystallization process is provided. We will explain the problems with crystallization during operation as they are faced by industrial users. An incentive for the research is given in Section 1.3 and from this incentive we will formulate the goals that motivate the research that has been conducted. Finally, the outline of this thesis will be given in Section 1.4.

1.1 Introduction to crystallization processes

In general, separation methods in chemical industry exploit differences in properties of components in the mixture. By exposing the mixture of materials to conditions where the various components of a mixture behave differently, the components can be separated. In separation processes involving crystallization one exploits differences in phase change behavior of materials.

Crystallization may be defined as a phase change in which a crystalline product is obtained from a solution, as in [Myerson, 2002, section 1.1]. In this context, a solution has to be interpreted in a broad sense, namely as a mixture of two or more species in a homogeneous phase. This covers mixtures of components in gas phase and melts [Myerson, 2002, section 1.1]. In this thesis we only consider crystallization where the solution is a liquid phase and where the driving force for crystallization is generated by cooling of the solution. In such a process, the crystallized component and the residue can be separated, for instance, by filtration. A more detailed description on mechanisms involved in crystallization is given in Section 2.1.

Crystallization has applications in the manufacturing of a broad range of material in chemical process industry, in the bulk industry as well as in the fine chemical industry.

Production of salts, semiconductors, food, fertilizers, paints, resins and waste treatment are just a few examples of processes where crystallization has major applications. An interesting feature of crystallization processes is that the characteristics of the solid material produced by these processes often have a large influence on the quality of the final product. For instance in food manufacturing, the characteristics of the products obtained by crystallization might effect the consistency, structure and taste of a product [Myerson, 2002, Crystallization in foods p.287].

Crystallization is also an important technique used in the pharmaceutical industry. Since there are high demands on purity of active pharmaceutical ingredients (API), crystallization is used widely for purification and separation of intermediates in the production process. Also the vast majority of the final products of pharmaceutical industry is manufactured in solid and crystalline form, which are obtained from crystallization of solutions. In the pharmaceutical industry, the characteristics of the solid material have important consequences, for instance:

- The particle characteristics might have an effect on the bio-availability [1].
- The particle characteristics might have an effect on the stability and sensitivity of the product during storage.

Especially in the industries that produce specialty chemicals and products with high value, such as the pharmaceutical industry, the specifications on products are tight and demands on specifications, predictability, precision and quality are high. Therefore, there is a large demand for reproducibility and predictability. The urgency to gain control over reproducibility and predictability is reflected in efforts by of industry and the supervisory authorities such as the Fedaral Drug Authority (FDA) to introduce Process Analytical Technology (PAT) and Quality by Design (QbD) in industrial environments.

In order to understand how the material properties are related to the crystallization process and to understand if and how these properties might be influenced by the way the process is operated, it is relevant to get a thorough understanding and insight in the physics of crystallization in more detail. We will come back to this discussion later and in Section 2.1 the crystallization process will be discussed. Next we will discuss the issues in crystallization that are faced by industry.

1.2 Industrial issues with crystallization

Despite the numerous applications of crystallization processes in industry, the unit operations involving crystallization are known as sensitive parts of the process chain. Due to the problems with crystallization processes, they are known in industrial environments as unpredictable and irreproducible. The unpredictable and irreproducible behavior of the processes has a large impact on the economic and operational aspects of the process. First of all, the behavior induces large variations in the quality of the final products, which in general is not desired. Although it is often technically possible to rework material that does not meet quality specifications, these procedures need specific authorizations by

[1] The term bio-availability refers to the fraction of, and the rate with which, a dose of administered drug reaches the desired site in the body without undergoing changes.

the FDA and are in general not desired in industry. Such a procedure has a negative impact on the production costs and capacity of a plant and demands for additional interaction by the operators. Moreover, pharmaceutical components are produced following certified production procedures, which in general do not allow for additional or batch to batch specific procedures.

In order to quantify the quality of crystalline products various measurable characteristics are of importance. The most important industrially relevant characteristics with respect to quality are given:

Crystal size and crystal size distribution: Specification on the crystalline product are given in terms of size or volumetric measures. Typical measures are a prescribed crystal size distribution, a prescribed number of quantiles of the distribution, and the mean and median of the crystal size.

Crystal morphology: Materials can crystallize to crystals with a number of different internal structures, called polymorphism. A specification on a product can be given in terms of the mass fraction of polymorphic types with respect to the total mass of the particle population.

Crystal shape: The shape of particles can be characterized by classification of shapes, in classes of spherical, cubic, octahedron, etc. Most often, all particles are of the same shape class and a multidimensional crystal size distribution might be used to quantify the shapes present in a population.

Purity: Depending on the components in a solution, undesired components such as pollutants and solvent molecules might be integrated in the particles during the growth process. The purity of particles can be specified on a mass fraction basis.

It is important to remark that crystal morphology and crystal shape are often related. It is well known that [Mersmann, 2001, section 5.3] the impurities might cause reduction or even blockage of growth of certain crystal faces. Therefore, also the crystal shape and purity are often related.

The question on which characteristics are of importance for the quality of a specific product, differs from product to product and from case to case. We give some examples of how the characteristics might influence important properties:

- Properties of the crystalline material, such as dissolution rate and bio-availability often vary strongly between the polymorphic types of crystals.
- The flow properties, also known as flowability, of a mixture of crystals and residue is known to depend on the shape and size of the crystals.
- A small particle size might result in a product in which crystals can be packed together in a very dense manner. Such a product might be very difficult to filter.
- A crystalline product with included liquids might be difficult to dry.

From the examples it is evident that downstream processing of the intermediates might heavily depend on the properties of the crystalline material. Therefore, the particle characteristics are not only of concern for the production of the final product but are also important for the production of intermediates. In general, the pharmaceutical industry desires products with a narrow crystal size distribution, a uniform crystal shape, a high fraction of specified morphology and high purity and demands high reproducibility

of these characteristics. Moreover, customers tend to relate reproducibility to professionalism and understanding of a production process by a manufacturer. As such, reproducibility is an important aspect to sustain the relationship between consumer and manufacturer.

Numerous external sources that influence the crystallization process and the characteristics of the final particles can be identified. There are known causes of influence that are quite general for batch crystallization processes, which include:

Impurities The presence of a second chemical component or impurity. Small quantities (concentrations of less than 1 *ppm*) of materials present in the solution can alter the physical mechanisms involved in crystal growth. This reflects in, for instance, changes of the shape of crystals in presence of impurities. Moreover, growth rate and nucleation kinetics can be affected by orders of magnitudes [Mersmann, 2001, chapter 5.3].

Variation in feedstock composition The feedstock of material in the crystallization processes originates often from the preceding unit operations. Slight variation in composition in general occurs due to different sources or apparently small differences of material properties or handling of the material.

Variation in operating conditions Small variations in the operation conditions can result in large changes in product quality. The production facilities for batch crystallization are often only automated to a semi automatic level. Operators execute the subsequent steps in the recipe, inherently with small batch to batch variations.

Disturbance Environmental disturbances on the process can induce large deviations of the product characteristics. Disturbances can, for instance, be caused by the undesired interaction between different pieces of equipment which are connected to the same utility network. An example is a disturbance on the temperature of the cooling medium, which might depend on the demand of coolant on the complete site.

Since not all of the external sources can be prevented, there is a demand from industry to develop methods that enable robust operation of the crystallization process in the presence of these perturbations and sources of disturbance.

The particle characteristics can, in general, not be measured on-line in production facilities. The crystal purity, morphology, shape and size characteristics are in general examined on a sample basis, in a laboratory environment after the product has been crystallized completely. Moreover, there is a number of important mechanisms involved in the growth of crystals which lack predictability but that are known to be of influence on the product quality. For instance, for most processes,

- Models that can be used to quantitatively predict the effect of specific impurities on the crystal growth rate do not exist.
- The effect of operating conditions on crystal shape and morphology is not known.
- The mechanisms responsible for the creation of poly-morphs are not known in detail.

Since quantitative models for these mechanisms do not exist, the state-of-the-art dynamical models for batch crystallization processes do not take this type of quality char-

acteristics into account. In Chapter 2, the models for batch crystallization that are available will be introduced.

1.3 Incentives and problem statement

As discussed in the previous section, the mechanisms involved in crystallization are sensitive to external influences, such as the presence of impurities, feedstock variations, variations in operation condition and external disturbances. Therefore, industrial processes that involve crystallization often show behavior which is perceived as irreproducible and unpredictable. On the other hand, the industry demands methods and strategies of operation which guarantee robust, reliable and predictable process behavior and can be applied in an industrial setting and on an industrial scale. These demands put specific requirements on the methods to be developed. The requirements are:

Robustness The operation methods need to be insensitive to or at least capable of handling small variations in the environment, the feedstock, the material properties and external disturbances. With small we mean as large as reasonable based on physical considerations.

Predictability It is demanded that a process behaves predictably, such that the resulting properties of a product can be predicted a priori based on applied initial and operating conditions of the process.

Reliability The process can be run in a (rough) industrial environment. Potentially unsafe operation modes need to be avoided. The equipment needed to implement the methods needs to be suitable and sufficiently robust for use in industrial environments. Interaction and maintenance is only allowed at predefined moments and not when the process is in operation.

Development of methods that meet these demands is the incentive of the research described in this thesis. It is our belief that general techniques and methods in the field of model-based control, optimization and estimation can contribute to development of these methods. In this thesis we explore to what extent these methods can be used to enable robust, reliable and predictable operation of the batch cooling crystallization process. The problem statement of this thesis is the following:

Problem statement:
Given the available models, knowledge of crystallization, state-of-the-art industrial equipment and measurement technology, analyze the possibilities to operate the current batch cooling crystallization processes in such a way that the quality parameters are reproducible and predictable. If possible, develop control methods that achieve this goal.

We recognize that various aspects are relevant to finding a solution to this problem statement. For instance, it is of key importance to understand the process behavior, to be able to infer information of the process during operation and to influence the process behavior. Based on the problem statement the following research topics have been defined:

Process analysis Analyze which sensors are necessary to be able to obtain a reliable estimate of the states [2] of the process. Analyze if it is possible to influence the desired quality parameters independently and to what extent this is possible. Analyze to what extent it is possible to control and steer the current process.

Controller development Development of control methods which enable robust and reproducible operation of crystallization processes. The design of the operational procedure can be part of the design.

Sensor development Development of sensors that enable to measure relevant process variables (such as the liquid concentration and crystal size distribution) and that enable the reliable reconstruction of the state of the process.

Estimator development Given the measurement techniques known for crystallization processes, develop estimation methods which infer reliable information on the state of the system from the available measurements.

New actuation methods Study what kind of modifications on the process equipment help to improve the robust operation of batch cooling crystallization processes.

A part of these research topics has been covered in this thesis. In order to enable the analysis of the dynamic behavior of process, a generic dynamic model for the batch crystallization process will be presented in Chapter 2. The purpose of this chapter is to provide a generic model for batch cooling crystallization processes that enables to perform basic analysis and to avoid unnecessary complexity.

In Chapter 3 the observability and controllability properties of the generic batch cooling crystallization model are analyzed. This analysis provides insight in the chances for success of the development of (model based) estimation and control methods and therefore is a necessity when one desires to develop control and estimation methods.

In Chapter 4 a method for the control of the supersaturation in a batch cooling crystallization process is development. The development of this method contributes to the goal of development of control methods that enable robust and reproducible operation of crystallization processes since the supersaturation is considered to be one of the most important variables that influences the growth of crystals.

Since online measurements for crystallization processes are expensive and known to be unreliable in industrial applications, a large part of this thesis is devoted to the development of model based estimation methods for crystallization processes. In the Chapters 5, 6 and 7 the development of estimators for crystallization processes will be presented. The development of estimators for crystallization processes is all but trivial since crystallization processes are described by non-linear infinite dimensional models. To reduce the mathematical complexity the problem of estimator design has been studied in a linear setting. In Chapters 5 a method for the synthesis of optimal estimators for linear infinite dimensional systems will be presented. In Chapter 6 the approximation and implementation of these estimators will be discussed. The focus in the Chapters 5 and 6 is on the analysis of the methods for estimator design of infinite dimensional systems. In Chapter 7 the methods developed in the previous chapters are used to

[2] In the context of dynamic process models, "state" refers to the memory of a process. In [Polderman and Willems, 1998, Definition 4.3.3] the definition of state is given in a precise manner. Roughly speaking the state is "the collection of variables of a system containing all the information about the past required to be able to understand what the future may look like.".

obtain an estimator for batch cooling crystallization processes. The estimator has been implemented and tested in a simulation environment.

The development of sensors has been restricted to the evaluation and application of current commercially available measurement methods. The development of new actuation methods for batch crystallization processes is not covered and left for future research. In the next section we will provide a detailed overview of the content of this thesis.

1.4 Outline and reading guide for this thesis

This section presents an outline of this thesis, which contains eight chapters. The first chapter is an introduction of the project and provides the motivation of the research described in this thesis. Chapter 2 till Chapter 7 present the results that have been achieved in the research project. In the final chapter, Chapter 8, the conclusions on the studied topics will be summarized and some reflections on the implications for the process will be given. The last chapter also contains a number of recommendations for future work. The thesis contains besides results on engineering aspects that are relevant for crystallization also the mathematical analysis that is necessary for development of control and estimation methods. The readers which are not comfortable with the mathematical treatment can skip the analysis without any problem and are encouraged to read the introduction and conclusions of the chapters. We will give a detailed overview per chapter in the remainder of this section.

Chapter 2 - Modeling of batch cooling crystallization processes

This chapter provides a technical introduction to the batch cooling crystallization process. The chapter begins with an introduction describing the physical aspects of crystallization and the main mechanisms that are of importance for the crystallization process. Based on these mechanisms, a dynamic model for the batch cooling crystallization process will be introduced. The model will serve as a reference model for the analysis of the crystallization process and implementation of the control and estimation methods. The model that will be derived belongs to the class of nonlinear distributed parameter systems.

Chapter 3 - Observability and controllability of crystallization processes

This chapter provides an analysis of the observability and controllability properties of batch crystallization processes. Roughly speaking, observability indicates to what extent it is possible to infer information on the state of the system from measurement of specific variables of the process. Similarly, the controllability indicates to what extent it is possible to steer the process from an initial state to any arbitrary desired state. In order to provide a sound basis for the analysis and discussion on both topics, the chapter begins with the formal definition of the concepts of observability and controllability. The results will be derived from these concepts.

Chapter 4 - Control of batch cooling crystallization by feedback linearization

In this chapter the development and analysis of a method for control of batch crystallization processes by control of the supersaturation level is presented. We believe that the control of supersaturation is of large value, since supersaturation is considered to be the driving force behind crystal growth and nucleation. The control method that will be presented is based on an application of the method of feedback linearization. In the analysis, special care has been taken to show that the method is robust to model uncertainties and therefore remains functional in the presence of modeling errors and in practical situations. In order to test the proposed method, a control scheme based on the theoretical analysis has been implemented in an industrial environment.

Chapter 5 - Estimation for distributed parameter systems

This chapter considers the design of optimal estimators for distributed parameter systems. Since measurements of operating conditions and product properties in a crystallization process in an industrial environment have limited accuracy (especially at small particle size), it is necessary to develop model based estimation methods. Such methods can be used to combine online measurements with the existing knowledge on process dynamics, in order to obtain accurate estimates of the process states. The crystallization process is a distributed parameter system, therefore it is necessary to study the design of estimators for distributed parameter systems. In this chapter we will show how optimal estimators can be designed for linear distributed parameter systems in a systematic way. We will discuss two types of estimators based on different design criteria. The first type of estimator will minimize the Hilbert-Schmidt norm of the error system. The second type of estimator will minimize the L_2-gain of the error system. The methods to design the optimal estimators are based on the duality between estimation problems and control problems, which we will present in the introduction of the chapter. The analysis will be based on the estimation problem with a finite time horizon. Special attention will be given to the analysis of knowledge of the initial conditions of a process.

Chapter 6 - Approximation and implementation of estimators

This chapter considers the implementation of estimators for distributed parameter systems. The analysis in Chapter 5 will show that the optimal estimator for distributed parameter systems is an infinite dimensional system itself. Therefore, this estimator cannot be implemented on a digital computer. In Chapter 6 we will study three methods to approximate the infinite dimensional optimal estimator by a finite dimensional estimator, which *can* be implemented. We will pay attention to the performance of the approximate estimator compared with the optimal estimator. We will show how an estimator for a system with heat diffusion and an estimator for a system with convection can be implemented.

Chapter 7 - Estimators design and implementation for crystallization

In this chapter the theory of Chapter 5 and Chapter 6 will be combined to build an estimator for the batch cooling crystallization process that has been introduced in Chapter 2. Since the process model for batch cooling crystallization is nonlinear we will base the estimator design for this system on a linear approximation of the model. Simulation results will show the performance of the estimator.

Chapter 8 - Conclusion and Recommendations

In the last chapter we present conclusions on the research which has been presented in this thesis. We will indicate how these results relate to the problem statement which has been introduced. Moreover, we will provide recommendations for future research.

1.5 About the project

The research contained in this thesis is part of the project *PH-00-04 Intelligent observer and control design for industrial batch cooling crystallization*. This project is an initiative of the Institute for Sustainable Process Technology (ISPT) and is a collaboration between pharmaceutical industry, SME's and universities in The Netherlands. Within the project PH-00-04, the following industrial and academic partners have been cooperating.

- Albemarle Catalysts,
- Merck Sharp & Dohme,
- DSM Research,
- Friesland Campina DOMO,
- Perdix Analytical Systems,
- Ipcos Boxtel B.V.,
- Institute for Sustainable Process Technology (ISPT),
- Delft University of Technology - Department Process and Energy,
- Delft University of Technology - Department DCSC,
- Eindhoven University of Technology - Control Systems, Faculty of Electrical Engineering.

CHAPTER 2

Modeling of batch cooling crystallization processes

Abstract

This chapter provides an introduction on the aspects of crystallization which are relevant for control of batch crystallization processes. The chapter starts with a process description. Based the process description a dynamic model will be introduced that serves as a basis for the examples discussed in this thesis. At the end of this chapter the sensors for online measurement on crystallization processes will be discussed.

In this chapter a general dynamic model for crystallization processes will be presented. The model serves as a basis for the work presented in the subsequent chapters of this thesis. The aim of the model is to describe the dynamic behavior of the system under study in such a way that it is suitable for analysis of the process and design of control methodologies for the process. That is, the model is based on a simple but realistic process description, in which the dominant aspects of crystallization processes are present. It is important to remark that it is not the aim to obtain an exact process model valid for all processes, but that the goal is to obtain a generalized model serving the purpose of enabling the analyzes made in this thesis. Such a generalized model can be specialized to a specific process by minor changes in the structure and identification of kinetic relations and parameters. The idea is that such a generalized model is better suited for analysis and research purposes. The reasoning being this approach is that the main conclusions of a sound analysis must be independent of the exact realization of a model describing all details of a process and must be valid as long as the key process mechanisms are represented well in an adequate mathematical model. First a description

of mechanisms present in the crystallization process will be given. In the remainder of the chapter an dynamic state space model for the crystallization process will be derived.

2.1 Process description of a crystallization process.

A key characteristic for a crystallization process is the presence of at least two thermodynamic phases, known as the *liquid phase* and the *solid phase*. In a crystallization process the liquid phase contains at least the solvent and the solute. Moreover, additional agents for stabilization of the compound, reactants and impurities might be present. The solid phase consists of the population of particles of crystalline material. In this thesis only batch processes in which there is no significant exchange of mass between the process and the environment are considered.

Moreover, the following additional assumptions on the crystallization process under study are made:

- The solution is a dilute solution. That is, the volume of solvent, solute and solid can be approximated well by the volume of the solvent.
- The solvent does not take part in the crystallization process.
- Particles are single crystals and do not consist of agglomerates of crystals.
- There are no effects of impurities in the liquid on the solubility, crystal growth and nucleation rate.
- There is only one polymorphic form present in the process.
- The process is ideally mixed.

The first two of these assumptions have been made to avoid an unnecessary complication of the crystallization model. In principle, it is possible to drop the assumptions and increase the complexity of the model, but this does not change the main characteristics of the batch crystallization process. In the literature, the condition on agglomerate formation is often not made explicitly. However, if agglomerates do influence the evolution of the process then one should include the state of agglomerates in the model of the system and one has to include the formation and evolution of agglomerates in the dynamics of the process model. In practical industrial systems, agglomerate of crystals (also known as agglomerates) are often present. In what sense and how they precisely do influence the growth of particles is beyond the scope of this thesis.

The two phases in the process do have a mutual influence on each other by various mechanisms. For instance, due to the crystallization of matter, there is a transfer of mass between the solid and liquid phase. The particles in the system can be altered by various mechanisms:

Growth Solid particles can increase in size due to uptake of dissolved material from the liquid phase. The transition process from solution to crystalline material is known as crystallization[1] or crystal growth.

[1] It must be noted that the word crystallization refers to the formation of crystalline material out of a gas phase or a liquid phase, but that in process industry the term crystallization process refers to the process in which growth, dissolution, nucleation and breakage might be present simultaneously.

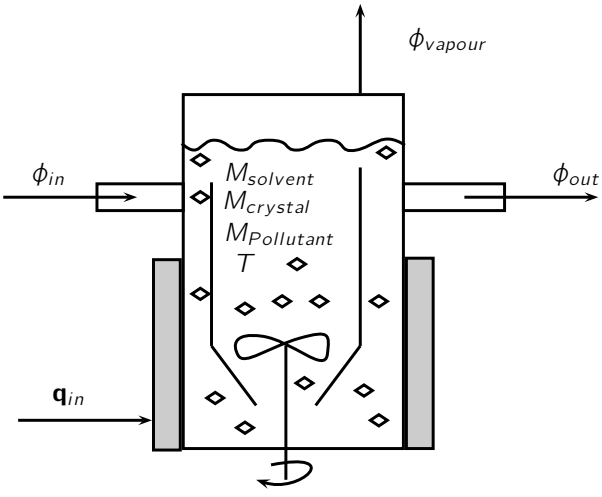

Figure 2.1: General schematic of a batch cooling crystallizer.

Dissolution Particles can decrease in size due to the transfer of material from the crystal surface to the liquid phase. This mechanism is known as dissolution.

Nucleation New crystalline particles can be created if the process conditions are right. This mechanism is known as nucleation. There are various mechanisms and causes which can lead to the formation of new particles. The classification in primary and secondary nucleation mechanisms is the most well known classification [Mersmann, 2001]. Primary nucleation refers to nucleation that is not accommodated by crystalline material and secondary nucleation refers to nucleation that is assisted by crystalline material.

Breakage Particles can break into multiple fractions, either due to forces from the internal structure of the particle or due to external forces acting on the particles. This mechanism is known as breakage or fragmentation. The attrition of particles is often considered as main source of small particles.

Due to the simultaneous growth, dissolution, nucleation and breakage of particles, the population of particles in a process is continuously subject to change. How such changes in the population of particles can be modeled is explained in Section 2.2.1. In the next subsection the physical mechanisms relevant for nucleation, dissolution and crystal growth are described.

Batch crystallization processes in industry are mostly carried out in general purpose reactors with a volume in the order between $0.1\,m^3$ and $10\,m^3$. Such a general purpose reactor is often a glass or a stainless steel, glass lined, stirred tank reactor, which is frequently equipped with baffles to improve mixing behavior. This type of reactors is equipped with a cooling and heating jacket for thermal control of the system. A picture of such a reactor is given in Figure 2.1. When working with organic solvents, the reactor will also be equipped with a vacuum pressure control system to control the exhaust of vapors.

2.1.1 Physics of nucleation and crystal growth

The term crystallization refers to the physical process in which molecules arrange to form solid matter, called crystals.Typical examples are the crystallization of a component from a solution or a melt. The aspect that makes crystallization interesting to be used as separation technology is the high selectivity in which molecules are selected to be added to the solid matter. In this section the physical aspects of this process which are relevant for the dynamic model will be discussed. The interested reader can find a detailed discussion on the physics behind the mechanisms of crystal growth in [Mersmann, 2001].

The fundamental driving force for crystal growth is the difference in chemical potential of the given substance in the transferring and transferred state in the solution and in the crystal [Mullin, 2001, p.128]. The crystal growth rate is also influenced by the mass transport between the surface layer of the particle and its environment. The driving force for these mechanism is the concentration difference between the crystal surface and the environment.

At a given temperature there is a maximum amount of solute that can dissolve in the solvent. The concentration at which the solution (measured in the ratio of solute mass and solvent mass) is saturated is described by the saturation curve $c_{sat}(T)$ [$\mathrm{kg_{solute}/kg_{solvent}}$], where T is the solvent temperature. When this maximum concentration is reached, the solution is said to be saturated. With respect to the saturation curve the solution can be undersaturated, saturated or supersaturated, depending on whether the solute concentration is less than, equal to or greater than the saturation curve, respectively. In this thesis it will be assumed that the solubility increases strictly with the temperature T, that is $c_{sat}(T_1) < c_{sat}(T_2)$ for all $T_1 < T_2$, (or equivalently $\frac{\mathrm{d}c_{sat}}{\mathrm{d}T}(T) > 0$ for all T).

The supersaturation level is commonly expressed by the difference between the solute concentration c and the saturation curve $c_{sat}(T)$. The absolute supersaturation $S_a(c,T)$ and relative supersaturation $S_r(c,T)$ are defined by:

$$S_a(c,T) = c - c_{sat}(T) \qquad \textit{and} \qquad S_r(c,T) = \frac{S_a(c,T)}{c_{sat}(T)}. \tag{2.1a,b}$$

In practical applications it is common to consider not the chemical potential directly, but either the absolute or relative supersaturation measure for the driving force for both crystal growth and nucleation. Figure 2.2 shows a typical concentration temperature diagram of a solvent-solute combination, with the solubility line and the undersaturated and supersaturated zones. For completeness, the diagram also shows the metastable zone width limit which is often used in industrial environments. The metastable zone width line or limit divides the supersaturated region in a metastable zone and unstable zone [Mullin, 2001, Section 3.12]. In the metastable zone spontaneous nucleation is improbable, but crystal growth will occur once crystals are present. In the unstable zone spontaneous nucleation is possible and not inevitable on the long term. In practice an accurate determination of the metastable zone width is difficult, which is amongst other reasons due to the limited capabilities of online sensors to detect small particles. It is well known that the measured meta stable zone might depend on the operation conditions, equipment, scaling and mixing effects [Kadam, 2012]. Therefore, the existence

of the meta stable zone and the concept of the metastable zone limit as partitioning of the concentration temperature plane in distinct zones is disputed and might need reconsideration.

There are various methods to generate supersaturation in a solution. For industry relevant methods are:

1. Cooling crystallization: The solubility of solute in a solvent in general depends on the temperature. For solid-solvent combinations of which the solubility increases with temperature, supersaturation can be generated by cooling of a saturated solution.
2. Evaporative crystallization: By evaporation of solvent from a solution, the concentration of the solute in the solvent increases. This mechanism causes supersaturation if applied to a saturated solution.
3. Reactive crystallization: Due to the addition of an extra component in the solution the solubility properties of a solvent might be altered and cause supersaturation of a solution.

The choice which method will be applied in an industrial case depends, amongst others, on the solute properties, the solvent properties, the slope of the solubility curve, the tendency toward scaling and the efficiency of the methods for a specific case. Also a combination of the methods is applied in industry to increase yield or decrease production time.

Cooling crystallization is often employed when a high purity of the product is desired but requires a significant dependency of the solubility on temperature. A drawback of the cooling crystallization processes are the relatively low yield and the sensitivity for scaling phenomena. Evaporative crystallization is often employed when the solubility is less dependent on temperature or when a high yield is desired. A drawback of evaporative crystallization is that it is energy intensive and requires relatively complex equipment compared to cooling crystallization. Reactive crystallization is often employed when high yield is desired.

Although in general it is assumed that supersaturation is the driving force behind crystal growth, growth of the particles can depend on the condition of the particle itself and the condition of the liquid phase. For instance, the presence of impurities or irregularities on the crystal surface might alter the crystal growth rate and characteristic significantly.

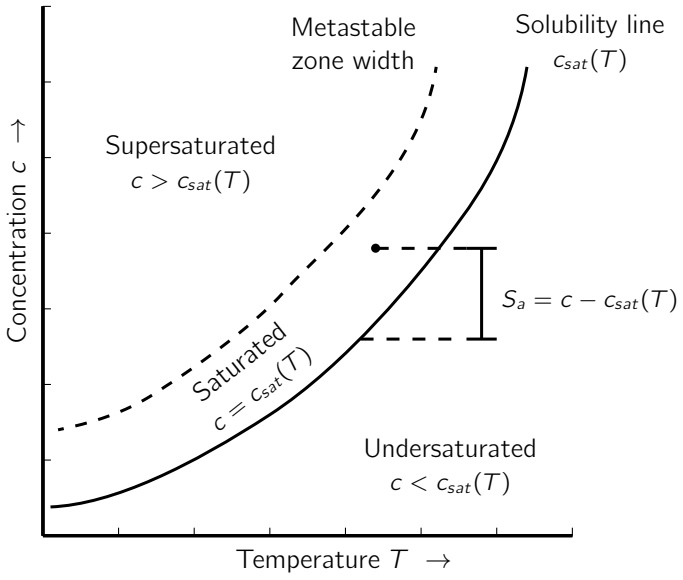

Figure 2.2: Concentration - Temperature diagram with solubility line.

2.2 A model for batch cooling crystallization processes

In this section a dynamic model for batch cooling crystallization processes will be derived. First a model for the dynamic modeling of the particle population and the conservation laws for energy and mass will be introduced. Then, by combination of these models, a general model applicable to batch cooling crystallization processes will be derived.

2.2.1 Model of the particle population

In this section a method for modeling of a process with contains a population of particles will discussed. In industrial crystallization processes the solid phase can consist of a large number of particles per volumetric unit of suspension. More than 10^9 particles per m^3 is common. Since this number is large, models which deal with particles individually, have extreme high computational demands. To circumvent this, macroscopic models based on statistical properties of the population of particles will be introduced. These models describe properties of a complete population, rather than properties of individual particles. Such models will be called population models. The usage of population models has been reported in a wide range of applications such as grinding, aerosol coagulation, and granulation of particles, but also modeling of cell populations in biology. The usage of population models in crystallization processes has been introduced in [Hulburt and Katz, 1964].

First , the state of a particle population with N particles in a compartment with volume V will be modeled. For this purpose, the concept of a number density distribution

represented by $n_V(x)$ will be introduced. Assume that particles in a population are characterized by a size parameter x such as for example length, surface area or volume, where $x \in [0, \bar{x})$ with $\bar{x} > 0$. Define the number density n_V as a distribution, that is, n_V is such that the total number of particles with parameter x in the interval $[x_1, x_2]$ present in a compartment with volume V is given by:

$$\int_{x_1}^{x_2} n_V(x)\mathrm{d}x.$$

Clearly, the number density distribution is normalized such that:

$$N = \int_0^{\bar{x}} n_V(x)\mathrm{d}x.$$

is the total number of particles in the volume V.

The number distribution $n(x)$ (also known as number density function), for an infinitesimal volume V is defined by the limit process:

$$\int_{x_1}^{x_2} n(x)\mathrm{d}x = \lim_{V \to 0} \frac{1}{V} \int_{x_1}^{x_2} n_V(x)\mathrm{d}x.$$

The number distribution $n(x)$ can be used to model the state of crystallization processes per volumetric unit of the process. For a more extensive introduction to population models in the context of crystallization the reader is referred to [Randolph and Larson, 1971] and [Ramkrishna, 2000]. For a introduction to population models in a more mathematical context we refer to [Engel and Nagel, 2000, Section 6.1] and [Webb, 1985].

In models of crystallization processes is often assumed that the state of the particle population can described uniquely by the number density distribution of a characteristic property x of the particles. The volume of the particle is a possible choice and it is becoming increasingly popular to use multiple characteristic properties, for instance two characteristic lengths of the particles. This leads to multidimensional population densities. In this thesis it will be assumed that the state of the particle population can be completely described by the length of the particle, which will be denoted by ℓ. Therefore, it is assumed that the state of a population can be described by a function $n(\ell) \in \mathbb{R}$ with unit m^{-1} *per volumetric unit*. Moreover, it is assumed that the population density distributions are in the class $\mathcal{N} = L_2(\mathbb{L}, \mathbb{R})$ with $\mathbb{L} = [0, \bar{\ell}]$ for some $\bar{\ell} \in \mathbb{R}^+$. $\bar{\ell}$ represents the length of the largest crystal that can occur in the process. From a mathematical point of view this assumption can be subject to discussion and one can argue that $\mathcal{N} = L_1(\mathbb{L}, \mathbb{R})$, which is a Banach space, is more natural. However, the choice for $\mathcal{N} = L_2(\mathbb{L}, \mathbb{R})$ has been made since this is a Hilbert space. In a Hilbert space the solution of optimization problems can be done by exploitation both the existence of an inner product and completeness of the function space, whereas optimization problems in L_1 require a deeper mathematical analysis.

It will be assumed that the volume fraction occupied by the particles in the population can be calculated from the population density function. Therefore, it is supposed that there exists a functional $V : \mathcal{N} \to \mathbb{R}$ that calculates the total volume of the particles

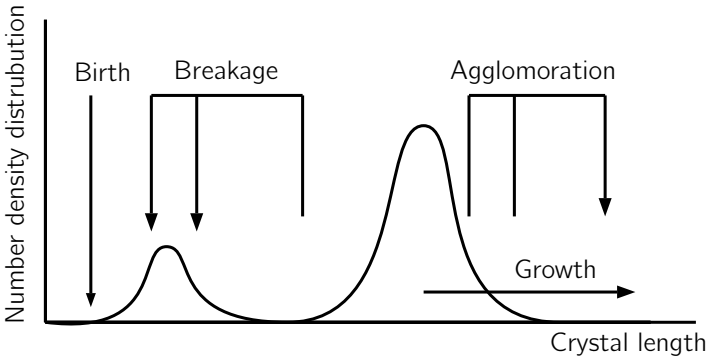

Figure 2.3: Population balance and various phenomena present in the crystallization process.

represented by a population density distribution. A commonly used function V, for the case where the particles are characterized by the edge length ℓ is given by:

$$V(n) = \int_0^{\bar{\ell}} v(\ell) n(\ell) \mathrm{d}\ell \tag{2.2}$$

where $v(\ell)$ is a polynomial expression depending on the particle shape. Remark that the unit of $V(n)$ is $\frac{m^3}{m^3}$. When growth manifest itself in three dimensions of the particle one considers $v(\ell) \approx \ell^3$, when growth manifest itself in two dimensions of the particle one considers $v(\ell) \approx \ell^2$ and when growth manifest itself in only one dimension of the particle one considers $v(\ell) \approx \ell$. The model leaves freedom for other polynomial relations between ℓ and v as long as physics are respected.

The population of particles can be subject to change due to various mechanisms and therefore it is assumed that the number density distribution is a time dependent distribution, which will be denoted by $n \in L_2(\mathbb{L} \times \mathbb{T}, \mathbb{R})$, where $\mathbb{L}$ and $\mathbb{T}$ denotes the length interval and time interval under consideration. In this situation the volume fraction obtained by the solid phase will change with time as defined by the mapping $t \mapsto V(n(\cdot, t))$ and will be denoted by $[V(n)](t)$ and $V(n(\cdot, t))$. A graphical representation of these mechanisms acting on the particle size distribution is given in Figure 2.3. The mechanisms responsible for change of the particle size distribution are which are described in Section 2.1. The evolution of the population density distribution can be described by the so called balance equation for the population. The mechanisms can be incorporated in the balance equations will be described in the following subsection.

Growth

Growth of particles in the population balance can be modeled as a convection process with a velocity equal to the growth rate of the particles. Suppose there exists a time dependent number density distribution $n(\ell, t)$, describing particles with length ℓ which growth with rate $G(\ell)$. Consider the number of particle in the interval $[\ell_1, \ell_1 + \Delta\ell]$, given

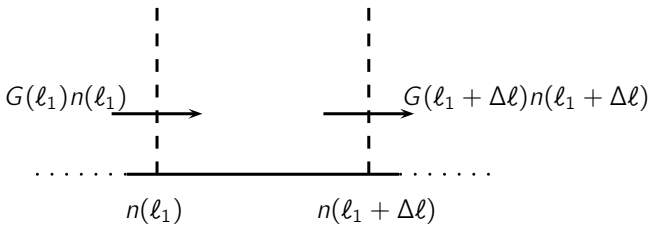

Figure 2.4: Growth process.

by $\int_{\ell_1}^{\ell_1+\Delta\ell} n(\ell)\mathrm{d}\ell$. The change of the number of particles in the interval $\ell \in [\ell_1, \ell_1+\Delta\ell]$ is equal to the flux of particles across the boundaries of the interval, which is graphically represented by Figure 2.4. Therefore, the change of number of particles in the interval $[\ell_1, \ell_1+\Delta\ell]$ can be modeled by:

$$\frac{\partial}{\partial t}\int_{\ell_1}^{\ell_1+\Delta\ell} n(\ell,t)\mathrm{d}\ell = G(\ell_1)n(\ell_1,t) - G(\ell_1+\Delta\ell)n(\ell_1+\Delta\ell,t).$$

Observe that by the Fundamental Theorem of Calculus the right hand side can be rewritten as:

$$\frac{\partial}{\partial t}\int_{\ell_1}^{\ell_1+\Delta\ell} n(\ell,t)\mathrm{d}\ell = \int_{\ell_1}^{\ell_1+\Delta\ell} -\frac{\partial G(\ell)n(\ell,t)}{\partial \ell}\mathrm{d}\ell.$$

Since this holds for all $\ell_1 > 0$ and $\Delta\ell > 0$, it follows that $n(\ell,t)$ satisfies the partial differential equation:

$$\frac{\partial n}{\partial t} = -\frac{\partial Gn}{\partial \ell}, \tag{2.3}$$

where G is the (possibly size dependent) growth rate, with $G(\ell) \in \mathbb{R} > 0$. This equation needs a boundary condition on $n(0,\bar{\ell})$ in order to be well posed. In case of size independent growth one has $G \in \mathbb{R}$. In case of size dependent growth G is a function of ℓ. In crystallization processes the growth rate can be a function of the concentration and temperature, which will be shown in Section 2.2.3.

Dissolution

Dissolution is the release of material from the solid phase to the liquid phase. As a result crystals decrease in size. Dissolution has been far less studied than crystal growth but is under ideal circumstances assumed to be reciprocal to growth. Therefore, dissolution can be modeled by the equation.

$$\frac{\partial n}{\partial t} = \frac{\partial Dn}{\partial \ell},$$

where D is the (possibly size dependent) dissolution rate, with $D > 0$. It must be remarked that this equation needs a boundary condition on $n(0,\bar{\ell})$ if $\bar{\ell} < \infty$, in order to be well posed.

If crystal growth and dissolution were purely diffusion controlled in nature, they would exhibit a true reciprocity. The faces of a crystal would grow and dissolve at the same rate and the rate of crystallization would equal the rate of dissolution at a given temperature and equal driving forces. In [Mullin, 2001] it can be found that these conditions rarely occur in practice. Crystals dissolve much faster than they grow and up to a fivefold difference is not uncommon. The large rate of dissolution and attempts to identify kinetics can also be found in [Matthews et al., 1996]. The dissolution rate can also be a function of the concentration and temperature.

Nucleation

Due to the mechanism of nucleation new crystalline particles can come into existence. The particles generated by nucleation are of very small size. It is common practice [Myerson, 2002, section 10.3] to model nucleation as boundary condition on the population balance equation in the following way. When the birth rate and growth rate at time t equal $B(t)$ respectively $G(t)$, then the following boundary condition is applied:

$$n(0,t) = \frac{B(t)}{G(t)}.$$

Alternatively, nucleation can be modeled by addition of particles in a certain size range to the number density distribution. For instance, when it is assumed that after nucleation particles have a length within the interval $\ell_0 \pm \epsilon$ then the increase in the number of particles in this size interval is described by

$$\frac{\partial n}{\partial t} = B(t)w(\ell)$$

where $w(\ell)$ is a weighting function and is, for instance. given by:

$$w(\ell) = \begin{cases} \frac{1}{2\epsilon} & \text{if } \ell_0 - \epsilon < \ell < \ell_0 + \epsilon, \\ 0 & \text{else.} \end{cases}$$

Breakage or Fragmentation

The process of particle breakage can be modeled by the fragmentation equation. A fundamental treatment of the theory of particle breakage is given in [Filippov, 1961]. The effect of particle breakage can be described by the follow equation:

$$\frac{\partial n}{\partial t}(\ell,t) = [En](\ell,t) = -\beta(\ell)n(\ell,t) + \int_0^{\bar{\ell}} \beta(y)P(\ell,y)n(y,t)\mathrm{d}y$$

where $\beta(\ell) > 0$ is the rate of breakage of particles with length ℓ and $P(x,y)$ is the breakage kernel. The first term $-\beta(\ell)n(\ell,t)$ describes to the removal of particles of size ℓ from the number distribution due to breakage of these particles. The second term $\int_0^{\bar{\ell}} \beta(y)P(\ell,y)n(y,t)\mathrm{d}y$ describes the addition of particles at size ℓ as a result of breakage of particles of larger sizes.

There are some physical constraints on $P(x, y)$. Obviously, the breakage rate and breakage kernel have to be such that the conservation of mass is respected. Since breakage can only decrease size it follows that $P(x, y) = 0$ for $x > y$. Moreover, for binary breakage, i.e. breakage of a particle into precisely two parts, it follows that: $P(x, y) = P(y - x, y)$. In practical applications the identification of a breakage model is difficult. An overview of the modeling of particle breakage is given in [Valentas and Amundson, 1966] and overview of breakage models is given in [Peterson et al., 1985].

Population balance model with growth, breakage and nucleation

The combined model for a number density distribution of the particle population subject to change due to growth, nucleation and breakage is given by:

$$\frac{\partial n}{\partial t} = \frac{\partial G n}{\partial \ell} + En = \frac{\partial G n}{\partial \ell} - \beta(\ell) n(\ell, t) + \int_0^{\bar{\ell}} \beta(y) P(\ell, y) n(y, t) \mathrm{dy} \tag{2.4}$$

with boundary condition $n(0, t) = \frac{B(t)}{G(t)}$. Here G is the growth rate ($G(t) > 0$ for all t), B is the nucleation rate, β is the fragmentation rate and P is the fragmentation kernel. In practical applications one will often neglect the effect of fragmentation and one will set $\beta = 0$.

2.2.2 Mass and energy balance

All models that are considered here are based on two conservation laws:

1. Conservation of mass. The total change of mass that is stored in the system and exchanged with its environment is zero.
2. Conservation of energy: The total change in energy stored in the system and the exchange of energy between a system and its environment is zero.

The mass and energy balance serve as basis to establish the structure of the dynamic model and will be discussed individually in the following subsection.

Mass balance

The conservation of mass serves as basis to determine the relation between the masses of the various components in the crystallizer. The conservation of mass reflects that the change of the mass of a component in the reactor equals the difference between the flux into and the flux out of the component through the boundaries of the system. Since it has been assumed that there is no significant exchange of mass between the process and the environment it follows that the total mass present in the system is constant. In batch crystallization processes there are two components present, the solvent and the to-be-crystallized component. The mass of the solvent will be indicated by $m_s\,[kg]$, the mass of the solute will be indicated by $m_l\,[kg]$ and the mass of the solid component will be indicated by $m_c\,[kg]$.

From the assumption that there is no mass exchange between the process and the environment, the mass balance dictates that:

$$\frac{\mathrm{d}m_s}{\mathrm{d}t} = 0, \tag{2.5}$$

$$\frac{\mathrm{d}m_l}{\mathrm{d}t} + \frac{\mathrm{d}m_c}{\mathrm{d}t} = 0. \tag{2.6}$$

Enthalpy balance

The conservation of energy serves as a basis to derive a model for the enthalpy and thereby for the temperature of the system. The conservation of energy reflects that the change of the energy in the system equals the inflow and outflow of energy through the boundaries of the system. There are several mechanisms that influence the enthalpy stored in the reactor.

- Exchange of thermal energy between the reactor and the thermal jacket by heat conduction, denoted by $Q_j\,[J/s]$.
- Exchange of thermal energy between the reactor and the environment by heat conduction, denoted by $Q_0\,[J/s]$.
- The release of energy due to crystallization, denoted by $Q_c\,[J/s]$.

Let $E_T\,[J]$ denote the enthalpy in the reactor. It follows from the law of conservation of energy that the energy in the system satisfies the equation:

$$\frac{\mathrm{d}E_T}{\mathrm{d}t} = Q_0 + Q_j + Q_c. \tag{2.7}$$

It is assumed that the diffusion processes can be modeled by a first order equation. Let $T\,[^\circ\mathrm{C}]$ denote the reactor temperature, $T_j\,[^\circ\mathrm{C}]$ denote the jacket temperature and $T_0\,[^\circ\mathrm{C}]$ denote the environmental temperature, then the heat flows follow from Fourier's law and can be modeled as follows:

$$Q_0 = h_0(T_0 - T), \tag{2.8}$$

$$Q_j = h_j(T_j - T), \tag{2.9}$$

where $h_0, [J/(s^\circ\mathrm{C})]$ is the heat transfer coefficient between environment and reactor, $h_j, [J/(s^\circ\mathrm{C})]$ is the heat transfer coefficient between the thermal jacket and reactor.

Moreover it is assumed that the heat flow due to crystallization is linear with respect to the rate of crystallization, such that it can be modeled by:

$$Q_c = \Delta H V_r R(t), \tag{2.10}$$

where $\Delta H\,[J/kg]$ represents the enthalpy of crystallization and $R(t)\,[kg/sm^3]$ denotes the rate of crystallization per volumetric unit of slurry. The rate of crystallization $R(t)$ is given by:

$$R(t) = \rho_c \frac{\mathrm{d}V(n(\cdot, t))}{\mathrm{d}t},$$

where $\rho_c\,[kg/m^3]$ is the specific crystal density and V is the volume function given by Equation 2.2. Let $C_p\,[J/^\circ\mathrm{C}]$ denote the heat capacity of the reactor and its content, then the temperature in the reactor can be determined as follows:

$$T = \frac{E_T}{C_p}. \tag{2.11}$$

Often, the heat capacity of the reactor will be approximated by the heat capacity of the slurry inside the reactor and one will use $C_p \approx V_r \rho c_p$ where $V_r\,[m^3]$ is the reactor volume and $\rho\,[\mathrm{kg/m^3}]$ and $c_p\,[\mathrm{J/kgK}]$ are the density specific heat capacity of the solvent. A dynamic model for the temperature in the reactor is then obtained by combination of the Equations (2.7), (2.8), (2.9), (2.10) and (2.11),

$$\frac{\mathrm{d}T}{\mathrm{d}t} = \frac{1}{V_r \rho c_p}(Q_0 + Q_j + Q_c) = \alpha_0(T_0 - T) + \alpha_j(T_j - T) + \frac{\Delta H}{\rho c_p} R(t).$$

where $\alpha_0 = \frac{h_0}{V_r \rho c_p}$ and $\alpha_j = \frac{h_j}{V_r \rho c_p}$ are the thermal time constants of the system.

2.2.3 Kinetic relations

In the balance equations given in this chapter, the rates G and B have not been defined. The domain of the functions G and B has been defined. Independent of the values of G and B the mass and energy balances are conservative. However, what lacks is the value of these functions and with that the rate of change of the state variables in the models. In chemical engineering these equations are known as kinetic relations or kinetics. The word kinetics means [Oxford, 2010] here "relating to or resulting from motion". For chemical processes, the interaction between particles originates from the collision between particles and therefore from the motion of particles and the kinetics involved here.

Depending on whether growth is diffusion or surface integration controlled, the absolute or relative supersaturation is the driving force for crystal growth [Mersmann, 2001]. It is often assumed that the crystal growth rate is size independent and can be modeled by an empirical power law of either the absolute or relative supersaturation. In this thesis this assumption is adopted and it is assumed that the growth rate satisfies the relation:

$$G(c,T) = \begin{cases} k_g S(c,T)^g & \text{if } S(c,T) > 0 \\ 0 & else \end{cases}, \tag{2.12}$$

where, $k_g > 0$ is the exponential factor, $g > 0$ is the growth rate exponent and S is either the relative or absolute supersaturation level.

For nucleation, it is assumed that the rate of nucleation is dependent on the supersaturation as well. In case of secondary nucleation it is assumed that the driving force is the absolute supersaturation level [Mersmann, 2001, p.6]. Moreover, it is assumed that the total volume present in the solid phase is of influence on the nucleation rate. It is assumed that the nucleation rate can be modeled the empirical power law:

$$B(c,T,n) = \begin{cases} k_b S_a(c,T)^b \rho_c V(n(\cdot,t)) & \text{for } S_a(c,T) > 0 \\ 0 & else \end{cases} \tag{2.13}$$

where, $k_b > 0$ is the exponential factor, $b > 0$ is the birth rate exponent, S_a is the absolute supersaturation level, $V(n(\cdot, t))$ is the volume fraction of the solid phase and ρ_c is the density of the crystalline material.

2.2.4 Reference model for batch crystallization process.

Cooling crystallization reference process

In the pharmaceutical industry, cooling crystallization processes are mostly carried out in general purpose reactors with a volume between $0.1\,\mathrm{m}^3$ and $10\,\mathrm{m}^3$. In this section the dynamic model for the the particle population, the mass balance equation and thermal energy balance equation are combined in order to obtain a general model for a batch crystallization process. It will be assumed that the batch cooling crystallization process is carried out in a vessel with a volume of $1\,m^3$, which will be denoted by V_r.

The concentration of the solute in the process has been defined as ratio between the solute mass and solvent mass, i.e. $c = \frac{m_l}{m_s}$. Therefore, the change of concentration with respect to time satisfies the relation:

$$\frac{\mathrm{d}c}{\mathrm{d}t} = \frac{\mathrm{d}}{\mathrm{d}t}\frac{m_l}{m_s}.$$

Using the mass balance for the closed system (Equations 2.5 and 2.6), this can be rewritten to:

$$\frac{\mathrm{d}c}{\mathrm{d}t} = -\frac{1}{m_s}\frac{\mathrm{d}m_c}{\mathrm{d}t}.$$

The volume fraction occupied by the solid phase can be computed by the functional $V(n)$. Therefore, the solid mass can be computed by

$$m_c = \rho_c V_r V(n),$$

where $\rho_c\,[kg/m^3]$ is the solid density. From the assumption that the solution is dilute it follows that

$$m_s \approx \rho V_r,$$

where $\rho\,[kg/m^3]$ is the solvent density. From the combination of these equations it follows that:

$$\frac{\mathrm{d}c}{\mathrm{d}t} = -\frac{\rho_c}{\rho}\frac{\mathrm{d}V(n)}{\mathrm{d}t}.$$

From the latter equation it follows that the concentration is not a state in the system, since it is linearly dependent on the particle distribution. It follows by integration of the left and right hand side, that when initial conditions are given by $c(0) = c_0$ and $n(\ell, 0) = n_0(\ell)$ that $c(t)$ satisfies:

$$c(t) = c_0 + \frac{\rho_c}{\rho}\left[V(n_0(\cdot)) - V(n(\cdot, t))\right]. \tag{2.14}$$

The latter equation is the direct result from the assumption that the system does not exchange mass with the environment.

By combination of the population balance equation (2.4), the energy balance, the mass balance and the kinetic Equations (2.12), (2.13) the system can be modeled. It follows that if $S_a(c,T) > 0$, then $G(c,T) > 0$. The following set of equations describes the dynamics of the system:

$$\frac{\partial n}{\partial t} = -\frac{\partial G n}{\partial \ell}, \tag{2.15a}$$

$$\frac{\mathrm{d}T}{\mathrm{d}t} = \alpha_j \left[T_j - T\right] + \alpha_0 \left[T_0 - T\right] + \frac{\Delta H}{\rho c_p} R(t), \tag{2.15b}$$

$$n(0,t) = \frac{B(c,T,n)}{G(c,T)}, \tag{2.15c}$$

where the states are $n(\ell,t) \in L_2(\mathbb{L}\times\mathbb{T},\mathbb{R})$, $T(t) \in \mathbb{R}$ is the reactor temperature, $T_j(t) \in \mathbb{R}$ is the jacket temperature, $T_0(t) \in \mathbb{R}$ is the environmental temperature. The constants $\alpha_j = \frac{h_j}{C_T}$ and $\alpha_0 = \frac{h_0}{C_T}$ are the thermal time constants. The growth rate $G(c,T)$ and nucleation rate $B(c,T,n)$ are dependent on the reactor temperature and the concentration via the supersaturation. The concentration satisfies Equation (2.14) in which V is the volume fraction function for the crystal size distribution $n(\ell,t)$ and is given by (2.2).

Moreover, in the situation where $S_a(c,T) < 0$ and $D(c,T) > 0$, it follows by combination of the population balance Equation (2.4), the energy balance, the mass balance and the kinetic Equations (2.12), (2.13) that the system can be modeled by the following set of equations:

$$\frac{\partial n}{\partial t} = \frac{\partial D n}{\partial \ell}, \tag{2.16a}$$

$$\frac{\mathrm{d}T}{\mathrm{d}t} = \alpha_j \left[T_j - T\right] + \alpha_0 \left[T_0 - T\right] + \frac{\Delta H}{\rho c_p} R(t), \tag{2.16b}$$

where $D(c,T) > 0$ is the dissolution rate and the boundary condition $n(\bar{\ell},t) = 0$ holds.

In this thesis will be assumed that the volume fraction of the solid phase can be computed by the function V given by Equation (2.2) with $v(\ell) = k_v \ell^3$, where k_v is the shape factor, determined by geometry of the crystals. For cubic particles it follows that $k_v = 1$. By use of integration by parts $\frac{\mathrm{d}}{\mathrm{d}t}[V(n)](t)$ can, in the situation of particle growth, be rewritten to:

$$\frac{\mathrm{d}}{\mathrm{d}t}[V(n)](t) = k_v G(c,T) \left(\left[\ell^3 n(\ell,t)\right]_{\ell=0}^{\bar{\ell}} - 3\int_0^{\bar{\ell}} \ell^2 n(\ell,t)\mathrm{d}\ell \right). \tag{2.17}$$

In the situation of the dissolution of particles a similar expression holds.

It is important to make some remarks with respect to the model which has been introduced. Well posedness [2] of the population balance equations (2.15) and (2.16) is

[2] A problem is said to be well posed (in the sense Hadamard) if: 1) a solution to the problem exists, 2) the solution is unique, and 3) the solution depends continuously on the problem data.

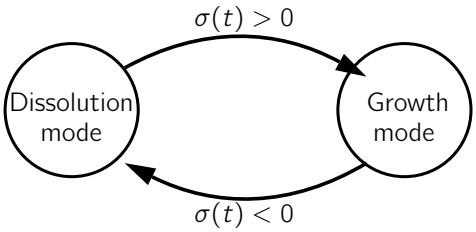

Figure 2.5: Automaton corresponding to the hybrid behavior of crystallization processes. The switching function $\sigma(t)$ is equal to the level of supersaturation in the system, i.e. $\sigma(t) = S_a(c(t), T(t))$.

of course of importance. In order to establish uniqueness of solutions one boundary condition is necessary and allowed. Please notice that:

- If $S_a(c, T) > 0$, the model is well posed if and only if a boundary condition at $\ell = 0$ and the initial condition are specified. That is $n(0, t) = \eta_0(t)$ with $\eta_0(t) \in \mathbb{R}$, $n(\ell, 0)$ is given and $n(\ell, 0)$ and $T(0)$ are given.
- If $S_a(c, T) < 0$ and $\bar{\ell} < \infty$ the model is well posed if and only if a boundary condition at $\ell = \bar{\ell}$ and the initial condition are specified. That is $n(\bar{\ell}, t) = \eta_{\bar{\ell}}(t)$ with $\eta_{\bar{\ell}}(t) \in \mathbb{R}$ is given and $n(\ell, 0)$ and $T(0)$ are given.

The system can be interpreted as a hybrid nonlinear distributed parameter system. The consequence is that if the sign of $S_a(c, T)$ changes, the system switches between the growth mode and dissolution mode, which is illustrated with Figure 2.5. Therefore, three modes of operation can be distinguished namely

Supersaturated operation The process operates only in the supersaturated region for the complete time interval $\mathbb{T}$.

Undersaturated operation The process operates only in the undersaturated region region for the complete time interval $\mathbb{T}$.

Mixed super and under saturated operation The process alternates between the undersaturated or supersaturated region for during the time interval $\mathbb{T}$.

The initial conditions of the process determine in which mode one can operate the process. Clearly, the initial conditions have to be compatible with the operational modes. The three modes of operation are illustrated in the concentration-temperature diagram as shown in Figure 2.6.

Two additional classes U^G and U^D of the input signals for input T_j will be defined, which contain the input signals that keep the process inside the supersaturated and undersaturated mode respectively. Define U^G and U^D as follows:

$$U^G(c_0, n_0, T_0) := \left\{ T_j \in L_2(\mathbb{T}; \mathbb{R}) \,\middle|\, S(c, T) > 0 \text{ for all } t \in \mathbb{T} \text{ and (2.15) holds.} \right\} \tag{2.18}$$

$$U^D(c_0, n_0, T_0) := \left\{ T_j \in L_2(\mathbb{T}; \mathbb{R}) \,\middle|\, S(c, T) < 0 \text{ for all } t \in \mathbb{T} \text{ and (2.16) holds.} \right\} \tag{2.19}$$

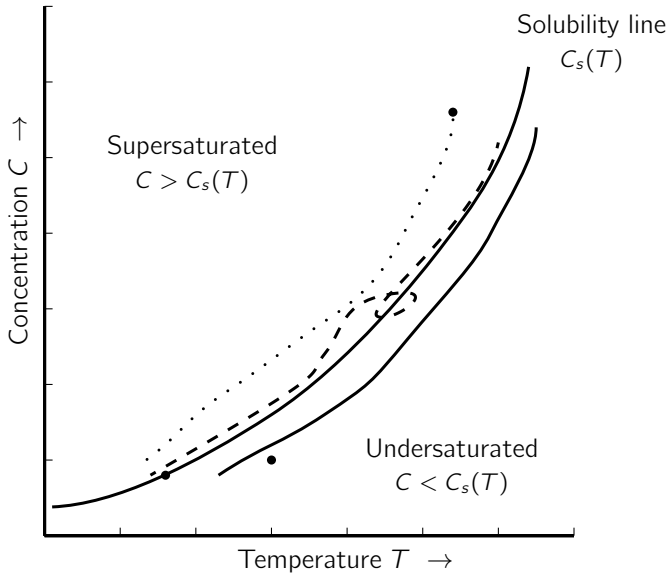

Figure 2.6: Concentration - Temperature diagram with three modes of operation. Supersaturated operation (dotted line), Under-saturated operation (straight line) and Mixed super and under saturated operation (dash dotted line).

Note that $U^G(T_0, c_0, n_0) = \emptyset$ ($U^D(T_0, c_0, n_0) = \emptyset$) whenever the initial conditions (n_0, c_0, T_0) are such that $S(c_0, T_0) \leq 0$ ($S(c_0, T_0)) \geq 0$).

The model which we have introduced exhibits hybrid, nonlinear and infinite dimensional characteristics. Although the individual types of systems have been studied in detail and quite advanced analysis methods exist for these systems, theory for systems that are hybrid, nonlinear and infinite-dimensional is not mature yet. Therefore, in this thesis we will assume that the process will only operate in one of the two modes and does not switch between the modes. The subsets U^G and U^D will be used in Chapter 3 in the context of the analysis of the observability and controllability of the crystallization process.

2.3 Model approximation by moment transformation

A very popular method to deal with the complexity of population balance models is obtained by application of the moment transformation [Mersmann, 2001]. The moment transformation is known as the method of moments and has been reported the first time in [Hulburt and Katz, 1964] in the context of population balance models. Crystallization models obtained by transformation of the population balance models are known as moments models. The method of moments has severe limitations when it comes to more complicated crystallization models. In this section we introduce the method of moments and highlight its properties.

Table 2.1: Popular of moments of a particle length density distribution.

Symbol and Definition	Dimension
$\mu_0(t) = \int_0^{\bar{\ell}} n(\ell, t) d\ell$	$[1/m^3]$
$\mu_1(t) = \int_0^{\bar{\ell}} \ell n(\ell, t) d\ell$	$[m/m^3]$
$\mu_2(t) = \int_0^{\bar{\ell}} \ell^2 n(\ell, t) d\ell$	$[m^2/m^3]$
$\mu_3(t) = \int_0^{\bar{\ell}} \ell^3 n(\ell, t) d\ell$	$[m^3/m^3]$

The moments transformation $M_i : L_2(0, \bar{\ell}) \to \mathbb{R}$ assigns for every positive integer i a number to a distribution $n \in L_2(0, \bar{\ell})$. The i-th moment of the distribution n is given by:

$$\mu_i = M_i(n) = \int_0^{\bar{\ell}} \ell^i n(\ell) \mathrm{d}\ell. \tag{2.20}$$

In case the domain $\mathbb{L}$ represents the length of particles in the distribution, the units of the first four moments $\mu_0, \mu_1, \mu_2, \mu_3$ of the distribution, shown in Table 2.1, have a dimension that has a physical interpretation. This makes the moment transformation particular popular under chemical and process engineers. However, some cautions need to be exerted with interpreting these numbers as physical quantities.

The method of moments has some limitations. Calculation of the moment from a distribution is rather straightforward. However, calculation of a distribution from a given finite number of moments, the inverse problem, is rather involved. Several researchers from various fields have studied this problem in detail. From a mathematical point of view, the inverse problem is known as Hausdorff moment problem [Talenti, 1987] for $L_2(0, 1)$ and as Stieltjes moment problem $L_2(0, \infty)$. In [Talenti, 1987] it has been shown that the Hausdorff moment problem in general is ill-posed, in the sense that the solution does not depend smoothly on the moments. Some results can be obtained, especially when a priori information on the shape of the distribution is taken into account. For narrow distributions reconstruction remains cumbersome [John et al., 2007].

The moment transformation is a popular transformation to deal with the infinite dimensional state space of the population balance equation. Application of the moment transformation is known as the "method of moments", and will be introduced in the remainder of this section.

2.3.1 Method of moments applied to population balance equations

The method of moments can be considered as a special case of a Galerkin projection or the method of weighted residuals. We will make the assumption that there the exists an size $\bar{\ell}$ such that for all $\ell > \bar{\ell}$,$n(\ell, t) = 0$ for all $t \geq 0$, that is we assume that the crystal

remains smaller than $\bar{\ell}$ for all $t \geq 0$. We call n a weak solution of (2.4) with respect to Φ if $n \in L_2$ and (2.21) holds.

$$\langle \frac{\partial n}{\partial t} + \frac{\partial G n}{\partial \ell} - En, \phi \rangle = 0 \quad \text{for all } \phi \in \Phi \tag{2.21}$$

The method of moments considers $\Phi = \text{span}\{\ell^i\}_0^\infty$ and it is easy to see that this is equivalent to:

$$\langle \frac{\partial n}{\partial t} + \frac{\partial G n}{\partial \ell} - En, \ell^i \rangle = 0 \quad \text{for all } i = 0, 1, 2, ... \tag{2.22}$$

Under certain assumptions, which we will state next, an approximation of (2.4) can be obtained from (2.22). After rearrangement, (2.22) can be expressed as follows:

$$\langle \frac{\partial n}{\partial t}, \ell^i \rangle = -\langle \frac{\partial G n}{\partial \ell}, \ell^i \rangle + \langle En, \ell^i \rangle \quad \text{for all } i = 0, 1, 2, ...$$

Depending on the particular characteristics of G and E this can be simplified. Important cases are those in which the growth rate is independent of the size: $G \in \mathbb{R}$, or cases with a growth rate with polynomial dependence on size $G(\ell) = \sum_{k=0}^{K} \gamma_k \ell^k$. In the derivation above, the coefficients γ_k might depend on other variables than ℓ, such as time, concentration or temperature. For those cases it follows that:

$$\langle \frac{\partial n}{\partial t}, \ell^i \rangle = -\sum_{k=0}^{K} \gamma_k \langle \frac{\partial \ell^k n}{\partial \ell}, \ell^i \rangle + \langle En, \ell^i \rangle \quad \text{for all } i = 0, 1, 2, ...$$

Using integration by parts this can be rewritten as:

$$\langle \frac{\partial n}{\partial t}, 1 \rangle = -\sum_{k=0}^{K} \gamma_k ([\ell^k n(\ell, t)]_{\ell=0}^{\ell=\infty} + \langle En, 1 \rangle$$

$$\langle \frac{\partial n}{\partial t}, \ell^i \rangle = -\sum_{k=0}^{K} \gamma_k ([\ell^{i+k} n(\ell, t)]_{\ell=0}^{\ell=\infty} - i\langle n, \ell^{i+k-1} \rangle) + \langle En, \ell^i \rangle \quad \text{for } i = 1, 2, ...$$

With use of the definition of moments, Equation (2.20) and the assumption $n(\ell, t) = 0$ for $\ell > \bar{\ell}$, condition (2.21) can now be expressed as a system of an infinite but countable number of ordinary differential equations in the moments:

$$\frac{\mathrm{d}\mu_0}{\mathrm{d}t} = \gamma_0 n(0, t) + \langle En, 1 \rangle, \tag{2.23a}$$

$$\frac{\mathrm{d}\mu_i}{\mathrm{d}t} = i \sum_{k=0}^{K} \gamma_k \mu_{i+k-1} + \langle En, x^i \rangle. \tag{2.23b}$$

From the system of equations (2.23) it follows that for general growth and breakage relations each moment μ_i depends at least on the moments u_j with $j = i - 1, ..., i + K - 1$. Therefore, in general, the system of equations (2.23) cannot be truncated to a

finite number of differential equations without violating (2.21). This is a fundamental limitation of the method of moments.

For the special case in which there is no particle breakage and the growth rate is linear with the particle length ($E = 0$ and $K \leq 1$) truncation of (2.23) to a finite set of differential equations is possible at an arbitrary order. This property has made the method of moments extremely popular and widely used in crystallization research. After truncation, one obtains a simple model, given by:

$$\frac{\mathrm{d}\mu_0}{\mathrm{d}t} = \gamma_0 n(0,t) \tag{2.24a}$$

$$\frac{\mathrm{d}\mu_i}{\mathrm{d}t} = i(\gamma_0 \mu_{i-1} + \gamma_1 \mu_i) \tag{2.24b}$$

This is generally referred to as the moments model.

2.3.2 Moment model for batch crystallization

The moment transformation can be applied to the reference model, which is given by the Equations (2.15). We will make the following assumptions:

- The growth rate $G(c,T)$ is independent of ℓ,
- The volume fraction of the solid phase is given by

$$V(n) = \int_0^\infty k_v \ell^3 n(\ell) \mathrm{d}\ell.$$

- The nucleation rate can be modeled by the rate equation

$$B(c,T,n) = k_b S_a(c,T)^b V(n).$$

We define the moments $\mu_0, \mu_1, \ldots$ as in Equation (2.20). It follows that $k_v \mu_3 = V(n)$. Therefore, by Equation (2.14) the concentration can be related to μ_3 and satisfies:

$$c(t) = c_0 + \frac{\rho_c}{\rho} k_v \left[\mu_{3,0} - \mu_3(t)\right], \tag{2.25}$$

where c_0 is the initial concentration and $\mu_{3,0}$ is the initial third moment and is given by $\mu_{3,0} = V(n_0)$. The rate of crystallization $R(t)$ satisfies:

$$R(t) = 3\rho_c G(c(t), T(t)) \mu_2(t).$$

By use of the moment transformation, the batch model crystallizer model 2.15 can be transformed to the model:

$$\frac{\mathrm{d}\mu_0}{\mathrm{d}t} = \frac{k_b}{k_v} \rho_c S_a(c,T)^b \mu_3, \tag{2.26a}$$

$$\frac{\mathrm{d}\mu_i}{\mathrm{d}t} = i G(c,T) \mu_{i-1}, \qquad \text{for } i = 1, 2, \ldots \tag{2.26b}$$

$$\frac{\mathrm{d}T}{\mathrm{d}t} = \alpha_j \left[T_j - T\right] + \alpha_0 \left[T_0 - T\right] + \frac{\Delta H}{\rho c_p} 3\rho_c k_v G(c,T) \mu_2. \tag{2.26c}$$

We remark that this model is only representative for the crystallization process when it is operated in a regime where $G(c(t), T(t)) \geq 0$ for all t, that is T_j has to be chosen such that $T_j \in U^G$ as defined by Equation (2.18). This has to be kept in mind when the moment model is used. Moreover, we remark that only the states $\mu_i > 0$ for $i = 0, 1, 2, 3$ are of physical relevance and that this property is inherited from the positivity of the number density function. Since truncation of the moment model at $i = 3$ results in a closed system of equations, it is common to use the moment model with the four states μ_0, μ_1, μ_2 and μ_3.

2.4 Online Measurement Equipment

An important aspect in the development of online optimization and control methods is the availability of measurements of the process variables. Various devices exist to perform measurements in the two thermodynamic phases of crystallization processes. For the online measurement of the concentration of solute in the liquid phase, commercially available solutions exist. These devices can be implemented in an industrial environment. An overview of the sensors that have been tested in this project can be found in [Kadam, 2012]. Determination of the concentration can be done by a refractive index measurement or by measurement of the attenuation spectra of infrared light. Experience has shown that fouling of sensors can cause severe problems. The online measurement of the state of the particle population is more problematic in an industrial environment with current technology. For the measurement of the particle size distribution various devices exist based on different measurement principles. Popular measurement principles exploit the measurement of the attenuation spectra of ultra sound and in situ microscopy in combination with image processing. Also the measurement of reflection patterns by a rotating light beam is possible and used in FBRM (Focused Beam Reflectance Measurement) devices. Potential problems in the online measurement of the particle size that have been identified are:

- Problems with accuracy of the measurements occur when the volume fraction of particles becomes large.
- The measurement devices are in general sensitive to particle shape and need an extensive calibration.
- The measurement of small particles is typically not accurate, unreliable or even impossible.

Especially the last issue is of large importance for modeling, online optimization and control purposes. If measurement devices are insensitive for small particles, it is impossible to accurately determine the instant at which nucleation does take place. The measurement of nucleation will therefore be delayed until particles have grown to a detectable size. This should to be taken into account when kinetic data and nucleation models are identified. The implication for online control is that the feedback path for small particles will contain a uncertain (probably large) delays and that the delay will severely degrade the possibility to correct for the presence small particles by feedback methods.

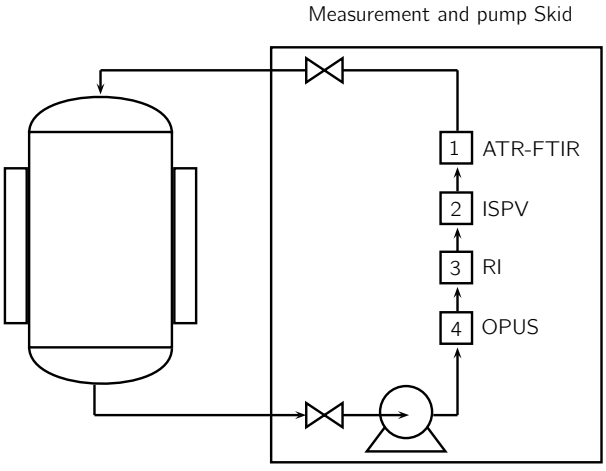

Figure 2.7: Flow diagram skid

2.4.1 Measurement Skid

In the context of the ISPT project a system for online measurements on batch crystallization processes in industrial environments has been developed. The system consists of a temperature controlled circulation line, a circulation pump, a number of commercially available sensors and an electrical cabinet for data processing. The circulation line is connected to the batch crystallizer by use of heat traced hoses. The system provides a means to perform measurements on industrial crystallization processes while it avoids the necessity to perform changes to the process equipment. The latter property makes it suitable for industrial environments, where changes to process equipment imply large costs due to downtime. Moreover, especially in pharmaceutical environments, the changes to processes have large implications for the certification of equipment. A flow diagram of the measurement system is given in Figure 2.7.

The measurement system consists of two parts, called skids. One skid houses the pump system, the second skid houses the sensors and electronics systems for the sensors. The skid contains four sensors, based on different measurement principles:

ATR-FTIR - Bruker Optics (MATRIX-MF) Spectrometer used for the measurement of the concentration of solute in liquid phase. The sensor is based on the ATR-FTIR (Attenuated Total Reflectance - Fourier Transform Infrared) principle.

Refractive index - K-Patents (PR-23-IA) Refractive index sensor, used for concentration measurement of the liquid phase.

Ultrasound diffraction - Sympatec (OPUS) Sensor for crystal size distribution. The measurement is based on the extinction spectrum of ultrasound due to the particle population.

In situ microscope - Perdix Analytical Systems (ISPV) In situ microscope system with flow trough cell and back flash light illumination. In combination with image processing software this sensor forms a means to measure for crystal size distribution.

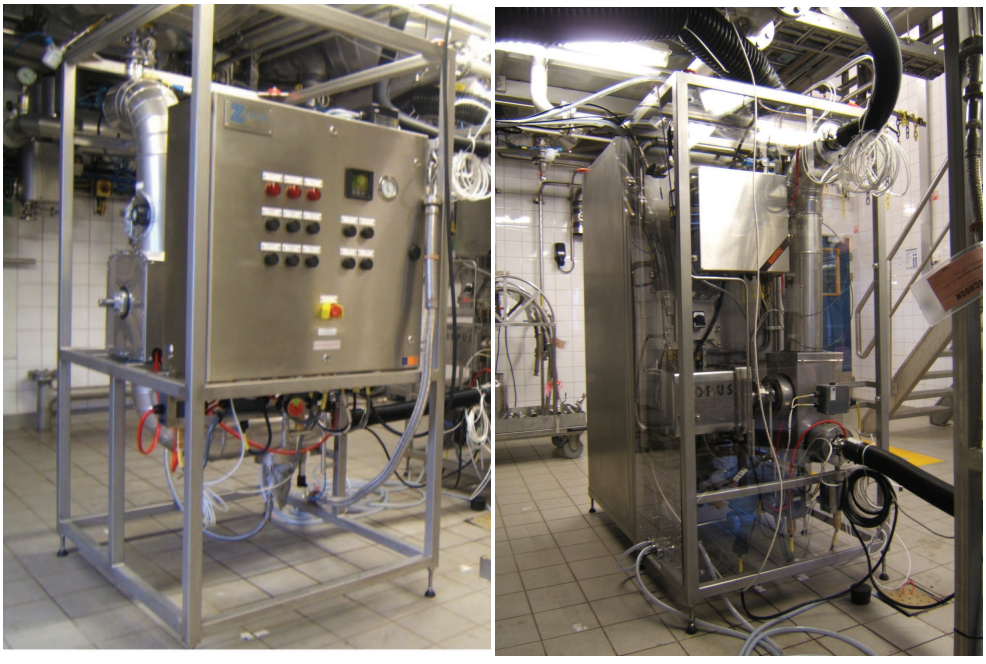

(a) Pump skid (b) Measurement Skid

Figure 2.8: Photograph of measurement skid located at MSD Apeldoorn.

The sensors are mounted in the measurement skid and can be remotely read out via the industrially standardized OPC protocol. The measurement system is certified to operate in explosive environments and is compliant with the (tight) sanitary requirements which are demanded by pharmaceutical industry. A photograph of the measurement system operational at MSD Apeldoorn during the period October till December 2010, is shown in Figure 2.8.

CHAPTER 3

Observability and controllability of crystallization processes

Abstract

In this chapter the controllability and observability of the batch crystallization process will be studied. Observability and controllability are important properties of a model of a process. Controllability indicates to what extent the states of a system can be steered to desired values. Likewise, observability indicates to what extend one can obtain information on the state of a system from available measurements.

In this chapter the analysis of the observability as well as the controllability properties of batch crystallization processes will be presented. We consider the question which sensors need to be installed on a batch crystallization process to obtain sufficient information to predict the future evolution of the state of the process. This question can be answered by analysis of the observability of the process. The controllability of the batch crystallization process is of relevance to steer the states, (for instance the crystal size distribution, temperature or level of supersaturation) of a process to certain desired states in finite time.

First, in Section 3.1 an introduction to the concept observability will be given. We explain how observability can be analyzed and what observability means in the context of batch crystallization processes. Thereafter, the observability of the population balance model given by Equations (2.15) in combination with a concentration sensor and a particle size measurement will be analyzed. Since in crystallization research the moment models

given by Equations (2.26) play a central role, the observability properties of these models will be analyzed separately.

In Section 3.3 an introduction to the concept of controllability will be given. We explain what is needed to analyze controllability and what this means in the context of batch crystallization processes. Thereafter, the controllability of the population balance model for batch crystallization given by the Equations (2.15) will be analyzed. The controllability of the moment models given by Equations (2.26) will be analyzed separately.

The contribution of this chapter is the analysis of the observability and controllability of the batch cooling crystallization process model. We remark that the introduction of the sections on observability and controllability have a fundamental character in which we go back to the definitions of observability and controllability. This introduction is necessary since the process model of batch cooling crystallization is a nonlinear infinite dimensional system, such that well known analysis methods for linear finite dimensional or nonlinear finite dimensional system cannot be applied directly.

3.1 Observability

In this section we provide an introduction to observability. Subsequently, the observability of batch crystallization processes in combination with a concentration sensor and particle size measurement will be presented.

3.1.1 Introduction to observability

Observability is the property that indicates if and to what extent information of the states of a system can be obtained from measurements. This concept is well studied in system theory. For finite dimensional linear systems the concept is classical and well known [Kailath, 1980]. For infinite dimensional linear systems the concept is also well studied and can be found in, for instance, [Curtain and Zwart, 1995]. For finite dimensional non linear systems observability also has been studied and can be found in for instance [Nijmeijer and Van der Schaft, 1990]. Since we deal with a nonlinear and infinite dimensional system, we have chosen to present a definition of the concept of observability that is suitable for this situation and which is compatible with the approaches mentioned above.

Let us consider a system Σ given by:

$$\Sigma : \begin{cases} \dot{x} = f(x, u), \\ y = h(x), \end{cases} \tag{3.1}$$

with $x(t) \in X$, $y(t) \in Y$ and $u(t) \in U$, and X, U and Y Hilbert spaces and $t \in \mathbb{T}$ with $\mathbb{T} = [0, \tau)$ where $\tau > 0$. Moreover, introduce the set of admissible inputs $\mathcal{U} \subset U^{\mathbb{T}}$. We assume that f is sufficiently smooth, in the sense that for every $u \in \mathcal{U}$ and every $x_0 \in X$ the solution $x(t, 0, x_0, u)$ of the differential equation (3.1) with initial condition $x(0) = x_0$ and admissible input u is uniquely defined on the time interval $\mathbb{T}$.

Let $y(t, 0, x_0, u)$ denote the output of system Σ corresponding to the initial condition $x(0) = x_0$ and input u, that is $y(t, 0, x_0, t) = h(x(t, 0, x_0, t))$. Moreover we introduce the concept of a *system map* for the system Σ.

Definition 3.1.1 (System map)
The system map of the system Σ on $\mathbb{T}$ is the map $\mathcal{G}^\tau : X \times \mathcal{U} \to \mathcal{Y}$,defined by

$$[\mathcal{G}^\tau(x_0, u)](t) := y(t, 0, x_0, u) \quad \text{for } t \in \mathbb{T}$$

where both $\mathcal{U}$ and $\mathcal{Y}$ are subsets of L_2, i.e. $\mathcal{U} \subset L_2(\mathbb{T}, U)$ and $\mathcal{Y} \subset L_2(\mathbb{T}, Y)$.

We introduce the concept of a *distinguishable pair of states* as follows.

Definition 3.1.2 (Distinguishable pair of states)
Two states $x_1, x_2 \in X$ are said to be distinguishable for (3.1) *on $\mathbb{T}$, if for every admissible input function $u \in \mathcal{U}$ the mappings $t \mapsto y(t, 0, x_1, u)$ and $t \mapsto y(t, 0, x_2, u)$, for $t \in [0, \tau]$ corresponding to initial condition $x(0) = x_1$ resp. $x(0) = x_2$ are not identical on their common domain of definition, i.e.*

$$\mathcal{G}^\tau(u, x_1) \neq \mathcal{G}^\tau(u, x_2) \quad \text{for all } u \in \mathcal{U}.$$

We are now in the position to make precise what observability is and introduce the definitions for two types of observability:

Definition 3.1.3 (Approximately observable)
The system Σ is called approximately observable on $[0, \tau]$ (for some finite $\tau > 0$) if knowledge of the input in $\mathcal{U}$ and output in $\mathcal{Y}$ determines the initial state uniquely.

Definition 3.1.4 (Exactly observable)
The system Σ is called exactly observable on $[0, \tau]$ (for some finite $\tau > 0$) if the initial state can be uniquely and continuously constructed from the knowledge of the input in $L_2(\mathbb{T}, U)$ and the output in $L_2(\mathbb{T}, Y)$.

We make the following observations.
Remark 3.1.1. Approximate observability and exact observability is also defined for autonomous systems.
Remark 3.1.2. Note that *exact observability* implies *approximate observability* but that the converse is not true.
Remark 3.1.3. Approximate observability of a system on the interval $[0, \tau]$, implies approximate observability of the system on the interval $[0, \tau']$ for $\tau' \geq \tau$.
Remark 3.1.4. The notion of "approximate" observability is common in literature. However the indication "approximate" is not self explanatory here and is due to the duality relationship between observability and controllability. In the context of controllability the notion "approximate controllability" is more appropriate, see for instance [Curtain and Zwart, 1995, Definition 4.1.3].

The following theorem shows the relation between the existence of indistinguishable states of a system and approximate observability.

Theorem 3.1.1
The following two statements are equivalent:

1. *Every pair of states $x_1 \in X$, $x_2 \in X$ with $x_1 \neq x_2$, is a distinguishable pair of states for system* (3.1) *on* $\mathbb{T}$.
2. *The system* Σ *is approximately observable.*

Proof.
$(1 \Rightarrow 2)$ Let every pair of states $x_1 \in X$ and $x_2 \in X$ is a distinguishable pair of states for system (3.1) on $\mathbb{T}$ and assume that the system Σ is *not* approximately observable. Since every pair x_1, x_2 is distinguishable, for a given pair (u, y) with $y = G^\tau(u, x_1)$ there does not an x_2 such that $y = G^\tau(u, x_2)$ which implies that (u, y) yields x_1. This contradicts with the assumption, therefore the system is approximately observable.
$(1 \Leftarrow 2)$ Let the system Σ be approximately observable and assume there exist a pair of states $x_1 \in X$ and $x_2 \in X$ that is *indistinguishable*. The assumption implies that there exist indistinguishable pairs $x_1 \neq x_2$ and an input signal $u \in \mathcal{U}$ such that $y_1 = \mathcal{G}^\tau(u, x_1) = \mathcal{G}^\tau(u, x_2) = y_2$ for all $\tau \in \mathbb{T}$. This contradicts with approximate observability since given an input $u \in \mathcal{U}$, approximate observability implies that two pairs (u, y_1) and (u, y_2) with $y_1 = y_2$ yield $x_1 = x_2$. □

From the definition of an observable system it now follows why observability is an important property. In an observable system the possibility that the evolution of two distinct initial states x_1 and x_2 in combination with an input signal u generate one and exactly the same measurement is excluded.

We have the following theorem for falsification of exact observability and approximate observability from the system map $\mathcal{G}^\tau(u, x_0)$.

Theorem 3.1.2
The system Σ *is neither exactly observable or approximately observable on* $[0, \tau]$ *if there exists a pair of not identical initial states* $x_1, x_2 \in X$, *i.e.* $x_1 \neq x_2$ *which is not distinguishable for* $t \in [0, \tau]$.

Proof. The proof follows immediately from the definition. □

Analogously to the definition of approximate and exact observability, we introduce the notion of approximate observability on a set and exact observability on a set.

Definition 3.1.5 (Approximately observable on a set $X_0 \subset X$)
Let $X_0 \subset X$. *The system* Σ *is called approximately observable* X_0 *on* $[0, \tau]$ *(for some finite* $\tau > 0$*) if knowledge of the input in* $\mathcal{U}$ *and output in* $\mathcal{Y}$ *determines the initial state* $x_0 \in X_0$ *uniquely.*

Definition 3.1.6 (Exactly observable on a set $X_0 \subset X$)
Let $X_0 \subset X$. *The system* Σ *is called exactly observable on* $[0, \tau]$ *(for some finite* $\tau > 0$*) if the initial state* $x_0 \in X_0$ *uniquely can be uniquely and continuously constructed from the knowledge of the input in* $L_2(\mathbb{T}, U)$ *and the output in* $L_2(\mathbb{T}, Y)$.

For finite dimensional nonlinear systems and infinite dimensional linear systems results exist to characterize observability in more detail. We will introduce the most important results for both classes. For linear infinite dimensional systems, we have the following

situation. Consider a linear infinite dimensional system Σ_{lin},

$$\Sigma_{lin} : \begin{cases} \dot{x} = Ax + Bu, \\ y = Cx, \end{cases}$$

where the linear operator $A : D(A) \to X$, $D(A) \subset X$, is the infinitesimal generator of semigroup operator $T(t) : X \to X$ for $t \in \mathbb{T}$

For the system Σ_{lin} we introduce the observability map, as done in [Curtain and Zwart, 1995]:

Definition 3.1.7 (Observability map for linear systems)
The observability map of the system Σ_{lin} on $[0, \tau]$, is the bounded linear map $\mathcal{C}^\tau : X \to L_2([0, \tau]; Y)$ defined by $\mathcal{C}^\tau x = CT(\cdot)x$.

Moreover we introduce the controllability map for the system Σ_{lin}:

Definition 3.1.8 (Controllability map for linear systems)
The controllability map of the system Σ_{lin} on $[0, \tau]$, is the bounded linear map $\mathcal{B}^\tau : L_2([0, \tau]; U) \to X$ defined by $\mathcal{B}^\tau u = \int_0^\tau T(\tau - s)Bu(s)\mathrm{d}s$.

Note that for linear systems $\mathcal{C}^\tau x = \mathcal{G}^\tau(0, x)$ and $C\mathcal{B}^\tau u = \mathcal{G}^\tau(u, 0)$, such that the system map of the system Σ_{lin} is given by $\mathcal{G}^\tau(x_0, u) = \mathcal{C}^\tau x_0 + C\mathcal{B}^\tau u$. Due to linearity it follows that observability only depends on properties of $\mathcal{C}^\tau x_0$. Exact and approximate observability for the linear system can be characterized by the following lemma, which is shown in [Curtain and Zwart, 1995, Corollary 4.1.14].

Lemma 3.1.3
For the linear system Σ_{lin}, we have the following necessary and sufficient condition:

(a) The system is approximately observable on $[0, \tau]$ if and only if $\ker \mathcal{C}^\tau = \{0\}$, i.e. $CT(t)z = 0$ on $t \in [0, \tau]$ implies $z = 0$.
(b) The system is exactly observable on $[0, \tau]$ if and only if $\ker \mathcal{C}^\tau = \{0\}$ and $\mathcal{C}^\tau$ has closed range.

For finite dimensional nonlinear systems we are in a different situation. Consistent with the definition of local observability in [Nijmeijer and Van der Schaft, 1990] we introduce the following definition for local observability of the system Σ.

Definition 3.1.9 (Locally observable at x_1)
The system Σ is called locally observable at x_1 on $\mathbb{T}$ (for some finite $\tau > 0$) if there exists a neighborhood W of x_1 such that for every neighborhood $V \subset W$ and for all states $x_2 \in V$, we have that

$$\mathcal{G}^\tau(u, x_1) = \mathcal{G}^\tau(u, x_2) \quad \text{for every } u \in \mathcal{U} \text{ implies } x_1 = x_2.$$

Definition 3.1.10
The system Σ is called locally observable if the system Σ is called locally observable for every $x_1 \in X$.

We remark that (global) approximate observability implies local approximate observability, but that the converse is not true.

We will now discuss observability for nonlinear finite dimensional systems and a sufficient condition to characterize local observability in more detail. Consider finite dimensional nonlinear systems of the form:

$$\Sigma_{nlin} : \begin{cases} \dot{x} = f(x) + \sum_{j=1}^{k} g_j(x)u_j, \\ y_i = h_i(x), \end{cases} \tag{3.2}$$

with $x(t) \in M$, with $M \subset \mathbb{R}^n$, $U \subset \mathbb{R}^m$ $Y \subset \mathbb{R}^p$ for $n, p, q < \infty$ and $i \in \{1, ..., p\}$. For systems of the form (3.2) the following characterization of local observability is known. First we introduce the concept of a observation space. We will use the notion of a Lie-derivative, which is introduced in the Appendix A.1.

Definition 3.1.11 (Observation space [Nijmeijer and Van der Schaft, 1990])
The observation space $\mathcal{O}$ of system (3.2) *is the linear space of functions defined on M containing $h_1, .., h_p$ and all repeated Lie-derivatives $L_{X_1}L_{X_2}...L_{X_k}h_i$ with $i \in \{1, ..., p\}$ and X_j for $j \in \{1, ..., k\}$ in the set $\{f, g_1, ..g_m\}$.*

Then we introduce the concept of the observability co-distribution by the following definition:

Definition 3.1.12 (Observability co-distribution [Nijmeijer and Van der Schaft, 1990])
Let the observability co-distribution, denoted by $d\mathcal{O}$ be defined as follows by:

$$d\mathcal{O}(x_0) = span\{dH(x_0) | H \in \mathcal{O}\}. \tag{3.3}$$

Here $dH(x_0)$ denotes the differential of H at x_0.

The following theorem can be used to test if a system is locally observable at a certain state $x_0 \in M$.

Theorem 3.1.4 (Local observability for finite dimensional systems
[Nijmeijer and Van der Schaft, 1990])
Consider the system (3.2) *with $dim(M) = n$. Assume that $dim(d\mathcal{O}(x_0)) = n$. Then the system is locally observable at x_0.*

Proof. For the proof we refer to [Nijmeijer and Van der Schaft, 1990]. □

Corollary 3.1.5
The system (3.2) *is locally observable if the system is locally observable for any $x_0 \in M$.*

Theorem 3.1.4 can be used to test local observability, by calculation of the dimension of the span of a subset of the Lie-derivatives at point x_0. We remark that the observation space $\mathcal{O}$ contains all repeated Lie-derivatives. Therefore it depends from case to case if one can successfully analyze the local observability of the system with this theorem by calculation of a finite number of Lie-derivatives.

In the next section we will use the previously defined concepts of observability to analyze the batch cooling crystallization process.

3.2 Observability of a batch cooling crystallization process

In this section we will analyze the observability of the batch crystallization process as introduced in Chapter 2. It is important to analyze the observability of a process since by such an analysis it becomes apparent to which extent is it possible to infer information on the state of a process from measurements with a given sensor.

Since observability depends on the availability of the sensors in the process, we will discuss two different configurations. We will analyze observability of a process modeled by the population balance model (2.15) in presence of a concentration sensor in Section 3.2.1 and in the presence of a population sensor in Section 3.2.2. In Section 3.2.2 we will analyze the observability of the moment model in presence of a concentration sensor.

The analysis of the observability properties of the model of the batch crystallization process has been carried out on an model in which mechanisms of secondary significance have been neglected. This has been done to avoid an unnecessary complicated analysis and to keep the problem tractable. In our analysis we will assume that the crystallization enthalpy and the heat exchange with the environment are negligibly small. That is, we set $\Delta H = 0$ and $\alpha_0 = 0$ in Equation (2.15). Moreover we will assume that the level of secondary nucleation is small and we set $B(c, T, n) = 0$. To summarize, we assume that the process is modeled by a population balance model, such as is given by Equation (2.15). That is,

$$\frac{\partial n}{\partial t} = -\frac{\partial G(c,T)n}{\partial \ell}, \tag{3.4a}$$

$$\frac{\mathrm{d}T}{\mathrm{d}t} = \alpha(T_j - T), \tag{3.4b}$$

with boundary condition $n(0,t) = 0$ and initial condition $n(\ell, 0) = n_0(\ell)$ and where n is the population balance, T is the reactor temperature, T_j is the jacket temperature. The operator growth rate G is assumed to be size independent and to be dependent on concentration and temperature $G := G(c,T)$. In the analysis we only consider operation in regimes $G > 0$ so that the population balance equation (3.4) remains well defined for all $t \geq 0$. As described in Section 2.2.4, the concentration and mass of the particles in the solid phase are related via the algebraic equation (2.6), which is due to the mass conservation. For simplicity, in this section it will be assumed that $\frac{\rho_c}{\rho} = 1$, such, the concentration can be expressed as function of the population balance. By use of equation (2.14), one obtains:

$$c(t) = c_0 - V(n - n_0)(t) = c_0 + V(n_0) - [V(n)](t), \tag{3.5}$$

where c_0 is the initial concentration, $n_0(\cdot) = n(\cdot, 0)$ is the population balance at time $t = 0$ and $n(\ell, t)$ is the population balance at time t, and $V(\cdot)$ the volume function defined in Equation (2.2).

In this section we assume that the volume of the particles in the population $n(\ell, t)$ can be calculated from linear combinations of the first k moments of the population $n(\ell, t)$,

i.e. $v(\ell) = \sum_{i=0}^{k} v_i \ell^i$ where $v_i \in \mathbb{R}$ are arbitrary coefficients. With $n \in L_2(\mathbb{L} \times \mathbb{T}, \mathbb{R})$, the total volume of particles at time t per volumetric unit of liquid is given by

$$[V(n)](t) = \int_0^\infty \sum_{i=0}^{k} v_i \ell^i n(\ell, t) \mathrm{d}\ell, \tag{3.6}$$

as described in Section 2.2.

3.2.1 Observability of population balance model from concentration measurements

In this section we consider a batch crystallizer, equipped with a concentration measurement $c(t)$ and temperature measurement $T(t)$. That is, we equip the model with the following output equation:

$$y(t) = C_{sens}\left(\begin{bmatrix} n(\cdot, t) \\ T(t) \end{bmatrix}\right) = \begin{bmatrix} c_0 + V(n_0) - V(n)(t) \\ T(t) \end{bmatrix}. \tag{3.7}$$

Since the model is nonlinear and infinite dimensional, the usual technique for studying observability does not apply. Therefore we follow a different path. We first simplify the problem setting to the linear convection equation and analyze this setting. Then we use the results from the linear convection equation to obtain results on the observability of the model (3.4) given by Equations (3.4), (3.7).

Observability of a linear advection problem

Consider the following system:

$$\frac{\partial n}{\partial t} = An = -\frac{\partial n}{\partial \ell}, \tag{3.8a}$$

$$y(t) = Cn(\cdot, t) := \int_0^\infty \ell^k n(\ell, t) \mathrm{d}\ell, \tag{3.8b}$$

with boundary condition $n(0, t) = 0$, initial condition $n(\ell, 0) = n_0(\ell)$, $n(\cdot, t) \in L_2(0, \infty)$ and the operator as defined in (3.8b) with k a positive integer. In this section we will study approximate observability of the system given by Equations (3.8).

The operator A is the infinitesimal generator of the left-shift semigroup $\mathcal{T}(t)$, with:

$$[\mathcal{T}(t)n](\ell) = \begin{cases} n(\ell - t) & \text{if } \ell - t > 0 \\ 0 & else \end{cases} \tag{3.9}$$

The system under consideration is a linear infinite dimensional system. Therefore, we can use Theorem 3.1.3 to study if the system is approximately observable.

Theorem 3.2.1
Consider the system defined by Equations (3.8) *and let* $\mathcal{C}^\tau n = C\mathcal{T}(\cdot)n$ *be the observability map associated with* (3.8)*, where* $\mathcal{T}(\cdot)$ *is the semigroup defined in* (3.9)*. The kernel of the observability map is given by:*

$$\ker \mathcal{C}^\tau = \left\{ n \in L_2(0,\infty) | \int_0^\infty \ell^i n(\ell) \mathrm{d}\ell = 0 \quad \textit{for } i = \{0,1,2,...,k\} \right\}, \tag{3.10}$$

and the system is not approximately observable.

The proof of this theorem is based on a simple observation that relates time responses with moments of the initial condition. Before we proceed with the proof, we introduce the following lemma:

Lemma 3.2.2
Let $f \in L_2(0,\infty)$ *and let* $k \in \mathbb{N}$ *an positive integer. Then*

$$\int_t^\infty \ell^k f(\ell - t) \mathrm{d}\ell = 0 \quad \textit{for all } t \geq 0 \tag{3.11}$$

if and only if

$$\int_0^\infty \ell^i f(\ell) \mathrm{d}\ell = 0 \quad \textit{for } i \in \{0,...,k\}. \tag{3.12}$$

Proof. Introduce the coordinate change $\sigma = \ell - t$ to Equation (3.11). With use of the Binomial theorem of Newton it follows that:

$$\int_t^\infty \ell^k f(\ell - t) \mathrm{d}\ell = \int_0^\infty (\sigma + t)^k f(\sigma) \mathrm{d}\sigma = \sum_{i=0}^{k} \binom{k}{i} t^{k-i} \int_0^\infty \sigma^i f(\sigma) \mathrm{d}\sigma.$$

This is a k-th order polynomial in t with coefficients defined by $\int_0^\infty \sigma^i f(\sigma) \mathrm{d}\sigma$, from which the assertion follows. □

Proof of Theorem 3.2.1. First we will calculate the kernel of the observability map $\mathcal{C}^\tau n_0$ of the system. The map $\mathcal{C}^\tau n_0$ is given by $\mathcal{C}^\tau n_0 = C\mathcal{T}(\cdot)n_0$ with

$$C\mathcal{T}(t)n_0 = \int_0^\infty \ell^k (\mathcal{T}(t)n_0)(\ell) \mathrm{d}\ell. \tag{3.13}$$

With use of the explicit representation of the semigroup $\mathcal{T}(\cdot)$, c.f. (3.9) this can be rewritten as:

$$C\mathcal{T}(t)n_0 = \int_t^\infty \ell^k n_0(\ell - t) \mathrm{d}\ell \quad . \tag{3.14}$$

It now follows from Lemma 3.2.2 that $\mathcal{C}^\tau n_0 = 0$ if and only if the moments $\alpha_i = \int_0^\infty \ell^i n_0(\ell) \mathrm{d}\ell$ are zero for $i = \{0,...,k\}$. Since, there always exists an $n_0 \neq 0$, with $\alpha_i = 0$ for $i = \{0,...,k\}$, we conclude by lemma 3.1.3 (b), that the system is not approximately observable on $[0,\tau]$. Remark that this result is independent of τ. Hence, the system is not approximately observable for any $\tau > 0$.

□

Remark 3.2.1. The result of Theorem 3.2.1 admits a straightforward generalization if the measurement (3.8b) is replaced by a measurement of the form:

$$y(t) = C_{ext1} n(\cdot, t) = \begin{bmatrix} \int_0^\infty \ell^k n(\ell, t) \mathrm{d}\ell \\ \int_0^\infty \ell^{k-1} n(\ell, t) \mathrm{d}\ell \\ \vdots \\ \int_0^\infty \ell^0 n(\ell, t) \mathrm{d}\ell \end{bmatrix} \tag{3.15}$$

that contain multiple measurements up to order k. We claim that the system (3.8) with measurement (3.15) is not approximately observable as the kernel of $\mathcal{C}^\tau_{ext1} n_0 := C_{ext1} \mathcal{T}(\cdot) n_0$ equals the right hand side of (3.10), i.e. $\ker \mathcal{C}^\tau_{ext1} = \ker \mathcal{C}^\tau$.

The results can also be generalized to more general measurement functions of the form:

$$y(t) = C_{ext2} n(\cdot, t) := \int_0^\infty \sum_{i=1}^{k} v_i \ell^i n(\ell, t) \mathrm{d}\ell. \tag{3.16}$$

with coefficients $v_i \in \mathbb{R}$. That is, the system (3.8) with measurement (3.16) is not approximately observable. This results from linearity of C_{ext2}.

For population balance models, Theorem 3.2.1 has the following consequence. Suppose we consider the system (3.8) with the measurements (3.8b) with (or equivalently (3.15) or (3.16)) and with two initial distributions $n_1(\ell) \in L_2(\mathbb{L}))$ and $n_2(\ell) \in L_2(\mathbb{L}))$ such that the first k moments are equal. That is $\int_0^\infty \ell^i n_1(\ell) \mathrm{d}\ell = \int_0^\infty \ell^i n_2(\ell) \mathrm{d}\ell$ for $i = 0, ..., k$. Then the measurements due to evolution of n_1 are equal to measurements due to evolution of n_2. Therefore the initial conditions n_1 and n_2 are indistinguishable in the measurements of the system.

This can be seen as follows. Let $\Delta n(\ell) = n_2(\ell) - n_1(\ell)$, then the first k moments $\int_0^\infty \ell^k \Delta n(\ell) \mathrm{d}\ell$ are equal to 0 The outputs (due to the evolution of initial distribution $n_1(\ell)$ resp. $n_2(\ell)$) are equal, i.e.:

$$y_2(t) = \int_t^\infty \ell^k n_2(\ell - t) \mathrm{d}\ell = \int_t^\infty \ell^k (n_1(\ell - t) + \Delta n(\ell - t)) \mathrm{d}\ell = y_1(t)$$

since $\Delta n(\ell - t)$ has been constructed such that:

$$\int_t^\infty \ell^k \Delta n(\ell - t) \mathrm{d}\ell = 0 \quad \text{for all } t \in [0, \infty).$$

Therefore, one cannot conclude from an measured output $y(t)$ whether that output is due to initial condition $n_1(\ell)$ or $n_2(\ell)$.

Conversely, it follows from Theorem 3.2.1 that if the two distributions $n_1(\ell) \in L_2(\mathbb{L})$ and $n_2(\ell) \in L_2(\mathbb{L})$ such that one of their first k moments are not equal, then the measurements due to evolution of n_1 are not equal to measurements due to evolution of n_2. Therefore one can infer from the measurement y_1 and y_2 what values of the first k moments of the distributions n_1 and n_2 are.

Remark 3.2.2. Please note that due to linearity of the measurement equation the analysis of observability in principle focuses on the observability of the *difference* between

two distributions and as such the focus is on the contribution of this *difference in the distributions* in the measurement signals. Therefore, as a result of the linearity of the measurement with respect to the distributions it is sufficient to analyze the distinguishably of the measurement of the distribution difference from the zero distribution. Remark that the difference between distributions can be a distribution with *negative* values.

One might wonder how for this system indistinguishable distributions look like. We will show that it is possible to construct indistinguishable distributions. In Appendix B.1 we present Theorem B.1.1, which enables us to construct indistinguishable distributions. As an example, we will construct two indistinguishable functions $n_1(\ell)$ and $n_2(\ell)$. We set $n_1(\ell) = 0$, such that the difference is given by $\Delta n(\ell) = n_1(\ell) - n_2(\ell) = -n_2(\ell)$. We construct Δn such that the first k moments are zero with use of Theorem B.1.1. We choose the parameters $k = 3$, $n_2(0) = 0$, $\alpha_1, ...\alpha_5 = 0$ and $\alpha_6 = \frac{1}{24}$, and obtain the distribution $n_2(\ell)$ that is indistinguishable from $n_1(\ell) = 0$, shown in Figure 3.1.

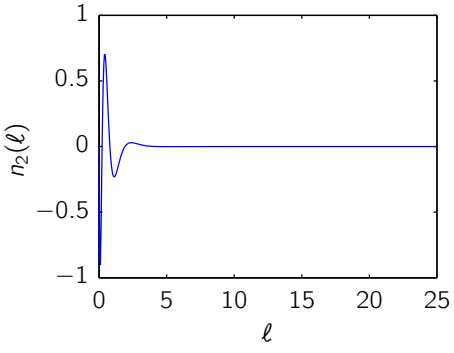

Figure 3.1: The function $n_2(\ell)$ that is indistinguishable from $n_1(\ell) = 0$ by either the measurements (3.8b), (3.15) or (3.16) on the system (3.8), constructed by use of Theorem B.1.1 with parameters $k = 3$, $n_2(0) = 0$, $\alpha_1, ...\alpha_5 = 0$ and $\alpha_6 = \frac{1}{24}$.

Remark 3.2.3. It is important to note that the first moment of the difference between *indistinguishable* distributions is zero. Therefore, an distribution $n_2(\ell)$ indistinguishable $n_1(\ell) = 0$ either is identical to zero or $n(\ell)$ is positive for some ℓ as well as negative for some ℓ. Negative values of $n(\ell)$ have no physical interpretation, and one might argue that this type of distributions are not relevant for crystallization processes. We argue that for the observability problem they do have relevance since we are concerned with *differences* in distributions.

We will now proceed with the analysis of the observability properties of the batch crystallization process with concentration sensor.

Observability for the batch crystallization process

We study the observability of the population balance model (3.4) in which a concentration sensor and temperature sensor are used, such as given by Equations (3.7).

Contrary to the linear advection equation, explicit solutions to the system of equations

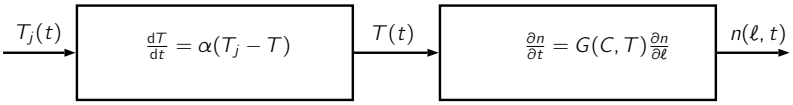

Figure 3.2: Illustration of model (2.15) as cascade of two subsystems systems.

are not known, which complicates the analysis. In order to prove that the system is not approximatly observable, we apply Theorem 3.1.2 and we show the existence for a pair of two initial conditions that generate identical output signals. We state the main result of this section as follows:

Theorem 3.2.3
Consider the system (3.4) *with the measurement* (3.7) *and the volume function* $V(n)$ *as defined by equation* (3.6). *The system is not approximately observable. Moreover, let* $[n_1(\ell,t), T_1(t)]$ *and* $[n_2(\ell,t), T_2(t)]$ *be the solutions to system* (3.4) *with initial conditions* $[n_{0,1}(\ell), T_{0,1}]$ *resp.* $[n_{0,2}(\ell), T_{0,2}]$, *with* $T_{0,1} = T_{0,2}$ *and an input signal* $T_j \in U^G$. *Let* $\mathcal{G}^\tau : L_2(\ell) \times \mathbb{R} \to \mathbb{R}^2$ *denote the system map, as defined in definition 3.1.1 and let the measurements* y_1, y_2 *be defined as* $y_1 = \mathcal{G}^\tau(n_{0,1}, T_{0,1}, T_j)$ *and* $y_2(t) = \mathcal{G}^\tau(n_{0,2}, T_{0,2}, T_j)$. *If the first* k *moments of* $n_{0,1}(\ell)$ *and* $n_{0,2}(\ell)$ *are equal, i.e.* $\int_t^\infty \ell^i n_{0,1}(\ell)\mathrm{d}\ell = \int_t^\infty \ell^i n_{0,2}(\ell)\mathrm{d}\ell$ *for* $k = 1, ..., k$, *then the measurements* $y_1(t)$ *and* $y_2(t)$ *are equal for all* $t \in \mathbb{T}$.

Since the system under consideration is non-linear, we are not able to define a linear semigroup operator and we are not able to define the observability map of the system as in definition 3.1.7. Therefore, we will follow a different approach.

We will prove the theorem later in this section. First we introduce some lemmas, which enable us to analyze solutions of the system (3.4). First we observe that the system consists of a cascade of two systems, i.e. the evolution of the state n is influenced by the state T, but the evolution of T is not influenced by the state n. This is represented in Figure 3.2.

Observe that, for a given solution $[n(\ell,t), T(t)]$ to the Equations (3.4), we can calculate the trajectories of c and G a-posteriori, i.e. we can evaluate $V(n(\cdot,t))$ and $G(c(t), T(t))$ along the solution. We define the function $\Gamma : \mathbb{T} \to \mathbb{R}$ and $\Lambda : \mathbb{T} \to \mathbb{R}$ as follows:

$$\Gamma(t) := G(c(t), T(t)) = G(c_0 + V(n_{0,i}) - [V(n)](t), T(t)) \tag{3.17}$$

$$\Lambda(t) := V(n(\cdot,t)) = \int_0^\infty \sum_{i=0}^{k} v_i \ell^i n(\ell,t)\mathrm{d}\ell \tag{3.18}$$

It follows that the function $\Gamma(t)$ defines the solution to the Equations (3.4) in terms of a parametrization of the initial condition. This becomes more apparent in the following lemma:

Lemma 3.2.4
Consider the time variant system:

$$\frac{\partial n}{\partial t} = -\frac{\partial \Gamma(t) n}{\partial \ell}, \tag{3.19}$$

with $t \in [0, \tau]$, $n(0,t) = 0$, $n(\cdot, 0) = n_0(\cdot) \in L_2(0, \infty)$, $\Gamma(t) \in L_2(\mathbb{T}; \mathbb{R})$ *and* $w(t) := \int_0^t \Gamma(\tau) \mathrm{d}\tau > 0$ *for all* t. *The solution to Equation* (3.19) *is given by* $n(\ell, t)$*:*

$$n(\ell, t) = \begin{cases} n_0(\ell - w(t)) & \text{if } w(t) \leq \ell \\ 0 & \text{else.} \end{cases}$$

Proof. We show that $n(\ell, t)$ satisfies (3.19). Therefore, we calculate the derivatives of n with respect to t and ℓ:

$$\frac{\partial n}{\partial \ell} = \frac{\partial n_0(\ell - w(t))}{\partial \ell} = \frac{\partial n_0(\ell)}{\partial \ell}$$

and

$$\frac{\partial n}{\partial t} = \frac{\partial n_0(\ell - w(t))}{\partial t} = -\frac{\partial w(t)}{\partial t}\frac{\partial n_0}{\partial \ell} = -\Gamma(t)\frac{\partial n_0}{\partial \ell},$$

Therefore:

$$\frac{\partial n}{\partial t} = -\Gamma(t)\frac{\partial n_0}{\partial \ell} = -\Gamma(t)\frac{\partial n}{\partial \ell} = -\frac{\partial \Gamma(t) n}{\partial \ell},$$

which is (3.19). We conclude $n(\ell, t)$ satisfies (3.19). □

We will now show that for a given initial condition $n_0(\ell)$, the trajectory $\Gamma(t)$ defined by Equation (3.17), satisfies a non-homogeneous ordinary differential equation, which can be parametrized by $n_0(\ell)$ and $\frac{\partial T}{\partial t}$.

Theorem 3.2.5

Consider the system (3.4) *and let* $\Gamma(t)$ *be defined by* (3.17). *For given initial condition* n_0, c_0, T_0*, and input* T_j*, and boundary condition* $n(0,t) = 0$, $\Gamma(t)$ *satisfies the equation:*

$$\begin{pmatrix} \dot{\Gamma}(t) \\ \dot{w}(t) \end{pmatrix} = \begin{pmatrix} -\frac{\partial G}{\partial c}\Gamma(t) \sum_{i=1}^{k} \sum_{j=0}^{i-1} i v_i \binom{i-1}{j} w(t)^{i-j-1} \int_0^\infty \sigma^j n_0(\sigma) \mathrm{d}\sigma + \frac{\partial G}{\partial T}\frac{\partial T}{\partial t} \\ \Gamma(t) \end{pmatrix}. \quad (3.20)$$

with $w(0) = 0$ *and* $\Gamma(0) = G(c_0, T_0)$.

Proof. Differentiate $\Gamma(t)$ defined by (3.17) with respect to t.

$$\dot{\Gamma} = \frac{\partial G}{\partial c}\frac{\partial c}{\partial t} + \frac{\partial G}{\partial T}\frac{\partial T}{\partial t}$$

Differentiate (3.5) to obtain $\frac{\partial c}{\partial t} = -\frac{\partial V(n)}{\partial t}$ and substitute this:

$$\dot{\Gamma} = -\frac{\partial G}{\partial c}\frac{\partial V(n)}{\partial t} + \frac{\partial G}{\partial T}\frac{\partial T}{\partial t}$$

Then substitute $V(n) = \int_0^\infty \sum_{i=0}^{k} v_i \ell^i n(\ell, t) \mathrm{d}\ell$

$$\dot{\Gamma} = -\frac{\partial G}{\partial c}\int_0^\infty \sum_{i=0}^{k} v_i \ell^i \frac{\partial}{\partial t} n(\ell, t) \mathrm{d}\ell + \frac{\partial G}{\partial T}\frac{\partial T}{\partial t}$$

Use that $n(\ell, t)$ satisfies Equation (3.4) to derive:

$$\dot{\Gamma} = \frac{\partial G}{\partial c} \int_0^\infty \sum_{i=0}^{k} v_i \ell^i \Gamma(t) \frac{\partial n}{\partial \ell} \mathrm{d}\ell + \frac{\partial G}{\partial T} \frac{\partial T}{\partial t}$$

Using integration by parts the equation can be rewritten to:

$$\dot{\Gamma} = \frac{\partial G}{\partial c} \Gamma(t) \sum_{i=0}^{k} v_i \left([\ell^i n(\ell, t)]_0^\infty - \int_0^\infty i\ell^{i-1} n(\ell, t) \mathrm{d}\ell \right) + \frac{\partial G}{\partial T} \frac{\partial T}{\partial t},$$

which can be rearranged to:

$$\dot{\Gamma} = \frac{\partial G}{\partial c} \Gamma(t) \left(v_0 \left[n(\infty, t) - n(0, t) \right] - \sum_{i=1}^{k} i v_i \int_{w(t)}^\infty \ell^{i-1} n_0(\ell - w(t)) \mathrm{d}\ell \right) + \frac{\partial G}{\partial T} \frac{\partial T}{\partial t}.$$

Introduce the coordinate change $\sigma = \ell - w(t)$ to obtain:

$$\dot{\Gamma} = \frac{\partial G}{\partial c} \Gamma(t) \left(v_0 \left[n(\infty, t) - n(0, t) \right] - \sum_{i=1}^{k} i v_i \int_0^\infty (\sigma + w(t))^{i-1} n_0(\sigma) \mathrm{d}\sigma \right) + \frac{\partial G}{\partial T} \frac{\partial T}{\partial t}.$$

With use of the Binomial theorem of Newton it follows that $(\sigma + w(t))^{i-1} = \sum_{j=0}^{i-1} \binom{i-1}{j} w(t)^{i-j-1} \sigma^j$, such that:

$$\dot{\Gamma} = - \frac{\partial G}{\partial c} \Gamma(t) \sum_{i=1}^{k} \sum_{j=0}^{i-1} i v_i \binom{i-1}{j} w(t)^{i-j-1} \int_0^\infty \sigma^j n_0(\sigma) \mathrm{d}\sigma + \frac{\partial G}{\partial T} \frac{\partial T}{\partial t}.$$

□

We introduce the following theorem, which considers the non-uniqueness of a growth trajectory $\Gamma(t)$.

Theorem 3.2.6
Let $[n_1(\ell, t), T(t)]$ and $[n_2(\ell, t), T(t)]$ be the solutions to system (3.4) with initial conditions $n_{0,1}(\ell)$ resp. $n_{0,2}(\ell)$ and an input signal $T_j(t)$. If $\int_0^\infty \ell^i n_{0,1}(\ell) \mathrm{d}\ell = \int_0^\infty \ell^i n_{0,2}(\ell) \mathrm{d}\ell$ for $i = 1, ..., k$, then

$$\Gamma_1(t) = \Gamma_2(t) \quad \textit{for all} \quad t \in [0, \infty).$$

Proof. We analyze the trajectories (Γ_1, w_1) and (Γ_2, w_2) for n_1 and n_2 respectively and we will show that they satisfy the same differential equation with equal initial conditions. From Theorem 3.2.5 it follows that (Γ_1, w_1) satisfies the equation:

$$\begin{pmatrix} \dot{\Gamma}_1 \\ \dot{w}_1 \end{pmatrix} = \begin{pmatrix} -\frac{\partial G}{\partial c} \Gamma_1 \sum_{i=1}^{k} \sum_{j=0}^{i-1} i v_i \binom{i-1}{j} w_1^{i-j-1} \int_0^\infty \sigma^j n_{0,1}(\sigma) \mathrm{d}\sigma + \frac{\partial G}{\partial T} \frac{\partial T}{\partial t}. \\ \Gamma_1 \end{pmatrix} \tag{3.21}$$

with $w_1(0) = 0$ and $\Gamma_1(0) = G(c_0, T_0)$. Similarly, (Γ_2, w_2) satisfies:

$$\begin{pmatrix} \dot{\Gamma}_2 \\ \dot{w_2} \end{pmatrix} = \begin{pmatrix} -\frac{\partial G}{\partial c}\Gamma_2 \sum_{i=1}^{k}\sum_{j=0}^{i-1} i v_i \binom{i-1}{j} w_2^{i-j-1} \int_0^\infty \sigma^j n_{0,2}(\sigma)\mathrm{d}\sigma + \frac{\partial G}{\partial T}\frac{\partial T}{\partial t}, \\ \Gamma_2 \end{pmatrix} \tag{3.22}$$

with $w_2(0) = 0$ and $\Gamma_2(0) = G(c_0, T_0)$. With use of the assumption $\int_0^\infty \ell^i n_{0,1}(\ell)\mathrm{d}\ell = \int_0^\infty \ell^i n_{0,2}(\ell)\mathrm{d}\ell$ for $i = 1, ..., k$, the system of equations (3.22) can be rewritten to:

$$\begin{pmatrix} \dot{\Gamma}_2 \\ \dot{w_2} \end{pmatrix} = \begin{pmatrix} -\frac{\partial G}{\partial c}\Gamma_2 \sum_{i=1}^{k}\sum_{j=0}^{i-1} i v_i \binom{i-1}{j} w_2^{i-j-1} \int_0^\infty \sigma^j n_{0,1}(\sigma)\mathrm{d}\sigma + \frac{\partial G}{\partial T}\frac{\partial T}{\partial t}, \\ \Gamma_2 \end{pmatrix} \tag{3.23}$$

with $w_2(0) = 0$ and $\Gamma_2(0) = G(c_0, T_0)$. It follows from (3.21) and (3.23) that (Γ_1, w_1) and (Γ_2, w_2) satisfy the same differential equation, with equal initial conditions. Therefore we conclude that $(\Gamma_1, w_1) = (\Gamma_2, w_2)$. □

We are now ready to prove Theorem 3.2.3. For this we prove the existence of two initial conditions which generate equal measurements. By Theorem 3.1.2 this shows that the system is not approximately observable.

Proof of Theorem 3.2.3. By Theorem 3.2.6 we have that the growth rate $\Gamma_1(t)$ and $\Gamma_2(t)$ are equal. From the assumptions it follows that $V(n_{0,1}) = V(n_{0,2})$. Define the distribution $\Delta n_0(\ell)$ by $\Delta n_0(\ell) = n_{0,2}(\ell) - n_{0,1}(\ell)$. It follows from the assumptions that $\int_0^\infty \ell^i \Delta n_0(\ell)\mathrm{d}\ell = 0$ for $i = 1, ..., k$. From Lemma 3.2.4 and $n_{0,2}(\ell) = n_{0,1}(\ell) + \Delta n_0(\ell)$ it follows that n_2, can be expressed as follows:

$$n_2(\ell, t) = \begin{cases} n_{0,1}(\ell - w_2(t)) + \Delta n_0(\ell - w_2(t)) & \text{if } w_2(t) > 0 \\ 0 & \text{else} \end{cases}$$

where $w_2(t) = \int_0^t \Gamma_2(\tau)\mathrm{d}\tau$.

Therefore, the volume in the distributions n_1 and n_2 as function of time, i.e. $[V(n_1)](t)$ and $[V(n_2)](t)$ evaluated along the trajectories $[n_1(\ell, t), T(t)]$ and $[n_2(\ell, t), T(t)]$ are equal. Indeed:

$$\begin{aligned} [V(n_2)](t) &= \int_0^\infty \sum_{i=0}^{k} v_i \ell^i n_2(\ell, t)\mathrm{d}\ell \\ &= \sum_{i=0}^{k} v_i \left[\int_{w_2(t)}^\infty \ell^i n_1(\ell - w_2(t))\mathrm{d}\ell + \int_{w_2(t)}^\infty \ell^i \Delta n(\ell - w_2(t))\mathrm{d}\ell \right] \end{aligned}$$

Since $\int_0^\infty \ell^i \Delta n_0(\ell)\mathrm{d}\ell = 0$ for $i = 1, ..., k$, this equals:

$$\begin{aligned} [V(n_2)](t) &= \sum_{i=0}^{k} v_i \int_{w_2(t)}^\infty \ell^i n_1(\ell - w_2(t))\mathrm{d}\ell \\ &= \int_{w_1(t)}^\infty \sum_{i=0}^{k} v_i \ell^i n_1(\ell - w_1(t))\mathrm{d}\ell = V(n_1)(t) \end{aligned}$$

From this it follows that the outputs $y_1(t)$ and $y_2(t)$ are equal, i.e.:

$$y_2(t) = \begin{bmatrix} C_0 + V(n_{0,2}) - [V(n_2)](t) \\ T(t) \end{bmatrix} = \begin{bmatrix} C_0 + V(n_{0,1}) - [V(n_1)](t) \\ T(t) \end{bmatrix} = y_1(t)$$

By Theorem 3.1.2 it follows that the system is not approximately observable. □

For crystallization processes the results of Theorem 3.2.3 have the following consequence. Suppose there exist two initial distributions $n_1(\ell)$ and $n_2(\ell)$ such that

$$\int_t^\infty \ell^i n_{0,1}(\ell)\mathrm{d}\ell = \int_t^\infty \ell^i n_{0,2}(\ell)\mathrm{d}\ell$$

for $k = 1, ..., k$. Then outputs $y_1(t)$ and $y_2(t)$ will be equal for all $T_j \in U^G$. Therefore, it is not possible to distinguish if a measurement due to the evolution of distribution $n_{0,1}$ from a measurement due to the evolution of distribution $n_{0,2}$. As such the system is not approximately observable. Conversely, it again follows that if the two distributions $n_1(\ell) \in L_2(\mathbb{L})$ and $n_2(\ell) \in L_2(\mathbb{L})$ are such that one of their first k moments are not equal, then the measurements due to evolution of n_1 are not equal to measurements due to evolution of n_2. Therefore one can infer from the measurement y_1 and y_2 what values of the first k moments of the distributions n_1 and n_2 are.

3.2.2 Observability of population balance model from particle size distribution sensor

In this section we study the observability of the batch crystallization process equipped with a particle size distribution sensor and a temperature sensor. Various types of particle size distribution sensors are available on the market. The measurement device described in Section 2.4 contains two particle size distribution sensor.

We consider sensors, which measure the number of particles in a certain size class. We assume that there are k classes. The output space Y is therefore $Y = \mathbb{R}^k$. We assume that the measurement is linear and can be represented by the map $F : L_2(0, \infty) \to Y$. The sensor is assumed to be functional for particles with sizes between ℓ_{min} and ℓ_{max} and that the sensor does covers the domain $[\ell_{min}, \ell_{max}]$ completely, i.e.:

$$F(n(\ell)) = 0 \quad \text{implies} \quad n(\ell) = 0 \quad \text{for all } \ell \in [\ell_{min}, \ell_{max}].$$

The classes are centered around the points $\ell_1, \ell_2, ..., \ell_k$ with distance $\Delta\ell$ between the points, i.e. $\Delta\ell = \frac{\ell_{max} - \ell_{min}}{k}$ and $\ell_i = \ell_{min} + (i - \frac{1}{2})\Delta\ell$, thus $\ell_1 = \ell_{min} + \frac{\Delta\ell}{2}, \ell_2 = \ell_{min} + \frac{3\Delta\ell}{2}, ..., \ell_k = \ell_{max} - \frac{\Delta\ell}{2}$. We will assume $\Delta\ell > \ell_{min}$, which is reasonable in practice.

The sensors are modeled by weighting functions $w_i(\ell)$ which indicate the probability that a particle of size ℓ is classified to be in size class $i \in \{1, .., k\}$ The observation operator $F : L_2(0, \infty) \to Y$, representing such a sensor is given by:

$$Fn = \begin{bmatrix} f_1 \\ \vdots \\ f_k \end{bmatrix} n \quad \text{with} \quad f_i n = \int_0^\infty w_i(\ell) n(\ell)\mathrm{d}\ell. \tag{3.24}$$

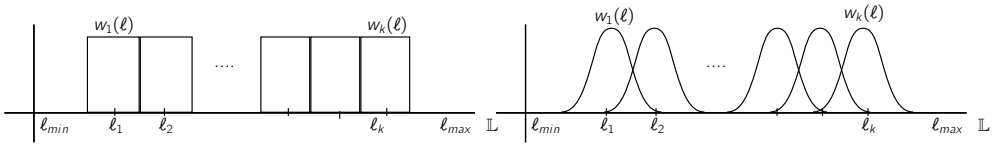

(a) Ideal classification (b) Approximate classification

Figure 3.3: Illustration of a set of possible CSD sensors

We assume that the system can be modeled by the model given by Equations (3.4) and we equip this model with the following output equation:

$$y = \begin{bmatrix} Fn & T \end{bmatrix}^\top = \begin{bmatrix} f_1 n & \dots & f_k n & T \end{bmatrix}^\top. \tag{3.25}$$

We distinguish different types of classification models. The first case is ideal classification in which the sensor performs the classification task ideally, i.e. it classifies the particle to belong in the right class with probability one. This case can be modeled by introduction of the binary classification functions w_i:

$$w_i(\ell) = \begin{cases} 1 & \text{if } \ell \in [\ell_i \pm \frac{\Delta\ell}{2}], \\ 0 & else, \end{cases} \tag{3.26}$$

as depicted in Figure 3.3a.

In the second case, we model sensors which does not classify particles ideally. We call this approximate classification and assume that a model of the classification process is available in the form of more general weighting functions $w_i(\ell)$. We assume that the weights w_i are symmetric around the center of the class and non-negative, i.e.

$$w_i(\ell_i + \ell) = w_i(\ell_i - \ell) \geq 0. \tag{3.27}$$

An example of this situation is shown if Figure 3.3b.

Since the batch crystallization process is nonlinear it is not possible to use the result on linear infinite dimensional systems to analyze observability. Therefore, we first simplify the problem setting to the linear advection equation and analyze this setting. Then we use the results from the linear advection equation to obtain results for the model given by Equation (3.4).

Observability of advection equation with population sensor

Consider the linear advection system:

$$\frac{\partial n}{\partial t} = -\frac{\partial n}{\partial \ell} \tag{3.28}$$

with initial condition $n(\cdot, 0) = n_0 \in L_2(0, \infty)$ and boundary condition $n(0, t) = 0$ for all $t \geq 0$. We augment the system with the sensor $y = Fn$ given by (3.24) and study whether the system is observable with this particle size sensor.

The solution to the state equation given by:

$$n(\ell, t) = [\mathcal{T}(t)n_0](\ell) = \begin{cases} n_0(\ell - t) & \text{if } \ell - t > 0 \\ 0 & else \end{cases} \tag{3.29}$$

Here, $\mathcal{T}$ is the semigroup with infinitesimal generator $-\frac{\partial}{\partial \ell}$.

To study observability, we introduce, conform definition 3.1.7, the observability map $\mathcal{C}^\tau$ on $[0, \tau]$ of the system (3.28) with sensor (3.29), as the bounded linear map $\mathcal{C}^\tau : X \to L_2(0, \tau; \mathbb{R}^k)$ defined by $\mathcal{C}^\tau n = F\mathcal{T}(\cdot)n$. In the situation that the population sensors performs ideal classification i.e. with weighting functions (3.26), we characterize the kernel of the observability map by the following theorem.

Theorem 3.2.7
Consider the system (3.28) *with sensor* (3.29) *and weighting functions* (3.26) *and observability map* $\mathcal{C}^\tau n = F\mathcal{T}(\cdot)n$. *If* $\tau \geq \Delta\ell$ *then*

$$\ker \mathcal{C}^\tau = \{n \in L_2(0, \infty) | n(\ell) = 0 \quad \text{for } \ell < \ell_{max}\}$$

Proof. We study the kernel of

$$\mathcal{C}^\tau n = F\mathcal{T}(\cdot)n \begin{bmatrix} f_1\mathcal{T}(\cdot)n \\ \vdots \\ f_k\mathcal{T}(\cdot)n \end{bmatrix}.$$

For the individual components of $F\mathcal{T}(t)n$ we have:

$$f_i\mathcal{T}(t)n = \int_0^\infty w_i(\ell)\mathcal{T}(t)n(\ell)\mathrm{d}\ell = \int_t^\infty w_i(\ell)n(\ell - t)\mathrm{d}\ell.$$

For the specific choice of weighting functions w_i as in (3.26), w_i has compact support in $[\ell_i - \frac{\Delta\ell}{2}, \ell_i + \frac{\Delta\ell}{2}]$ and it follows that:

$$f_i\mathcal{T}(t)n = \int_{\max(t, \ell_i - \frac{\Delta\ell}{2})}^{\max(t, \ell_i + \frac{\Delta\ell}{2})} n(\ell - t)\mathrm{d}\ell.$$

Here, we have used the max-operation to implement the discontinuous character of $\mathcal{T}(t)n(\ell)$. Introduce the coordinate change $\sigma = \ell - t$ to the latter equation and rewrite $f_i\mathcal{T}(t)n$ as follows:

$$f_i\mathcal{T}(t)n = \int_{\max(0, \ell_i - \frac{\Delta\ell}{2} - t)}^{\max(0, \ell_i + \frac{\Delta\ell}{2} - t)} n(\sigma)\mathrm{d}\sigma.$$

We introduce $N(\ell)$ as the anti-derivative of $n(\ell)$. In terms of $N(\ell)$ we can rewrite the latter equation to:

$$f_i\mathcal{T}(t)n = N(\max(0, \ell_i + \frac{\Delta\ell}{2} - t)) - N(\max(0, \ell_i - \frac{\Delta\ell}{2} - t)).$$

We use $\ell_i = \ell_{min} + (i - \frac{1}{2})\Delta\ell$ and it follows that:

$$f_i\mathcal{T}(t)n = N(\max(0, \ell_{min} + i\Delta\ell - t)) - N(\max(0, \ell_{min} + (i-1)\Delta\ell - t)).$$

It follows that $f_i\mathcal{T}(t)n = 0$ if and only if $N(\ell_i + \frac{\Delta\ell}{2} - t) = N(\max(0, \ell_i - \frac{\Delta\ell}{2} - t))$.

We repeat this for all components of $F\mathcal{T}(t)n$. It follows that $F\mathcal{T}(\cdot)n = 0$ if and only if

$$F\mathcal{T}(\cdot)n = \begin{bmatrix} f_1\mathcal{T}(\cdot)n \\ f_2\mathcal{T}(\cdot)n \\ \vdots \\ f_k\mathcal{T}(\cdot)n \end{bmatrix} = \begin{bmatrix} N(\max(0, \ell_{min} + \Delta\ell - \cdot)) - N(\max(0, \ell_{min} - \cdot)) \\ N(\max(0, \ell_{min} + 2\Delta\ell - \cdot)) - N(\max(0, \ell_{min} + \Delta\ell - \cdot)) \\ \vdots \\ N(\max(0, \ell_{min} + k\Delta\ell - \cdot)) - N(\max(0, \ell_{min} + (k-1)\Delta\ell - \cdot)) \end{bmatrix} = 0.$$

It follows that $F\mathcal{T}(t)n = 0$ for all $t \geq 0$ if and only if $N(\max(0, \ell_{min} + i\Delta\ell - t)) = N(\max(0, \ell_{min} + (i-1)\Delta\ell - t))$ for $i = \{1 \ldots k\}$ and $t \geq 0$. We conclude that distributions with $N(\ell) = 0$ for $\ell \in [0, \ell_{max}]$ are distributions such that $F\mathcal{T}(t)n = 0$ for all $t > \Delta\ell$. Since $n(\ell) = \frac{\partial N}{\partial \ell}(\ell, t)$. This implies that distributions with $n(\ell) = 0$ for $\ell \in [0, \ell_{max}]$ are unobservable for any $t > \Delta\ell$. □

From Theorem 3.2.7 it follows that is is sensible to introduce the following decomposition of $L_2(0, \infty)$:

$$L_2(0, \infty) = L_2(0, \ell_{max}) \oplus L_2(\ell_{max}, \infty).$$

The subspace $L_2(0, \ell_{max})$ is the subspace that is approximately observable for $\tau > \Delta\ell$, the subspace $L_2(\ell_{max}, \infty)$ is the subspace of not distinguishable distributions for this sensor.

In the situation that the population sensors performs approximate classification i.e. with weighting functions (3.27), the observability map can be defined analogously. We have not been able to characterize the kernel of the observability map in this situation for general weighting functions $w_i(\ell)$. It is conjectured that for positive and symmetric weighting functions w_i with compact support $[\ell_i - \frac{\Delta\ell}{2}, \ell_i + \frac{\Delta\ell}{2}]$, the subspace $L_2(0, \ell_{max})$ is approximately observable for $\tau > \Delta\ell$. The formal proof is open for future research.

Observability of crystallization process with population sensors

Since the batch crystallization process is nonlinear we have not been able to conduct a rigorous observability analysis for the process with a population sensor. However, when the growth rate of the particles is positive and constant in time, the population balance equation is equivalent to the system (3.28). Therefore, it follows that if the growth rate of the particles is positive and constant in time, the subspace $L_2(0, \ell_{max})$ is approximately observable for some $\tau > 0$. The analysis for the case with a time variant growth rate has been left for future research.

3.2.3 Observability of the truncated moment model

In Section 2.3 it is explained that it is a very popular in the field of chemical engineering to analyze the crystallization process with use of the truncated moment model. In this section we analyze the observability of the moment model truncated at the fourth moment

and equipped with a concentration and temperature measurement. For completeness we repeat the model:

$$\frac{\mathrm{d}\mu_0}{\mathrm{d}t} = 0, \tag{3.30a}$$
$$\frac{\mathrm{d}\mu_i}{\mathrm{d}t} = iG(c,T)\mu_{i-1}, \quad \text{for } i = 1,2,3 \tag{3.30b}$$
$$\frac{\mathrm{d}T}{\mathrm{d}t} = \alpha(T_j - T) \tag{3.30c}$$
$$y = \begin{bmatrix} c \\ T \end{bmatrix} = \begin{bmatrix} c_0 + \mu_{3,0} - \mu_3 \\ T \end{bmatrix} \tag{3.30d}$$

where c_0 is the initial concentration of the process, $\mu_{3,0} = \int_0^\infty \ell^3 n_0(\ell)\mathrm{d}\ell$ is the initial third moment, $G(c,T)$ is the concentration and temperature dependent growth function and T_j is the temperature of the reactor jacket and functions as input of the system. We remark that this model is only representative for the crystallization process when it is operated in a regime where $G(c(t),T(t)) \geq 0$ for all t, that is T_j has to be chosen such that $T_j \in U^G$ as defined by Equation (2.18). Moreover, we remark that only the states where $\mu_i > 0$ for $i = 0,1,2,3$ are of physical relevance. We indicate the state space for which both conditions hold by X^G, i.e.

$$X^G = \left\{ x \in \mathbb{R}^5 | x = \mathrm{col}(\mu_0, ..., \mu_3, T), G(c,T) > 0, \mu_i > 0 \text{ for } i = \{0,1,2,3\} \right\} \tag{3.31}$$

In order to show that the system is locally observable on the subset $x \in X^G$ we use Theorem 3.1.4.

The model can be represented as an input affine nonlinear finite dimensional model, as follows:

$$\Sigma_{mom} \begin{cases} \dot{x} = & f(x) + g(x)u \\ y = & h(x) \end{cases} \tag{3.32a}$$

where:

$$x = \begin{bmatrix} \mu_0 \\ \mu_1 \\ \mu_2 \\ \mu_3 \\ T \end{bmatrix}, \quad u = T_j, \quad f(x) = \begin{bmatrix} 0 \\ G(C,T)\mu_0 \\ 2G(C,T)\mu_1 \\ 3G(C,T)\mu_2 \\ -\alpha T \end{bmatrix}, \quad g(x) = \begin{bmatrix} 0 \\ 0 \\ 0 \\ 0 \\ \alpha \end{bmatrix}, \tag{3.32b}$$

$$h(x) = \begin{bmatrix} h_1(x) \\ h_2(x) \end{bmatrix} = \begin{bmatrix} C \\ T \end{bmatrix} = \begin{bmatrix} C_0 + \mu_{3,0} - \mu_{3.} \\ T \end{bmatrix} \tag{3.32c}$$

And we have the following result for the moment model.

Theorem 3.2.8
Consider the system Σ_{mom} given by Equation (3.32). The system is locally observable for $x \in X^G$.

Proof. We will verify local observability by Theorem 3.1.4. Theorem 3.1.4 states that we have to show that $dim(d\mathcal{O}) = 5$ for all $x \in X^G$. The first, second and third order Lie derivatives of h with respect to combinations of the vector fields f and g have been calculated symbolically in order to analyze the dimension of $d\mathcal{O}(x)$ for $x \in X^G$. The detailed results on the symbolic calculations are given in Appendix B.2. It follows that a subspace $d\mathcal{O}'(x)$ of $d\mathcal{O}(x)$ can be constructed by the following Lie-derivatives:

$$
\begin{aligned}
d\mathcal{O}'(x) &= \text{span}\,\{dh_1(x), dh_2(x), dL_f h_1(x), dL_f L_f h_1(x), dL_g L_f h_1(x), dL_f L_f L_f h_1(x)\} \\
&= \text{span}\,\{ \begin{bmatrix} 0 \\ 0 \\ 0 \\ 1 \\ 0 \end{bmatrix}, \begin{bmatrix} 0 \\ 0 \\ 0 \\ 0 \\ 1 \end{bmatrix}, \begin{bmatrix} 0 \\ 0 \\ -3G \\ -3G_c\mu_2 \\ -3G_T\mu_2 \end{bmatrix}, \begin{bmatrix} 0 \\ -2G^2 \\ 18GG_c\mu_2 \\ * \\ * \end{bmatrix} \begin{bmatrix} 0 \\ 0 \\ -3G_T \\ -3G_{Tc}\mu_2 \\ -3G_{TT}\mu_2 \end{bmatrix}, \begin{bmatrix} -2G^3 \\ * \\ * \\ * \\ * \end{bmatrix} \}
\end{aligned}
$$

where $*$ indicates a nonzero entry. When we analyze $d\mathcal{O}'$, it follows that $dim(d\mathcal{O}') = 5$ for all states $x_0 \in X^G$ such that $\{\mu_0, \mu_1, \mu_2, \mu_3\} > 0$ and $G(c, T) > 0$. Therefore, we may conclude that $dim(d\mathcal{O}) = 5$ for every $x_0 \in X^G$ and that the system is locally observable on X^G. □

Theorem3.2.8 implies that the system (3.30a) is locally observable for every $x_0 \in X^G$. It is interesting to note that, since the states in the moment model are the moments μ_0, μ_1, μ_2 and μ_3 and the temperature T this result is compatible with the outcome of the analysis of the population balance model in combination with the concentration sensor, which is presented in Section 3.2.1.

3.3 Controllability

In this section the controllability of a batch cooling crystallization process will be discussed. Controllability is the system theoretic concept that indicates whether a set of states can be reached from a given set of initial states in finite time. The concept is of interest for batch cooling crystallization processes since it indicates to what extent one can steer between the states of the processes, in this case the population balance and the temperature of the reactor. The controllability of a process plays a role in answering questions like:

- To what extent can one steer a process from an undesired state to a desired state.
- To what extent can one find control methods which reduce the sensitivity of a process to disturbances.
- What is the compromise on optimization and optimal operation, if the process is not controllable?

First, an brief introduction about the concept of controllability will be given in this section. Subsequently, we will study the controllability of batch cooling crystallization processes.

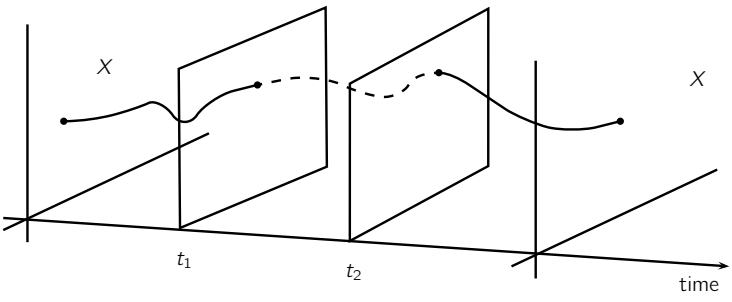

Figure 3.4: Illustration of a controllable system.

3.3.1 Introduction to controllability

It is important to make precise what controllability means. Consider a system Σ given by the state space evolution:

$$\dot{x} = f(x, u), \tag{3.33}$$

with $x(t) \in X$, $y(t) \in Y$ and $u(t) \in U$, and where X, U and Y are Hilbert spaces and $t \in \mathbb{T} = [0, \tau)$, with $\tau > 0$. Moreover, introduce the space of admissible inputs $\mathcal{U} \subset U^{\mathbb{T}}$. We assume that f is sufficiently smooth, in the sense that for every $u \in \mathcal{U}$ and every $x_0 \in X$ the solution $x(t, t_0, x_0, u)$ of the differential Equation (3.1) with initial condition $x(t_0) = x_0$ and admissible input $u \in \mathcal{U}$ is uniquely defined on the time interval $\mathbb{T}$. From [Nijmeijer and Van der Schaft, 1990] we recall the definition of a controllable system:

Definition 3.3.1 (Controllable system)
The system (3.33) *is called controllable if for any two points $x_1, x_2 \in X$ there exists a finite time τ and an admissible control function $u \in \mathcal{U} : [0, \tau] \to U$ such that $x(\tau, 0, x_1, u) = x_2$.*

Figure 3.4 shows a graphical representation of the idea that we steer a state x at time $t = t_1$ to different value at $t = t_2$.

Moreover we will introduce the concept of a reachable set.

Definition 3.3.2 (Reachable set)
Let $x_1 \in X$, let $\tau > 0$ and let V be an open neighborhood of x_1. Define the reachable set from x_1, $\mathcal{R}^V(x_1, \tau)$, as follows:

$$\mathcal{R}^V(x_1, \tau) = \{x_2 \in X | \text{there exists } u \in U^{[0,\tau]} \text{ such that } x(\tau, 0, x_1, u) = x_2 \text{ and } x(t, 0, x_1, u) \in V \text{ for all } t \in [0, \tau]\}$$

It follows that for a controllable system, the union of all reachable sets $\mathcal{R}^X(x_1, \tau)$ for $\tau > 0$ for every $x_1 \in X$ equals the space X, i.e

$$\bigcup_{\tau > 0} \mathcal{R}^X(x_1, \tau) = X \quad \text{for all } x_1 \in X.$$

Similarly, it follows that for a not controllable system, there exists at least one $x_1 \in X$ such that the union of all reachable sets $\mathcal{R}^X(x_1, \tau)$ for $\tau > 0$ does not equal the space X, i.e.

$$\bigcup_{\tau>0} \mathcal{R}^X(x_1, \tau) \neq X \quad \text{for some } x_1 \in X.$$

In the next section we will show that for batch crystallization processes there are large restrictions on the reachable sets in the case where we only consider particle growth or dissolution. Then this property of not controllable systems is used to show that the batch crystallization processes is not controllable.

3.3.2 Controllability analysis of batch crystallization processes

In this section the controllability properties of the model of a batch crystallizer, given by the Equations (2.15) will be analyzed. The controllability of processes which involve population equations has been studied before. In [Semino and Ray, 1995] an introduction to controllability for balance systems is given. The controllability of an evaporation continuous crystallizer has been analyzed and reported in [Eek and Bosgra, 2000]. In [Kalbasenka et al., 2005] an analysis of controllability of population balance in evaporation batch crystallization is given. This analysis is based on the characteristic curves in solutions of the population balance equation.

In [Zhang et al., 2010] and [Hang et al., 2010] the reachable sets of a population balance models has been studied in the context of batch crystallization processes. The analysis is based on the numerical approximation by the method of characteristics. The reachability of particle size distributions in semi-batch emulsion polymerization has been studied in [Wang and Doyle III, 2004]. The control of the particle size distributions in continuous processes by a receding horizon control algorithm has been reported in [Henson, 2003].

The model (2.15) for batch crystallization is a hybrid nonlinear distributed parameter model. Since systematic methods for analysis of controllability of hybrid nonlinear distributed parameter systems do not exist, we will restrict our analysis to the case in which no switching occurs. That is, we will assume that the input, which is the jacket temperature T_j, is either such that the system is supersaturated for all $t \geq 0$ or is such that the system is under saturated for all $t \geq 0$. This is represented by $T_j \in U^G$ with U^G defined by Equation (2.18) and $T_j \in U^D$ with U^D defined by Equation (2.19), respectively. We will assume that there is no breakage of particles and that the initial condition of the process is given by $n(\ell, 0) = n_0(\ell)$. For both operation modes we will characterize the reachable set.

First, we consider the growth-only scenario as defined in Section 2.2.4. In this case the process is described by:

$$\frac{\partial n}{\partial t} = -G(c, T)\frac{\partial n}{\partial \ell}, \tag{3.34a}$$

$$\frac{\mathrm{d}T}{\mathrm{d}t} = \alpha(T_j - T), \tag{3.34b}$$

with boundary condition $n(0,t) = B(n(\ell,t), T(t))$, initial conditions $n(\ell,0) = n_0(\ell)$, $T(0) = T_0$ and input $T_j \in U^G$, hence the system is supersaturated for all $t \geq 0$.

The solution to the system of Equations (3.34) with initial condition (n_0, T_0) is given by:

$$n(\ell,t) = \begin{cases} n_0(\ell - w_G(t)), & \text{if: } \ell - w_G(t) > 0, \\ B(n(\ell, t - \frac{\ell}{w_G(t)}), t - \frac{\ell}{w_G(t)}), & \text{else,} \end{cases} \tag{3.35a}$$

and

$$T(t) = e^{-\alpha t} T_0 + \int_0^t \alpha e^{-\alpha(t-\tau)} T_j(\tau) \mathrm{d}\tau \tag{3.35b}$$

with: $w_G(t) = \int_0^t G(c(\tau), T(\tau))\mathrm{d}\tau$. Note that since $G(c(t), T(t)) \geq 0$ for all $t > 0$, it follows that $w_G(t) \geq 0$, for $t \geq 0$.

Moreover, we consider the dissolution-only scenario as defined in Section 2.2.4 and assume that the process is described by:

$$\frac{\partial n}{\partial t} = D(c,T)\frac{\partial n}{\partial \ell}, \tag{3.36a}$$

$$\frac{\mathrm{d}T}{\mathrm{d}t} = \alpha(T_j - T), \tag{3.36b}$$

with initial conditions $n(\ell,0) = n_0(\ell)$, $T(0) = T_0$ and input $T_j \in U^D$, hence the system is undersaturated for all $t \geq 0$.

Let (n_0, T_0) be an initial condition of (3.36), then the solution to the system is given by:

$$n(\ell,t) = n_0(\ell + w_D(t)) \tag{3.37a}$$

and

$$T(t) = e^{-\alpha t} T_0 + \int_0^t \alpha e^{-\alpha(t-\tau)} T_j(\tau) \mathrm{d}\tau \tag{3.37b}$$

with: $w_D(t) = \int_0^t D(c(\tau), T(\tau))\mathrm{d}\tau$. Note that since $D(c(t), T(t)) \geq 0$ for all $t > 0$, it follows that $w_D(t) \geq 0$, for $t \geq 0$.

For the systems (3.34) and (3.36) we will characterize the reachable sets from the initial condition (n_0, T_0).

Let (n_0, T_0) be an initial condition of (3.34), let V_G be a neighborhood of (n_0, T_0) and consider the reachable set $R_G^V((n_0, T_0), \tau)$ for $\tau > 0$ defined by:

$$R_G^{V_G}((n_0, T_0), \tau) = \Big\{(n, T) \in L_2(\mathbb{L}, \mathbb{R}) \times \mathbb{R} | \exists T_j \in U^G \text{and for all } t \in \mathbb{T} \text{ (3.34) holds}\Big\}.$$

Let V_D be a neighborhood of (n_0, T_0) and consider the reachable set $R_D^{V_D}((n_0, T_0), \tau)$ defined by:

$$R_D^{V_D}((n_0, T_0), \tau) = \Big\{(n, T) \in L_2(\mathbb{L}, \mathbb{R}) \times \mathbb{R} | \exists T_j \in U^G \text{and for all } \tau \in \mathbb{T} \text{ (3.36) holds}\Big\}.$$

With use of the explicit solutions (3.35) the reachable set from (n_0, T_0) can be characterized by:

$$R_G^{V_G}((n_0,T_0),t) = \Big\{(n(\cdot,t),T(t)) \in L_2(\mathbb{L},\mathbb{R}) \times \mathbb{R} \Big| \exists T_j \in U^G,$$
$$n(\ell,t) = \begin{cases} n_0(\ell - w(t)) & \text{if: } \ell - w_G(t) > 0 \\ B(n(\ell, t - \frac{\ell}{w_G(t)}), t - \frac{\ell}{w_G(t)}) & \text{else.} \end{cases}$$

and

$$T(t) = e^{-\alpha t}T_0 + \int_0^t \alpha e^{-\alpha(t-\tau)}T_j(\tau)\mathrm{d}\tau \Big\}$$

with: $w_G(t) = \int_0^t G(c(\tau),T(\tau))\mathrm{d}\tau$.

With use of the explicit solutions (3.37) from (n_0, T_0) can be characterized by:

$$R_D^{V_D}((n_0,T_0),t) = \Big\{(n(\cdot,t),T(t)) \in L_2(\mathbb{L},\mathbb{R}) \times \mathbb{R} \Big| \exists T_j \in U^G,$$
$$n(\ell,t) = n_0(\ell + w_D(t))$$

and

$$T(t) = e^{-\alpha t}T_0 + \int_0^t \alpha e^{-\alpha(t-\tau)}T_j(\tau)\mathrm{d}\tau \Big\}$$

with: $w_D(t) = \int_0^t D(c(\tau),T(\tau))\mathrm{d}\tau$.

It is important to recognize that the reachable set depends on the initial concentration c_0 and the initial condition of the process. From the reachable set $R_G^{V_G}$ it follows that from the initial conditions (n_0, T_0) it is not possible to reach a distribution n_1 that cannot be represented as $n_0(\ell - \gamma)$ with a constant $\gamma > 0$. As such, we conclude that the system (3.34) is not controllable with the admissible set of inputs $T_j \in U_G^V$. Similarly, from the reachable set $R_G^{V_D}$ it follows that from the initial conditions (n_0, T_0) it is not possible to reach a distribution n_1 that cannot be represented as $n_0(\ell + \gamma)$ with an constant $\gamma > 0$. As such, we conclude that the system (3.37) is not controllable with the admissible set of inputs $T_j \in U_G^V$.

We conclude that if we do assume that the system does not switch between the growth and dissolution mode during operation, the batch crystallization process is not controllable. We cannot draw a conclusion about the controllability of the batch crystallization process when we pose not assumption on the switching behavior. However, it is known that controller design for switching systems is difficult. Therefore, although that the system might be controllable by exploitation of the switching behavior, the design of a controller that can take this switching behavior into account will be challenging.

The analysis shows that, under the assumption that the given model holds, it is not possible to steer the process from an arbitrary distribution to an arbitrary different distribution without switching between growth and dissolution.

3.4 Conclusions and Recommendations

Conclusions

In this chapter the concepts observability and controllability have been introduced in the context of a nonlinear system with infinite dimensional state spaces. The definitions have been applied to study the observability and controllability of batch cooling crystallization processes which can be modeled with the model 2.15. Since the process model is hybrid, nonlinear and infinite dimensional, we have restricted the analysis to operation in regimes where the process is either supersaturated or undersaturated.

In the first part of the chapter we have provided an analysis of the observability properties of batch crystallization processes in the presence of a concentration measurement and in the presence of a population size. We have restricted the analysis to operation regimes in which the system is supersaturated and only growth takes place, in order to limit the complexity of the problems. From the analysis of the observability of the process in presence of a concentration sensor, we draw the conclusion that there exist populations that generate equal measurements. Therefore, we conclude that the system is not observable. We have characterized states which are indistinguishable in terms of the moments of the states and provide a constructive algorithm to generate examples of indistinguishable states. From the analysis it follows that if the process is equipped with measurements of the k-th moment of the number density distribution, the moments $\mu_0, ..., \mu_k$ of the number density distribution are observable, but the moments $\mu_{k+1}, \mu_{k+2}, ...$ are not observable. Moreover, the analysis of the observability properties shows that if one is interested in only the first moments $\mu_0, \mu_1, \mu_2, \mu_3$ of the distribution there is, from observability point of view, no need to install a population sensor in the process. It must be noted that in the process model and the analysis we assume that the initial concentration c_0 is known. This is a result of the assumption that there is no mass exchange between the process and the environment. The outcome of the observability analysis depends on this assumption.

For the analysis of the observability of the process in presence of a population size sensor, we have introduced a model of a population size sensor with ideal classification and an model for a population size sensor with approximate classification. The observability of the process in combination with a population size sensor with ideal classification has been analyzed in case of a constant growth rate has been analyzed. It follow that the process is approximately observable in this situation. In case the growth rate is not constant the analysis cannot be completed completely and approximate observability is conjectured. The analysis of the observability of the process with an population size sensor with approximate classification could be complete due the mathematical complexity and is left for future research.

In the second part of the chapter we have provided an analysis of the controllability properties of batch crystallization processes. In order to limit the complexity of the analysis, we have restricted the analysis to operation regimes in which the system is only supersaturated or only undersaturated. The analysis shows that the process is not controllable, when the process is restricted to these operation modes. We cannot draw

conclusions on operation modes that cover supersaturation as well as undersaturation.

3.4.1 Recommendations

In the analysis of the observability we have only analyzed whether there exists a pair of two states that generate exactly the same measurement signal to draw conclusions on observability. However, it might be that a pair of two states exist that generates *almost* the same measurement signal. Then, from mathematical point of view the system is approximately observable, but in practice the reconstruction of the states might be cumbersome. It would be interesting to analyze if it is possible to extend the analysis of exact observability in this direction. The analysis of the controllability properties shows that, under the assumption that the given model holds, it is not possible to steer the process from an arbitrary distribution to an arbitrary different distribution without switching between growth and dissolution. Therefore, when one desires to have influence one the final crystal size distribution, one needs to explore possibilities to make the process controllable.

CHAPTER 4

Control Of Batch Cooling Crystallization By Feedback Linearization

Abstract

In this chapter a method for control of the supersaturation level in a batch cooling crystallizer is presented and analyzed. The method is based on feedback linearization. The sensitivity of the control method to model uncertainties and measurement disturbances has been analyzed and is supported by an simulation study. The methods has been evaluated in an experimental environment on an industrial scale process and show the potential of the presented approach.

In order to produce crystalline products which meet high quality standards, it is of large importance to enable the reproducible operation of batch crystallization processes. One of the necessities for reproducible operation is the possibility to create reproducible operating conditions. In this chapter a method which enables the creation of reproducible operating conditions is presented. For reproducible operation of a crystallization process the number of particles in a batch and the driving force during the batch are of high importance. In this chapter the method of feedback linearization will be introduced. Based on the method of feedback linearization, a control scheme to control the super saturation level in a crystallizer is developed. Beside the development of the method, we analyze in this chapter the applicability of the method of feedback linearization in an industrial environment. The control law that will be presented is an explicit control law, which can be combined with linear control techniques to control the process. In contrast

to online-optimization based methods such as implicit MPC, the control law is explicit, which is nice from analysis point of view. The theoretical analysis of the method has been published in [Jansen, 2011] and [Vissers et al., 2011b]. The experimental results have been published in [Vissers et al., 2011a].

The idea to control the supersaturation in a crystallization process is not completely new. Control of supersaturation by use of PID control and bang-bang control can be found in [Alatalo, 2010] and [Khan et al., 2011]. An application of feedback linearization on batch cooling crystallization processes can be found in [Corrioua and Rohani, 2002] and [Xie et al., 2002]. The method of feedback linearization is closely related to the concept of differentially flatness, used in the analysis of nonlinear systems. An analysis of differentially flatness of batch cooling crystallization processes and controller synthesis by use of this property can be found in [Vollmer, 2004].

4.1 Feedback linearization

In this section a method for linearization of the input output dynamics of a process by feedback, known as feedback linearization will be introduced. The method of feedback linearization is well described in literature, for instance see [Khalil, 1992, Chapter 13], [Sastry, 1999, Chapter 9], [Nijmeijer and Van der Schaft, 1990, Chapter 6].

Input-output feedback linearization considers a method to linearize the input-output behavior of a system, by interconnection of the system with a state feedback controller (commonly called state feedback law) which has been designed in such a way that the input-output dynamics of the interconnected system can be described by a linear mapping.

This is reflected in the following definition:

Definition 4.1.1
System $\dot{x} = f(x) + g(x)u$ with $y = h(x)$ is called input/output linearizable if a state dependent control law $u = \Psi(x, v)$ exists, which accommodates a linear mapping $v \mapsto y$.

State feedback linearization can be used to linearize a system by feedback, such that the resulting closed loop system can be controlled by linear control method such as PID control, $\mathcal{H}_\infty$ control, or model predictive control (MPC).

In Figure 4.1 a graphical representation of the state feedback setup is shown.

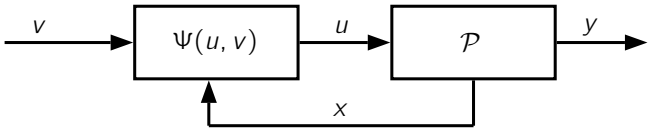

Figure 4.1: State feedback setup

The concept of feedback linearization has been researched quite extensively. We present the some important results in the context of single input single output systems (SISO

systems). The Lie derivative is a mathematical tool that appears to be quite very useful for the analysis of of nonlinear systems. An introduction is given in Appendix A.1.

We introduce the concept of relative degree of a system by the following definition:

Definition 4.1.2
System $\dot{x} = f(x) + g(x)u$ with $y = h(x)$ is said to have relative degree r if the following two condition hold:

$$L_g L_f^k h(x) = 0 \quad \text{for} \qquad k = 0, \dots, r-2 \tag{4.1a}$$
$$L_g L_f^{r-1} h(x) \neq 0 \tag{4.1b}$$

The relative degree of the system can be considered as the number of times we have to differentiate the output y before the input u appears explicitly and appears to be useful to characterize if a system is feedback linearizable. The following theorem gives a necessary and sufficient condition for linearizablility of a system by feedback.

Theorem 4.1.1
The system $\dot{x} = f(x) + g(x)u$, $y = h(x)$ is input/output linearizable if and only if the system has relative degree r with $0 < r < \infty$. The proof is given in [Kravaris and Chung, 1987].

A general method to synthesize a state feedback law that renders input-output dynamics of the interconnected system linear is given by the following theorem.

Theorem 4.1.2
Consider an input/output linearizable dynamical system with relative degree r that assumes the form,

$$\dot{x}_1 = f_1(x), \tag{4.2a}$$
$$\dot{x}_2 = f_2(x) + g(x)u, \tag{4.2b}$$
$$y = h(x), \tag{4.2c}$$
$$x = [x_1, x_2]^\top, \quad f = [f_1, f_2]^\top.$$

Define a state feedback law

$$\Psi(x, v) := \frac{v - \sum_{k=0}^{r} \beta_k L_f^k h(x)}{\beta_r L_g L_f^{r-1} h(x)}, \tag{4.3}$$

and the coordinate transformation

$$\begin{bmatrix} \eta \\ \zeta \end{bmatrix} = \begin{bmatrix} \eta \\ \zeta_1 \\ \vdots \\ \zeta_r \end{bmatrix} = \begin{bmatrix} x_1 \\ L_f^0 h(x) \\ \vdots \\ L_f^{r-1} h(x) \end{bmatrix}. \tag{4.4}$$

Then: By defining $u = \Psi(x, v)$ in the system from Equation (4.2), the input/output mapping, $v \mapsto y$, is a linear system of the form,

$$\dot{\zeta} = A\zeta + Bv, \tag{4.5a}$$
$$y = C\zeta. \tag{4.5b}$$

Proof. From the definition of the Lie derivative (A.1), and definition (4.1) it follows that for the system 4.2 we have,

$$\frac{dy}{dt} = \frac{\partial h}{\partial x}\frac{\partial x}{\partial t} = \langle d_x h, f(x) + g(x)\rangle = L_f h(x) + L_g h(x)u = L_f h(x),$$
$$\frac{d^2y}{dt^2} = \langle d_x L_f h(x), f(x) + g(x)u\rangle = L_f^2 h(x) + L_g L_f h(x)u = L_f^2 h(x).$$

In general to follows that:

$$\begin{aligned}\frac{d^k y}{dt^k} &= \langle d_x L_f^{k-1} h(x), f(x) + g(x)u\rangle,\\ &= L_f^k h(x) + L_g L_f^{k-1} h(x)u = L_f^k h(x) \quad \text{for } k = 0, \ldots, r-1,\\ \frac{d^r y}{dt^r} &= L_f^r h(x) + L_g L_f^{r-1} h(x)u.\end{aligned}$$

When the feedback control law $u = \Psi(x, v)$ from Equation (4.3) has been applied, the closed loop system can be described by,

$$\begin{aligned}\frac{d^k y}{dt^k} &= L_f^k h(x) \qquad k = 1, \ldots, r-1,\\ \frac{d^r y}{dt^r} &= L_f^r h(x) + L_g L_f^{r-1} h(x)u,\\ &= \frac{v}{\beta_r} - \sum_{k=0}^{r-1} \frac{\beta_k}{\beta_r} L_f^k h(x),\end{aligned}$$

and can be re-written in matrix form as,

$$\begin{bmatrix} \frac{dy}{dt} \\ \frac{d^2y}{dt^2} \\ \vdots \\ \\ \frac{d^ry}{dt^r} \end{bmatrix} = \begin{bmatrix} 0 & 1 & 0 & \ldots & 0 \\ 0 & 0 & 1 & \ldots & 0 \\ \vdots & \vdots & \ddots & & 0 \\ \vdots & \vdots & & 0 & 1 \\ \frac{-\beta_0}{\beta_r} & \frac{-\beta_1}{\beta_r} & \frac{-\beta_2}{\beta_r} & \ldots & \frac{-\beta_{r-1}}{\beta_r} \end{bmatrix} \begin{bmatrix} y \\ \frac{dy}{dt} \\ \vdots \\ \vdots \\ \frac{d^{r-1}y}{dt^{r-1}} \end{bmatrix} + \begin{bmatrix} 0 \\ 0 \\ \vdots \\ \vdots \\ \frac{1}{\beta_r} \end{bmatrix} v. \tag{4.6}$$

This a system of the form,

$$\dot{\zeta} = A\zeta + Bv, \tag{4.7a}$$
$$y = C\zeta, \tag{4.7b}$$

with $\zeta = [\zeta_1, \ldots, \zeta_r]^\top = [L_f^0 h(x), \ldots, L_f^{r-1} h(x)]^\top$. □

Corollary 4.1.3
The input/output behavior of the closed loop system is governed by,

$$\sum_{k=0}^{r} \beta_k \frac{d^k y}{dt^k} = v. \tag{4.8}$$

The transfer function is given by,

$$G_l(s) = \frac{y(s)}{v(s)} = \frac{1}{\beta_r s^r + \beta_{r-1} s^{r-1} + \cdots + \beta_1 s + \beta_0}, \tag{4.9}$$

showing that the coefficients $\beta_{(\cdot)}$ define the poles of the feedback linearized system $G_l(s)$.

In practice, the model parameters in the Lie derivatives of the state feedback law $\Psi(x, v)$ will never exactly match the real process parameters. Therefore, it is usefull to study the situation where some parameters are considered to be uncertain. Define parameter vector $\theta \in \mathbb{R}^p$, which contains p uncertain parameters and which is contained by the set of possible parameter values $\Theta \subset \mathbb{R}^p$. We use $\theta_n \in \mathbb{R}^p$ to represent the nominal parameter vector of the uncertain parameters.

Consider the state dynamics in the system from Equation (4.2) to be uncertain, i.e.:

$$\begin{aligned} f(x, \theta) &= f(x, \theta_n) + f_\delta(x), \\ &= f_n(x) + f_\delta(x). \end{aligned}$$

The resulting state feedback closed-loop system can be approximated by a linear system with additive uncertainty, according to the following theorem based on [Sampath et al., 2002].

Theorem 4.1.4
Consider an input/output linearizable dynamical system under additive uncertainty and relative degree r which is independent of θ:

$$\dot{x}_1 = f_{n1}(x) + f_{\delta 1}(x), \tag{4.10a}$$
$$\dot{x}_2 = f_{n2}(x) + f_{\delta 2}(x) + g(x)u, \tag{4.10b}$$
$$y = h(x), \tag{4.10c}$$
$$x = [x_1, x_2]^\top,$$
$$f_n = [f_{n1}, f_{n2}]^\top, \quad f_\delta = [f_{\delta 1}, f_{\delta 2}]^\top.$$

Define the nominal state feedback law based on the nominal state equations,

$$\Psi_n(x, v) := \frac{v - \sum_{k=0}^{r} \beta_k L_{f_n}^k h(x)}{\beta_r L_g L_{f_n}^{r-1} h(x)}, \tag{4.11}$$

and the nominal coordinate transformation

$$\begin{bmatrix} \eta \\ \xi \end{bmatrix} = \begin{bmatrix} \eta \\ \xi_1 \\ \vdots \\ \xi_r \end{bmatrix} = \begin{bmatrix} x_1 \\ L_{f_n}^0 h(x) \\ \vdots \\ L_{f_n}^{r-1} h(x) \end{bmatrix}. \tag{4.12}$$

Then: By defining $u = \Psi_n(x, v)$ in the system from Equation (4.10), the input/output mapping, $v \mapsto y$, can be written as an uncertain linear system of the form,

$$\dot{\xi} = A(\theta)\xi + Bv + W_d d, \tag{4.13a}$$
$$y = C\xi, \tag{4.13b}$$

where W_d is a linear time invariant weight, $|d| \leq 1$ represents a perturbation and $A(\theta)$ represents the uncertain state matrix.

Proof. Applying the nominal coordinate transformation (4.12) on the uncertain system (4.10) results in the following representation,

$$\begin{aligned}
\dot{\eta} &= f_{n1}(\eta) + f_{\delta 1}(\eta) \\
\frac{d\xi_k}{dt} &= \langle d_x L_{f_n}^{k-1} h, f_n + f_\delta + gu \rangle = L_{f_n}^k h + L_{f_\delta} L_{f_n}^{k-1} h \qquad k = 1, \ldots, r-1, \qquad (4.14) \\
\frac{d\xi_r}{dt} &= \langle d_x L_{f_n}^{r-1} h, f_n + f_\delta + gu \rangle = L_{f_n}^r h + L_{f_\delta} L_{f_n}^{k-1} h + L_g L_{f_n}^{r-1} h(x) u,
\end{aligned}$$

When we apply the nominal feedback law $u = \Psi_n(x, v)$ (4.11), the closed-loop system can be described by,

$$\begin{aligned}
\frac{d\xi_k}{dt} &= L_{f_n}^k h + L_{f_\delta} L_{f_n}^{k-1} h = \xi_{k+1} + L_{f_\delta} L_{f_n}^{k-1} h, \qquad k = 1, \ldots, r-1 \qquad (4.15) \\
\frac{d\xi_r}{dt} &= L_{f_n}^r h + L_{f_\delta} L_{f_n}^{r-1} h + \frac{1}{\beta_r} \left[v - \sum_{k=0}^{r} \beta_k L_{f_n}^k h(x) \right] \\
&= \frac{v}{\beta_r} - \sum_{k=0}^{r-1} \frac{\beta_k}{\beta_r} \xi_{k+1} + L_{f_\delta} L_{f_n}^{r-1} h, \qquad (4.16)
\end{aligned}$$

where we have used $\xi_k = L_{f_n}^{k-1} h$. For convenience, this system of equations can be written in matrix form as follows:

$$\begin{bmatrix} \frac{d\xi_1}{dt} \\ \frac{d\xi_2}{dt} \\ \vdots \\ \vdots \\ \frac{d\xi_r}{dt} \end{bmatrix} = \begin{bmatrix} 0 & 1 & 0 & \ldots & 0 \\ 0 & 0 & 1 & \ldots & 0 \\ \vdots & \vdots & \ddots & & 0 \\ \vdots & \vdots & & 0 & 1 \\ \frac{-\beta_0}{\beta_r} & \frac{-\beta_1}{\beta_r} & \frac{-\beta_2}{\beta_r} & \ldots & \frac{-\beta_{r-1}}{\beta_r} \end{bmatrix} \begin{bmatrix} \xi_1 \\ \xi_2 \\ \vdots \\ \vdots \\ \xi_r \end{bmatrix} + \begin{bmatrix} 0 \\ 0 \\ \vdots \\ \vdots \\ \frac{1}{\beta_r} \end{bmatrix} v + \begin{bmatrix} \Delta_1 \\ \Delta_2 \\ \vdots \\ \vdots \\ \Delta_r \end{bmatrix}$$

$$y = \begin{bmatrix} 1 & 0 & \ldots & 0 \end{bmatrix} \xi,$$

where we have introduced $\Delta_k(\eta, \xi, \theta) = L_{f_\delta} L_{f_n}^{k-1} h(x)$. Contribution from uncertain parameter $\Delta_k(\eta, \xi, \theta) = L_{f_\delta} L_{f_n}^{k-1} h(x)$ depends on η, ξ and θ. To isolate the ξ dependent part, each Δ_k can be written as,

$$\begin{aligned}
\Delta_k &= \frac{\partial \Delta_k}{\partial \xi_1} \xi_1 + \frac{\partial \Delta_k}{\partial \xi_2} \xi_2 + \cdots + \frac{\partial \Delta_k}{\partial \xi_r} \xi_r + \tilde{\Delta}_k(\eta, \xi, \theta) \\
&= \delta_{k1}(\theta) \xi_1 + \delta_{k2}(\theta) \xi_2 + \cdots + \delta_{kr}(\theta) \xi_r + \tilde{\Delta}_k(\eta, \xi, \theta)
\end{aligned}$$

where $\tilde{\Delta}_k$ contains all parts of Δ_k which are not linearly dependent of ξ and is treated as a disturbance term. The closed-loop system can be re-written in matrix form:

$$\begin{bmatrix} \frac{d\xi_1}{dt} \\ \frac{d\xi_2}{dt} \\ \vdots \\ \vdots \\ \frac{d\xi_r}{dt} \end{bmatrix} = \begin{bmatrix} \delta_{11} & 1+\delta_{12} & \delta_{13} & \ldots & \delta_{1r} \\ \delta_{21} & \delta_{22} & 1+\delta_{23} & \ldots & \delta_{2r} \\ \vdots & \vdots & \ddots & & \vdots \\ \vdots & \vdots & & \ddots & 1+\delta_{(r-1)r} \\ \delta_{r1} - \frac{\beta_0}{\beta_r} & \delta_{r2} - \frac{\beta_1}{\beta_r} & \delta_{r3} - \frac{\beta_2}{\beta_r} & \ldots & \delta_{rr} - \frac{\beta_{r-1}}{\beta_r} \end{bmatrix} \begin{bmatrix} \xi_1 \\ \xi_2 \\ \vdots \\ \vdots \\ \xi_r \end{bmatrix} + \begin{bmatrix} 0 \\ 0 \\ \vdots \\ \vdots \\ \frac{1}{\beta_r} \end{bmatrix} v + \begin{bmatrix} \tilde{\Delta}_1(\eta,\xi,\theta) \\ \tilde{\Delta}_2(\eta,\xi,\theta) \\ \vdots \\ \vdots \\ \tilde{\Delta}_r(\eta,\xi,\theta) \end{bmatrix},$$

$$y = \begin{bmatrix} 1 & 0 & \ldots & 0 \end{bmatrix} \xi,$$

where the δ_{ij} are dependent on θ.

For this system a uncertainty model with structured and unstructured uncertainties can be found. This uncertainty model has the space representation,

$$\dot{\xi} = A(\theta)\xi + Bv + W_d d,$$
$$y = C\xi.$$

where $d \in \mathbb{R}^{n+p}, ||d|| \leq 1$, and the matrix $W_d \in \mathbb{R}^{q \times r}$, which is such that $W_d = col(w_{d1}, ..., w_{dr})$ with $w_{d1}^\top \in \mathbb{R}^{n+p}$ and

$$|\tilde{\Delta}_i(\eta, \xi, \theta)| \leq w_{di} d \qquad \text{for all } [\eta, \xi] \in X, \theta \in \Theta \text{ and for all } ||d|| \leq 1.$$

□

With this system representation it is possible to use linear robust control theory for the design of an $\mathcal{H}_\infty$-controller.

4.2 Supersaturation control by feedback linearization

In this section the method of feedback linearization will be employed to derive a control strategy for control of the supersaturation of a batch cooling crystallization process. As mentioned in Section 2.2.3 it is generally assumed that supersaturation is the driving force for crystal growth and of strong influence on nucleation rate. Therefore it is reasonable to expect that by control of the supersaturation in a process in a manner robust to disturbances and model mismatch, the crystal growth and nucleation rate will behave predictable. In this section we start with the introduction of a process model for a batch cooling crystallizer, based on the model introduced in Section 2.3.1. Subsequently we derive the control law for feedback linearization, the disturbance models for robust controller design and we present the design of a H_∞ controller and a linear MPC controller for the feedback linearized system. We analyze the effectiveness of the feedback linearization approach by analysis of the tracking performance and disturbance sensitivity of the controlled feedback linearized system.

4.2.1 Feedback Linearization of the nominal moment model

The non-linear model, introduced in Section 2.3.1, can be written as,

$$\dot{x} = f(x) + g(x)u,$$
$$y = h(x).$$

where the jacket temperature is defined as the system input $u = T_j$ and,

$$f(x) = \begin{bmatrix} B(\mu_3, T) \\ G(\mu_3, T)\mu_0 \\ 2G(\mu_3, T)\mu_1 \\ 3G(\mu_3, T)\mu_2 \\ -\frac{\rho_c k_v}{\rho c_p(\mu_3)} \Delta H_c(\mu_3) 3G(\mu_3, T)\mu_2 - \frac{UA_c}{\rho V c_p(\mu_3)} T \end{bmatrix} \qquad g(x) = \begin{bmatrix} 0 \\ 0 \\ 0 \\ 0 \\ \frac{UA_c}{\rho V c_p(\mu_3)} \end{bmatrix}$$

$$x = \begin{bmatrix} \mu_0 & \mu_1 & \mu_2 & \mu_3 & T \end{bmatrix}^\top \qquad h(x) = S_a(x)$$

We assume that the absolute supersaturation $S_a(x)$ and concentration $c(t)$ can be calculated from the states by the following relations:

$$s_a(x) = c(\mu_3) - c_{sat}(T) \tag{4.17}$$

$$c(t) = c_0 + \rho_c k_v h(\mu_{3,0} - \mu_3(t)) \quad \text{with } c(0) = c_0. \tag{4.18}$$

Here, the initial solute concentration is represented by c_0, ρ_c represents the crystal density, h is a conversion factor equal to the volume of slurry[1] per mass of solvent, and $\mu_{3,0} = \mu_3(0)$.

It is assumed that the initial conditions are defined by,

$$T(0) = T_0,$$

$$\mu_i(0) = \mu_{i,Seed} = \int_0^\infty L^i f_{Seed}(L) dL, \ i = 0, \ldots, 3$$

where $f_{seed}(L)$ represents the CSD at initial time.

The crystal nucleation (birth rate) and crystal growth are assumed to be given by the following empirical expressions, which are based on the relative supersaturation,

$$B(t) = k_b k_v S_r(t)^b \mu_3(t), \tag{4.19}$$

$$G(t) = k_g S_r(t)^g. \tag{4.20}$$

Here, k_b, k_g, b, g, and k_v are defined as respectively, the nucleation coefficient, growth coefficient, nucleation exponent, growth exponent, and the volume shape factor. The birth rate approximates the effects of secondary nucleation.

We assume that the saturation curve, temperature dependent enthalpy of crystallization and concentration dependent heat capacity are known. Typically this kind of data is obtained from quadratic fits of polynomials on measured data and we assume that:

$$c_{sat}(T) = A_0 + A_1 T + A_2 T^2, \tag{4.21}$$

$$\Delta H_c(c) = B_0 + B_1 c + B_2 c^2, \tag{4.22}$$

$$c_p(c) = C_0 + C_1 \left(\frac{c}{1+c} \right) + C_2 \left(\frac{c}{1+c} \right)^2. \tag{4.23}$$

For simulation we have setup a simulation scenario of crystallization of $KNO3$ in a crystallizer with a volume of $1m^3$. The physical properties of $KNO3$ have been taken from [Matthews et al., 1996].

[1] The entire mass of material in the reactor, comprising solvent, solute and solid crystals.

Table 4.1: Data used for setup of simulation scenario with a crystallizer with a volume of $1m^3$.

Simulation parameters	Symbol	Value	Unit
Vessel volume	V	1	m^3
Heat transfer coefficient · area	UA_c	54521	$\frac{J}{min°C}$
Sample time	T_s	1/6	min
Initial conditions	Symbol	Value	Unit
Initial vessel temperature	T_0	57.9894	°C
Initial concentration	c_0	1.0483	$\frac{g(KNO_3)}{g(H_2O)}$
Initial moments	$\mu_0(0)$	$9.75 \cdot 10^7$	$\frac{\#}{V}$
	$\mu_1(0)$	$3.9 \cdot 10^4$	$\frac{m}{V}$
	$\mu_2(0)$	15.6	$\frac{m^2}{V}$
	$\mu_3(0)$	$6.2 \cdot 10^{-3}$	$\frac{m^3}{V}$
Initial mass seed crystals	M_0	13176	g
Initial CSD	$n_{seed}(L,0)$	$n_p e^{\frac{-(\ell-\bar{\ell}_0)^2}{2\sigma^2}}$	#
CSD peak value	n_p	$7.78 \cdot 10^{12}$	#
Mean crystal length	ℓ_0	400	μm
Crystal length standard deviation	σ	5	μm

The first time-derivative of the output depends explicitly on the input u, which makes the relative order $r = 1$. By application of Theorem 4.1.1 it follows that the system is feedback linearizable. A state feedback law can be found by use of Theorem 4.1.2. As done in Equation (4.3), a feedback law is defined as follows:

$$u = \Psi(x, v) = \frac{v - \beta_0 h(x) - \beta_1 L_f h(x)}{\beta_1 L_g h(x)}, \tag{4.24}$$

with

$$\begin{aligned} L_f h(x) &= \left[\frac{\partial h}{\partial \mu_0} \quad \frac{\partial h}{\partial \mu_1} \quad \frac{\partial h}{\partial \mu_2} \quad \frac{\partial h}{\partial \mu_3} \quad \frac{\partial h}{\partial T}\right] f(x) = \frac{\partial h(\mu_3, T)}{\partial \mu_3} f_4 + \frac{\partial h(\mu_3, T)}{\partial T} f_5 \\ &= -3\rho_c k_v h G(\mu_3, T)\mu_2 + \frac{\partial C_{sat}}{\partial T}(T)\left[\frac{\rho_c k_v}{\rho c_p(\mu_3)} \Delta H_c(\mu_3) 3G(\mu_3, T)\mu_2 + \frac{UA_c}{\rho V c_p(\mu_3)} T\right] \\ L_g h(x) &= \left[\frac{\partial h}{\partial \mu_0} \quad \frac{\partial h}{\partial \mu_1} \quad \frac{\partial h}{\partial \mu_2} \quad \frac{\partial h}{\partial \mu_3} \quad \frac{\partial h}{\partial T}\right] g(x) = \frac{\partial h(\mu_3, T)}{\partial T} g_5(\mu_3) \\ &= -\frac{\partial C_{sat}(T)}{\partial T} \frac{UA_c}{\rho V c_p(\mu_3)} \end{aligned}$$

4.2.2 Derivation of a uncertainty model for robust control

Parametric uncertainty is considered for the growth rate parameters in Equation (4.20). That is, we assume

$$k_g = k_{g_n} + W_{kg}\delta_{kg}, \tag{4.25}$$

$$g = g_n + W_g \delta_g, \tag{4.26}$$

where $(k_{g_n}, g_n) \in \Theta \subset \mathbb{R}^2$ is a vector of nominal parameters, and δ_i is a real valued uncertainty with $|\delta_i| \leq 1$. W_{kg} and W_g represent weights to define the uncertainty bound. This implies that the growth rate can be described as a nominal and disturbed part according to,

$$\begin{aligned} G(\mu_3, T) =& k_g S_a^g = (k_{g_n} + W_{kg}\delta_{kg}) S_a^{(g_n + W_g\delta_g)}, \\ =& (k_{g_n} + W_{kg}\delta_{kg}) \left(S_a^{g_n} + \Delta_S\right), \\ =& \underbrace{k_{g_n} S_a^{g_n}}_{G_n(\mu_3,T)} + \underbrace{k_{g_n}\Delta_S + W_{kg}\delta_{kg}\left(S_a^{g_n} + \Delta_S\right)}_{G_\delta(\mu_3,T)}, \end{aligned} \tag{4.27}$$

where $\Delta_S := S_a^{(g_n + W_g\delta_g)} - S_a^{g_n}$. With G_n and G_δ as in Equation (4.27), an uncertain model of the form (4.10) is defined by,

$$\dot{x} = f_n(x) + f_\delta(x) + g(x)u \tag{4.28}$$

$$y = c(x) - c_{sat}(x) \tag{4.29}$$

where,

$$f_n(x) = \begin{bmatrix} B(\mu_3, T) \\ G_n(\mu_3, T)\mu_0 \\ 2G_n(\mu_3, T)\mu_1 \\ 3G_n(\mu_3, T)\mu_2 \\ -\frac{3\rho_c k_v}{\rho}\frac{\Delta H_c(\mu_3) G_n(\mu_3, T)\mu_2}{c_p(\mu_3)} - \frac{UA_c}{\rho V c_p(\mu_3)} T \end{bmatrix} \qquad g(x) = \begin{bmatrix} 0 \\ 0 \\ 0 \\ 0 \\ \frac{UA_c}{\rho V c_p(\mu_3)} \end{bmatrix}$$

$$f_\delta(x) = \begin{bmatrix} 0 \\ G_\delta(\mu_3, T)\mu_0 \\ 2G_\delta(\mu_3, T)\mu_1 \\ 3G_\delta(\mu_3, T)\mu_2 \\ -\frac{3\rho_c k_v}{\rho}\frac{\Delta H_c(\mu_3) G_\delta(\mu_3, T)\mu_2}{c_p(\mu_3)} \end{bmatrix} \qquad x = \begin{bmatrix} x_a \\ \hline x_b \end{bmatrix} = \begin{bmatrix} \mu_0 \\ \mu_1 \\ \hline \mu_2 \\ \mu_3 \\ T \end{bmatrix}$$

The relative order of the system is 1. With a nominal state feedback law as in Equation (4.24) applied to the system and a nominal coordinate transformation defined as $[\eta, \xi_1]^\top = [x_a, h(x_b)]^\top$, a linear system representation is written as in Equation (4.15) and (4.16).

$$\dot{\xi}_1 = -\frac{\beta_0}{\beta_1}\xi_1 + \frac{1}{\beta_1} v + \Delta_1(x_b) d \tag{4.30a}$$

$$y = \xi_1 \tag{4.30b}$$

Where,

$$\begin{aligned} \Delta_1(x_b) =& L_{f\delta} h(x_b) = \frac{\partial h(x_b)}{\partial x_4} f_{\delta 4} + \frac{\partial h(x_b)}{\partial x_5} f_{\delta 5}, \\ =& 3\rho_c k_v G_\delta \mu_2 \left((A_1 + 2A_2 T)\frac{\Delta H_c}{\rho c_p} - h \right). \end{aligned} \tag{4.31}$$

As $\Delta_1(x_b)$ is state dependent, an upper bound is defined by,

$$W_d := \max_{x_b \in \mathcal{X}_r} |\Delta_1(x_b)|, \tag{4.32}$$

which represents the maximum value of Δ_1 over the relevant set of states $\mathcal{X}_r$.

Table 4.2: Parameter uncertainty.

Parameter	Nominal	Interval	Unit
g	1.32	± 0.03	-
$\log_e(k_g)$	8.849	± 0.112	$10^{-6}\frac{m}{min}$

With the final controller the supersaturation will be bounded. Together with the vessel temperature range, this defines a representable set of states that might be encountered during normal process operation. Let

$$\mathcal{X}_r := \{x_b = \begin{bmatrix} \mu_2 \\ \mu_3 \\ T \end{bmatrix} \mid 0 \leq S_a(\mu_3, T) \leq \bar{S}_a, \underline{T} \leq T \leq \bar{T}\}. \tag{4.33}$$

Here $\mu_2 = (\frac{\mu_3}{\mu_{0_{init}}})^{2/3}\mu_{0_{init}}$ is used to estimate the second moment. Figure 4.2 shows the state space representation of the state feedback linearized system where, $A = -\frac{\beta_0}{\beta_1}$, $B = \frac{1}{\beta_1}$ and $C = 1$. W_d is multiplied by B^{-1} to write the system as a nominal plant P_n with a scaled input disturbance.

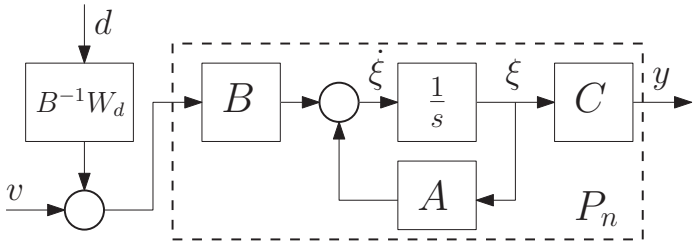

Figure 4.2: Linear representation of the state feedback system as a nominal plant with an input disturbance term

4.2.3 Supersaturation State Feedback Analysis

Simulations are carried out to investigate the effects of parameter mismatch and measurement noise on the linearization performance of the supersaturation state feedback law in Equation (4.24). A desired supersaturation level of $S_d = 2 \cdot 10^{-3}$ is defined to be maintained by the linearized system. The dc-gain of the representing linear system $G_l(s)$ as in Equation (4.9) is given by β_0^{-1}. Setting $v = \beta_0 \cdot S_d$ accommodates an output S_d.

Parameter Mismatch in Growth Kinetics

For this simulation, the growth rate parameters, k_g and g, are assumed to deviate from the nominal parameter values. The nominal values are adopted from [Matthews et al., 1996] and summarized in Appendix E. The estimation confidence region for the parameters is used as a bound on the parameter variation, see table 4.2. The state feedback law $\Psi(x, v)$ depends on the nominal physical parameters of the crystallizer model,

$\theta_n := [k_{g_n}, g_n]$. The real process parameter values are represented by $\theta := [k_g, g]$, where $\theta_n \neq \theta$ due to parameter mismatch.

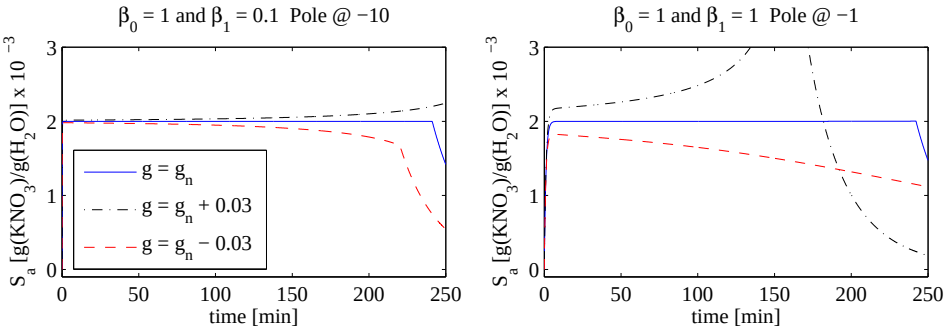

Figure 4.3: Response of the system in three simulations to evaluate the effect of parameter mismatch in growth exponent g. The simulation result shows that the sensitivity to mismatch in g is dependent on the location of the closed loop pole. The sensitivity decreases when the close loop pole moves from the origin.

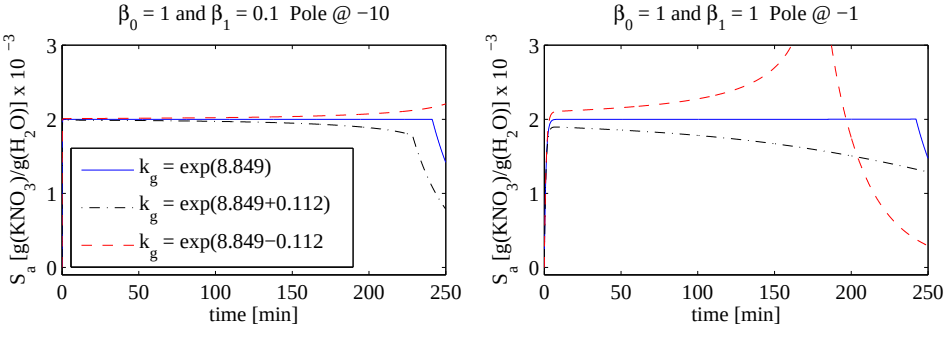

Figure 4.4: Response of the system in three simulations to evaluate the effect of parameter mismatch in growth factor k_g. The simulation result shows that the sensitivity to mismatch in k_g is dependent on the location of the closed loop pole. The sensitivity decreases when the close loop pole moves from the origin.

Figures 4.3 and 4.4 show that parameter mismatch leads to inaccurate linearization. When the real growth rate is smaller than the nominal growth rate in the state feedback law, the response becomes unstable, continuously raising the growth rate in an exponential manner. A larger actual growth rate results in a more conservative feedback law. The closed loop pole, defined by β_0 and β_1, influences how fast the system becomes unstable. With the closed loop pole further in the left half plane, the linearization is less sensitive for parameter variations than for the pole close to the origin.

We can conclude that the linearization performance degrades for parameter mismatch in the growth kinetics. However, this can be compensated by extra feedback control on the supersaturation output, in combination with the proper choice of parameters $(g_n, k_{g_n}, \beta_0, \beta_1)$.

Temperature Measurement Noise

Noise will be present on the available measurements, used in the state feedback linearization function. Noise, which is represented by δ_x in Figure 4.5, is added to the temperature measurement to simulate the effects. The measurement noise δ_x is modeled by white noise, ${\sigma_n}^2 = 0.01°\mathrm{C}$.

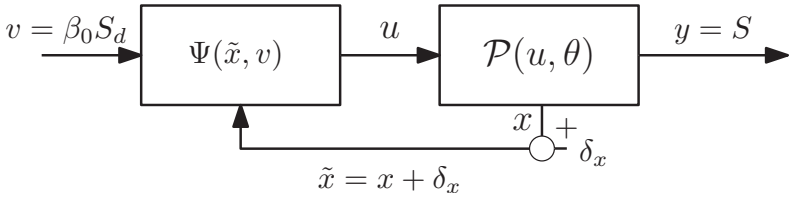

Figure 4.5: State Feedback analysis setup.

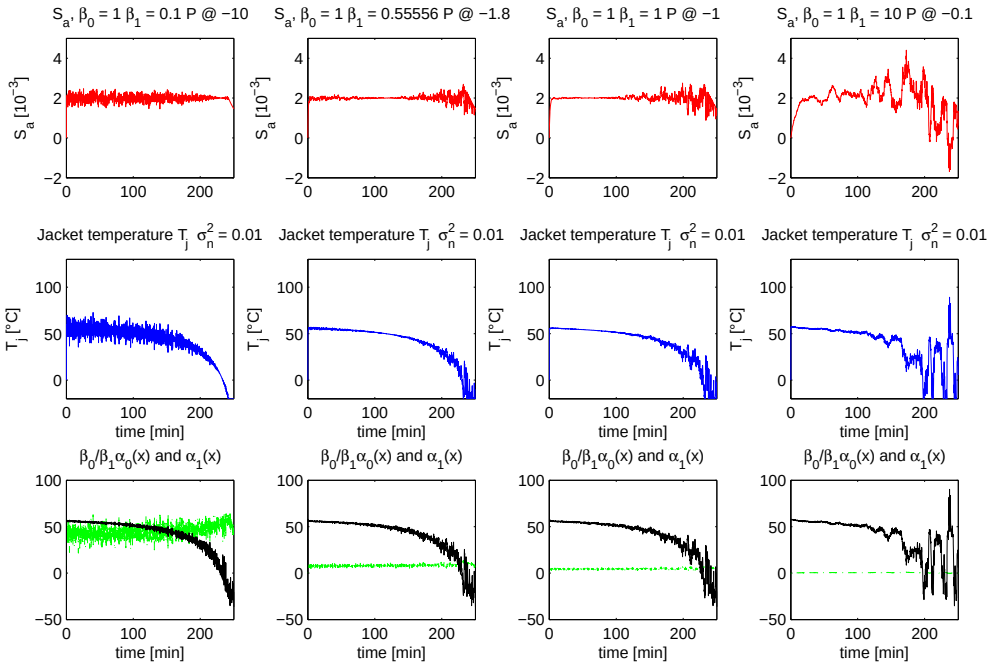

Figure 4.6: Response of the system in state feedback configuration to evaluate the effect temperature measurement noise on the controlled jacket temperature and the resulting supersaturation. The four simulations show the influence of the parameter $\frac{\beta_0}{\beta_1}$ and the contributions of the components α_0 and α_1 (defined in Equation (4.34)) in the output signal of the feedback controller.

From Figure 4.6 is seen that the average jacket temperature is very similar to the optimal temperature profile for a constant supersaturation as proposed in [Miller, 1993]. Additionally, Figure 4.6 shows some remarkable results. The closed loop pole influences the noise sensitivity which is changing during the process. For some regions, measure-

ment noise is completely suppressed, while amplified for other parts during the batch. The source can be found in the construction of the state feedback law. Recall the state feedback law from Equation (4.24), which can be rewritten in terms of $\phi(x)$ and $\alpha(x) = \frac{\beta_0}{\beta_1}\alpha_0(x) + \alpha_1(x)$ by,

$$u = \frac{1}{\beta_1}\underbrace{\frac{1}{L_g h(x)}}_{\phi(x)} v + \frac{\beta_0}{\beta_1}\underbrace{\frac{-h(x)}{L_g h(x)}}_{\alpha_0(x)} + \frac{\beta_1}{\beta_1}\underbrace{\frac{-L_{f_n} h(x)}{L_g h(x)}}_{\alpha_1(x)}. \tag{4.34}$$

Temperature dependency in the $\phi(x)$ term is small and can be neglected for this analysis. The influence of small differences in T can be examined by a first order Taylor expansion for $\alpha(x)$ around x^*,

$$\alpha(x)|_{(x \approx x^*)} = \alpha(x^*) + \frac{\partial \alpha(x)}{\partial T}(x - x^*) + \mathcal{O}^2 \tag{4.35}$$

where

$$\frac{\partial \alpha(x)}{\partial T}(x - x^*) = \left(\frac{\beta_0}{\beta_1}\frac{\partial \alpha_0(x)}{\partial T} + \frac{\partial \alpha_1(x)}{\partial T}\right)(x - x^*). \tag{4.36}$$

From this can be seen that changes in $\alpha(x)$ due to temperature fluctuations are reduced to zero when,

$$\frac{\beta_0}{\beta_1} = -\frac{\partial \alpha_1(x)}{\partial T}\left(\frac{\partial \alpha_0(x)}{\partial T}\right)^{-1}. \tag{4.37}$$

This can be confirmed from Figure 4.6, where the amplitude of fluctuations in $\alpha_0(x)$ is scaled by $\frac{\beta_0}{\beta_1}$ and for some part during the batch cancels the fluctuations in $\alpha_1(x)$.

4.2.4 Advanced Linear Controller design

In the previous section it has been shown that state feedback linearization can be used to linearize the input-output mapping for the absolute supersaturation of the crystallizer model. Two advanced linear controllers are designed, based on the linear system representation to track a desired supersaturation trajectory S_d. First, a robust controller is designed according to the $\mathcal{H}_\infty$ framework. Second, a Model Predictive Controller is designed, making predictions based on the nominal linear system representation.

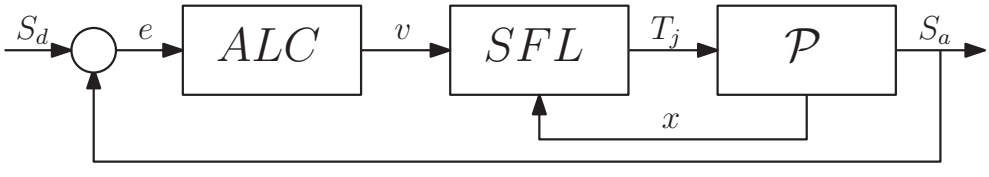

Figure 4.7: Complete control setup, Advanced Linear Control (ALC) combined with State Feedback Linearization (SFL).

$\mathcal{H}_\infty$ Controller Design

A weighted sensitivity setup as in Figure 4.8 is used to design a robust controller. $\mathcal{H}_\infty$-synthesis is used to find a controller K_∞ that optimizes the infinity norm of the closed loop transfer function $\mathcal{T}$,

$$\mathcal{T} = \begin{bmatrix} \mathcal{T}_{d\to\tilde{vd}} & \mathcal{T}_{r\to\tilde{vd}} \\ \mathcal{T}_{d\to\tilde{y}} & \mathcal{T}_{r\to\tilde{y}} \\ \mathcal{T}_{d\to\tilde{e}} & \mathcal{T}_{r\to\tilde{e}} \end{bmatrix} = \begin{bmatrix} W_{vd}SB^{-1}W_d & W_{vd}RW_r \\ W_yTB^{-1}W_d & W_yTW_r \\ W_eTB^{-1}W_d & W_eSW_r \end{bmatrix} \tag{4.38}$$

The sensitivity, complementary sensitivity and control sensitivity are defined respectively as, $S = (I+P_nK_\infty)^{-1}$, $T = P_n(I+P_nK_\infty)^{-1}$ and $R = K_\infty(I+P_nK_\infty)^{-1}$. The weights are chosen to balance the controller performance and robustness. The input filter $W_{vd}(s)$ is high pass to penalize high frequency input signals. The filter on the tracking error W_e is low pass to focus control on low frequency tracking errors. The output filter W_y is set to 0 to focus on sensitivity shaping. The filters are defined as,

$$W_r = 1,\ W_d = 0.1,\ W_{vd} = \frac{15s+10}{s+15},\ W_e = \frac{0.4s+0.4}{s+0.002}.$$

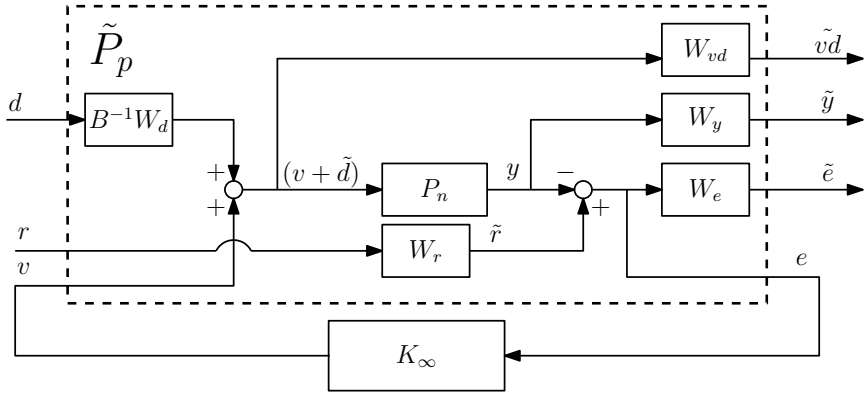

Figure 4.8: Setup for $\mathcal{H}_\infty$-synthesis.

The settings for the $\mathcal{H}_\infty$-controller for $\beta_0 = 1$ and $\beta_1 = 0.5$ are given by,

$$A = -2,\ B = 2,\ C = 1,\ K_\infty \in \mathbb{R}^3,\ \|\mathcal{T}\|_\infty \leq 0.9487.$$

This concludes the design of a robust controller for the state feedback linearized system and accounts for parameter uncertainty in the growth parameters. Simulations results are presented in Section 4.2.5.

Model Predictive Controller Design

A MPC-controller is designed to obtain a control input which minimizes a quadratic cost criterion based on predictions from the nominal linearized model. The nominal linear model P_n, as in Figure 4.2, is discretized using the zero order hold method. The discrete-time state space model is given by $P_d = [A_d, B_d, C_d, D_d]$. To create a cost criterion as a function of input changes $\Delta v_{(k)}$, the discrete-time state space model is transformed into an Incremental Input Output (IIO) model [van den Boom and Stoorvogel, 2010].

$$\begin{bmatrix} y_{(k)} \\ \Delta\xi_{(k+1)} \end{bmatrix} = \begin{bmatrix} I & C_d \\ 0 & A_d \end{bmatrix} \begin{bmatrix} y_{(k-1)} \\ \Delta\xi_{(k)} \end{bmatrix} + \begin{bmatrix} 0 \\ B_d \end{bmatrix} \Delta v_{(k)}$$
$$y_{(k)} = \begin{bmatrix} I & C_d \end{bmatrix} \begin{bmatrix} y_{(k-1)} \\ \Delta\xi_{(k)} \end{bmatrix}$$

which can be written as,

$$\xi_{i(k)} = A_i \xi_{i(k-1)} + B_i \Delta v_{(k)}, \tag{4.39a}$$
$$y_{(k)} = C_i \xi_{i(k-1)}. \tag{4.39b}$$

The quadratic cost criterion comprises the predicted tracking error $e_{(k)}$, and future input changes $\Delta v_{(k)}$. To make the MPC-controller less dependent of the state feedback parameters β_1 in B_i, the input change penalty matrix R is pre- and post-multiplied by $B_i = [0, \frac{1}{\beta_1}]^\top$. This equalizes the contribution of Δv in the tracking error and input-change weighting in the cost function, defined as

$$\mathcal{J}(\xi_{i(0)}, V_\Delta) = e_{(N)}^\top P e_{(N)} + \sum_{k=0}^{N-1} \left(e_{(k)}^\top Q e_{(k)} + \Delta v_{(k)}^\top \tilde{R} \Delta v_{(k)} \right) \tag{4.40}$$
$$V_\Delta = [\Delta v_{(0)}, \Delta v_{(1)}, \ldots, \Delta v_{(N-1)}]^\top$$
$$e_{(k)} = y_{(k)} - r_{(k)} = C_i \xi_{i(k-1)} - r_{(k)}$$
$$\tilde{R} = B_i^\top R B_i$$
$$V_{\text{opt}} = \arg\min_V \mathcal{J}(\xi_{(0)}, V_\Delta) \tag{4.41}$$

The MPC control horizon is chosen to be equal to the prediction horizon given by $N = 60$. The final penalty matrices are given by, $R = 750$, $Q = 1$, and $P = 1$.

Although MPC is famous for taking constraints into account, this is not straightforward in combination with state feedback linearization [Deng et al., 2009]. In some cases, the technique known as constraint mapping is effective [Henson and Seborg, 1997]. In the case of cooling crystallization, actuator constraints are defined for the jacket temperature $T_j = u \in [\underline{u}, \bar{u}]$. After state feedback linearization $u = \phi(x_b)v + \alpha(x_b)$, v has to be such that $u \in [\underline{u}, \bar{u}]$. This introduces nonlinear state dependency into the constraints on the linearized input v.

$$\begin{array}{ccc} \underline{u} \leq & \phi(x_b)v + \alpha(x_b) & \leq \bar{u} \\ \dfrac{\underline{u} - \alpha(x_b)}{\phi(x_b)} \leq & v & \leq \dfrac{\bar{u} - \alpha(x_b)}{\phi(x_b)} \quad \forall\, x_b \in \mathcal{X}_r \end{array}$$

A set of allowed inputs $\mathcal{V}$, satisfying the state dependent constraints over the realistic set of states $\mathcal{X}_r$, is defined by,

$$\mathcal{V} = \left\{ v \in [\underline{v}, \bar{v}] \mid \underline{v} \geq \frac{\underline{u} - \alpha(x_b)}{\phi(x_b)}, \bar{v} \leq \frac{\bar{u} - \alpha(x_b)}{\phi(x_b)} \ \forall x_b \in \mathcal{X}_r \right\}$$

which is empty for $\mathcal{X}_r$ defined by Equation (4.33). The upper and lower bounds $\underline{v}$ and $\bar{v}$ intersect, making it impossible to find bounds satisfying the constraints for the complete set of states.

4.2.5 Simulation results in closed loop configuration

Simulations are carried out to investigate the performance and robustness of linear control techniques on the state feedback linearized system. First the situation of parameter mismatch has investigated by illustrating a tracking problem. Secondly, the noise sensitivity of the control law has been investigated for an external disturbance on the jacket temperature and for measurement noise. For all simulations the jacket temperature is limited to stay between $-20°\mathrm{C}$ and $+130°\mathrm{C}$. To guarantee equal conditions and make comparison more reliable, a fixed noise sequence is used for every simulation. The standard deviation of the tracking error is denoted by σ_e and is used as a measure for controller performance. The tracking error is defined as ($e = S_a - S_d$), where S_a represents the absolute supersaturation, and S_d represents the desired supersaturation trajectory and is represented by the red-dashed line in the figures.

Growth Rate Parameter Mismatch

The same variation of the growth rate parameters is used as in the analysis part in Subsection 4.2.3. The nominal values and upper and lower bounds are given in table 4.2. The nominal state feedback law $\Psi_n(x, v)$ is based on the nominal parameter values. The state feedback parameters are chosen as $\beta_0 = 1$, $\beta_1 = 0.5$, and define a closed loop pole of P_n at -2. The batch time is approximately 4 hours.

Three situations are simulated, case (1) nominal case where [$g = 1.32$, $k_g = \exp(8.849) \cdot 10^{-6}$], case (2) growth rate is smaller than estimated [$g = 1.32 + 0.03$, $k_g = \exp(8.849 - 0.112) \cdot 10^{-6}$], and case (3) growth rate is larger than estimated [$g = 1.32 - 0.03$, $k_g = \exp(8.849 + 0.112) \cdot 10^{-6}$]. Two different supersaturation trajectories are being tracked to check controller stability and tracking performance for all cases.

Figure 4.9 shows the response of the $\mathcal{H}_\infty$- and MPC-controller for the supersaturation output, linear input v, jacket temperature and vessel temperature for a smooth input trajectory. For case (1) and (2) the output tracking is good throughout the complete batch. The standard deviation of the tracking error, which is related to the error weight W_e, for the $\mathcal{H}_\infty$-controller is smaller than 0.15 $mg(KNO_3/H_2O)$. For the MPC controller σ_e is smaller than 0.05 $mg(KNO_3/H_2O)$. The IIO-structure in the cost function $\mathcal{J}$ results in a small steady state tracking error. The ability to anticipate on the input trajectory results in a noncausal output tracking response. From the response of the

linear input v for the nominal case (1), it is seen that the state feedback linearized system indeed behaves as a first order linear system. For case (2) and (3) the growth parameter mismatch cause the linearization to be inaccurate, which is compensated by the linear controllers as can be seen from the response of the linear input v. However, for case (3) the growth rate is higher than estimated. This results in such a fast crystal growth that the cooling rate should be increased beyond the limit of the jacket temperature range to maintain the desired supersaturation trajectory. Therefore, after about 160 minutes the jacket temperature is saturated at $-20°\mathrm{C}$, causing the supersaturation to collapse. The tracking error for case (3) represents the error of the first 160 minutes. Figure 4.10 shows the same responses as in Figure 4.9, only this time for a

Table 4.3: Standard deviation of the output error for the smooth trajectory.

Controller	σ_e (1)	σ_e (2)	σ_e (3)	Unit
$\mathcal{H}_\infty$	1.393	1.195	1.453	$10^{-4}[g_{KNO_3}/g_{H_2O}]$
MPC	0.068	0.263	0.519	$10^{-4}[g_{KNO_3}/g_{H_2O}]$

non-smooth input trajectory. The supersaturation trajectory can be maintained within actuator limits for all parameter variations. Again the tracking error is small, where the MPC controller is very accurate by anticipating on the trajectory and a steady state error of less than $0.001\,mg(KNO_3/H_2O)$ for the response between 60 and 140 minutes. The exponential nature of the saturation curve with respect to temperature can be seen from the vessel temperature response for the nominal case (1). Between 60 and 140 minutes the supersaturation is kept constant. The matching jacket temperature results in a negative exponential temperature drop, theoretically tending towards minus infinity if the supersaturation trajectory was not returning to zero. This emphasizes the fact that the jacket temperature will always reach the actuator limits up to the end of the batch when the desired supersaturation is nonzero.

Table 4.4: Standard deviation of the output error for the non-smooth trajectory.

Controller	σ_e (1)	σ_e (2)	σ_e (3)	Unit
$\mathcal{H}_\infty$	0.648	0.571	0.947	$10^{-4}[g_{KNO_3}/g_{H_2O}]$
MPC	0.053	0.092	0.420	$10^{-4}[g_{KNO_3}/g_{H_2O}]$

Also the inaccurate linearization due to parameter mismatch can be seen from the response of the linear input v. For case (3) both controller outputs v tend towards infinity. However, due to the finite nature of the crystallization process the control output is bounded. Overall, both controllers perform well in the presence of parameter mismatch in the growth parameters.

Jacket Temperature Disturbance

Another possible source of modelling errors can be due to disturbances on the jacket temperature. This can be caused by for example, changes in temperature or pressure of the cooling medium. Actuator disturbance is considered by adding a low frequency

disturbance d_1 to the jacket temperature input, where d_1 is modelled by low-pass filtering of normally distributed white noise (see Equation (4.42) and Figure 4.11).

$$\dot{T} = -\frac{3\rho_c k_v}{\rho}\frac{\Delta H_c(\mu_3)G(\mu_3,T)\mu_2}{c_p(\mu_3)} - \frac{UA_c}{\rho V c_p(\mu_3)}(T - T_j + d_1) \tag{4.42a}$$

$$d_1(s) = \frac{1}{s+0.1}n(s) \tag{4.42b}$$

$$\sigma_n = 0.4^{\circ}\mathrm{C}\ \mu_n = 0 \tag{4.42c}$$

Again the three cases of parameter mismatch where simulated in combination with jacket disturbance. The resulting standard deviation on the output tracking error for both trajectories are given in table 4.5 and 4.6. The supersaturation output and the jacket temperature input response for the smooth reference trajectory of both the $\mathcal{H}_\infty$- and MPC-controller are shown in Figure 4.12.

Controller	σ_e (1)	σ_e (2)	σ_e (3)	Unit
$\mathcal{H}_\infty$	1.417	1.239	1.415	$10^{-4}[g_{KNO_3}/g_{H_2O}]$
MPC	0.299	0.410	0.522	$10^{-4}[g_{KNO_3}/g_{H_2O}]$

Table 4.5: Standard deviation of the output error for the smooth trajectory.

Both controllers manage to achieve a tracking error of less than 0.1 $mg(KNO_3/H_2O)$. From table 4.5 it can be concluded that the MPC-controller is almost four times as accurate as the $\mathcal{H}_\infty$-controller. This is mainly due to the anticipation on the trajectory resulting in a smaller tracking error. For the non-smooth trajectory with less setpoint changes, the difference between MPC- and $\mathcal{H}_\infty$-control is only twice as good, see table 4.6.

This concludes that this approach is able to compensate for low frequency fluctuations in the jacket temperature of industrial batch cooling crystallizers.

Controller	σ_e (1)	σ_e (2)	σ_e (3)	Unit
$\mathcal{H}_\infty$	0.718	0.678	0.904	$10^{-4}[g_{KNO_3}/g_{H_2O}]$
MPC	0.299	0.344	0.394	$10^{-4}[g_{KNO_3}/g_{H_2O}]$

Table 4.6: Standard deviation of the output error for the non-smooth trajectory.

Measurement Noise

Actual noise on the temperature sensor was examined from experimental data, see the blue dashed line in Figure 4.13. The sensor noise is modelled as discrete white noise with $\sigma_n = 0.024^{\circ}\mathrm{C}$. A small part of the noise sequence is shown in Figure 4.13 by the red solid line. The influence of measurement noise is best illustrated by setting the supersaturation reference to a fixed value.

From Figure 4.14 it can be seen that the response is very similar to the uncontrolled constant input case as in Figure 4.6 for the state feedback pole at -1.8. The state feedback law shows to be very sensitive to measurement noise, as was shown in Section 4.2.3. Noise sensitivity of the state feedback law is small only within a certain range of process states. This range can be influenced by changing the state feedback closed loop pole. This gives reason to investigate the performance of a time variant state feedback law and time variant linear controller to exploit the use of different state feedback parameters throughout the batch. In the next section we will study this approach.

Moreover, it is interesting to study what the possibilities and implications are of filtering of the measured variables. One has to take into account that additional filtering might degrade the performance of the feedback linearization due to additional phase delays. This study is beyond the scope of this chapter and is left open for future research.

Time Variant State Feedback

The analysis in Section 4.2.3 showed a strong relation between the noise sensitivity for temperature measurements and the closed loop pole of the linearized system, given by $\frac{\beta_0}{\beta_1}$. The relation was described by Equation (4.37), which represents the closed loop pole for which the noise sensitivity is optimal at a given state x. This is used to determine the optimal poles over the state trajectories of a nominal batch simulation.

We present an approach in which we switch the gain $\frac{\beta_0}{\beta_1}$ in the feedback law by a pre-programmed schedule. By discretizing this optimal pole trajectory, a set of closed loop poles is obtained, which correspond to different linear models $[P_1, P_2, \ldots, P_n] \in \mathcal{P}$. From the optimal pole locations, we will select 5 discrete values. The scheduling method switches between the gains in the feedback linearization law. Figure 4.15 shows the optimal pole trajectory and the discretized set of closed loop poles, defining 5 linear models $(P_1, \ldots, P_5)$. The maximal pole is set to -1, and the minimal pole is set to -10. The blue line indicates which linear model should be used at a given time instant. Figure 4.16 shows the supersaturation output for the time variant MPC (blue solid line), and the MPC with a linear model with the closed loop pole located at -2. Also the linear model planning is shown, indicating at what time instant the time variant MPC switches model.

The result is seen from the supersaturation output and jacket temperature input in Figure 4.16. In the beginning of the batch both controllers use almost the same model, so the response is very similar. However, during the end of the batch the time variant MPC uses a prediction model and feedback law with the pole at -7.5, instead of -2 for the time invariant MPC. This results in a far less aggressive jacket temperature input and less disturbed supersaturation output.

4.2.6 Conclusions and discussion on super saturation control

In this section the application of the state feedback linearization method to batch cooling crystallization has been presented. In order to take parametric model uncertainty

into account a method for uncertainty modeling of a feedback linearized system with uncertain parameter has been introduced. State feedback linearization has been successfully applied and tested in a simulation environment with the nonlinear industrial seeded batch cooling crystallizer model and has shown to provide the ability to use advanced linear control.

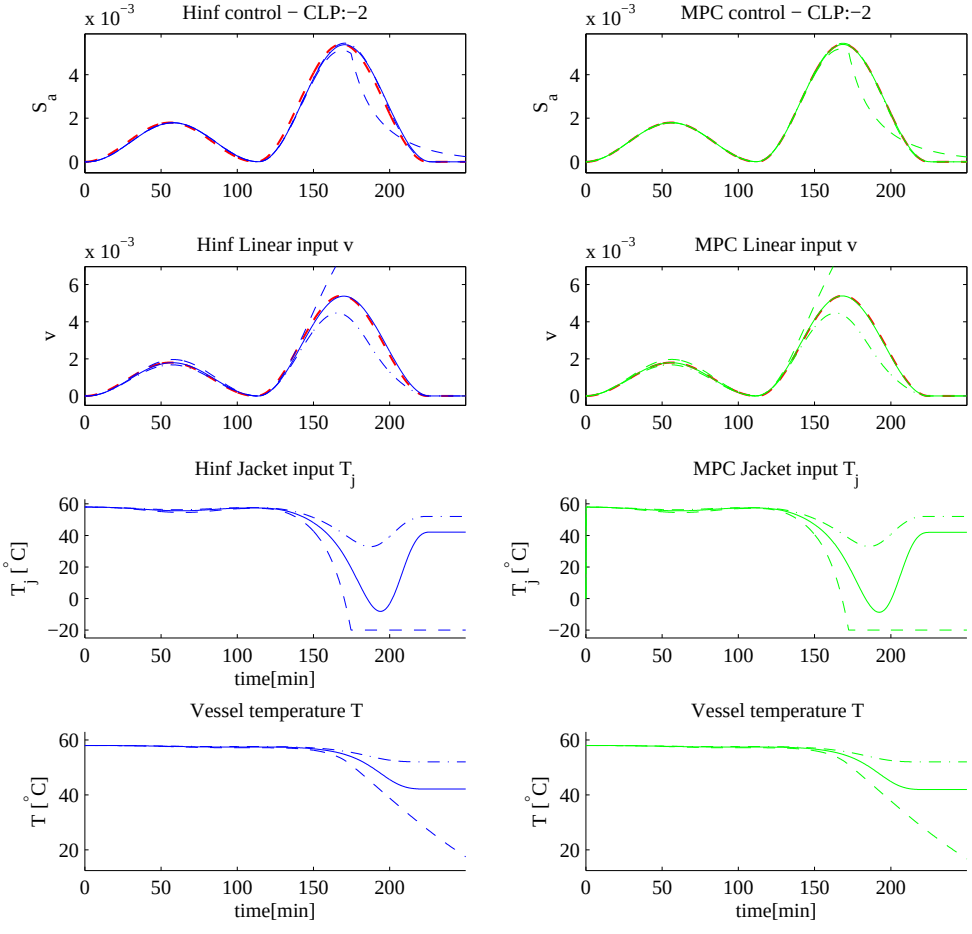

Figure 4.9: Simulation of feedback linearization in combination with MPC and H_infty-control for tracking of a smooth super-saturation trajectory, in absence of measurement noise and in presence of parameter mismatch. Proper tracking is observed for both control methods as long actuator limits are not active. Solid line: case(1), Dash-dotted line: case(2), Dashed line: case(3).

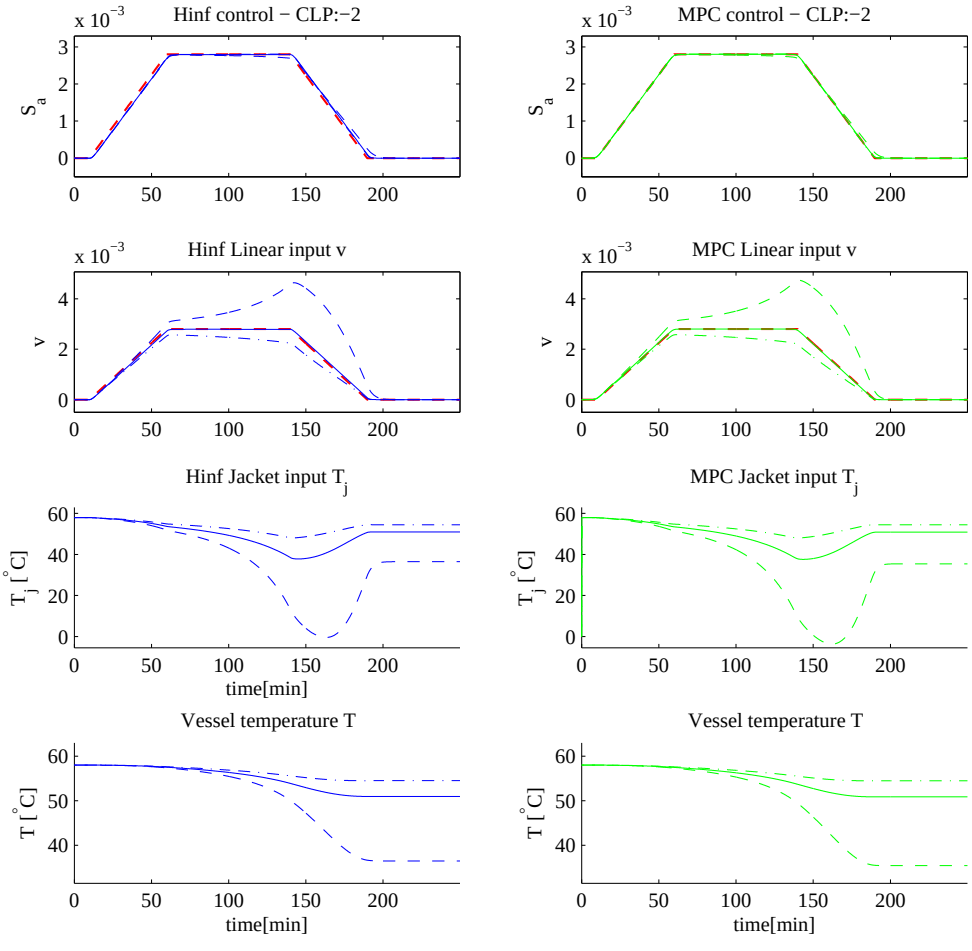

Figure 4.10: Simulation of feedback linearization in combination with MPC and H_infty-control for tracking of a non-smooth super-saturation trajectory, in absence of measurement noise and in presence of parameter mismatch. Proper tracking is observed for both control methods. Solid line: case(1), Dash-dotted line: case(2), Dashed line: case(3).

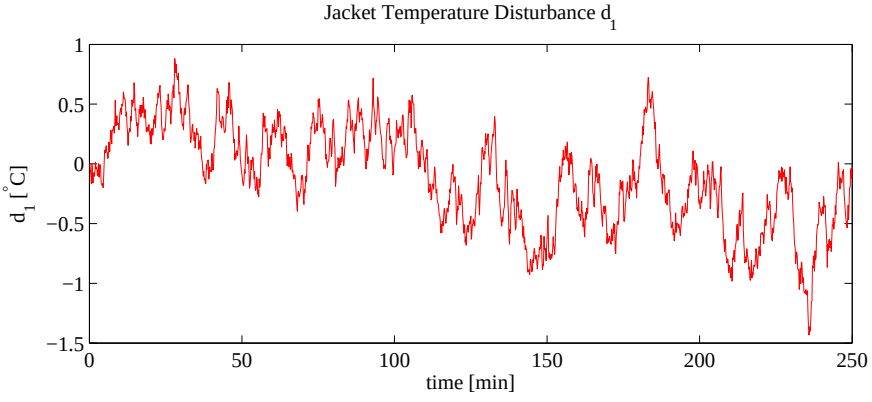

Figure 4.11: Illustrative example of jacket temperature disturbance d_1 used in simulation examples.

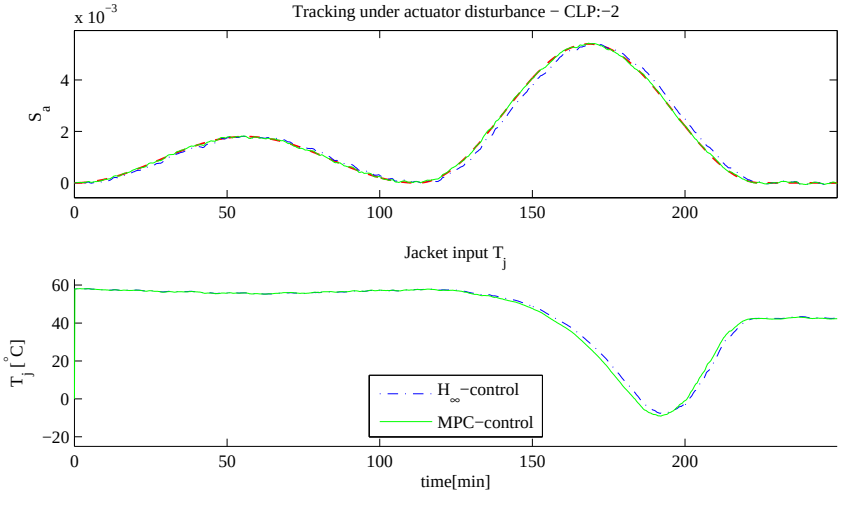

Figure 4.12: Absolute supersaturation and jacket temperature during simulations with jacket temperature disturbance as shown in Figure 4.11. The simulation result shows that the sensitivity of the control setup with respect to disturbances in the jacket temperature are low.

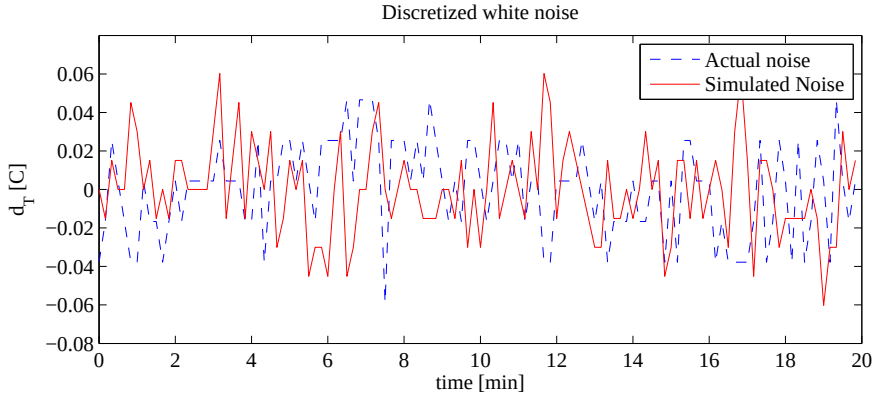

Figure 4.13: Temperature sensor noise as observed in industrial environment and simulated temperature measurement noise used in simulation examples.

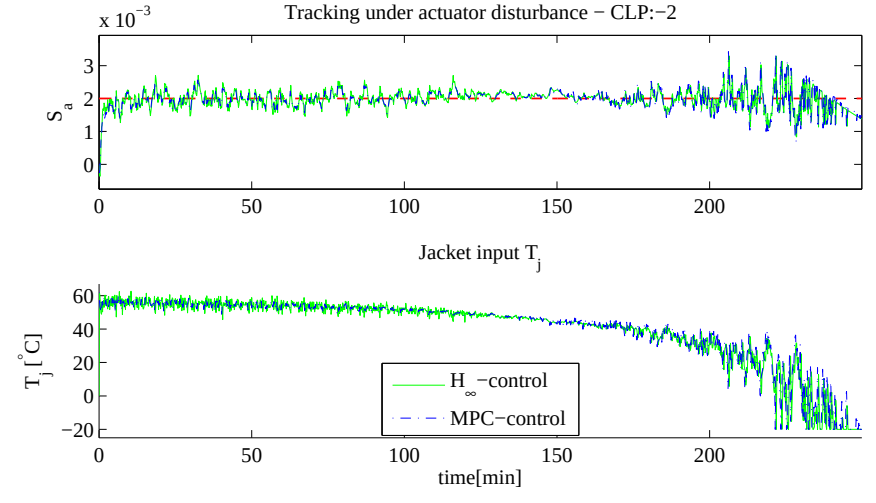

Figure 4.14: Absolute supersaturation and jacket temperature during simulations in presence of temperature measurement noise. The simulation shows that the influence of the temperature measurement noise on the jacket temperature and the resulting absolute supersaturation depends on the time. The sensitivity is maximal during the end of the batch.

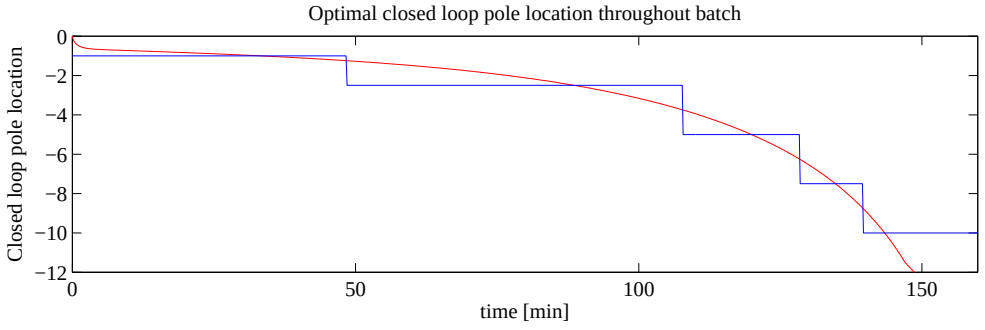

Figure 4.15: Closed loop pole optimal for 5 time instances throughout nominal batch operation. The optimal pole location has been calculated by use of Equation (4.37).

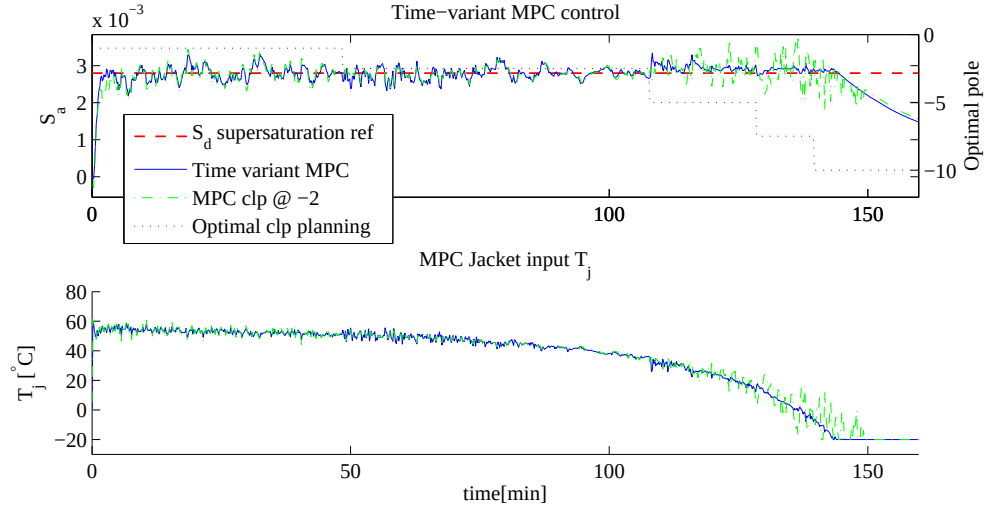

Figure 4.16: Absolute supersaturation and jacket temperature during simulations with a combination of invariant feedback linearization and time invariant MPC and a combination of time variant feedback linearization and time variant MPC following Figure 4.15. The simulation shows that by the time variant approach the sensitivity of the process with respect to the measurement noise can be reduced.

4.3 Control of supersaturation by approximate feedback linearization.

Although various types of model based control technology for batch crystallization have been developed in the past [Braatz, 2002; Nagy and Braatz, 2003; Mesbah, 2010] , industrial acceptation and implementation of these methods is hampered by high costs for the development of the methods and the necessary models as well as the complexity of the methods. Most of these methods do rely on the knowledge of the states of the process, since they are based on state feedback techniques. For crystallization processes, this implies that a reliable online measurement or estimate of both the particle size distribution and the solute concentration are in general necessary for implementation of advanced control methods. In practical situations particle size measurements are difficult to get operational in a industrial environment. Also the crystal growth rate kinetics of a crystallization process might not be known for practical reasons, for instance due to the lack of modeling data or the lack of a particle size measurement. Therefore, it is important to determine to what extent crystallization processes can be controlled with methods that demand a lower level of automation and less information on the process dynamics.

In this section we study the possibilities for tracking control of the absolute supersaturation in absence of measurements of the particle phase. We present a method for supersaturation control, which can be interpreted as approximation of the feedback linearization law (4.24). This method for supersaturation control has been implemented and experimentally validated in a production environment of MSD Apeldoorn during a experimental campaign in December 2011.

In this section we again study a system that can be modeled by the moment model introduced in Section 2.3.1. For simplicity, we assume that the specific heat capacity c_p and crystallization enthalpy H_c are constant. Hence, the model under consideration is given by:

$$\begin{aligned} \dot{x} &= f(x) + g(x)u, \\ y &= h(x), \end{aligned}$$

where the input is the jacket temperature, $u = T_j$ and,

$$f(x) = \begin{bmatrix} B(\mu_3, T) \\ G(\mu_3, T)\mu_0 \\ 2G(\mu_3, T)\mu_1 \\ 3G(\mu_3, T)\mu_2 \\ -\frac{\rho_c k_v}{\rho c_p}\Delta H_c 3G(\mu_3, T)\mu_2 - \alpha T \end{bmatrix} \qquad g(x) = \begin{bmatrix} 0 \\ 0 \\ 0 \\ 0 \\ \alpha \end{bmatrix}$$

$$x = \begin{bmatrix} \mu_0 & \mu_1 & \mu_2 & \mu_3 & T \end{bmatrix}^\top \qquad h(x) = S_a(x)$$

where $\alpha = \frac{UA_c}{\rho V c_p}$. Moreover we introduce the tracking error, as the difference between the reference and realized value:

$$e = r - y. \tag{4.43}$$

We will make use of the observation that during the initial phase of the process, i.e. when $\mu 2$ and μ_3 are small and when operated under low supersaturation, the product $G(\mu_3, T)\mu_2$ is small.

First we make the assumption that $G(\mu_3, T)\mu_2 = 0$. In this situation the control law:

$$u = K \left[\alpha \frac{\partial C_{sat}}{\partial T}(T)\right]^{-1} e + T \tag{4.44}$$

asymptotically stabilizes e for $K < 0$. The variable K is the tuning parameter of the controller and it will be shown to be the time constant of the system under feedback with (4.44). The proof of this assertion follows when one considers the error dynamics, which are given by:

$$\dot{e} = \dot{r} - \dot{y} = \dot{r} - \frac{\partial c}{\partial t} + \frac{\partial C_s}{\partial T}(T)(-\frac{\rho_c k_v}{\rho c_p}\Delta H_c 3 G(\mu_3, T)\mu_2 + \alpha(T_j - T)). \tag{4.45}$$

By substitution of the control law in (4.45) it follows that the closed loop error dynamics satisfy the equation:

$$\dot{e} = Ke + \dot{r} - \frac{\partial c}{\partial t} - \frac{\partial C_s}{\partial T}(T)\frac{\rho_c k_v}{\rho c_p}\Delta H_c 3 G(\mu_3, T)\mu_2.$$

Under the assumption that $G(\mu_3, T)\mu_2 = 0$ (which implies that $\frac{\partial c}{\partial t} = 0$) it follows that the closed loop error system is asymptotically stable and that the time constant is defined by K:

$$\dot{e} = Ke + \dot{r}.$$

Of course, it is important to consider the implications of the assumption $G(\mu_3, T)\mu_2 = 0$. The term $-\frac{\partial c}{\partial t} - \frac{\partial C_s}{\partial T}(T)\frac{\rho_c k_v}{\rho c_p}\Delta H_c 3 G(\mu_3, T)\mu_2$ in Equation (4.45) account for the decrease in concentration due to consumption of solute by crystal growth and the change in supersaturation due to change of temperature of the reactor as a result of the enthalpy uptake or release due to crystallization. For cases that the enthalpy change ΔH_c is small, the effect of the concentration change dominates. As long as the system operates at positive supersaturation, $\frac{\partial c}{\partial t}$ is negative. It follows that for this situations e is remains positive for all t, which indicates that the $r > y$, that is the realized supersaturation is lower than the reference value. Although not ideal, this situation seems acceptable for most industrial applications. For cases in which the enthalpy change ΔH_c is not negligible and positive, the total contribution of the term is again negative. The same reasoning applies and therefore the realized supersaturation will be lower than the reference value. For cases in which the enthalpy change ΔH_c is not negligible and negative, the contribution of $-\frac{\partial c}{\partial t} - \frac{\partial C_s}{\partial T}(T)\frac{\rho_c k_v}{\rho c_p}\Delta H_c 3 G(\mu_3, T)\mu_2$ can be positive as well as negative and not decisive answer can be given in general.

Although the control law (4.44) does not provide perfect tracking for all scenarios, it also has important positive properties. First of all, the control law does not desire kinetic data of the crystallization process. The saturation curve and an estimate of the thermal constant is the only necessary information for implementation. Secondly, no information about the first three moments is necessary. Therefore a measurement or estimator of

these moments does not have to be present for implementation. These two properties make that the control law can be implemented with less effort and cost than is necessary for the implementation of more advanced control methods.

It might be of interest to reconsider the feedback linearization law (4.24) in this context. It follows that the presented approach is equivalent to application of an approximation of this state feedback law in combination with a P-controller. For completeness we repeat (4.24):

$$u = \psi(x, v) = \frac{v - \beta_0 h(x) - \beta_1 L_f h(x)}{\beta_1 L_g h(x)}.$$

Under the assumption that $G \approx 0$ and $\mu_2 \approx 0$, the Lie-derivatives $L_f h(x)$ and $L_g h(x)$ can be approximated by:

$$L_f h(x) \approx \alpha \frac{\partial C_{sat}}{\partial T}(T) T \qquad L_g h(x) \approx -\alpha \frac{\partial C_{sat}}{\partial T}(T) \tag{4.46}$$

The feedback linearization law $\psi(x, v)$ can be approximated by $\tilde{\psi}(x, v)$:

$$\tilde{\psi}(x, v) = \frac{v - \beta_0 h(x) - \beta_1 \alpha \frac{\partial C_{sat}}{\partial T}(T) T}{-\beta_1 \alpha \frac{\partial C_{sat}}{\partial T}(T)} = \beta_1^{-1} \left[\alpha \frac{\partial C_{sat}}{\partial T}(T) \right]^{-1} (\beta_0 h(x) - v) + T.$$

Careful comparison of the approximate feedback law $\tilde{\psi}(x, v)$ with the controller given by Equation (4.44) shows that both laws are identical when $v = \beta_0 h(x) + K\beta_1 e$ is substituted in $\tilde{\psi}(x, v)$. The identity v can be interpreted as proportional feedback of the error combined with a feed forward term, which follows from rearrangement of v:

$$v = [\beta_0 - K\beta_1]\, h(x) + K\beta_1 r.$$

4.3.1 Implementation and experimental test

The controller given by Equation (4.44) has been implemented in a industrial environment of MSD Apeldoorn. A general purpose reactor with a volume of $1000L$ has been used as experimental environment, shown in Figure 4.19. The crystallizer is a stirred tank stainless steel reactor, equipped with combined cooling and heating jacket, vacuum and pressure regulation system and temperature measurement in the bottom and standard DCS for data acquisition.

The controller has been tested during one seeded batch experiment on a volume of $900L$ with the pharmaceutical compound Androsta-1,4-diene-3,17-dione,cyclic 17-(2,2-dimethyltrimethylene acetal), abbreviated as $ADD - NEOP$. The solvent is a mixture of pure ethanol (99.5% v/v) and triethyl amine (0.5% v/v). The latter is added as a stabilizer.

The required temperature measurements of the reactor and jacket temperature are acquired from the DCS system and the concentration measurements are acquired with

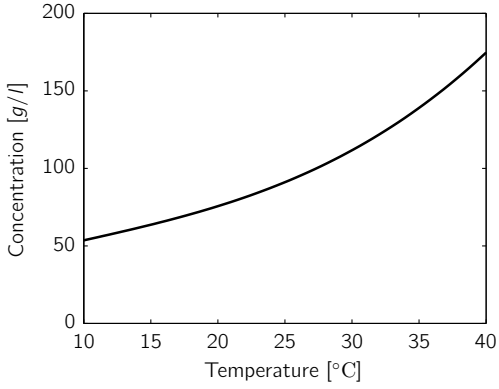

Figure 4.17: Solubility of $ADD - NEOP$.

a K-Patents PR-23 refractive index sensor. The concentration sensor has been mounted on a measurement skid, which is presented in Section 2.4 and has been developed in the context of the project. The solubility of $ADD - NEOP$ has been determined by a dissolution experiment in which the crystallized compound has been dissolved by a slow linear increase of the solvent temperature. A parametrization of the solubility as function of the literature $C_s(T)$ been obtained by a least square fit of a third order polynomial function on the measured temperature and concentration data, which has resulted in the following polynomial:

$$C_s(T) = 32.68 + 2.468T - 5.912 \cdot 10^{-2}T^2 + 2.155 \cdot 10^{-3}T^3.$$

A graph of the modelled solubility function $C_s(T)$ of $ADD - NEOP$ measured solubility given in Figure 4.17.

The control law has been implemented in the INCA software environment from IPCOS B.V.. The saturation controller has been implemented as master controller, in a master/slave configuration with a controller for the jacket temperature. The slave controller is digitally implemented PID-controller with a sample time of 5 seconds. Figure 4.18 shows a schematic representation of the implemented control architecture. The time constant α of the thermal dynamics of the reactor has been estimated with a step test using the jacket temperature to be approximately 20 minutes. The tuning parameter K of the controller was set to 900 seconds.

During the experiment the approximately 100 Kg of $ADD - NEOP$ was crystallized from solution. Figure 4.20 shows the measured supersaturation and its reference. The figure shows the tracking of the desired supersaturating after the controller was turned on at 10:40h. Step changes in the reference profile have been applied to shown the convergence of super saturation to the setpoint. True first order behavior is observed from tracking of changes of the set- point and the time constant of the closed loop indeed approximately matched the value of K. At 13:30h approximately the measured saturation does not meet the expectations. Sensor fouling is the most likely cause. The sensor recovered due to immediate additional heat supply to the sensor using thermal tracing system of the skid.

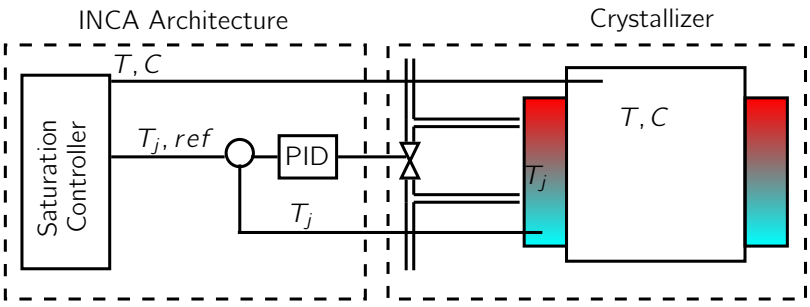

Figure 4.18: Schematic representation of the control architecture that has been implemented for test of the supersaturation controller.

4.3.2 Conclusions

A system for online regulation of the supersaturation during batch cooling crystallization has been presented. The presented approach is of lower complexity than previously developed methods. Furthermore, it is based on concentration measurements only and therefore it might be cheaper and easier to implement.

The presented control method is based only on the solubility curve of the solid/solvent combination in the process and no kinetic information is needed to design the control law. This makes the implementation in industrial environment feasible, since a need for determination of kinetic laws or parameters would demand additional experiments and increase the costs significantly. The solubility can be calculated online from the temperature measurement and the concentration can be measured using relatively cheap equipment.

Experimental results show the system can be applied successfully in an industrial environment. The control method enables proper control of the supersaturation in a crystallization process for situations where material consumption is small. Therefore the method is effective for start up phases of batch processes. Also for processes with material consumption reasonable performance can be expected, but a supersaturation that is lower than the reference value will be realized.

4.3.3 Recommendations

The experiment for validation of the supersaturation controller has been carried out only in one experiment. Although this single experiment is sufficient to show the effectiveness of the controller method for supersaturation control, it has not been possible to study the effect of supersaturation control on the product quality in this experimental campaign. In order to demonstrate a positive effect of tight supersaturation control on product quality, an experimental campaign with a statistically significant number of experiments and the possibility to evaluate and quantify product quality has to be carried out.

Figure 4.19: General purpose reactor *HR4RES12* at former plant of MSD Apeldoorn.

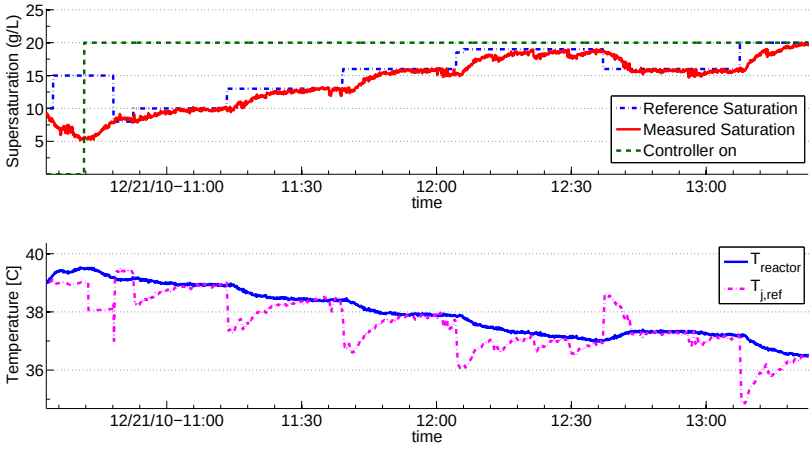

Figure 4.20: Step response test with designed supersaturation controller.

4.4 Conclusion and recommendations on supersaturation control

In this chapter a method for the control of the supersaturation level in batch cooling crystallization processes has been presented.

4.4.1 Conclusions

The method is based on the feedback linearization of the nonlinear map between the jacket temperature and the supersaturation level, (i.e. the input output map described by the model for batch cooling crystallization processes) by use of a state feedback law. The effectiveness of the method has been analyzed in a theoretical analysis. It follows that after feedback linearization, the input/output map can be described by a first order linear system. In the analysis, special attention has been paid to the effect of modeling errors on the feedback linearization.

It has been shown that supersaturation feedback control is able to accurately compensate for errors in the supersaturation response, even in the presence of parameter mismatch or process disturbances. This results in reliable batch process control, which is of key importance for high-quality products and larger economical benefit. Moreover, the presented method provides a flexible approach where a process operator can directly manipulate the supersaturation level and allows the operator to design a customized supersaturation trajectory. There is no need for a supersaturation to temperature trajectory transformation to generate a proper input that can be used in conventional temperature control as in [Sampath et al., 2002], [Zhang, 2003].

The effectiveness of the presented control approach has been evaluated in a experiment, that is representative for industrial environments. In the experiment an approximation of the control law has been implemented. The control law has been approximated in such a way that only a concentration measurement is needed for implementation. The experiment shows that in the initial stage of the batch crystallization process (i.e. when the consumption rate is low) proper control of the supersaturation level can be achieved.

4.4.2 Recommendations

The method for supersaturation control by feedback linearization is a method based on nonlinear state feedback. Therefore, the availability of the complete state of the moment model is assumed in the analysis. In practical applications the state variables might not be measurable due to lack of sensors. In such a situation feedback linearization has to be applied in combination with a state observer for the process. The estimate of the state will be inherently subject to an estimation error. It is of importance to analyze what the influence of the estimation error is on the method of feedback linearization. We have not presented this analysis, which is open for future research.

In this chapter we have studied the sensitivity of the feedback linearized model with respect to sensor noise in the temperature measurement. The effect of sensor noise shows to be signification and not negligible. We have not paid attention to sensor noise and static errors in the measurement of the moment μ_2 and μ_3. It is recommended to perform this analysis in future research.

The analysis has shown that by feedback linearization can result in control input to the process which contain fast and aggressive control actions. It has been shown that this can be due to amplification of the sensor noise. Given the rather slow thermal dynamics of the process and the fact that the process dynamics change much slower than the noise component in the measurement signal, one can question the necessity of the presence of fast components in the input for the linearization performance of the feedback system. Therefore, it is interesting to study what the possibilities and implications are of filtering of the measured variables. One has to take into account that additional filtering might degrade the performance of the feedback linearization due to additional phase delays.

CHAPTER 5

Estimation for Distributed Parameter Systems

Abstract

This chapters considers the problem of designing estimators to estimate non-measured outputs of infinite dimensional systems on which a finite number of measurements are taken in real-time. The design of estimators will be treated as an optimization problem in which the estimation error is minimized. In this optimization problem the performance of the estimators is measured either by the Hilbert-Schmidt norm or by the induced L_2-gain of the error-system. It is shown that for those criteria, both optimization problems are equivalent to a dual regulator design problem. For both problems, a complete solution is derived which, in turn, provides explicit solutions of the optimal estimator design problems.

5.1 Introduction

Distributed parameter systems occur in numerous engineering applications. The problem of estimating non-measured outputs in a distributed system is of key importance to infer information of system variables from partial information. Partial information is typically based on measurements or observed outputs and can be inferred from sensors or measurements. One typically distinguishes estimation from filtering problems. Estimation problems are concerned with the (optimal) approximation of non-observed

variables from measurements. Filtering problems deal with the estimation of state variables. Both estimators and filters infer estimates of variables in a causal manner from observed data. This means that estimates of non-measured variables will not depend on anticipated (or future) values of the measured quantities, which is a necessity when one desires to operate the estimator or filter in an real-time environment. The development of non-causal filters has not been covered in this chapter. We will illustrate the necessity of estimators for infinite dimensional system by two examples. The first one is motivated by the research on crystallization processes. The second one concerns an example of temperature estimation in materials.

Example 5.1.1 (Crystal population estimation)
Consider a crystallizer with a population of particles, characterized by the size distribution $n(\ell, t)$ *where* ℓ *is the particle length and* t *is time. The crystallizer is equipped with a number of sensors, which are able to count the number of crystals that are present in the reactor and whose length (or size) is in a specific range. See Figure 5.1, where* y_i *denote the measurements and* z_1 *is the crystal size of interest. The evolution of the population can be modeled by crystallization models as presented in Section 2.15. This gives the time-varying length distribution* $n(\ell, t)$*. One is interested in a reconstruction of the actual population balance* $n(\ell, t)$ *from a finite number of measurements* $y_1, \ldots, y_n$ *where* $y_i(t) = \int_{\ell_i^-}^{\ell_i^+} n(\ell, t)\mathrm{d}\ell$ *represents a counter for a sensor that considers particle sizes of length* ℓ *with* $\ell_i^- \leq \ell \leq \ell_i^+$ *only.*

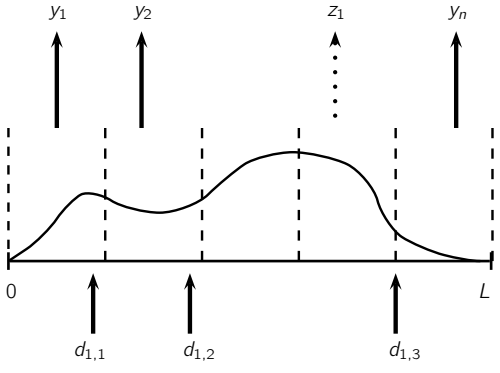

Figure 5.1: Output estimation problem on crystal size population in crystallization processes.

As a second example we introduce the following (fictitious, but rather realistic) example.

Example 5.1.2 (Heat diffusion)
Consider a one dimensional slab of a semiconductor on the domain $[0, L]$*, as depicted in Figure 5.2 with heat producing elements such as transistors distributed over the domain. Due to diffusion, heat that is locally produced will spread trough the slab. This can be modeled by Fouriers law of heat diffusion. The slab is equipped with n (non-collocated) temperature sensors distributed over the slab and which measure the temperature* y_i *at a specific location of the slab. One is interested in estimating the temperature at the non-measured locations indicated by* z_i*, so as to monitor the condition of the components.*

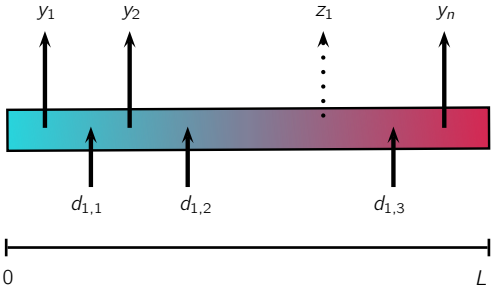

Figure 5.2: Output estimation problem on heat diffusion problem.

A nice feature of the framework of estimation in infinite dimensional systems that we will consider here, is that it is applicable to all kinds of engineering problems that involve spatial-temporal systems. In abstract form, the estimation problem is depicted in Fig. 5.3. It involves a given dynamical system that is affected by noise and that produces noise-corrupted measurements y, which are subsequently used to estimate a non-observed signal z. The estimator to be designed is a causal system that processes measurements y to estimates $\hat{z}$ of z. In this chapter we present a complete solution to the problem of synthesizing output estimators for linear distributed parameter systems that are optimal in the sense that they either minimize the Hilbert-Schmidt norm or the L_2-gain of the system that generates the estimation error. The optimal estimators will be called the optimal Hilbert-Schmidt norm output estimator and optimal L_2-gain output estimator for linear distributed parameter systems, respectively. Both design criteria will be discussed in detail in Section 5.2.

The chapter is organized as follows. A precise formulation of the estimator design problem is given in Section 5.2. Then we will introduce an alternative formulation of the plant Σ_p, which enables to formulate the estimator design problem in a more convenient mathematical framework. The connection between estimation and control problems will be studied in Section 5.4 and is at the basis of a duality result that we will derive first. In this Section we will also develop the mathematical tools that enable deriving solutions for estimation problems from control problems. In Section 5.5 the estimation problem for Hilbert-Schmidt norm criterion will be solved and in Section 5.6 the estimation problem for the L_2-gain criterion will be solved.

For finite dimensional systems it is known that there is a strong relation between estimation and control problems, which is usually evidenced using arguments from duality

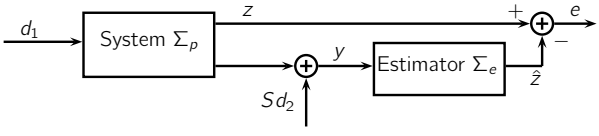

Figure 5.3: Interconnection of plant and estimator.

theory. This relation is studied for instance in [Mutsaers and Weiland, 2009] for finite dimensional systems and in [Vissers and Weiland, 2010] for an estimator design for distributed parameter systems based on the Hilbert-Schmidt norm criterion. In this chapter, we will generalize these results to infer a complete solution of the optimal L_2-gain estimator design problem in an infinite dimensional setting.

5.1.1 Notation:

We denote the inner product associated with a Hilbert space X by $\langle\,,\,\rangle$. With $\mathbb{T} \subseteq \mathbb{R}$ a time set, the induced inner product on $L_2(\mathbb{T}, X)$ is denoted by $\langle\langle\,,\,\rangle\rangle$. That is, for $x, x' \in L_2(\mathbb{T}, X)$ $\langle\langle x, x'\rangle\rangle = \int_{\mathbb{T}} \langle x(\tau), x'(\tau)\rangle \mathrm{d}\tau$. We use $||\cdot||_2$ to indicate the 2-norm on X as well as the 2-norm on $L_2(\mathbb{T}, X)$. For a operator $B : L_2(\mathbb{T}, X) \to L_2(\mathbb{T}, X)$, its induced 2, 2-norm is the smallest number α for which $||Bx||_2 \leq \alpha ||x||_2$ for all $x \in L_2(\mathbb{T}, X)$. Also, $\mathbb{R}^{n\times m}$ is equipped with the structure of an inner product. The inner product on elements of $\mathbb{R}^{n\times m}$ is denoted by $\langle M_1, M_2\rangle = \mathrm{tr}\, M_1^* M_2$ where tr represents the trace. Let $\mathcal{M}$ denote the function space $L_2(\mathbb{T}\times\mathbb{T}, \mathbb{R}^{n\times m})$ with inner product $\langle\langle M_1, M_2\rangle\rangle = \iint_{\mathbb{T}\times\mathbb{T}} \langle M_1(\tau_1, \tau_2), M_2(\tau_1, \tau_2)\rangle \mathrm{d}\tau_1 \mathrm{d}\tau_2$ and corresponding norm $||M||_2 = \langle\langle M, M\rangle\rangle^{\frac{1}{2}}$. Moreover we introduce the time restriction operator

$$\sigma_\tau : L_2(\mathbb{T}, X) \to L_2(\mathbb{T}, X)$$

for $\tau \in \mathbb{R}^+$ by :

$$(\sigma_\tau x)(t) = \begin{cases} x(t) & \text{for } t \leq \tau, \\ 0 & \text{for } t > \tau. \end{cases}$$

5.2 Problem statement

Let X be a Hilbert space, and let $Y = \mathbb{R}^m$, $Z = \mathbb{R}^n$, $D_1 = \mathbb{R}^{d_1}$ and $D_2 = Y$ be Euclidean spaces equipped with the standard inner product. Consider the system Σ_p with states $x(t) \in X$, outputs $z(t) \in Z$, measurements $y(t) \in Y$ and disturbances $d_1(t) \in D_1$, $d_2(t) \in D_2$, given by:

$$\Sigma_p : \begin{cases} \dot{x} = Ax + Gd_1 \\ y = Cx + Sd_2 \\ z = Hx \end{cases} \tag{5.1}$$

The operator $A : D(A) \to X$ is a linear (possible unbounded) operator and A is the generator of a strongly continuous semi-group operator $T(t) : X \to X$. In this work we consider time instants $t \in \mathbb{T} = [0, t_e]$ with $t_e \in [0, \infty)$. It is assumed that $T(t)$ is exponentially stable, i.e. there exists positive constants α and M such that for all $x_0 \in X$, $||T(t)x_0|| \leq Me^{-\alpha t}||x_0||$ for all $t \in \mathbb{T}$. Moreover, we assume that the pair (A, C) is $\mathbb{T}$-observable, which means that $x_0 = 0$ whenever $CT(t)x_0 = 0$ for all $t \in \mathbb{T}$. Let the disturbances be $d_1 \in L_2(\mathbb{T}, D_1)$ and $d_2 \in L_2(\mathbb{T}, D_2)$.

Remark 5.2.1. In this setting, the output $z(t)$ represents the signal to be estimated. The outputs z are not measurable in practice at the process and are here only used to formulate the estimator design problem, cf. Figure 5.3

We introduce a second system Σ_e, called the estimator, which is the realization of a linear mapping $L_2(\mathbb{T}, Y) \to L_2(\mathbb{T}, Z)$. The estimator is connected to Σ_p, as shown in Figure 5.3 and the estimation error is defined as $e = z - \hat{z}$. We allow Σ_e to be time variant and demand that it is causal and such that it can be represented by the input/output-map:

$$\Sigma_e(M) : \hat{z}(t) := \int_0^t M(t,\tau) y(\tau) \mathrm{d}\tau, \tag{5.2}$$

where integration kernel M is required to be in the class $\mathcal{M}$, which is defined by:

$$\mathcal{M} = \left\{ M \in L_2(\mathbb{T} \times \mathbb{T}, \mathbb{R}^{\dim(Y)\times\dim(Z)}) \mid M(t,\tau) = 0 \text{ whenever } \tau > t \right\}.$$

We indicate the parametrization of the estimator with respect to M by $\Sigma_e(M)$ when this is convenient.

Remark 5.2.2. Depending on the application, the initial condition x_0 in (5.1) is assumed to be known or unknown. We will treat both cases. The case in which x_0 is known is without loss of generality covered by the case in which $x_0 = 0$. This can be seen as follows. If we assume that x_0 is known, it follows that the outputs $y(t)$ and $z(t)$ are given by:

$$\begin{bmatrix} y(t) \\ z(t) \end{bmatrix} = \begin{bmatrix} y_0(t) \\ z_0(t) \end{bmatrix} + \begin{bmatrix} y_d(t) \\ z_d(t) \end{bmatrix},$$

with:

$$\begin{bmatrix} y_0(t) \\ z_0(t) \end{bmatrix} = \begin{bmatrix} C \\ H \end{bmatrix} T(t) x_0, \qquad \begin{bmatrix} y_d(t) \\ z_d(t) \end{bmatrix} = \int_0^t \begin{bmatrix} C \\ H \end{bmatrix} T(t-\tau) G d_1(\tau) \mathrm{d}\tau + \begin{bmatrix} S \\ 0 \end{bmatrix} d_2(t).$$

It follows that y_d and z_d are solutions of (5.1) with $x_0 = 0$. Let $\hat{z}_d$ be the output of an estimator for the case with $x_0 = 0$ and define $\hat{z}(t) := \hat{z}_d(t) + HT(t)x_0$. It follows that $e = z - \hat{z} = z_d - \hat{z}_d$. Consequently, the error is equal to the error in case in which $x_0 = 0$. That is, an estimator for the case with $x_0 \neq 0$ can be constructed from an estimator for the case where $x_0 = 0$, by addition of $HT(t)x_0$ to the estimate for z_d.

Depending on whether x_0 is assumed to be known or unknown, the system Σ_p defines a mapping $L_2(\mathbb{T}, D_1 \times D_2) \to L_2(\mathbb{T}, Y \times Z)$ or $X \times L_2(\mathbb{T}, D_1 \times D_2) \to L_2(\mathbb{T}, Y \times Z)$, respectively. In either case, $\Sigma_p(d_1, d_2)$ or $\Sigma_p(x_0, d_1, d_2)$ is defined by the output (y, z) of (5.1) with $x(0) = 0$ and $x(0) = x_0$, respectively, and disturbance input d_1 and d_2.

The interconnection of Σ_p with Σ_e, denoted by $\Sigma_p \wedge \Sigma_e$ is defined by the transfer between the disturbances d_1 and d_2 and the error e. More precisely, the composite system is defined by the mapping

$$\Sigma_p \wedge \Sigma_e : X \times L_2(\mathbb{T}, D_1 \times D_2) \to L_2(\mathbb{T}, Z)$$

if x_0 is unknown and by

$$\Sigma_p \wedge \Sigma_e : L_2(\mathbb{T}, D_1 \times D_2) \to L_2(\mathbb{T}, Z)$$

if x_0 is known. The explicit characterization of $\Sigma_p \wedge \Sigma_e$ for the case of an unknown initial conditions is given by:

$$e(t) = z(t) - \hat{z}(t) = Hx(t) - \int_0^t M(t,\tau)(Cx(\tau) + Sd_2(\tau))\mathrm{d}\tau, \tag{5.3a}$$

$$\text{with:} \quad x(t) = T(t)x_0 + \int_0^t T(t-\tau)Gd_1(\tau)\mathrm{d}\tau. \tag{5.3b}$$

The characterization of $\Sigma_p \wedge \Sigma_e$ for the case of known initial conditions can be obtained analogously by setting $x_0 = 0$ in (5.3b).

In order to deal (in a systematic manner) with the question how the estimator Σ_e should be designed or synthesized, we specify the requirements on the interconnection of the estimator and the plant. A possible way to do this is to specify performance requirements on the operator that implements the mapping $\Sigma_p \wedge \Sigma_e$. In this chapter we will use norms on $\Sigma_p \wedge \Sigma_e$ to define the design problem. Specifically, we introduce the design criterion $J(M)$:

$$J(M) = ||\Sigma_p \wedge \Sigma_e(M)||,$$

for different norms on the operator $\Sigma_p \wedge \Sigma_e(M)$. We distinguish the following design problems:

Problem 5.1 (Determination of infimum)
For the case of known and/or unknown initial condition of (5.1)*, find* γ^{opt} *such that*

$$\gamma^{opt} = \inf_{M \in \mathcal{M}} ||\Sigma_p \wedge \Sigma_e(M)||.$$

Problem 5.2 (Determination of optimal estimator)
For the case of known and/or unknown initial condition of (5.1)*, find an optimal estimator* $M^{opt} \in \mathcal{M}$ *such that*

$$J(M^{opt}) = \gamma^{opt},$$

if it exists.

Problem 5.3 (Determination of the set of optimal estimators)
Determine the set $\mathcal{M}^{opt}$ *such that*

$$\mathcal{M}^{opt} = \{M \in \mathcal{M} | \gamma^{opt} = ||\Sigma_p \wedge \Sigma_e(M)||\}.$$

Problem 5.4 (Determination of a almost optimal estimator)
For all $\epsilon > 0$*, find* $M_\epsilon^{opt} \in \mathcal{M}$ *such that*

$$\gamma^{opt} \leq ||\Sigma_p \wedge \Sigma_e(M_\epsilon^{opt})|| \leq \gamma^{opt} + \epsilon.$$

Of course, these problems crucially depend on the chosen performance index. In this chapter we will consider the design problem for two norms which we will call the induced norm and the Hilbert-Schmidt norm. The norms will be introduced next by the Definitions 5.2.1 and 5.2.4.

Definition 5.2.1 (Induced norm)
Let $\mathcal{U}$ and $\mathcal{Y}$ be arbitrary Hilbert spaces and suppose $K : \mathcal{U} \to \mathcal{Y}$ is a linear map . Then the induced norm of the operator K is defined by:

$$||K|| := \sup_{0 \neq u \in \mathcal{U}} \frac{||Ku||}{||u||},$$

where $||u||$ is the norm in $\mathcal{U}$ and $||Ku||$ is the norm in $\mathcal{Y}$.

When we consider an operator that represents the input output map of a dynamic system operating on L_2-spaces, we will also call the induced norm of that operator the (induced) L_2-gain of the system.

In the context of our estimator design problem with unknown initial condition, the input space $\mathcal{U}$ is defined by $\mathcal{U} = X \times L_2(\mathbb{T}, D_1 \times D_2)$. We define the criterion $J_{02,2}(M)$ as the gain of the system after interconnection with the estimator $\Sigma_e(M)$ by:

$$J_{02,2}(M) := ||\Sigma_p \wedge \Sigma_e(M)||_{02,2} = \sup_{\substack{d_1 \in L_2(\mathbb{T}, \mathcal{D}_1) \\ d_2 \in L_2(\mathbb{T}, \mathcal{D}_2) \\ x_0 \in X}} \frac{||e||_2}{\sqrt{||x_0||_2^2 + ||d_1||_2^2 + ||d_2||_2^2}},$$

where e satisfies equation (5.3a). Similarly, in the case with known initial condition the input space $\mathcal{U}$ is defined by $\mathcal{U} = L_2(\mathbb{T}, D_1 \times D_2)$. We define the criterion $J_{2,2}(M)$ as the L_2-gain of the system after interconnection with the estimator $\Sigma_e(M)$, i.e.:

$$J_{2,2}(M) := ||\Sigma_p \wedge \Sigma_e(M)||_{2,2} := \sup_{\substack{d_1 \in L_2(\mathbb{T}, \mathcal{D}_1) \\ d_2 \in L_2(\mathbb{T}, \mathcal{D}_2)}} \frac{||e||_2}{\sqrt{||d_1||_2^2 + ||d_2||_2^2}},$$

where e satisfies equation (5.3a) for $x_0 = 0$. In either case $M \in \mathcal{M}$.

Secondly, we introduce the Hilbert-Schmidt norm. It is defined in terms of the following class of operators:

Definition 5.2.2 (Linear integral operator)
Let $U = \mathbb{R}^p$, $Y = \mathbb{R}^m$ and let $K : L_2(\mathbb{T}, U) \to L_2(\mathbb{T}, Y)$ be a linear bounded operator defined for $u \in L_2(\mathbb{T}, U)$ by

$$(Ku)(t) := \int_{\mathbb{T}} k(t, s)u(s)\mathrm{d}s, \quad \text{for } t \in \mathbb{T}. \tag{5.4}$$

Any such operator K is said to be an integral operator and k is called the integration kernel.

In this chapter integral operators are used to represent time variant linear systems. Within the class of integral operators a subclass of operators can be defined. The class of Hilbert-Schmidt operators is defined as follows:

Definition 5.2.3 (Hilbert-Schmidt operator)
Let $U = \mathbb{R}^p$, $Y = \mathbb{R}^m$ and let $K : L_2(\mathbb{T}, U) \to L_2(\mathbb{T}, Y)$ be a linear bounded integral operator defined by equation (5.4) *with $k \in L_2(\mathbb{T} \times \mathbb{T}, \mathbb{R}^{p \times m})$. Any such operator K is said to be of Hilbert-Schmidt type.*

We will now introduce the Hilbert-Schmidt norm.

Definition 5.2.4 (Hilbert-Schmidt norm)
Let K be an operator of Hilbert-Schmidt type. Then the Hilbert-Schmidt norm $||K||_{HS}$ is defined by:

$$||K||_{HS} := ||k||_2 = \Big(\iint_{\mathbb{T}\times\mathbb{T}} ||k(t,s)||^2 \mathrm{d}t\mathrm{d}s \Big)^{\frac{1}{2}}.$$

Please note that in the context of our estimator design problems, the Hilbert-Schmidt operator is only well defined for linear state space systems with initial condition $x_0 = 0$. The operator K in Definition 5.2.3 cannot be defined for state space systems with non zero initial conditions. It follows that the operator $\Sigma_p \wedge \Sigma_e$ only can be a Hilbert-Schmidt operator if $x_0 = 0$. For the estimator design problems that minimize the Hilbert Schmidt norm of $\Sigma_p \wedge \Sigma_e$ this means that we will only consider the situation with known initial conditions (i.e. $x_0 = 0$). For this situation it follows from (5.3a) that:

$$k(t,\tau)\begin{bmatrix} d_1(\tau) \\ d_2(\tau) \end{bmatrix} = HT(t-\tau)Gd_1(\tau) - M(t,\tau)C\int_0^\tau T(\tau-\sigma)Gd_1(\sigma)\mathrm{d}\sigma + M(t,\tau)Sd_2(\tau). \tag{5.5}$$

An explicit representation for $k(t,\tau)$ is given in the following Lemma.

Lemma 5.2.1
Let k be the integration kernel of the integral operator that is a realization of the system $\Sigma_g \wedge \Sigma_e$. Then:

$$k(t,\tau) = \begin{bmatrix} HT(t-\tau)G + \int_\tau^t M(t,\sigma)CT(\sigma-t)G\mathrm{d}\sigma & M(t,\tau)S \end{bmatrix} \tag{5.6}$$

Proof. The proof follows directly from the observation that:

$$\int_0^t \int_0^\tau M(t,\tau)CT(\tau-\sigma)Gd_1(\sigma)\mathrm{d}\sigma\mathrm{d}\tau = \int_0^t \int_\sigma^t M(t,\tau)CT(\tau-\sigma)G\mathrm{d}\tau d_1(\sigma)\mathrm{d}\sigma,$$

which is obtained by interchange of the order of integration. □

The optimization problem therefore amounts to minimizing

$$J_{HS}(M) := ||\Sigma_p \wedge \Sigma_e(M)||_{HS} = ||k||_2.$$

Please note that there is no a-priori guarantee that the integration kernel satisfies the property that $k \in L_2(\mathbb{T}\times\mathbb{T}, \mathbb{R}^{m\times p})$. However, by assumption we have that $M \in \mathcal{M}$, $T(t)$ is exponentially stable and that $\mathbb{T}$ is a finite time interval. Therefore, under these assumptions $k \in L_2(\mathbb{T}\times\mathbb{T}, \mathbb{R}^{m\times p})$.

In the context of linear systems, the three norms have important interpretations which make them of interest for engineering applications. The L_2-gain can be interpreted as the maximal (worst case) energy transfer by a system between the inputs and output. In this context this is the L_2-gain from the disturbances d_1, d_2 and mismatch due to unknown initial conditions to the estimator error. The Hilbert-Schmidt norm can be

interpreted as the integrated the energy in the time variant impulse response of the system.

In the next section we will show that the interconnection $\Sigma_p \wedge \Sigma_e(M)$ of the system and the estimator can be represented as the interconnection of a generalized plant with a controller. It will turn out that we can solve the estimator design problem for the generalized plant using duality theory.

5.3 Generalized plant

In the remainder of this chapter we will study the following generalized plant which provides an alternative representation of the estimator design problem. We introduce the system $\Sigma_g : (x_0, d_1, d_2, \hat{z}) \mapsto (e, y)$, the generalized plant associated with the estimator design problem for Σ_p, which is given by:

$$\Sigma_g : \begin{cases} \dot{x} = Ax + \begin{bmatrix} G & 0 & 0 \end{bmatrix} \begin{bmatrix} d_1 \\ d_2 \\ \hat{z} \end{bmatrix}, \quad \text{with } x(0) = x_0. \\ \begin{bmatrix} e \\ y \end{bmatrix} = \begin{bmatrix} H \\ C \end{bmatrix} x + \begin{bmatrix} 0 & 0 & -I \\ 0 & S & 0 \end{bmatrix} \begin{bmatrix} d_1 \\ d_2 \\ \hat{z} \end{bmatrix} \end{cases} . \tag{5.7}$$

This system is a realization of the operator $\Sigma_g : X \times L_2(\mathbb{T}, D_1 \times D_2 \times Z) \to L_2(\mathbb{T}, Z \times Y)$ that maps $(x_0, d_1, d_2, \hat{z}) \mapsto (e, y)$ and is given by:

$$(\Sigma_g(x_0, d_1, d_2, \hat{z}))(t) = \begin{bmatrix} H \\ C \end{bmatrix} \left[T(t)x_0 + \int_0^t T(t-\tau) \begin{bmatrix} G & 0 & 0 \end{bmatrix} \begin{bmatrix} d_1(\tau) \\ d_2(\tau) \\ \hat{z}(\tau) \end{bmatrix} \mathrm{d}\tau + \begin{bmatrix} 0 & 0 & -I \\ 0 & S & 0 \end{bmatrix} \begin{bmatrix} d_1(t) \\ d_2(t) \\ \hat{z}(t) \end{bmatrix} \right] . \tag{5.8}$$

The feedback interconnection of the generalized plant Σ_g and the estimator Σ_e is defined by sharing the variables y and $\hat{z}$ between Σ_g and Σ_e as shown in Figure 5.4a with $\Sigma_c = \Sigma_e$. This interconnection defines the operator $\Sigma_g \wedge \Sigma_e : X \times L_2(\mathbb{T}, D_1 \times D_2) \to L_2(\mathbb{T}, Z)$ for the case of unknown initial condition and $\Sigma_g \wedge \Sigma_e : L_2(\mathbb{T}, D_1 \times D_2) \to L_2(\mathbb{T}, Z)$ when the initial condition is known. Observe that the following holds.

Lemma 5.3.1
For every $M \in \mathcal{M}$ there holds that $\Sigma_p \wedge \Sigma_e(M) = \Sigma_g \wedge \Sigma_e(M)$.

Proof. The equivalence follows trivially from the structure of Σ_p and Σ_g. □

The lemma therefore states that the problem to design an estimator for the plant Σ_p in (5.1) as in Figure 5.3 is equivalent to the problem to design a controller or feedback controller Σ_e for Σ_g in (5.7) as in Figure 5.4a.

5.4 Duality between estimation and control

In the literature it is often stated that the control and estimation problem are dual problems. This duality has often been used to derive the solution for estimation problems, for instance in [Kailath, 1980, Chapter 4], [Kailath et al., 2000, chapter 15] and [Kwakernaak and Sivan, 1972, Section 4.4]. However, the meaning of the duality structure needs to be made precise in order to justify this observation. In this section we define the notion of a dual system for infinite dimensional systems. This has been done in [Van der Schaft, 1990] for finite dimensional systems and the approach taken there will be generalized to infinite dimensional systems where the state space is a Hilbert space. We will first characterize the dual system of Σ_g, by providing an explicit state space realization and use this to establish the connection between optimal estimation and the dual control problems. This enables to derive a solution to the estimator design problems on the bases of known solutions for optimal control problems.

5.4.1 Dual systems

In this section we will establish an interpretation of dual systems as Hilbert adjoint operators. Consider the general system Σ:

$$\Sigma : \begin{cases} \dot{x} = & \mathcal{A}x + \mathcal{B}u \\ y = & \mathcal{C}x + \mathcal{D}u \end{cases} \tag{5.9}$$

defined on the time interval $\mathbb{T}$. Assume $x(0) = x_0 \in X$, $u \in L_2(\mathbb{T}, U)$, $y \in L_2(\mathbb{T}, Y)$ and let $\mathcal{A} : D(\mathcal{A}) \to X$ be the infinitesimal generator of an exponentially stable semi group $\mathcal{S}(t)$ for $t \in \mathbb{T}$. It follows from [Curtain and Zwart, 1995] that the unique mild solution is given by:

$$\begin{aligned} y(t) =& \mathcal{C}\mathcal{S}(t)x_0 + \int_0^t \mathcal{C}\mathcal{S}(t-\tau)\mathcal{B}u(\tau)\mathrm{d}\tau + \mathcal{D}u(t), \quad \text{for } t \in \mathbb{T} \\ =:& \Sigma(x_0, u)(t) \end{aligned} \tag{5.10}$$

where we denote the system operator mapping from $(x_0, u) \in X \times L_2(\mathbb{T}, U)$ to $y \in L_2(\mathbb{T}, Y)$ by Σ. This mapping is well defined under the assumption that $\mathcal{S}$ is exponentially stable. Then we recall the definition of a adjoint operator and two properties.

Definition 5.4.1 (Hilbert adjoint operator)
[Kreyszig, 1989, Def. 10.1-2] Let $\mathcal{T} : \mathcal{D}(\mathcal{T}) \to H$ be a (possibly unbounded) densely defined linear operator in a complex Hilbert space H. Then the Hilbert adjoint operator $\mathcal{T}^* : \mathcal{D}(\mathcal{T}^*) \to H$ of $\mathcal{T}$ is defined as follows. The domain $\mathcal{D}(\mathcal{T}^*)$ of $\mathcal{T}^*$ consists of all $y \in H$ such that there is a $y^* \in H$ satisfying

$$\langle \mathcal{T}x, y\rangle = \langle x, y^*\rangle$$

for all $x \in \mathcal{D}(\mathcal{T})$. For each such $y \in \mathcal{D}(\mathcal{T}^*)$ the Hilbert adjoint operator $\mathcal{T}^*$ is defined in terms of that y^* by

$$y^* = \mathcal{T}^* y.$$

The following property relates the Hilbert-Schmidt norm of operators K and its ad-joint K^*:

Lemma 5.4.1
Let K be a Hilbert Schmidt operator and $||\cdot||_{HS}$ the Hilbert-Schmidt norm, then:

$$||K||_{HS} = ||K^*||_{HS}$$

Proof. K^* is well defined for any operator K and can be realized by $(K^*y)(t) = \int_{\mathbb{T}} k^*(s,t)y(s)\mathrm{d}s$, where k^* is the adjoint kernel, [Weidmann, 1980]. The property follows from the definition of $||K||_{HS}$

$$||K||_{HS}^2 := \iint_{\mathbb{T}\times\mathbb{T}} ||k(t,s)||_2^2 \mathrm{d}t\mathrm{d}s = \iint_{\mathbb{T}\times\mathbb{T}} ||(k(t,s))^*||_2^2 \mathrm{d}t\mathrm{d}s = ||K^*||_{HS}^2.$$

□

The following lemma relates the induced norm of operators K and its adjoint K^*:

Lemma 5.4.2
Let $\mathcal{U}$ and $\mathcal{Y}$ be arbitrary Hilbert spaces and suppose $K : \mathcal{U} \to \mathcal{Y}$ is a linear map and let K^* denote the adjoint of K. The induced norm of a operator K and the adjoint operator K^* are equal, i.e $||K|| = ||K^*||$.

This is a standard result for operators on a Hilbert space, and can be found in for instance [Kreyszig, 1989, thm 3.9-2].

In order to establish the notion of dual systems we treat linear systems as linear operators where the domain and range are Hilbert spaces. With use of Definition 5.4.1 we can now define the dual system as follows:

Definition 5.4.2 (Duality for systems with unknown initial condition)
Let Σ be a system with system operator Σ defined as in (5.10)*. The dual system of Σ, denoted by Σ^*, is the system with system operator $\Sigma^* : L_2(\mathbb{T}, Y) \to X \times L_2(\mathbb{T}, U)$, and is defined as the Hilbert adjoint of Σ. Hence, Σ^* is the operator for which $\langle\langle \Sigma(x_0, u), \tilde{y}\rangle\rangle = \langle\langle (x_0, u), \Sigma^*\tilde{y}\rangle\rangle$ for all $(x_0, u) \in X \times L_2(\mathbb{T}, U)$ and $\tilde{y} \in L_2(\mathbb{T}, Y)$. Here, $\langle\langle (x_0, u), (\tilde{x}_0, \tilde{u})\rangle\rangle := \langle x_0, \tilde{x}_0\rangle + \langle\langle u, \tilde{u}\rangle\rangle$.*

The following theorem relates the state space realizations of a system to the state space realization of its dual system. In order to prove the theorem, the following lemma is needed.

Lemma 5.4.3
Suppose the operator $\mathcal{A}$ with domain $D(\mathcal{A})$ is the infinitesimal generator of the semi-group $\mathcal{S}(t)$. Let the operator $\mathcal{A}^*$ be the adjoint operator of $\mathcal{A}$ and let for every t the operator $\mathcal{S}^*(t)$ be the adjoint operator of $\mathcal{S}(t)$. Then $\mathcal{A}^*$ is the infinitesimal generator of $\mathcal{S}^*(t)$.

Proof. Given that $\mathcal{A}$ generates $\mathcal{S}(t)$ and suppose $\bar{\mathcal{A}}$ is the generator of $\mathcal{S}^*(t)$. Then it

follows from the definitions of generator of the semigroup operator that:

$$\mathcal{A}x = \lim_{h\to 0} \frac{\mathcal{S}(t+h)x - \mathcal{S}(t)x}{h} \qquad \text{for } :x \in D(\mathcal{A})$$
$$\bar{\mathcal{A}}x = \lim_{h\to 0} \frac{\mathcal{S}^*(t+h)x - \mathcal{S}^*(t)x}{h} \qquad \text{for } :x \in D(\mathcal{A}^*)$$

From the definition of the adjoint operator of $\mathcal{A}$ it follows $\langle \mathcal{A}x_1, x_2\rangle = \langle x_1, \mathcal{A}^* x_2\rangle$ for all $x_1 \in D(\mathcal{A})$ and $x_2 \in D(\mathcal{A}^*)$. We infer:

$$\begin{aligned}\langle \mathcal{A}x_1, x_2\rangle &= \lim_{h\to 0} \frac{1}{h}\langle \mathcal{S}(t+h)x_1 - \mathcal{S}(t)x_1, x_2\rangle \\ &= \lim_{h\to 0} \frac{1}{h}(\langle x_1, \mathcal{S}^*(t+h)x_2 - \mathcal{S}^*(t)x_2\rangle) = \langle x_1, \bar{\mathcal{A}}x_2\rangle.\end{aligned}$$

Which shows $\mathcal{A}^* = \bar{\mathcal{A}}$ for $x \in D(\mathcal{A}) \cap D(\mathcal{A}^*)$ □

Theorem 5.4.4
Let the system operator $\Sigma : X \times L_2(\mathbb{T}, U) \to L_2(\mathbb{T}, Y)$ be defined by Equation (5.10). Then the dual operator $\Sigma^* : L_2(\mathbb{T}, Y) \to X \times L_2(\mathbb{T}, U)$ is given by $\Sigma^*\tilde{y} := (p_0, \tilde{u})$ with:

$$\begin{aligned}p_0 &= \int_0^{t_e} \tilde{\mathcal{S}}(0,\tau)\mathcal{C}^*\tilde{y}(\tau)\mathrm{d}\tau \\ \tilde{u}(t) &= \int_t^{t_e} \mathcal{B}^*\tilde{\mathcal{S}}(t,\tau)\mathcal{C}^*\tilde{y}(\tau)\mathrm{d}\tau + \mathcal{D}^*\tilde{y}(t)\end{aligned}$$

where $t \in \mathbb{T}$ and $\tilde{\mathcal{S}}(t,\tau) := S^*(\tau - t) : X \to X$ is the mild evolution operator with infinitesimal generator $-\mathcal{A}^*$ for $t \in \mathbb{T}$. Moreover the following differential equation with end-point condition $p(t_e) = 0$ is a realization of the operator Σ^*:

$$\Sigma^* : \begin{cases} \dot{p} = & -\mathcal{A}^* p - \mathcal{C}^*\tilde{y}, \\ \tilde{u} = & \mathcal{B}^* p + \mathcal{D}^*\tilde{y}. \end{cases} \tag{5.11}$$

Before we present the proof of Theorem 5.4.4 we introduce the following Lemma.

Lemma 5.4.5
Consider the system Σ^*, defined by Equation (5.11), with end-point condition $p(t_e) = p_{t_e}$. Then $p(t)$, defined by:

$$p(t) = \mathcal{S}^*(t_e - t)p_{t_e} + \int_t^{t_e} \mathcal{S}^*(\tau - t)\mathcal{C}^*\tilde{y}(\tau)\mathrm{d}\tau \quad \text{for } t \in \mathbb{T},$$

is a solution of Σ^*.

Proof. We differentiate p with respect to t and show that (5.11) holds.

$$\begin{aligned}\dot{p}(t) &= -\mathcal{A}^*\mathcal{S}^*(t_e - t)p(t_e) + \frac{\mathrm{d}}{\mathrm{d}t}\int_t^{t_e} \mathcal{S}^*(\tau - t)\mathcal{C}^*\tilde{y}(\tau)\mathrm{d}\tau \\ &= -\mathcal{A}^*\mathcal{S}^*(t_e - t)p(t_e) + \int_t^{t_e} \frac{\mathrm{d}}{\mathrm{d}t}\mathcal{S}^*(\tau - t)\mathcal{C}^*\tilde{y}(\tau)\mathrm{d}\tau - \mathcal{S}^*(t - t)\mathcal{C}^*\tilde{y}(t), \\ &= -\mathcal{A}^*\left(\mathcal{S}^*(t_e - t)p(t_e) + \int_t^{t_e} \mathcal{S}^*(\tau - t)\mathcal{C}^*\tilde{y}(\tau)\mathrm{d}\tau\right) - \mathcal{S}^*(t - t)\mathcal{C}^*\tilde{y}(t) \\ &= -\mathcal{A}^* p(t) - \mathcal{C}^*\tilde{y}(t).\end{aligned}$$

□

Proof of Theorem 5.4.4. In order to prove the Theorem, it will be validated whether Σ^* satisfies Definition 5.4.2. Given that $\mathcal{A}$ is the infinitesimal generator of a semigroup $\mathcal{S}(t)$ for $t \in \mathbb{T}$, it follows from Lemma 5.4.3 that $\mathcal{A}^*$ is the infinitesimal generator of $\mathcal{S}^*(t)$. Suppose $x_0, p_0 \in X$, $u(t), \tilde{u}(t) \in U$ and $y(t), \tilde{y}(t) \in Y$. Then, we observe that the following relation holds:

$$\frac{\mathrm{d}}{\mathrm{d}t}\langle x(t), p(t)\rangle + \langle y(t), \tilde{y}(t)\rangle = \langle u(t), \tilde{u}(t)\rangle$$

Indeed,

$$\begin{aligned}&\frac{\mathrm{d}}{\mathrm{d}t}\langle x(t), p(t)\rangle + \langle y(t), \tilde{y}(t)\rangle = \\ &\langle \mathcal{A}x(t) + \mathcal{B}u(t), p(t)\rangle + \langle \mathcal{C}x(t) + \mathcal{D}u(t), \tilde{y}(t)\rangle + \langle x(t), -\mathcal{A}^*p(t) - \mathcal{C}^*\tilde{y}(t)\rangle \\ &\qquad = \langle u(t), \mathcal{B}^*p(t)\rangle + \langle u(t), \mathcal{D}^*\tilde{y}(t)\rangle = \langle u(t), \tilde{u}(t)\rangle\end{aligned}$$

Hence, after integration over $\mathbb{T} = [0, t_e]$, we infer

$$\langle x(t_e), p(t_e)\rangle - \langle x_0, p(0)\rangle + \langle\langle \Sigma(x_0, u), \tilde{y}\rangle\rangle = \langle\langle u, \tilde{u}\rangle\rangle\,. \tag{5.12}$$

In particular, with the end-condition on $p(t_e) = 0$, we find:

$$\langle\langle \Sigma(x_0, u), \tilde{y}\rangle\rangle = \langle x_0, p(0)\rangle + \langle\langle u, \tilde{u}\rangle\rangle\,.$$

By definition, the left hand side equals $\langle\langle (x_0, u), \Sigma^*\tilde{y}\rangle\rangle$, so we infer that:

$$\langle\langle (x_0, u), \Sigma^*\tilde{y}\rangle\rangle = \langle x_0, p(0)\rangle + \langle\langle u, \tilde{u}\rangle\rangle\,.$$

This shows that $\Sigma^*\tilde{y} = (p_0, \tilde{u})$, where $p_0 = p(0)$ with $p(t)$ the solution of (5.11) given by:

$$\begin{cases} p(t) = & \mathcal{S}^*(t_e - t)p(t_e) + \int_t^{t_e} \mathcal{S}^*(\tau - t)\mathcal{C}^*\tilde{y}(\tau)\mathrm{d}\tau \\ \tilde{u}(t) = & \mathcal{B}^*p(t) + \mathcal{D}^*\tilde{y}(t) \end{cases}$$

Since $p(t_e) = 0$, this concludes the proof. □

We remark that the mild evolution operator $\tilde{\mathcal{S}}(t_e, t) := S^*(t_e - t)$ is not a semigroup operator, since $\tilde{\mathcal{S}}(t_e, t_1 + t_2) \neq \tilde{\mathcal{S}}(t_e, t_1)\tilde{\mathcal{S}}(t_e, t_2)$. However, $\tilde{\mathcal{S}}(t_e, t_e - t)$ is a semigroup operator with infinitesimal generator $\mathcal{A}^*$, since $\tilde{\mathcal{S}}(t_e, t_e - t) = S^*(t)$. We introduce the following corollary.

Corollary 5.4.6
Let the system operator $\Sigma : X \times L_2(\mathbb{T}, U) \to L_2(\mathbb{T}, Y)$ be defined by Equation (5.10) *and let $\Sigma^* : L_2(\mathbb{T}, Y) \to X \times L_2(\mathbb{T}, U)$ be the dual operator. Then $||\Sigma|| = ||\Sigma^*||$.*

This is an application of Lemma 5.4.2.

Theorem 5.4.4 and Corollary 5.4.6 consider the case where $\Sigma : X \times L_2(\mathbb{T}, U) \to L_2(\mathbb{R}, Y)$. Duality for operators $\Sigma : L_2(\mathbb{T}, U) \to L_2(\mathbb{R}, Y)$ can be defined equivalently. First we apply Definition 5.4.1 to define Σ^* for this case.

Definition 5.4.3 (Duality for systems with $x_0 = 0$)
Let Σ be a system with system operator Σ defined as in (5.10) *with $x_0 = 0$. The dual system of Σ, denoted by Σ^*, is the system with system operator $\Sigma^* : L_2(\mathbb{T}, Y) \to L_2(\mathbb{T}, U)$ and is defined as the Hilbert adjoint of Σ. Hence, Σ^* is the operator for which $\langle\langle \Sigma(u), \tilde{y} \rangle\rangle = \langle\langle u, \Sigma^* \tilde{y} \rangle\rangle$ for all $u \in L_2(\mathbb{T}, U)$ and $\tilde{y} \in L_2(\mathbb{T}, Y)$.*

A characterization of Σ^* is provided by the following theorem.

Theorem 5.4.7
Let the system operator $\Sigma : L_2(\mathbb{T}, U) \to L_2(\mathbb{T}, Y)$ be defined by Equation (5.10) *with $x_0 = 0$. Then the dual operator $\Sigma^* : L_2(\mathbb{T}, Y) \to L_2(\mathbb{T}, U)$ is given by $\Sigma^* \tilde{y} := \tilde{u}$ with:*

$$\tilde{u}(t) = \int_t^{t_e} \mathcal{B}^* \tilde{\mathcal{S}}(t, \tau) \mathcal{C}^* \tilde{y}(\tau) \mathrm{d}\tau + \mathcal{D}^* \tilde{y}(t)$$

where $t \in \mathbb{T}$ and $\tilde{\mathcal{S}}(t, \tau) := S^*(\tau - t) : X \to X$ is the mild evolution operator with infinitesimal generator $-\mathcal{A}^*$ for $t \in \mathbb{T}$. Moreover, also in this case (5.11) *is a state space realization of Σ^* with end point condition $p(t_e) = 0$.*

Proof. The proof of this theorem is identical to the proof of Theorem 5.4.4, when one sets $x_0 = 0$ in Equation (5.12). □

We introduce the following corollary.

Corollary 5.4.8
Let the system operator $\Sigma : L_2(\mathbb{T}, U) \to L_2(\mathbb{T}, Y)$ be defined by Equation (5.10) *with $x_0 = 0$ and let $\Sigma^* : L_2(\mathbb{T}, Y) \to L_2(\mathbb{T}, U)$ be the dual operator. Then $||\Sigma||_{HS} = ||\Sigma^*||_{HS}$ and $||\Sigma||_{2,2} = ||\Sigma^*||_{2,2}$.*

This is an application of the lemmas 5.4.1 and (5.4.2).

By the lemmas 5.4.1 and 5.4.2 we have shown that the operators Σ and Σ^* have equal L_2-gain and equal HS-norm. This property will enable us to relate the optimal HS estimation problem to the optimal LQR control problem and to relate the optimal L_2-gain estimator design problem to the optimal L_2-gain controller design problem, as we will show later in Subsection 5.4.3. First, we will use the duality theory of this section to obtain the dual systems of Σ_g, $\Sigma_e(M)$ and $\Sigma_g \wedge \Sigma_e(M)$.

5.4.2 Dual systems and interconnections

For the situation where the initial condition is unknown, consider the system Σ_g defined in (5.7) together with the corresponding system operator

$$\Sigma_g : X \times L_2(\mathbb{T}, D_1 \times D_2 \times Z) \to L_2(\mathbb{T}, Z \times Y).$$

Using Theorem 5.4.4 it follows that the adjoint system operator

$$\Sigma_g^* : L_2(\mathbb{T}, Z \times Y) \to X \times L_2(\mathbb{T}, D_1 \times D_2 \times Z)$$

satisfies:

$$(\Sigma_g^*(\tilde{e},\tilde{y})) = (p(0), \tilde{d}_1, \tilde{d}_2, \hat{\tilde{z}}) \quad \text{for} \quad t \in \mathbb{T},$$

where, for any $t \in \mathbb{T}$,

$$p(t) = \int_t^{t_e} T^*(\tau - t) \begin{bmatrix} H^* & C^* \end{bmatrix} \begin{bmatrix} \tilde{e}(\tau) \\ \tilde{y}(\tau) \end{bmatrix} \mathrm{d}\tau \tag{5.13}$$

$$\begin{bmatrix} \tilde{d}_1(t) \\ \tilde{d}_2(t) \\ \hat{\tilde{z}}(t) \end{bmatrix} = \begin{bmatrix} G^* \\ 0 \\ 0 \end{bmatrix} p(t) + \begin{bmatrix} 0 & 0 \\ 0 & S^* \\ -I & 0 \end{bmatrix} \begin{bmatrix} \tilde{e}(t) \\ \tilde{y}(t) \end{bmatrix}. \tag{5.14}$$

For the situation where the initial condition is known, consider the system Σ_g defined in (5.7) with $x_0 = 0$, together with the corresponding system operator

$$\Sigma_g : L_2(\mathbb{T}, D_1 \times D_2 \times Z) \to L_2(\mathbb{T}, Z \times Y).$$

Using Theorem 5.4.7 it follows that the adjoint system operator

$$\Sigma_g^* : L_2(\mathbb{T}, Z \times Y) \to L_2(\mathbb{T}, D_1 \times D_2 \times Z)$$

satisfies:

$$\Sigma_g^*(\tilde{e},\tilde{y}) = (\tilde{d}_1, \tilde{d}_2, \hat{\tilde{z}}) \quad \text{for} \quad t \in \mathbb{T},$$

with $(\tilde{d}_1, \tilde{d}_2, \hat{\tilde{z}})$ defined by Equation 5.14.

Moreover, as observed in Subsection 5.4.1, in either case a state space representation of the adjoint system Σ_g^* is given by:

$$\Sigma_g^* : \begin{cases} \dot{p} = -A^* p - \begin{bmatrix} H^* & C^* \end{bmatrix} \begin{bmatrix} \tilde{e} \\ \tilde{y} \end{bmatrix} \\ \begin{bmatrix} \tilde{d}_1 \\ \tilde{d}_2 \\ \hat{\tilde{z}} \end{bmatrix} = \begin{bmatrix} G^* \\ 0 \\ 0 \end{bmatrix} p + \begin{bmatrix} 0 & 0 \\ 0 & S^* \\ -I & 0 \end{bmatrix} \begin{bmatrix} \tilde{e} \\ \tilde{y} \end{bmatrix} \end{cases}, \tag{5.15}$$

with $p(t_e) = 0$.

Consider Σ_g together with its dual Σ_g^*. Let Σ_c be a linear causal map

$$\Sigma_c : L_2(\mathbb{T}, Y) \to L_2(\mathbb{T}, Z)$$

and let Σ_c^* be its dual. Consider the interconnected systems $\Sigma_g \wedge \Sigma_c$ and $\Sigma_g^* \wedge \Sigma_c^*$ as depicted in Figure 5.4. Then, depending on whether x_0 is considered unknown or known in Σ_g, we have that

$$\Sigma_g \wedge \Sigma_c : X \times L_2(\mathbb{T}, D_1 \times D_2) \to L_2(\mathbb{T}, Z)$$

or

$$\Sigma_g \wedge \Sigma_c : L_2(\mathbb{T}, D_1 \times D_2) \to L_2(\mathbb{T}, Z).$$

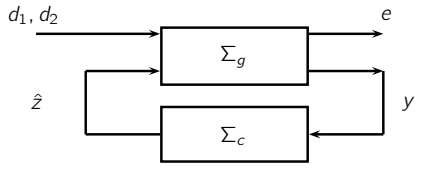

(a) Estimator design problem reformulated as controller design problem for a generalized plant Σ_g.

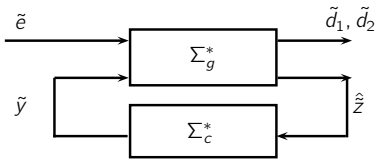

(b) Controller design problem for the dual system of the generalized plant Σ_g^*

Figure 5.4: Reformulations of the estimator design problem using a generalized plant and dualization of the problem.

This interconnection is shown in Figure 5.4a. Similarly, $\Sigma_g^* \wedge \Sigma_c^*$ defines a mapping $L_2(\mathbb{T}, Z) \to X \times L_2(D_1 \times D_2)$ or $L_2(\mathbb{T}, Z) \to L_2(\mathbb{T}, D_1 \times D_2)$ depending on whether the initial condition $x(0) = x_0$ in Σ_g is known or unknown, respectively. This interconnection is shown in Figure 5.4b.

We introduce the following lemma, which states basically that the operations of interconnection of Σ_g and Σ_c and dualization of Σ_g and Σ_c commute.

Lemma 5.4.9
Let Σ_g be given by (5.7) *and let the LTI map $\Sigma_c : L_2(\mathbb{T}, Y) \to L_2(\mathbb{T}, Z)$ be linear and causal. Then with either of the interpretations*

$$\Sigma_g \wedge \Sigma_c : X \times L_2(\mathbb{T}, D_1 \times D_2) \to L_2(\mathbb{T}, Z)$$

or

$$\Sigma_g \wedge \Sigma_c : L_2(\mathbb{T}, D_1 \times D_2) \to L_2(\mathbb{T}, Z),$$

we have that:

$$(\Sigma_g \wedge \Sigma_c)^* = \Sigma_g^* \wedge \Sigma_c^*.$$

Proof. The equality can be derived by a straightforward calculation of $(\Sigma_g \wedge \Sigma_c)^*$ and $\Sigma_g^* \wedge \Sigma_c^*$ using their state space representations. □

Now suppose that $\Sigma_c = \Sigma_e(M)$ is defined by the estimator given by Equation (5.2). Then the dual of the estimator Σ_c, i.e. $\Sigma_c^* = \Sigma_e^* : L_2(\mathbb{T}, Z) \to L_2(\mathbb{T}, Y)$ is represented by:

$$\Sigma_e^*(M) : \tilde{y}(t) = \int_t^{t_e} M^*(\tau, t)\tilde{z}(\tau)\mathrm{d}\tau, \tag{5.16}$$

We infer that $\Sigma_g^* \wedge \Sigma_e^*$ is represented by the Equations (5.19) below, in the sense that

$$(\Sigma_g^* \wedge \Sigma_e^*)\tilde{e} = (p_{cl}(0), \tilde{d}_1, \tilde{d}_2) \tag{5.17}$$

in the case of unknown initial conditions and

$$(\Sigma_g^* \wedge \Sigma_e^*)\tilde{e} = (\tilde{d}_1, \tilde{d}_2) \tag{5.18}$$

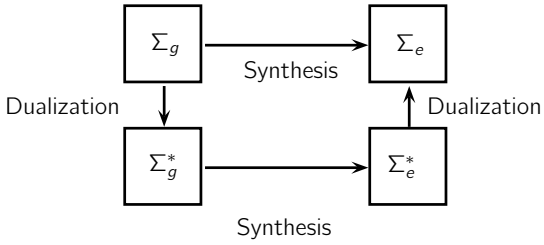

Figure 5.5: Direct design path and alternative design path for the design of estimator Σ_e.

in the case of known initial conditions ($x_0 = 0$). Here,

$$p_{cl}(t) = \int_t^{t_e} T^*(\tau - t) \begin{bmatrix} H^* & C^* \end{bmatrix} \begin{bmatrix} \tilde{e}(\tau) \\ -\int_\tau^{t_e} M^*(\sigma, \tau)\tilde{e}(\sigma)\mathrm{d}\sigma \end{bmatrix} \mathrm{d}\tau, \tag{5.19a}$$

$$\begin{bmatrix} \tilde{d}_1(t) \\ \tilde{d}_2(t) \end{bmatrix} = \begin{bmatrix} G^* \\ 0 \end{bmatrix} p_{cl}(t) + \begin{bmatrix} 0 & 0 \\ 0 & S^* \end{bmatrix} \begin{bmatrix} \tilde{e}(t) \\ -\int_t^{t_e} M^*(\tau, t)\tilde{e}(\tau)\mathrm{d}\tau \end{bmatrix}. \tag{5.19b}$$

5.4.3 Implications optimal estimation vs. optimal control

Note that by Lemma 5.3.1, we have that $\Sigma_p \wedge \Sigma_e(M) = \Sigma_g \wedge \Sigma_c$ whenever $\Sigma_c = \Sigma_e(M)$. The system $\Sigma_e^*(M)$ plays the role of Σ_c^* in Lemma 5.4.9 and is a controller for Σ_g^*. As such, the system $\Sigma_c = \Sigma_e^*(M)$ can be interpreted as an output feedback regulator for Σ_g^*.

We are now in the position to present the relation between estimator design and controller design. We will show that the estimator design Problems 5.1, 5.2, 5.3, and 5.4 can be formulated as regulator design problem for the dual system, interconnected as in Figure 5.4b. The aim of this approach is to solve the estimator design problem via reformulation of the estimation problem by dualization as control problem, then obtain the solutions to the resulting control problem and obtain the solutions for the estimation problem from the latter by dualization. This approach is shown in Figure 5.5.

The following two theorems show that this is possible.

Theorem 5.4.10
Consider Σ_p given by (5.1) *, Σ_g given by* (5.7) *and Σ_g^* given by* (5.15)*. Let $\Sigma_c = \Sigma_e(M)$ with $M \in \mathcal{M}$. Then:*

i. $J_{02,2}(M) := ||\Sigma_p \wedge \Sigma_e(M)||_{02,2} = ||\Sigma_g \wedge \Sigma_c||_{02,2} = ||(\Sigma_g \wedge \Sigma_c)^*||_{2,02} = ||\Sigma_g^* \wedge \Sigma_c^*||_{2,02}$,
ii. $J_{2,2}(M) := ||\Sigma_p \wedge \Sigma_e(M)||_{2,2} = ||\Sigma_g \wedge \Sigma_c||_{2,2} = ||(\Sigma_g \wedge \Sigma_c)^*||_{2,2} = ||\Sigma_g^* \wedge \Sigma_c^*||_{2,2}$,
iii. $J_{HS}(M) := ||\Sigma_p \wedge \Sigma_e(M)||_{HS} = ||\Sigma_g \wedge \Sigma_c||_{HS} = ||(\Sigma_g \wedge \Sigma_c)^*||_{HS} = ||\Sigma_g^* \wedge \Sigma_c^*||_{HS}$.

where $||\cdot||_{2,02}$ denotes the induced norm for operators in the class $L_2(\mathbb{T}, Z) \to X \times L_2(\mathbb{T}, D_1 \times D_2)$.

Proof. We prove i. The equality of $||\Sigma_p \wedge \Sigma_e(M)||_{02,2}$ and $||\Sigma_g \wedge \Sigma_c||_{02,2}$ follows from Lemma 5.3.1. The equality of $||\Sigma_g \wedge \Sigma_c||_{02,2}$ and $||(\Sigma_g \wedge \Sigma_c)^*||_{2,02}$ follows from Corollary 5.4.6. The equality of $||(\Sigma_g \wedge \Sigma_c)^*||_{2,02}$ and $||\Sigma_g^* \wedge \Sigma_c^*||_{2,02}$ follows from Lemma 5.4.9. The proof of (ii) and (iii) follows identically by application of Corollary 5.4.8. □

From this theorem the following important corollary follows.

Corollary 5.4.11
Let $\Sigma_c^* : L_2(\mathbb{T}, Z) \to L_2(\mathbb{T}, Y)$ *be given by*

$$\Sigma_c^*(M) : \tilde{y}(t) = \int_t^{t_e} M^*(\tau, t)\tilde{z}(\tau)\mathrm{d}\tau,$$

with $M \in \mathcal{M}$. *Then:*

i. $M \in \mathcal{M}$ *minimizes* $J_{02,2}(\cdot)$ *if and only if* M *minimizes* $||\Sigma_g^* \wedge \Sigma_c^*(\cdot)||_{2,02}$.
ii. $M \in \mathcal{M}$ *minimizes* $J_{2,2}(\cdot)$ *if and only if* M *minimizes* $||\Sigma_g^* \wedge \Sigma_c^*(\cdot)||_{2,2}$.
iii. $M \in \mathcal{M}$ *minimizes* $J_{HS}(\cdot)$ *if and only if* M *minimizes* $||\Sigma_g^* \wedge \Sigma_c^*(\cdot)||_{HS}$.

The proof of this corollary follows directly from Theorem 5.4.10 by the quality of the norms $||\Sigma_p \wedge \Sigma_e(M)||$ and $||\Sigma_g^* \wedge \Sigma_c^*(M)||$.

Corollary 5.4.11 shows how estimation problems and control problems are related. The norms which we have introduced, the induced norm and the Hilbert-Schmidt norm, do satisfy the property $||\Sigma|| = ||\Sigma^*||$, which we have shown in the Lemmas 5.4.2, and 5.4.1, respectively. Therefore, Corollary 5.4.11 can be used to solve the estimator design problem for these norms. In the following sections we will employ the duality result to derive the solutions to the Problems 5.1, 5.2, 5.3, and 5.4 for the design estimators for the case of the Hilbert-Schmidt norm and the induced $L_{2,2}$ norm. It will turn out that due to the specific structure of the equivalent regulator design problems, these problems admits an insightful solution based on a completion of the squares argument.

5.5 Optimal Hilbert-Schmidt norm estimator design

For distributed parameter systems, the solution of the optimal state estimation problem has been solved in a stochastic setting, for instance in [Curtain and Pritchard, 1978]. In this section we present a complete solution to the design of a deterministic optimal Hilbert-Schmidt norm output estimator for linear distributed parameter systems. The approach avoids stochastic interpretations of variables and is based on methods from functional analysis. For the finite dimensional H_2-estimator design problem on a infinite time horizon it is known that the problem is dual to the linear quadratic optimal control problem. We will generalize this result to the estimator design problem in an infinite dimensional setting on a finite time horizon. The result is a generalization of a result for finite dimensional systems presented in [Mutsaers and Weiland, 2009] and is based on [Curtain and Zwart, 1995]. In the first section we give a precise formulation of the optimal Hilbert-Schmidt norm estimator design problem. Subsequently, we introduce an equivalent dual linear quadratic (LQ) control problem and show that this problem can

be solved by using a completion of the squares argument. Finally the solution of the LQ-control problem is used to derive the optimal HS-estimator. It will be shown that the 2-norm criterion leads to a generalization of the well known Kalman estimator.

5.5.1 Formulation of the estimator design problem

In this section we consider the design of an optimal estimator, based on minimization of the Hilbert-Schmidt norm of the system $\Sigma_g \wedge \Sigma_e(M)$ obtained after interconnection of the plant with the estimator.

As design criterion we consider the functional $J : \mathcal{M} \to \mathbb{R}$ which represents the Hilbert-Schmidt norm of the interconnected systems Σ_g and $\Sigma_e(M)$:

$$J_{HS}(M) = ||\Sigma_g \wedge \Sigma_e(M)||_{HS}. \tag{5.20}$$

For this criterion we consider the Problems 5.1, 5.2, 5.3, and 5.4 stated in section 5.2. In the following section we will use the theory of duality from section 5.4.1 to introduce a regulator design problem that can be solved by a completion of the square argument.

5.5.2 Formulation of the dual control problem

In this section we will derive an optimal controller $\Sigma_c^*(M)$ for Σ_g^* which will be shown to be equivalent to the problem of minimization of J_{HS} in (5.20) over $M \in \mathcal{M}$.

Theorem 5.4.10 shows that the criterion (5.20) can be reformulated as:

$$J_{HS}(M) = ||\Sigma_g^* \wedge \Sigma_e^*(M)||_{HS}. \tag{5.21}$$

Then Corollary 5.4.11 states that it is possible to design a linear controller Σ_c^* : $L_2(\mathbb{T}, Z) \to L_2(\mathbb{T}, Y)$ that minimizes $||\Sigma_g^* \wedge \Sigma_c^*||_{HS}$ and obtain the solution for the estimator design problem by dualization of this controller by the following equivalence:

$$J_{HS}(M) = ||\Sigma_g \wedge \Sigma_e(M)||_{HS} = ||\Sigma_g^* \wedge \Sigma_e^*(M)||_{HS} \tag{5.22}$$

In this section the estimator design problem will be solved by minimization of (5.21) with respect to $M \in \mathcal{M}$. In order to characterize the Hilbert-Schmidt norm of the system $\Sigma_g^* \wedge \Sigma_e^*(M)$, i.e. $||\Sigma_g^* \wedge \Sigma_e^*(M)||_{HS}$ the integral operator associated to the system $\Sigma_g^* \wedge \Sigma_e^*(M)$ will be obtained in the following theorem.

Theorem 5.5.1
Consider the system $\Sigma_g^* \wedge \Sigma_e^*(M)$ as given by (5.18)*. The system $\Sigma_g^* \wedge \Sigma_e^*(M)$ can be represented as integral operator K with the realization:*

$$\begin{bmatrix} \tilde{d}_1(t) \\ \tilde{d}_2(t) \end{bmatrix} = (K\tilde{e})(t) = \int_{\mathbb{T}} \begin{bmatrix} K_M(t,s) \\ L_M(t,s) \end{bmatrix} \tilde{e}(s)\mathrm{d}s, \tag{5.23}$$

where K_M and L_M are given by:

$$K_M(t,s)=\begin{cases} G^*\big[T^*(s-t)H^* - \int_t^s T^*(\sigma-t)C^*M^*(s,\sigma)\mathrm{d}\sigma\big] & \text{for } 0\le t\le s,\\ 0 & s<t\le t_e, \end{cases} \tag{5.24a}$$

$$L_M(t,s)=\begin{cases} -S^*M^*(s,t), & \text{for } 0\le t\le s\\ 0 & \text{for } s<t\le t_e. \end{cases} \tag{5.24b}$$

Proof. The proof follows by interchanging the integration order in Equation (5.19). First, rewrite Equation (5.19a) to:

$$p_{cl}(t)=\int_t^{t_e} T^*(\tau-t)H^*\tilde{e}(\tau)\mathrm{d}\tau - \int_t^{t_e}\int_\tau^{t_e} T^*(\tau-t)C^*M^*(\sigma,\tau)\tilde{e}(\sigma)\mathrm{d}\sigma\mathrm{d}\tau.$$

Then the order of integration in the second integral is interchanged. Here is has been used that the integration domain represented by the inequalities $\tau\le\sigma\le t_e$ and $t\le\tau\le t_e$ is equivalent to the domain of integration represented by the inequalities $t\le\tau\le\sigma$ and $t\le\sigma\le t_e$, to obtain:

$$p_{cl}(t)=\int_t^{t_e} T^*(\tau-t)H^*\tilde{e}(\tau)\mathrm{d}\tau - \int_t^{t_e}\int_t^{\sigma} T^*(\tau-t)C^*M^*(\sigma,\tau)\mathrm{d}\tau\tilde{e}(\sigma)\mathrm{d}\sigma$$

Finally, the latter equation is rewritten as single integral.

$$p_{cl}(t)=\int_t^{t_e}\left[T^*(\tau-t)H^* - \int_t^{\tau} T^*(\sigma-t)C^*M^*(\tau,\sigma)\mathrm{d}\sigma\right]\tilde{e}(\tau)\mathrm{d}\tau$$

By use of this representation of $p_{cl}(t)$ in (5.19b) it follows that $\Sigma_g^*\wedge\Sigma_e^*$ can be represented by:

$$\begin{bmatrix}\tilde{d}_1(t)\\ \tilde{d}_2(t)\end{bmatrix}=\int_t^{t_e}\begin{bmatrix} G^*\left[T^*(\tau-t)H^* - \int_t^{\tau} T^*(\sigma-t)C^*M^*(\tau,\sigma)\mathrm{d}\sigma\right]\\ -S^*M^*(\tau,t)\end{bmatrix}\tilde{e}(\tau)\mathrm{d}\tau,$$

from shows (5.23), such that K_M and L_M follow. It has been demanded that the estimator Σ_e is causal (i.e. $M(t,s)=0$ for $s>t$). From this it follows that $M^*(s,t)=0$ for $s<t$. Therefore $L_M(t,s)=0$ for $s<t\le t_e$, which completes the proof. □

From Definition 5.2.4 it follows that the Hilbert-Schmidt norm of the integral operator K which implements $\Sigma_g^*\wedge\Sigma_e^*(M)$ can now be computed by evaluation of the following:

$$J_{\mathrm{HS}}(M)=||\Sigma_g^*\wedge\Sigma_e^*(M)||_{HS}=\left(\int_{\mathbb{T}}\int_{\mathbb{T}}\left\|\begin{bmatrix}K_M(t,s)\\ L_M(t,s)\end{bmatrix}\right\|_2^2\mathrm{d}t\,\mathrm{d}s\right)^{\frac{1}{2}}$$

Since $K_M(t,s)=0$ and $L_M(t,s)=0$ for $s<t\le t_e$, the latter is equal to:

$$J_{HS}(M)=||\Sigma_g^*\wedge\Sigma_e^*(M)||_{HS}=\left(\int_{\mathbb{T}}\int_0^{s}\left\|\begin{bmatrix}K_M(t,s)\\ L_M(t,s)\end{bmatrix}\right\|_2^2\mathrm{d}t\,\mathrm{d}s\right)^{\frac{1}{2}}. \tag{5.25}$$

In the next section we will consider the problem of estimator design for the situation $Z=\mathbb{R}$. We will solve the estimator design problem for this assumption and then generalize the solution to $Z=\mathbb{R}^n$.

5.5.3 Dual optimal control problem for $n = 1$

In this section we present a solution to the problem of minimization of the functional $J_{HS}(M)$ for the situation of estimation of a single output variable. That is $Z = \mathbb{R}$, or $n = 1$. We assume that the operator H is defined by $Hx = \langle h, x\rangle$ with $h \in X$. We will introduce an artificial linear infinite dimensional system and will show the relation between this system and the operators K_M and L_M for $Z = \mathbb{R}$. We will show that there is a relation between the estimator design problem and a linear quadratic regulator design problem for the artificial system. The solution of the linear quadratic regulator design problem for infinite dimensional systems is widely known and can be found in, for instance [Curtain and Zwart, 1995]. We will indicate how the solution of the LQR design problem can be used to solve the estimator design problem, which we will do in the next section.

Consider the following system:

$$\Sigma' : \begin{cases} \frac{\mathrm{d}\xi}{\mathrm{d}t}(t,s) & = -A^*\xi(t,s) - C^*w(t,s), \\ \kappa(t,s) & = G^*\xi(t,s), \\ \lambda(t,s) & = S^*w(t,s), \end{cases} \tag{5.26}$$

with end-point condition $\xi(t_e, s) = \xi_{t_e}$ and $w \in L_2(\mathbb{T} \times \mathbb{T}, Y)$ and $t \in [0, t_e]$. In this section the variable s will be considered to be fixed in the interval $\mathbb{T}$ and as such s will be interpreted as a parameter of the system Σ'. The following lemma shows how the solution to this system can be characterized.

Lemma 5.5.2
Consider the system Σ' with end-point condition $\xi(t_e, s) = \xi_{t_e,s}$ and $w \in L_2(\mathbb{T} \times \mathbb{T}, Y)$, $s \in [0, t_e]$ and $t \in [0, t_e]$. Then the solution $\xi(t, s)$ to Equations (5.26) is given by:

$$\xi(t,s) = T^*(t_e - t)\xi_{t_e} + \int_t^{t_e} T^*(\tau - t)C^*w(\tau, s)\mathrm{d}\tau. \tag{5.27}$$

Proof. We differentiate the right-hand side of (5.27) with respect to t to obtain:

$$\begin{aligned} \tfrac{\mathrm{d}\xi}{\mathrm{d}t}(t,s) &= -A^*T^*(t_e - t)\xi_{t_e} + \int_t^{t_e} AT^*(\tau - t)C^*w(\tau, s)\mathrm{d}\tau - T^*(t-t)C^*w(t,s), \\ &= -A^*\xi(t,s) - C^*w(t,s), \end{aligned}$$

where $T^*(t_e - t)$ is the mild evolution operator with infinitesimal generator $-A^*$. This shows that (5.27) satisfies the equations (5.26) and concludes the proof. □

Please note that the solutions of the system are only well defined for $t < t_e$ since the semigroup operator $T^*(t)$ is only defined for $t > 0$.

The following Theorem shows the relation between $K_M(t, s)$ and $L_M(t, s)$ and the system Σ' defined by equations (5.26).

Theorem 5.5.3
Consider the system Σ' given by equations (5.25) and fix $s \in \mathbb{T}$. Let $M \in \mathcal{M}$, let

$w(t,s) = -M^*(s,t)$, $w(t,s) = 0$ for $s < t < t_e$ and let $\xi(s,s) = \xi_s = h$. Let $\kappa(t,s)$ and $\lambda(t,s)$ be the outputs of the system (5.26)*. Then the following holds:*

$$K_M(t,s) = \kappa(t,s) \quad \textit{and} \quad L_M(t,s) = \lambda(t,s), \quad \textit{for} \;\; t \in [0,s].$$

Proof. It follows from Lemma 5.4.5 that since $w(t,s) = -M^*(s,t)$ and $\xi(s,s) = h$, the state $\xi(t,s)$ satisfies:

$$\xi(t,s) = T^*(s-t)h - \int_t^s T^*(\tau - t)C^*M^*(s,\tau)\mathrm{d}\tau, \quad \text{for} \;\; t \in [0,s],$$

Then it follows from Lemma 5.5.2 that $\kappa(t,s)$ and $\lambda(t,s)$ satisfy:

$$\begin{aligned}\kappa(t,s) =& G^*T^*(s-t)h - G^* \int_t^s T^*(\tau - t)C^*M^*(s,\tau), \mathrm{d}\tau \quad \text{for} \;\; t \in [0,s],\\ \lambda(t,s) =& S^*M^*(s,t).\end{aligned}$$

By Theorem 5.5.1, and the observation that $H^* = h$ it follows that $K_M(t,s) = \kappa(t,s)$ and $L_M(t,s) = \lambda(t,s)$ for $t \in [0,s]$. □

It now follows that the optimization criterion $J_{HS}(M)$ can be related to the system (5.26) in the following way.

Corollary 5.5.4
Let $M \in \mathcal{M}$ and let $\kappa(t,s)$ and $\lambda(t,s)$ be the output of the system (5.26) *with end-point condition $\xi(s,s) = \xi_s = h$ and input $w(t,s) = -M^*(s,t)$. Then $J_{HS}(M)$ equals:*

$$J_{HS}(M) = \left(\int_{\mathbb{T}} \int_0^s ||\kappa(t,s)||_2^2 + ||\lambda(t,s)||_2^2 \, \mathrm{d}t \, \mathrm{d}s \right)^{\frac{1}{2}}. \tag{5.28}$$

This result follows immediately from Theorem 5.5.3 since $K_M(t,s) = \kappa(t,s)$ and $L_M(t,s) = \lambda(t,s)$ for $0 < t < s$ under the conditions which have been assumed.

Theorem 5.5.5
Let $M \in \mathcal{M}$ and let ξ be the state of the system (5.26) *with end-point condition $\xi(t,s) = \xi_{s,s} = h$ and input $w(t,s) = -M^*(s,t)$. Then J_{HS}^2 can be rewritten as follows:*

$$J_{HS}^2(M) = \int_0^{t_e} \left[\langle h, \Pi(s)h \rangle + \int_0^s || - (SS^*)^{\frac{1}{2}} M^*(s,t) + (SS^*)^{-\frac{1}{2}} C\Pi(t)\xi(t,s)||_2^2 \, \mathrm{d}t \right] \mathrm{d}s$$

where the operator $\Pi(t) : X \to X$ with $t \in \mathbb{T}$ is defined as the unique self-adjoint solution to the Riccati differential equation:

$$\langle \xi_n, \dot{\Pi}\xi_m \rangle = \langle \xi_n, \Pi A^*\xi_m \rangle + \langle \Pi A^*\xi_n, \xi_m \rangle + \langle G^*\xi_n, G^*\xi_m \rangle - \langle (SS^*)^{-1}C\Pi\xi_m, C\Pi\xi_n \rangle, \tag{5.29}$$

for all $\xi_m, \xi_n \in D(A^*)$ with boundary condition $\Pi(0) = 0$.

Before this theorem will be proved, a general LQR design problem for the system (5.26) will be introduced. The solution of the linear quadratic regulator design problem for the system (5.26) will be presented and this solution will be used to prove Theorem 5.5.5 and to find the minimizer of the functional $J_{HS}(M)$.

Lemma 5.5.6
Consider the system (5.26) *with end-point condition* $\xi(s,s) = \xi_s \in X$ *and input* $w(\cdot,s) := w_s$ *where* $s \in \mathbb{T}$. *Moreover, consider the criterion* $J'(w_s,\xi_s)$, *defined by:*

$$J'(w_s,\xi_s) = \left(\int_0^s ||\kappa(t,s)||_2^2 + ||\lambda(t,s)||_2^2 \mathrm{d}t\right)^{\frac{1}{2}}. \tag{5.30}$$

Let $w_{s,opt} \in L_2(\mathbb{T},Y)$ *be the minimizer of* $J'(w_s,\xi_s)$ *i.e.:*

$$w_{s,opt} = \arg \inf_{w_s \in L_2(\mathbb{T},Y)} J'(w_s,\xi_s).$$

Then, $w_{s,opt}(t)$ *is unique and satisfies:*

$$w_{s,opt}(t) = -(SS^*)^{-1}C\Pi(t)\xi(t,s), \tag{5.31}$$

where the operator $\Pi(t) : X \to X$ *is defined as the unique self-adjoint solution to the Riccati differential equation* (5.29) *on the interval* $t \in [0,s]$. *Moreover, the value of infimum of* $J'(w_s,\xi_s)$ *is given by:*

$$J'(w_{s,opt},\xi_s) = \left(\langle \xi_s, \Pi(s)\xi_s\rangle - \langle \xi(0,s), \Pi(0)\xi(0,s)\rangle\right)^{\frac{1}{2}}.$$

Proof. We introduce the functional $V(\xi) = \langle \xi, \Pi\xi\rangle$ and differentiate the functional $V(\xi(t,s))$ with respect to t:

$$\frac{\mathrm{d}V(\xi(t,s))}{\mathrm{d}t} = \langle \dot{\xi}(t,s), \Pi\xi(t,s)\rangle + \langle \Pi\xi(t,s), \dot{\xi}(t,s)\rangle + \langle \xi(t,s), \dot{\Pi}\xi(t,s)\rangle.$$

Then we use that Π solves the Riccati equation for all $\xi \in D(A^*)$, and we evaluate $\frac{\mathrm{d}V(\xi(t,s))}{\mathrm{d}t}$ at $\xi(t,s)$ that satisfy the Equations (5.26). We omit the time indices for brevity and rewrite $\dot{V}$ as follows:

$$\begin{aligned}
\frac{\mathrm{d}V(\xi)}{\mathrm{d}t} =& \langle -A^*\xi - C^*w, \Pi\xi\rangle + \langle \Pi\xi, -A^*\xi - C^*w\rangle + \langle \xi, \Pi A^*\xi\rangle + \langle \Pi A^*\xi, \xi\rangle \\
&+ \langle G^*\xi, G^*\xi\rangle - \langle (SS^*)^{-1}C\Pi\xi, C\Pi\xi\rangle \\
=& -\langle C^*w, \Pi\xi\rangle - \langle \Pi\xi, C^*w\rangle + \langle G^*\xi, G^*\xi\rangle - \langle (SS^*)^{-\frac{1}{2}}C\Pi\xi, (SS^*)^{-\frac{1}{2}}C\Pi\xi\rangle \\
=& + \langle G^*\xi, G^*\xi\rangle - \langle (SS^*)^{\frac{1}{2}}w, (SS^*)^{-\frac{1}{2}}C\Pi\xi\rangle \\
&- \langle (SS^*)^{-\frac{1}{2}}C\Pi\xi, (SS^*)^{\frac{1}{2}}w\rangle - \langle (SS^*)^{-\frac{1}{2}}C\Pi\xi, (SS^*)^{-\frac{1}{2}}C\Pi\xi\rangle \\
=& + \langle G^*\xi, G^*\xi\rangle + \langle (SS^*)^{\frac{1}{2}}w, (SS^*)^{\frac{1}{2}}w\rangle - \\
&\langle (SS^*)^{\frac{1}{2}}w + (SS^*)^{-\frac{1}{2}}C\Pi\xi, (SS^*)^{\frac{1}{2}}w + (SS^*)^{-\frac{1}{2}}C\Pi\xi\rangle \\
=& + ||G^*\xi||_2^2 + ||(SS^*)^{\frac{1}{2}}w||_2^2 - ||(SS^*)^{\frac{1}{2}}w + (SS^*)^{-\frac{1}{2}}C\Pi\xi||_2^2
\end{aligned}$$

Hence, after integration of $\dot{V}$ over the index t in the interval $[0, s]$ and substitution of $G^*\xi = \kappa$ and $S^*w = \lambda$ it follows that:

$$\langle \xi(s,s), \Pi(s)\xi(s,s)\rangle - \langle \xi(0,s), \Pi(0)\xi(0,s)\rangle = \int_0^s ||\kappa(\tau,s)||_2^2 + ||\lambda(\tau,s)||_2^2 - ||(SS^*)^{\frac{1}{2}} w(\tau,s) + (SS^*)^{-\frac{1}{2}} C\Pi(\tau)\xi(\tau,s)||_2^2 \mathrm{d}\tau.$$

Rearrangement of the latter equation shows that:

$$J'^2(w_s, \xi_s) = \langle \xi(s,s), \Pi(s)\xi(s,s)\rangle - \langle \xi(0), \Pi(0)\xi(0)\rangle + \int_0^s ||(SS^*)^{\frac{1}{2}} w(\tau,s) + (SS^*)^{-\frac{1}{2}} C\Pi(\tau)\xi(\tau,s)||_2^2 \mathrm{d}\tau. \quad (5.32)$$

The term $\langle \xi(s,s), \Pi(s)\xi(s,s)\rangle - \langle \xi(0,s), \Pi(0)\xi(0,s)\rangle$ is independent of $w_s(t)$. Therefore, $J'(w_s, \xi_s)$ is minimized if

$$\int_0^s ||(SS^*)^{\frac{1}{2}} w(\tau,s) + (SS^*)^{-\frac{1}{2}} C\Pi(\tau)\xi(\tau,s)||_2^2 \mathrm{d}\tau = 0.$$

The integrand is a norm and therefore non-negative. We conclude that the integral is minimized if and only if the intergrand is zero for all $t \in [0, s]$. From this it follows that the minimizer of $J'(w_s, \xi_s)$ is unique and given by:

$$w_{s,opt}(t) = -(SS^*)^{-1} C\Pi(t)\xi(t,s) \quad \text{for } t < s.$$

Substitution of $w(s,t) = w_{opt}(s,t) = w_{s,opt}(t)$ in Equation (5.32) shows the infimum value of J'. □

From the structure of $w_{s,opt}$ it follows that the optimal input can be realized as a linear time dependent state feedback law, with a structure which is independent of the endpoint condition ξ_s and the value of s. The optimal control $w_{s,opt}$ can also be represented as output of the autonomous closed loop system.

Lemma 5.5.7
The minimizer $w_{s,opt}$ of J' given by Equation (5.30) *and end-point condition ξ_s, can be expressed as:*

$$w_{s,opt}(t) = -(SS^*)^{-1} C\Pi(t)\tilde{W}(t,s)\xi_s \quad \textit{for } t < s.$$

where $\Pi(t)$ is the solution of (5.29) *with $\Pi(0) = 0$. and $\tilde{W}(t,s) : X \to X$ for $t \in \mathbb{T}$ is the mild evolution operator with the infinitesimal generator $-A^* + C^*(SS^*)^{-1}C\Pi(t)$ on the interval $0 \le t \le s$.*

Proof. First remark that the structure of the Riccati equation (5.29) and the boundary condition on $\Pi(0)$ is independent of the values of s. The state and output trajectories which are the result of the optimal control in state feedback form, can be found by substitution of the optimal feedback law $w_{s,opt}$ into the system dynamics (5.26). The closed loop system is defined for $t < s$ and is given by Σ'_{cl}:

$$\Sigma'_{cl} = \begin{cases} \dot{\xi}_{cl}(t,s) = (-A^* + C^*(SS^*)^{-1}C\Pi(t))\xi_{cl}(t,s), \\ w_{s,opt}(t) = -(SS^*)^{-1}C\Pi(t)\xi_{cl}(t,s), \end{cases} \quad (5.33)$$

where $\xi_{cl}(s,s) = \xi_s$ and $t < s$.

It follows that $-A^* + C^*(SS^*)^{-1}C\Pi(t)$ is the infinitesimal generator of a mild evolution operator $W(t,s)$ on the interval $t \in [0,s]$, i.e. $W(t,s) : X \to X$ is such that:

$$(-A^* + C^*(SS^*)^{-1}C\Pi(t))\xi = \lim_{h\to 0} \frac{[\tilde{W}(t-h,s) - \tilde{W}(t,s)]\xi}{h}$$

for any $\xi \in D(-A^*)$, $0 \le t \le s$ and $s \in \mathbb{T}$. The closed loop system (5.33) is autonomous and the state trajectory of the system only depends on the boundary condition ξ_s. The trajectories satisfy:

$$\xi_{cl}(t,s) = \tilde{W}(t,s)\xi_s \quad \text{for } t < s.$$

By substitution of the latter into (5.31), $w_{s,opt}(t)$ can be written into closed loop form and completes the proof. □

We are now in the position to present the proof to Theorem 5.5.5.

Proof of Theorem 5.5.5. The assertion in Theorem 5.5.5 now follows from the observation that the theorem is a special case of Lemma 5.5.6 with $\xi(s,s) = h$ and $w(t,s) = -M^*(t,s)$. In particular we have by, Theorem 5.5.3, that

$$J_{HS}(M)^2 = \int_0^{t_e}\int_0^s ||\kappa(\tau,s)||_2^2 + ||\lambda(\tau,s)||_2^2 \mathrm{d}\tau\, \mathrm{d}s,$$

where κ and λ satisfy (5.26) with $\xi(s,s) = h$. First, rewrite the inner integral as done in Lemma 5.5.6, to:

$$J_{HS}(M)^2 = \int_0^{t_e} \Big[\langle \xi(s,s), \Pi(s)\xi(s,s)\rangle + \int_0^s ||(SS^*)^{\frac{1}{2}} w(\tau,s) + (SS^*)^{-\frac{1}{2}} C\Pi(\tau)\xi(\tau,s)||_2^2 \mathrm{d}\tau\Big]\mathrm{d}s.$$

where the operator $\Pi(t) : X \to X$ with $t \in \mathbb{T}$ is defined as the unique self-adjoint solution to the Riccati differential equation:

$$\langle \xi_n, \dot{\Pi}\xi_m\rangle = \langle \xi_n, \Pi A^*\xi_m\rangle + \langle \Pi A^*\xi_n, \xi_m\rangle + \langle G^*\xi_n, G^*\xi_m\rangle - \langle (SS^*)^{-1}C\Pi\xi_m, C\Pi\xi_n\rangle, \tag{5.34}$$

for all $\xi_m, \xi_n \in X$ and with boundary condition $\Pi(0) = \Pi_0$ where Π_0 is self-adjoint and positive semi-definite on $D(A^*)$. Then, by substitution of $w(t,s) = -M^*(t,s)$ and $\xi(s,s) = h$ it follows that

$$J_{HS}(M)^2 = \int_0^{t_e} \Big[\langle h, \Pi(s)h\rangle + \int_0^s || - (SS^*)^{\frac{1}{2}} M^*(s,\tau) + (SS^*)^{-\frac{1}{2}} C\Pi(\tau)\xi(\tau,s)||_2^2 \mathrm{d}\tau\Big]\mathrm{d}s.$$

□

We are now in the position to solve the problem of minimization ofJ_{HS} for $n = 1$, i.e. $Z = \mathbb{R}$. We will show that when $Z = \mathbb{R}$ and $Hx = \langle h, x\rangle$, a solution to minimization of the functional J' given by Equation (5.30) with $\xi_s = h$ provides a solution for the minimization of $J_{HS}(M)$.

Theorem 5.5.8
Consider the functional $J_{HS}(M)$ given by (5.20)*. The unique minimizer $M \in \mathcal{M}$ of $J_{HS}(M) = ||\Sigma_g^* \wedge \Sigma_e^*(M)||_{HS}$ is uniquely defined by:*

$$M_{opt}^*(s,t) = \begin{cases} (SS^*)^{-1}C\Pi(t)\xi(t,s) & \text{for } 0 \le t \le s, \\ 0 & \text{for } s < t \le t_e, \end{cases}$$

where $\xi(t,s)$ satisfies (5.26) *with boundary condition $\xi(s,s) = h$ and input $w(t,s) = -M_{opt}^*(s,t)$. The operator $\Pi(t) : X \to X$ with $t \in \mathbb{T}$ is defined as the unique self-adjoint solution to the Riccati differential equation* (5.34)*. The minimum value of $J_{HS}(M)$ is given by:*

$$J_{HS}(M_{opt}) = \left(\int_0^{t_e} \langle h, \Pi(s)h\rangle \mathrm{d}s \right)^{\frac{1}{2}}.$$

Proof. Let $M \in \mathcal{M}$ and let ξ be the state of the system (5.26) with end-point condition $\xi(s,s) = \xi_s = h$ and input $w(t,s) = -M^*(s,t)$. Then it follows from Theorem 5.5.5 that the criterion $J_{HS}(M)$ can be written as:

$$J_{HS}(M)^2 = \int_0^{t_e} \langle h, \Pi(s)h\rangle + \int_0^s || - (SS^*)^{\frac{1}{2}} M^*(s,t) + (SS^*)^{-\frac{1}{2}} C\Pi(\tau)\xi(\tau,s)||_2^2 \, \mathrm{d}\tau \, \mathrm{d}s. \quad (5.35)$$

where $\xi(t,s)$ satisfies (5.26) with $\xi(s,s) = h$ and $w(t,s) = -M^*(s,t)$ and where the operator $\Pi(t) : X \to X$ with $t \in \mathbb{T}$ be defined as the unique self-adjoint solution to the Riccati differential equation (5.34). It follows that the integrand is zero if and only if $M^*(t,s) = (SS^*)^{-\frac{1}{2}} C\Pi(t)\xi(t,s)$. The contribution of $\langle h, \Pi(s)h\rangle$ to $J_{HS}(M)^2$ is independent of the choice of M such that it must be concluded that M_{opt}^* is unique and is given by $M_{opt}^*(t,s) = (SS^*)^{-\frac{1}{2}} C\Pi(t)\xi(t,s)$. The value of $J_{HS}(M_{opt})$ follows by substitution of M_{opt} in (5.35). □

We are now in the position to solve the optimal estimator design problems by minimization of $J_{HS}(M)$ for $Z = \mathbb{R}$. First the design problem for a single to-be-estimated signal will be solved and then it will be generalized to the solution for $Z = \mathbb{R}^n$.

Theorem 5.5.9
Let $Z = \mathbb{R}$ and $Hx = \langle h, x\rangle$ and consider problem 5.2 for $J_{HS}(M)$ given by (5.20)*. The unique minimizer $M \in \mathcal{M}$ of $J_{HS}(M)$ is given by:*

$$M_{opt}(t,s) = \begin{cases} HU(t,s)\Pi(s)C^*(SS^*)^{-1} & \text{for } 0 \le s \le t \\ 0 & \text{for } t < s \le t_e \end{cases}$$

where the operator $\Pi(t) : X \to X$ with $t \in \mathbb{T}$ is defined as the unique self-adjoint solution to the Riccati differential equation:

$$\begin{aligned}\langle \xi_n, \dot{\Pi}\xi_m \rangle =& \langle \xi_n, \Pi A^* \xi_m \rangle + \langle \Pi A^* \xi_n, \xi_m \rangle \\ &+ \langle G^* \xi_n, G^* \xi_m \rangle - \langle (SS^*)^{-1} C\Pi \xi_m, C\Pi \xi_n \rangle, \quad \text{for all } \xi_m, \xi_n \in X\end{aligned} \tag{5.36}$$

with boundary condition $\Pi(0) = 0$ and $U(t,s)$ is the evolution operator with infinitesimal generator $A - \Pi(t)C^*(S^*S)^{-1}C$.

Proof. Theorem 5.5.8 shows that the unique minimizer of $||\Sigma_g^* \wedge \Sigma_e^*(M)||$ is given by

$$M_{opt}^*(s,t) = (SS^*)^{-1} C\Pi(t)\xi(t,s) \quad \text{for } t < s,$$

where $\xi(t,s)$ satisfies Equation (5.26) with $\xi(s,s) = h$, $w(t,s) = -M_{opt}^*(t,s)$ and where the operator $\Pi(t) : X \to X$ with $t \in \mathbb{T}$ is defined as the unique self-adjoint solution to the Riccati differential equation (5.34). By Lemma 5.5.7, it follows that $M_{opt}^*(s,t)$ can also be represented by the closed loop representation:

$$M_{opt}^*(s,t) = (SS^*)^{-1} C\Pi(t)\tilde{W}(t,s)h \quad \text{for } 0 < t < s,$$

where $\tilde{W}(t,s)$ is the mild evolution operator with infinitesimal generator $-A^* + C^*(SS^*)^{-1}C\Pi(t)$. Since it has been demanded that M_{opt} represents a causal estimator, it follows that $M_{opt}^*(s,t) = 0$ on the interval $s < t \leq t_e$. Therefor, $M_{opt}^*(s,t)$ is now defined on the rectangular interval $\mathbb{T} \times \mathbb{T}$ and is given by:

$$M_{opt}^*(s,t) = \begin{cases} (SS^*)^{-1} C\Pi(t)\tilde{W}(t,s)h & \text{for } 0 \leq t \leq s, \\ 0 & \text{for } s < t \leq t_e \end{cases}$$

We conclude that controller Σ_c^* that minimizes $||\Sigma_g^* \wedge \Sigma_c^*||_{HS}$ is given by:

$$(\Sigma_c^* \tilde{e})(t) = \int_t^{t_e} M_{opt}^*(s,t)\tilde{e}(s)\mathrm{d}s = \int_t^{t_e} (SS^*)^{-1} C\Pi(t)\tilde{W}(t,s)h\tilde{e}(s)\mathrm{d}s$$

and we conclude that $\Sigma_e^*(M) = \Sigma_c^*$.

By Corollary 5.4.11 it now follows that the estimator $\Sigma_e(M_{opt}) = [\Sigma_e(M_{opt})^*]^*$ is the unique minimizer of $J_{HS}(M) = ||\Sigma_g \wedge \Sigma_e(M)||$. Therefore, M_{opt} can be obtained by dualization of Σ_c^* and is given by:

$$M_{opt}(t,s) = HU(t,s)\Pi(s)C(SS^*)^{-1}, \quad \text{for } s < t.$$

where $U(t,s) : X \to X$ is the evolution operator with infinitesimal generator $A - \Pi(t)C^*(S^*S)^{-1}C$ □

By Corrolary 5.4.11 it now follows that for $Z = \mathbb{R}$ the solution to the optimal estimator design problem has an input/output map that can be represented by:

$$\Sigma_e(M_{opt}) : \hat{z}(t) = \int_0^t M_{opt}(t,s)y(s)\mathrm{d}s, \tag{5.37}$$

with $M_{opt}(t,s) = HU(t)\Pi(t)C(SS^*)^{-1}$.

Therefore, the optimal estimator for $Z = \mathbb{R}$ is represented by the mapping:

$$\Sigma_e(M_{opt}) : \hat{z}(t) = \int_0^t HU(t,s)\Pi(s)C^*(S^*S)^{-1}y(\tau)\mathrm{d}\tau. \tag{5.38}$$

5.5.4 Realization of the optimal estimator

Given the optimal convolution kernel of the optimal estimator as in Theorem 5.5.9 and the structure of the causal input output map (5.2) of the estimator, the input output map of the optimal estimator is known. The optimal estimator for $Z = \mathbb{R}$ is realized by the following state space system:

Theorem 5.5.10
Let $Z = \mathbb{R}$. The optimal estimator $\Sigma_e(M_{opt})$ which minimizes the norm $||\Sigma_p \wedge \Sigma_e(M)||_{HS}$ over all $M \in \mathcal{M}$, and solves the estimator design problem 5.2 for the Hilbert-Schmidt norm is given by:

$$\Sigma_e(M_{opt}) : \begin{cases} \dot{\alpha}(t) &= (A - \Pi(t)C^*(SS^*)^{-1}C)\alpha(t) + \Pi(t)C^*(S^*S)^{-1}y(t), \\ \hat{z}(t) &= H\alpha(t), \end{cases} \tag{5.39}$$

with initial condition $\alpha(0) = 0$.

Proof. Assume that $(A - \Pi(t)C^*(S^*S)^{-1}C)$ is the generator of evolution operator $U(t,s)$. Then the unique solution of this system is given by:

$$\hat{z}(t) = \int_0^t HU(t,s)\Pi(s)C(S^*S)^{-1}y(s)\mathrm{d}s = \int_0^t M_{opt}(t,s)y(s)\mathrm{d}s,$$

from, which it follows that $M_{opt}(t,s) = HU(t,s)\Pi(s)C(S^*S)^{-1}$, such that the system (5.39) is a realization of the optimal estimator. □

It follows from the structure of realization of the optimal estimator, that state evolution of the optimal estimator does not depend on the operator H. This can be specifically seen by the absence of H in the state-evolution by Equation (5.39) and the Riccati differential equation (5.29). As such the estimator $\Sigma_e(M_{opt})$ can be called a state estimator. Moreover the readout map of the optimal estimator is equal the to readout map of the system under study. Therefore generalization of the optimal estimator for one estimated output to an optimal estimator for system with a higher dimensional output, i.e. $Z = \mathbb{R}^n$, is straightforward. One can solve the optimal estimation problem for each output individually and combine these estimators. This results into an estimator with a n-dimensional readout map that equals the operator H of the original system Σ_p.

Theorem 5.5.11
Let $Z = \mathbb{R}^n$ and $Hx = \sum_{i=1}^n \langle h_i, x\rangle e_i$ where $h_i \in X$ and $\{e_i\}_{i=1}^n$ is the canonical basis in $\mathbb{R}^n$. The optimal estimator $\Sigma_e(M_{opt})$ which minimizes $||\Sigma_p \wedge \Sigma_e(M)||_{HS}$ over all

$M \in \mathcal{M}$, and solves the estimator design problem 5.2 for the Hilbert-Schmidt norm is given by:

$$\Sigma_e(M_{opt}) = \begin{cases} \dot{\alpha} & = (A - \Pi(t)C^*(SS^*)^{-1}C)\alpha + \Pi(t)C^*(S^*S)^{-1}y, \\ \hat{z} & = H\alpha. \end{cases} \tag{5.40}$$

With initial condition $\alpha(0) = 0$. Moreover, $J(M_{opt}) = (\sum_{i=1}^{n} \int_{\mathbb{T}} \langle h_i, \Pi(s)h_i \rangle \mathrm{d}s)^{\frac{1}{2}}$.

Proof. Consider for $i \in 1, ..., n$ the problem to minimize $J_{HS}(M)$ with $z_i = \langle h_i, x \rangle$. By Theorem 5.5.10 the solution is given by Equation (5.39) with $\hat{z}_i := \hat{z}_i = \langle h_i, \alpha \rangle$. Observe that for every $i \in 1, ..., n$ the evolution of α does not depend on h_i. Therefore we infer that:

$$\Sigma_e(M_{opt}) = \begin{cases} \dot{\alpha} & = (A - \Pi(t)C^*(SS^*)^{-1}C)\alpha + \Pi(t)C^*(S^*S)^{-1}y, \\ \begin{bmatrix} \hat{z}_1 \\ \vdots \\ \hat{z}_n \end{bmatrix} & = \begin{bmatrix} \langle h_1, \alpha \rangle \\ \vdots \\ \langle h_n, \alpha \rangle \end{bmatrix} = H\alpha, \end{cases} \tag{5.41}$$

is the estimator that solves the estimator design problem for $Z = \mathbb{R}^n$. □

By Theorem 5.5.11 as solution to the estimator design Problems 5.1 and 5.2 have been provided. The analysis also provides a solution to Problem 5.3, since by the applied completion of the squares argument it follows immediately that the optimal estimator is unique.

5.6 Optimal induced L_2-gain estimator design

In this section we consider the design of estimators, where we use the induced L_2-gain between the disturbance sources d_1 and d_2 and the estimation error e as design criterion. The L_2-gain can be interpreted as the worst case energy gain of signals, in which one compares the ratio of energy of signal at d_1 resp. d_2 and e for all possible signals d_1,d_2 with a finite amount of energy on the interval $\mathbb{T}$.

Optimal L_2-gain estimators arise in finite time estimation problems and are analogues to H_∞ estimators, which involve infinite time horizons of the to be estimated signals. The optimal L_2-gain estimator design problem is of relevance, since its solution enables the design of estimators in a robust estimation setting. In this way estimators for uncertain systems can be designed.

In the work of Van Keulen and Curtain, see for instance [Van Keulen, 1993], the design of H_∞-optimal output feedback controllers has been studied in an infinite dimensional setting. This work presents methods for coupled estimator and controller design, which are inherent in the H_∞ framework. Estimator design in the absence of a controller can be treated as a special case of the approach in [Van Keulen, 1993] and the resulting estimator will coincide with the estimator derived in this work. However, the derivation

of a complete solution to the optimal L_2-gain estimator design problem presented here is of independent interest as we consider this problem from different perspectives, including a game theoretic analysis.

The solution that is presented provides an intuitive interpretation to the problem, since it is based on a completion of the squares argument. This method has been used in [Bensoussan and Bernhard, 1992] to solve the optimal H_∞ regulator design problem for distributed parameter systems. The section is organized as follows. Firstly, we formalize the optimal L_2-gain estimator design problem for distributed parameter systems. Then we introduce an L_2-gain regulator design problem for a dual system and show the equivalence of the L_2-gain estimator design problem and the previously mentioned regulator design problem. Subsequently, we will provide a solution to the regulator design problem which is based on game theory and a completion of the squares argument. Using this result, an explicit state space realization of an optimal L_2-gain estimator is given. In the last section conclusions of the presented estimator design procedure are drawn.

5.6.1 Formulation of the design problem

In this section we study the Problems 5.1, 5.2, 5.3 and 5.4 for the design of estimators for system Σ_p (given by Equation (5.1)) in which we use the induced $L_{2,2}$-norm of the system $\Sigma_p \wedge \Sigma_e(M)$ as the design criterion $J(M)$. For completeness, we repeat that we will actually consider the design problem for the generalized plant Σ_g, given by Equation (5.7). In the context of unknown initial condition, we consider as design criterion $J_{02,2}(M)$ the induced L_2-gain of the system $\Sigma_g \wedge \Sigma_e$, given by:

$$J_{02,2}(M) := ||\Sigma_g \wedge \Sigma_e(M)||_{02,2} = \sup_{\substack{d_1 \in L_2(\mathbb{T},\mathcal{D}_1) \\ d_2 \in L_2(\mathbb{T},\mathcal{D}_2) \\ x_0 \in X}} \frac{||e||_2}{\sqrt{||x_0||_2^2 + ||d_1||_2^2 + ||d_2||_2^2}},$$

where e satisfies Equation (5.3a). In the context of known initial conditions we set $x_0 = 0$, we consider as design criterion $J_{2,2}(M)$ the L_2-gain of the system $\Sigma_g \wedge \Sigma_e$, given by:

$$J_{2,2}(M) := ||\Sigma_g \wedge \Sigma_e(M)||_{2,2} = \sup_{\substack{d_1 \in L_2(\mathbb{T},\mathcal{D}_1) \\ d_2 \in L_2(\mathbb{T},\mathcal{D}_2)}} \frac{||e||_2}{\sqrt{||d_1||_2^2 + ||d_2||_2^2}},$$

where e satisfies Equation (5.3a) for $x_0 = 0$ and we set $x_0 = 0$ in Equation (5.7).

In the remainder of this section we will study the design problem in the context of unknown initial condition, (i.e. minimization of $J_{02,2}(M)$) and will derive the solution for known initial conditions (i.e. minimization of $J_{2,2}(M)$) as special case of the latter. In the next subsection we will introduce our main result for L_2 estimator design, which relates the estimator design problem to the controller design problem.

5.6.2 Main results

The main result of this section will be to show the relation between four problems associated to Σ_g given by (5.7), Σ_g^* given by (5.15) and a two player zero sum differential game. We will show that for one of the problems a solution can be found, which can be used to solve the related problems and finally provide a solution to the estimator design problems defined in the Problems 5.1, 5.2, 5.3 and 5.4. Associated to Σ_g^* (given by Equation (5.15)), we introduce the functional $J_\gamma(\tilde{y}, \tilde{e}, p_{t_e})$, which is, for fixed $\gamma > 0$, defined as:

$$J_\gamma(\tilde{y}, \tilde{e}, p_{t_e}) = ||p(0)||_2^2 + ||\tilde{d}_1||_2^2 + ||\tilde{d}_2||_2^2 - \gamma^2||\tilde{e}||_2^2$$

and where $(\tilde{d}_1, \tilde{d}_2, \tilde{e})$ satisfy the system evolution of Σ_g^*, given by the differential equation in (5.15) with $p(t_e) = p_{t_e}$. We define the classes $\mathcal{Y}_f$ and $\mathcal{Z}_f$ of signals which can be realized by a causal feedback of the state of Σ_g^* as follows:

$$\begin{aligned}\mathcal{Y}_f := \{y \in L_2(\mathbb{T}, Y) |\ &\exists \pi_y(t) : L_2(\mathbb{T}, X) \to L_2(\mathbb{T}, Y) \text{ such that for all } t \in \mathbb{T} : \\ &y(t) = (\pi_y(t)p)(t) = (\pi_y(t)\sigma_t p)(t)\}, \\ \mathcal{Z}_f := \{e \in L_2(\mathbb{T}, Z) |\ &\exists \pi_e(t) : L_2(\mathbb{T}, X) \to L_2(\mathbb{T}, Z) \text{ such that for all } t \in \mathbb{T} : \\ &e(t) = (\pi_e(t)p)(t) = (\pi_e(t)\sigma_t p)(t)\}.\end{aligned}$$

We introduce the following problems:

P1 Find an estimator $\Sigma_e : L_2(\mathbb{T}, Y) \to L_2(\mathbb{T}, Z)$ for Σ_g such that the L_2-gain of the interconnection is less than γ, as shown in Figure 5.4a, i.e. $||\Sigma_g \wedge \Sigma_e(M)||_{2,2} < \gamma$.

P2 Find an output feedback regulator $\Sigma_c : L_2(\mathbb{T}, Z) \to L_2(\mathbb{T}, Y)$ such that the L_2-gain of the interconnection of Σ_g^* and Σ_c, as shown in Figure 5.4b, is less than γ, i.e. $||\Sigma_g^* \wedge \Sigma_c||_{2,2} < \gamma$.

P3 Find a causal state feedback regulator $\Sigma_s : L_2(\mathbb{T}, X) \to L_2(\mathbb{T}, Y)$, that it implements the map $p \mapsto y_s$ such that $y_s \in \mathcal{Y}_f$ with $y_s(t) = (\pi_y(t)p)(t) = F(t)p(t)$, such that the L_2-gain of the interconnection of Σ_g^* and Σ_s is less than γ, i.e. $||\Sigma_g^* \wedge \Sigma_s||_{2,2} < \gamma$.

P4 Two-player zero-sum differential game with full state information feedback and value function $J_\gamma(\tilde{y}, \tilde{e}, p_{t_e})$. Find a strategy $y_N \in \mathcal{Y}_f, e_N \in \mathcal{Z}_f$ such that a Nash equilibrium is established. This is characterized by:

$$J_\gamma(y_N, \tilde{e}, p_{t_e}) \leq J_\gamma(y_N, e_N, p_{t_e}) \leq J_\gamma(\tilde{y}, e_N, p_{t_e}),$$

for all $\tilde{y} \in L_2(\mathbb{T}, Y)$ and $\tilde{e} \in L_2(\mathbb{T}, Z)$.

In the remainder of this section we will show that the solution of problem $P4$ provides a solution to all of the problems stated above. We will show in the following theorems that the solution to problem $P4$ provides a solution to $P1$ since $P4$ solves $P3$, $P3$ solves $P2$ and $P2$ solves $P1$. In the next subsection the solution of problem $P1$ will be derived by use of the solution of $P4$ and the relation between the problems. First the relation between problem $P1$ and problem $P2$ is expressed by the following theorem.

Theorem 5.6.1 (relation $P1$ and $P2$)
The estimator Σ_e solves problem $P1$ if and only if the controller $\Sigma_c = \Sigma_e^*$ solves problem $P2$.

Proof. Let the solution to problem $P1$ be given by Σ_e. Then the system $\Sigma_g \wedge \Sigma_e$ is defined by the interconnection of Σ_g with Σ_e and satisfies $||\Sigma_g \wedge \Sigma_e||_{2,2} \leq \gamma$. We define $\Sigma_e^* : L_2(\mathbb{T}, Z) \to L_2(\mathbb{T}, Y)$ as the dual system of Σ_e. From Lemma 5.4.2 it follows that $||(\Sigma_g \wedge \Sigma_e)^*||_{2,2} \leq \gamma$. Moreover, from lemma 5.4.9 it follows that $(\Sigma_g \wedge \Sigma_e)^* = (\Sigma_g^* \wedge \Sigma_e^*)$, thus it follows that $||(\Sigma_g^* \wedge \Sigma_e^*)||_{2,2} \leq \gamma$. Therefore $\Sigma_c = \Sigma_e^*$ provides a solution to problem $P2$. The converse holds on the basis of the same arguments. □

Due to the special structure of the generalized plant, a solution to the state feedback regulator design problem $P3$ provides a solution to the output feedback regulator design problem $P2$.

Theorem 5.6.2 (Relation between $P3$ and $P2$)
Suppose that the state feedback regulator Σ_s implements a feedback law $y_s(t) = F(t)p(t)$ such that it solves $P3$. Then the system Σ_o,

$$\Sigma_o : \begin{cases} \dot{\xi}(t) = & (-A^* - C^*F(t))\xi(t) + H^*\tilde{\tilde{z}}(t) \quad \textit{with: } \xi(t_e) = 0, \\ \tilde{y}(t) = & F(t)\xi(t), \end{cases} \tag{5.42}$$

provides a solution to problem $P2$.

Proof. Let the regulator $\Sigma_s : y_s(t) = F(t)p(t)$ solve problem $P3$ and let Σ_o be as in (5.42). After interconnection of Σ_g^* with Σ_s the system $\Sigma_g^* \wedge \Sigma_s$ admits the following representation:

$$\Sigma_g^* \wedge \Sigma_s = \begin{cases} \dot{p}_s(t) = & (-A^* - C^*F(t))p_s(t) - H^*\tilde{e}(t) \quad \text{with: } p(t_e) = 0, \\ \tilde{d}_{1,s}(t) = & G^*p_s(t), \\ \tilde{d}_{2,s}(t) = & S^*F(t)p_s(t), \end{cases}$$

and $||\Sigma_g^* \wedge \Sigma_s|| < \gamma$. The interconnected system $\Sigma_g^* \wedge \Sigma_o$ has the representation:

$$\Sigma_g^* \wedge \Sigma_o : \begin{cases} \dot{p}_o(t) = & -A^*p_o(t) - C^*F(t)\xi(t) - H^*\tilde{e}(t) \quad \text{with: } p_o(t_e) = 0 \\ \dot{\xi}(t) = & (-A^* - C^*F(t))\xi(t) - H^*\tilde{e}(t) \quad \text{with: } \xi(t_e) = 0, \\ \tilde{d}_{1,o}(t) = & G^*p_o(t), \\ \tilde{d}_{2,o}(t) = & S^*F(t)\xi(t). \end{cases}$$

It easily follows that $\frac{\mathrm{d}}{\mathrm{d}t}(p_o - \xi) = -A^*(p_o - \xi)$. Therefore, if $p_o(t_e) = \xi(t_e)$ then $p_o(t) = \xi(t)$ for all $t \in \mathbb{T}$ and every $\tilde{e} \in L_2(\mathbb{T}, Z)$. From this it follows that if $p_o(t_e) = \xi(t_e)$ then $p_o(t) = p_s(t)$ for all $t \in \mathbb{T}$. We conclude that if $p_o(t_e) = \xi(t_e)$ then, $\tilde{d}_{1,s}(t) = \tilde{d}_{1,o}(t)$ and $\tilde{d}_{2,s}(t) = \tilde{d}_{2,o}(t)$ for every $\tilde{e} \in L_2(\mathbb{T}, Z)$, such that $||\Sigma_g^* \wedge \Sigma_o|| = ||\Sigma_g^* \wedge \Sigma_s||$. Since Σ_s solve problems $P3$ it follows that the interconnection $\Sigma_g^* \wedge \Sigma_s$ has L_2-gain less than γ. Thus we infer that $||\Sigma_g^* \wedge \Sigma_o|| < \gamma$ and that Σ_o solves problem $P2$. □

Next, we state the relation between problem $P4$ and problem $P3$. It will turn out that a Nash equilibrium strategy (y_N, e_n) with $y_N \in \mathcal{Y}_f$ and $e_N \in \mathcal{Z}_f$, provides a solution to the state feedback regulator design problem.

Theorem 5.6.3 (Relation between $P4$ and $P3$)
Suppose the strategy (y_N, e_N) establishes a Nash equilibrium for $J_\gamma(y, e, p_{t_e})$ and that $y_N \in \mathcal{Y}_f$. The causal operator π_y that maps that state p to y_N, is a state feedback regulator which solves $P3$.

Before we proceed with the proof of the theorems above, a two lemmas regarding the solution of $P4$ will be introduced.

We show that under full information feedback the two player zero sum differential game has an unique Nash-equilibrium. To do so, we first show that the value function J_γ can be rewritten in a more convenient form.

Lemma 5.6.4
Suppose there exists a symmetric operator $P(t)$, which is a solution of the differential equation:

$$\begin{aligned}\langle p_1, \dot{P} p_2\rangle = \langle PA^* p_1, p_2\rangle + \langle p_1, PA^* p_2\rangle \\ + \langle G^* p_1, G^* p_2\rangle - \langle P(C^*(SS^*)^{-1}C - \gamma^{-2}H^*H)Pp_1, p_2\rangle,\end{aligned} \tag{5.43}$$

for all $p_1, p_2 \in D(A^*)$ with $P(0) = I$. Then for all $(\tilde{d}_1, \tilde{d}_2, \tilde{e}, \tilde{y}, \tilde{z})$ that satisfy (5.15) with $p(t_e) = p_{t_e}$ we have:

$$J_\gamma(\tilde{y}, \tilde{e}, p(t_e)) = \langle p_{t_e}, P(t_e)p_{t_e}\rangle + ||(SS^*)^{\frac{1}{2}}\tilde{y} + (SS^*)^{-\frac{1}{2}}CPp||_2^2 - ||\gamma\tilde{e} - \gamma^{-1}HPp||_2^2 \tag{5.44}$$

Proof. For $p \in X$, we introduce the identity $V(p) = \langle p, Pp\rangle$ and differentiate the map $t \mapsto V(p(t))$ with respect to t.

$$\frac{\mathrm{d}V(p(t))}{\mathrm{d}t} = \langle p(t), P(t)\dot{p}(t)\rangle + \langle \dot{p}(t), P(t)p(t)\rangle + \langle p(t), \dot{P}(t)p(t)\rangle.$$

Then we substitute the dynamics of Σ_g^* for $\dot{p}$. Given that P solves the Riccati equation for all $p \in D(A^*)$, substitute $\dot{P}(t)$ with the Riccati equation with $p_1 = p_2 = p$. We omit the time index for brevity.

$$\begin{aligned}\frac{\mathrm{d}V(p)}{\mathrm{d}t} =& \langle Pp, (-A^*p - C^*\tilde{y} - H^*\tilde{e})\rangle + \langle -A^*p - C^*\tilde{y} - H^*\tilde{e}, Pp\rangle \\ &+ \langle PA^*p, p\rangle + \langle p, PA^*p\rangle + \langle G^*p, G^*p\rangle + \gamma^{-2}\langle HPp, HPp\rangle - \langle (SS^*)^{-1}CPp, CPp\rangle \\ =& \langle G^*p, G^*p\rangle + \langle -\tilde{e}, HPp\rangle + \langle HPp, -\tilde{e}\rangle + \gamma^{-2}\langle HPp, HPp\rangle \\ &- \langle CPp, \tilde{y}\rangle - \langle \tilde{y}, CPp\rangle - \langle (SS^*)^{-\frac{1}{2}}CPp, (SS^*)^{-\frac{1}{2}}CPp\rangle)\end{aligned}$$

Subsequently, one can reformulate this using a completion of the squares argument:

$$\begin{aligned}\frac{\mathrm{d}V(p)}{\mathrm{d}t} =& \langle G^*p, G^*p\rangle + \langle -\gamma\tilde{e} + \gamma^{-1}HPp, -\tilde{e}\gamma + \gamma^{-1}HPp\rangle - \gamma^2\langle \tilde{e}, \tilde{e}\rangle \\ &- \langle (SS^*)^{\frac{1}{2}}\tilde{y} + (SS^*)^{-\frac{1}{2}}CPp, (SS^*)^{\frac{1}{2}}\tilde{y} + (SS^*)^{-\frac{1}{2}}CPp\rangle + \langle (SS^*)^{\frac{1}{2}}\tilde{y}, (SS^*)^{\frac{1}{2}}\tilde{y}\rangle\end{aligned}$$

We use $d_1 = G^*p$ and $d_2 = S^*y$ and rearrange:

$$||\tilde{d}_1||_2^2 + ||\tilde{d}_2||_2^2 - \gamma^2||\tilde{e}||_2^2 = \frac{\mathrm{d}V(p)}{\mathrm{d}t} + ||(SS^*)^{\frac{1}{2}}\tilde{y} + (SS^*)^{-\frac{1}{2}}CPp||_2^2 - ||-\gamma\tilde{e} + \gamma^{-1}HPp||_2^2$$

After integration of the right- and left-hand side from $t = 0$ to $t = t_e$ one obtains an expression that equals the definition of $J_\gamma(\tilde{y}, \tilde{e}, p_{t_e})$:

$$J_\gamma(\tilde{y}, \tilde{e}, p_{t_e}) = \langle p(0), P(0)p(0)\rangle + \int_0^{t_e} ||\tilde{d}_1(t)||_2^2 + ||\tilde{d}_2(t)||_2^2 - \gamma^2||\tilde{e}(t)||_2^2 \mathrm{d}t =$$
$$\langle p_{t_e}, P(t_e)p_{t_e})\rangle + \int_0^{t_e} ||(SS^*)^{-\frac{1}{2}}CP(t)p(t) + (SS^*)^{\frac{1}{2}}\tilde{y}(t)||_2^2 - ||\gamma\tilde{e}(t) - \gamma^{-1}HP(t)p(t)||_2^2 \,\mathrm{d}t.$$

This concludes the proof. □

From the result above, a Nash equilibrium strategy that provides a solution to $P4$ follows immediately.

Lemma 5.6.5 (Solution to problem $P4$.)
The strategy (y_N, e_N) which is defined as:

$$e_N(t) = +\gamma^{-2}HP(t)p(t) \tag{5.45a}$$
$$y_N(t) = -(SS^*)^{-1}CP(t)p(t). \tag{5.45b}$$

establishes a unique Nash equilibrium. The value of the game under the equilibrium strategy is $J_\gamma(y_N, e_N, p_{t_e}) = \langle p_{t_e}, P(t_e)p_{t_e}\rangle$. Under the Nash equilibrium strategy the closed loop dynamics is given by:

$$\dot{p}_N(t) = (-A^* + (C^*(SS^*)^{-1}C - \gamma^{-2}H^*H)P(t))p_N(t), \quad \textit{with} \quad p_N(t_e) = p_{t_e}. \tag{5.46}$$

Proof. The closed loop dynamics follows immediately by substitution of the Nash equilibrium strategy into (5.15). Using Lemma 5.6.4 we rewrite the value function $J_\gamma(y,e,p(t_e))$ as in Equation (5.44). When the value function is evaluated at (5.45) the quadratic terms vanish. By convexity of the norms, uniqueness of the Nash equilibrium strategy follows and we have that $J_\gamma(y_N, e_N, p_{t_e}) \leq J_\gamma(y, e_N, p_{t_e})$ resp. $J_\gamma(y_N, e, p_{t_e}) \leq J_\gamma(y_N, e_N, p_{t_e})$. Therefore, the following inequality holds for all $y \in L_2(\mathbb{T}, \mathbb{R}^y)$ and $e \in L_2(\mathbb{T}, \mathbb{R}^z)$

$$J_\gamma(y_N, e, p_{t_e}) \leq J_\gamma(y_N, e_N, p_{t_e}) \leq J_\gamma(y, e_N, p_{t_e}),$$

which shows that y_N, e_N establishes a Nash equilibrium. The value at the equilibrium follows by evaluation of $J_\gamma(y_N, e_N, p_{t_e})$. From Equation (5.44) we infer that $J_\gamma(y_N, e_N, p_{t_e}) = \langle p_{t_e}, P(t_e)p_{t_e}\rangle$. □

Corollary 5.6.6
The unique Nash equilibrium strategy (y_N, e_N) can be realized by a static state feedback. Therefore it follows as result that $y_N \in \mathcal{Y}_f$ and $e_N \in \mathcal{Z}_f$ with mappings $\pi_y(t) = -(SS^*)^{-1}CP(t)$ and $\pi_e(t) = \gamma^{-2}HP(t)$.

We are now in the position to present the proof of Theorem 5.6.3.

Proof of Theorem 5.6.3. The relation between $P4$ and $P3$. Let (y_N, e_N) be a Nash equilibrium strategy for the functional J_γ. In Lemma 5.6.5 it has been shown that the equilibrium strategy is unique and thus we infer that y_N and e_N satisfy (5.45), a representation that is independent of p_{t_e}. Following corollary (5.6.6) the mappings $\pi_y(t) =$

and $\pi_e(t)$ are causal operators on p and independent of p_{t_e}. Define $\Sigma_s p := \pi_y(t)p$, then Σ_s is a state feedback controller for the system Σ_g^*. When Σ_s is interconnected with the system Σ_g^*, the output of the controller Σ_s is equal to $\pi_y(t)p = y_N$.

In Lemma 5.6.5 is has been shown that:

$$J_\gamma(y_N, e_N, p_{t_e}) = \langle p_{t_e}, P(t_e)p_{t_e}\rangle$$

The pair (y_N, e_N) establish a Nash equilibrium and therefore it follows that for all $e \in L_2(\mathbb{T}, Z)$

$$J_\gamma(y_N, e, p_{t_e}) \leq J_\gamma(y_N, e_N, p_{t_e})$$

From this we infer that that for all $e \in L_2(\mathbb{T}, Z)$

$$J_\gamma(y_N, e, p_{t_e}) \leq \langle p_{t_e}, P(t_e)p_{t_e}\rangle.$$

Specifically we find that $J_\gamma(y_N, e, 0) \leq 0$ for all $e \in L_2(\mathbb{T}, X)$ or equivalently:

$$J_\gamma(y_N, e, 0) = ||p(0)||_2^2 + ||\tilde{d_1}||_2^2 + ||\tilde{d_2}||_2^2 - \gamma^2||\tilde{e}||_2^2 < 0 \quad \text{for all } e \in L_2(\mathbb{T}, X),$$

where $p(0), d_1, d_2$ satisfy the evolution of (5.15) with $p(t_e) = 0$.

Therefore when the feedback controller $\Sigma_s p := \pi_y(t)p$ is interconnected to the system Σ_g^*, $||p(0)||_2^2 + ||\tilde{d_1}||_2^2 + ||\tilde{d_2}||_2^2 - \gamma^2||\tilde{e}||_2^2 \leq 0$ for all $\tilde{e} \in L_2(\mathbb{T}, X)$. This is equivalent to:

$$\frac{||p(0)||_2^2 + ||\tilde{d_1}||_2^2 + ||\tilde{d_2}||_2^2}{||\tilde{e}||_2^2} \leq \gamma^2. \quad \text{for all } \tilde{e} \in L_2(\mathbb{T}, X)$$

We take the square root on both sides and evaluate the supremum over $\tilde{e} \in L_2(\mathbb{T}, Z)$ to find:

$$\sup_{e \in L_2(\mathbb{T}, Z)} \frac{\sqrt{||p(0)||_2^2 + ||\tilde{d_1}||_2^2 + ||\tilde{d_2}||_2^2}}{||\tilde{e}||_2} \leq \gamma.$$

Therefore we conclude that if the system Σ_g^* is driven with $\tilde{y} = y_N = \pi_y(t)p$, the L_2-gain of the system is less or equal to γ, which concludes the proof. □

In this section we have shown the equivalence between the problems $P1$ and $P2$ and the relationship between the problems $P2$ and $P3$, problem $P3$ and $P4$ This enables to solves the optimal L_2-gain estimator design problem. The solution to this problem will presented in the next section.

5.6.3 Solution to estimator design problem.

In this section we will derive the solution to the optimal L_2-gain estimator design problem with use of the relations between the problems as established in the previous section. In Section 5.6.2 it has been shown that solution $y_N \in \mathcal{Y}_f, e_N \in \mathcal{Z}_f$ to problem $P4$ enables to solve problem $P3$, that solutions to problem $P3$ enable to solve $P2$ and that

the problem $P1$ and problem $P2$ are equivalent. An estimator which solves problem $P1$ can be obtained from dualization of the regulator Σ_c which solves problem $P2$ by Theorem 5.6.1. We will therefore show the existence of an regulator that solves P_2 and obtain Σ_e by dualization in the following two theorems. First we derive a solution to problem $P2$.

Theorem 5.6.7
Consider the system Σ_g^* given by 5.15 and problem P2 associated to it. The output feedback regulator Σ_c which solves P2 has the following realization:

$$\Sigma_c : \begin{cases} \dot{p}(t) = (-A^* + C^*(SS^*)^{-1}CP(t))p(t) + H^*\tilde{\hat{z}}(t), \quad \text{with } p(t_e) = 0, \\ \tilde{y}(t) = -(SS^*)^{-1}CP(t)p(t). \end{cases} \tag{5.47}$$

In this realization, $P(t)$ is the positive solution of the operator Riccati equation (5.49) *and satisfies the boundary condition $P(0) = I$.*

Proof. Lemma 5.6.5 shows that a Nash equilibrium strategy $y_N \in \mathcal{Y}_f, e_N \in \mathcal{Z}_f$ which solves $P4$ for the system Σ_g^* is given by (5.45), i.e:

$$e_N(t) = \pi_e(t)p(t) = \gamma^{-2}HP(t)p(t) \tag{5.48a}$$
$$y_N(t) = \pi_y(t)p(t) = -(SS^*)^{-1}CP(t)p(t) \tag{5.48b}$$

where $P(t)$ is the positive solution of the operator Riccati equation (5.49) with the boundary condition $P(0) = I$. By Theorem (5.6.3) it follows that the state feedback controller $\Sigma_s : y(t) = -(SS^*)^{-1}CPp(t)$ is a controller such that $||\Sigma_g^* \wedge \Sigma_s||_{2,2} \leq \gamma$ and therefore that Σ_s solves problem $P3$. Therefore, by Theorem 5.6.2 we infer that an output feedback regulator Σ_c which solves $P2$ has the realization given by Equation (5.47). □

We are now in the position to solve the estimator design problem $P1$.

Theorem 5.6.8 (Solution to estimator design problem $P1$)
Given the plant Σ_g and let $\gamma \in \mathbb{R}^+$ be such there exists a symmetric operator $P(t)$, which is for all $p_1, p_2 \in D(A^*)$ a solution of the differential equation:

$$\begin{aligned} \langle p_1, \dot{P}p_2\rangle = &\langle PA^*p_1, p_2\rangle + \langle p_1, PA^*p_2\rangle + \langle G^*p_1, G^*p_2\rangle \\ &- \langle P(C^*(SS^*)^{-1}C - \gamma^{-2}H^*H)Pp_1, p_2\rangle. \end{aligned} \tag{5.49}$$

with $P(0) = I$. Let the estimator Σ_e have the realization:

$$\Sigma_e : \begin{cases} \dot{\xi} = (A - PC^*(S^*S)^{-1}C)\xi + PC^*(SS^*)^{-1}y, \quad \text{with } \xi(0) = 0, \\ \hat{z} = H\xi, \end{cases} \tag{5.50}$$

where $P(t)$ is the solution to Riccati equation given by Equation (5.49)*. The estimator Σ_e solves problem $P1$, i.e. the L_2-gain of the interconnection $\Sigma_g \wedge \Sigma_e$, (as shown in Figure 5.4a) is less than γ, i.e. $||\Sigma_g \wedge \Sigma_e||_{2,2} < \gamma$. Moreover, the estimator solving problem $P1$ is given by the input/output mapping:*

$$\hat{z}(t) = \int_0^t HT_{P(t)C(S^*S)^{-1}C^*}(t-\tau)P(t)C^*(SS^*)^{-1}y(\tau)\mathrm{d}\tau,$$

where $t \in \mathbb{T}$ and $T_{P(t)C(S^*S)^{-1}C^*}$ is the mild evolution operator with infinitesimal generator $A - P(t)C(S^*S)^{-1}C^*$.

Proof. Theorem 5.6.1 shows that an estimator Σ_e which solves $P1$ for Σ_g can be obtained from a controller Σ_c that solves $P2$ for Σ_g^*. The controller Σ_c and estimator Σ_e are related as follows $\Sigma_e = \Sigma_c^*$. Let Σ_c be the controller that solves problem $P2$ as given by equation(5.47) in Theorem 5.6.7. By dualization of Σ_c we obtain:

$$\Sigma_e : \begin{cases} \dot{\xi} = (A - PC^*(S^*S)^{-1}C)\xi + PC^*(SS^*)^{-1}y, & \text{with } \xi(0) = 0, \\ \hat{z} = H\xi. \end{cases} \tag{5.51}$$

The system obtained after interconnection of the estimator Σ_e and the plant Σ_g, i.e. $\Sigma_g \wedge \Sigma_e = \Sigma_g \wedge \Sigma_c^*$, has L_2-gain equal the system $\Sigma_g^* \wedge \Sigma_c$ by lemma 5.4.9, such that we infer that $||\Sigma_g \wedge \Sigma_e||_{2,2} = ||\Sigma_g^* \wedge \Sigma_c||_{2,2} \leq \gamma$. □

Remark 5.6.1. In this section we have solved the problem $P1$, in which the value of γ is predefined. The solution for the original optimal estimator design problem, as defined by the Problems 5.1 and 5.2 can now be derived by minimization of the value γ. Typically this is done by use of the binary search algorithm.
Remark 5.6.2. The solution to the problems of minimization $J_{2,2}$ proceeds along identical lines. That, when the initial conditions are known (we set $x_0 = 0$) it follows that the solution to Problem 5.2 is equal to (5.50) with the initial condition to differential equation (5.43) set to $P(0) = 0$. It is interesting to see that in this situation for small t the contribution of the measured signal to the state evolution is negligible and that for small t the estimate is produced on the basis of the knowledge of the initial condition on the state of the system.

5.7 Infinite horizon estimation problems

The estimators that have been developed in this chapter are designed for estimation problems on finite time horizon. Note that our results for estimator designs derived in the Sections 5.5 and 5.6 are valid for any t_e, such that $0 < t_e < \infty$ and from the analysis it follows that for any $t_e \in [0, \infty)$ the optimal estimator is time variant.

In this section the design problem for time invariant causal estimators on the infinite time intervals will be discussed. That is, we are interested in causal and time invariant estimators that have a realization as integral operator:

$$\Sigma_e(M) : \hat{z}(t) = \int_{\mathbb{T}} M(t, \tau)y(\tau)\mathrm{d}\tau.$$

From the demand for causality it follows that M must be such that $M(t, \tau) = 0$ for $\tau > t$. From the demand for time-invariance it follows that M must such that $M(t, \tau) = M(t - \tau, 0)$ for all $t, \tau \in \mathbb{T}$. It is well known that integration kernels of linear time invariant systems are defined by the impulse response g of the system. Let the class of time invariant causal impulse responses be defined by:

$$\mathcal{G}_{LTI} = \{g \in L_2(\mathbb{T}, \mathbb{R}^{n \times m}) \mid g(t) = 0 \text{ for } t < 0\}.$$

Then, the class of linear time invariant causal integration kernels is given by $\mathcal{M}_{LTI}$:

$$\mathcal{M}_{LTI} = \{M(t,\tau) \mid \exists\, g \in \mathcal{G}_{LTI} \text{ such that } M(t,\tau) = g(t-\tau)\}.$$

We will use some abuse of notation by refering to the impulse response as $M(t) = M(t,0) = g(t)$.

In this section, we consider the estimator design Problems 5.1 and 5.2 for estimators with an integration kernel in the class $\mathcal{M}_{LTI}$. Often we will be interested in estimators which have a causal linear time invariant (LTI) realization, since their implementation and analysis is less complex than the implementation and analysis of time variant systems.

In this section the estimation problem on the interval $\mathbb{T} = [0,\infty)$ will be considered. The Hilbert-Schmidt norm is not a suitable norm in the context of linear time invariant systems on infinite time intervals. It follows that the norm is unbounded for any time invariant system on infinite time intervals.

Lemma 5.7.1
Let K be an integral operator $L_2(\mathbb{T},U) \to L_2(\mathbb{T},Y)$ defined on the interval $\mathbb{T} = [0,\infty)$, with integration kernel $k \in \mathcal{M}_{LTI}$ defined by the impulse response g with $g \neq 0$. Then:

$$||K||_{HS} = \int_{\mathbb{T}}\int_{\mathbb{T}} ||k(t,s)||_2^2 \mathrm{d}t\mathrm{d}s = \infty.$$

Proof. The unboundedness of the integral follows from the definition of $\mathcal{M}_{LTI}$. Since $k(t,s) = g(t-s)$ and that $g(t) = 0$ for $t < 0$, it follows that:

$$\begin{aligned}\int_{\mathbb{T}}\int_{\mathbb{T}} ||k(t,s)||_2^2 \mathrm{d}t\mathrm{d}s &= \int_0^\infty \int_0^\infty ||g(t-s)||_2^2 \mathrm{d}t\mathrm{d}s = \int_0^\infty \int_{-s}^\infty ||g(t)||_2^2 \mathrm{d}t\mathrm{d}s \\ &= \lim_{s\to\infty}\left[s\int_0^\infty ||g(t)||_2^2 \mathrm{d}t\right].\end{aligned}$$

□

In this section we introduce the impulse response norm and $L_{2,2}$-norm for systems operating on signals defined on $\mathbb{T} = [0,\infty)$. For a time invariant integral operator as defined by definition 5.2.2, that is defined by $k(t,\tau) = g(t-\tau)$ with $g \in \mathcal{G}_{LTI}$, these norms are defined by:

$$||\Sigma||_{\text{imp}} = \lim_{t_e\to\infty}\left(\int_0^{t_e} ||g(t)||_2^2 \mathrm{d}t\right)^{\frac{1}{2}} \tag{5.52}$$

$$||\Sigma||_{2,2} = \lim_{t_e\to\infty} \sup_{u\in L_2([0,t_e),U)} \frac{||Ku||_{L_2}}{||u||_{L_2}} \tag{5.53}$$

We remark that the impulse response norm can be shown to be equivalent to the well known $\mathcal{H}_2$-norm. The impulse response norm of an system Σ and the impulse response norm of the dual system Σ^* are equal, which will be shown in the following lemma.

Lemma 5.7.2
Let K be an intergral operator defined by impulse response $g \in \mathcal{G}_{LTI}$ and let $||\cdot||_{imp}$ be the impulse response norm. Then:

$$||K||_{imp} = ||K^*||_{imp}$$

Proof. K^* is well defined for any operator K and can be realized by $(K^*y)(t) = \int_{\mathbb{T}} g^*(s-t)y(s)\mathrm{d}s$, where g^* is the adjoint kernel. The property follows from the definition of $||K||_{\text{imp}}$:

$$||K||_{\text{imp}}^2 := \int_{\mathbb{T}} ||g(t)||_2^2 \mathrm{d}t = \int_{\mathbb{T}} ||g^*(t)||_2^2 \mathrm{d}t = ||K^*||_{\text{imp}}^2.$$

□

The latter lemma is equivalent to Lemma 5.4.1 for the Hilbert-Schmidt norm and Lemma 5.4.2 for the induced norm. Therefore, Theorem 5.4.10 remains valid for a criterion based on the impulse response norm and the optimal estimator design problem for a criterion based on the impulse response norm can be solved in the same manner.

This section is an extension of the Sections 5.5 ans 5.6. Therefore the results will be presented in a brief manner. Before we proceed with the results and proofs we make a technical remark. In the proofs we will apply a limit argument to bring the problem to the infinite time interval, i.e $t_e \to \infty$. This introduces some technical problems if we proceed the proofs exactly along the same line as in finite horizon case i.e $\mathbb{T} = [0, t_e]$. By dualization we have obtained systems (for instance Σ' and Σ_g^*) with endpoint conditions at $t = t_e$. Therefore it is not possible to conduct the limit argument immediately and we will chose to redefine for the dual systems $\mathbb{T}$ to $\mathbb{T} = [-t_e, 0]$, such that the end point condition is given at $t = 0$. Since the systems under consideration are time invariant, this does not pose any problem since the redefinition of $\mathbb{T}$ is a time shift.

In case that the impulse response norm is used as design criterion, the optimization criterion will be denoted by J_{imp} and is given by:

$$J_{\text{imp}}(M) = ||\Sigma_p \wedge \Sigma_e(M)||_{\text{imp}}.$$

The following result solves the estimator design problem for the criterion $J_{\text{imp}}(M)$ for $M \in \mathcal{M}_{LTI}$.

Theorem 5.7.3 (Optimal impulse response norm LTI estimator design for infinite horizon estimation.)
Consider the plant Σ_p defined by the Equation (5.1) *and the estimator Σ_e with realization*

$$\Sigma_e(M_{opt,LTI}) : \begin{cases} \dot{\xi} = (A - \Pi_\infty C^*(S^*S)^{-1}C)\xi + \Pi_\infty C^*(SS^*)^{-1}y, \\ \hat{z} = H\xi. \end{cases} \tag{5.54}$$

with $\xi(0) = 0$, where for all $\xi_n, \xi_m \in D(A^*)$ and Π_∞ is the solution of the implicit Riccati equation

$$\langle \xi_n, \Pi_\infty A^*\xi_m\rangle + \langle \Pi_\infty A^*\xi_n, \xi_m\rangle + \langle G^*\xi_n, G^*\xi_m\rangle - \langle (SS^*)^{-1}C\Pi_\infty\xi_m, C\Pi_\infty\xi_n\rangle = 0.$$

The estimator $\Sigma_e(M_{opt,LTI})$ is the unique minimizer of $J_{imp}(M) = ||\Sigma_p \wedge \Sigma_e(M)||_{imp}$ with $M \in \mathcal{M}_{LTI}$ and provides the unique solution to the estimator design Problems 5.2 restricted to the class of time invariant estimators.

The proof of this theorem follows the same line of reasoning as the proof of Theorem 5.5.10 and Theorem 5.5.11.

Based on the arguments in the proof of Theorem 5.5.11 we consider the case with $n = 1$, i.e. $H = \langle h, x\rangle$ with $h \in X$. Before we proceed with the proof of Theorem 5.7.3 we introduce the following lemma, that is analogous to Lemma 5.5.6 for the finite time horizon case.

Lemma 5.7.4
Consider the system Σ' given by

$$\Sigma' : \begin{cases} \dot{\xi}(t) = & -A^*\xi(t) - C^*w(t), \\ \kappa(t) = & G^*\xi(t), \\ \lambda(t) = & S^*w(t), \end{cases} \tag{5.55}$$

with end-point condition $\xi(0) = \xi_0$ and $w \in L_2(\mathbb{T}, Y)$ and $t \in \mathbb{T} = [-t_e, 0]$. The outputs $\kappa(t)$ and $\lambda(t)$ are uniquely defined for $t \in \mathbb{T}$. Moreover, consider the following functional:

$$J'(w, \xi_0)^2 := \lim_{t_e \to \infty} \int_{-t_e}^{0} ||\kappa(t)||_2^2 + ||\lambda(t)||_2^2 \mathrm{d}t. \tag{5.56}$$

The feedback $w(t) = -(SS^*)^{-1}C\Pi_\infty\xi(t)$ is the unique minimizer of $J'(w, \xi_0)^2$ in the class of static feedback laws, where Π_∞ is for all $\xi_n, \xi_m \in D(A^*)$ the solution of:

$$\langle \xi_n, \Pi_\infty A^*\xi_m\rangle + \langle \Pi_\infty A^*\xi_n, \xi_m\rangle + \langle G^*\xi_n, G^*\xi_m\rangle - \langle (SS^*)^{-1}C\Pi_\infty\xi_m, C\Pi_\infty\xi_n\rangle = 0. \tag{5.57}$$

Therefore, the minimizer w_{opt} of $J'(w, \xi_0)$ is given by $w_{opt}(t) = -(SS^*)^{-1}C\Pi_\infty\xi(t)$ and w_{opt} admits the representation $w_{opt}(t) = -(SS^*)^{-1}C\Pi_\infty\tilde{W}(t)\xi_0$ where $\tilde{W}(t)$ is the mild evolution operator with infinitesimal generator $-A^* + C^*(SS^*)^{-1}C\Pi_\infty$.

Proof. We apply the completion of the square argument. Define $V(\xi) = \langle \xi, \Pi_\infty\xi\rangle$. Then:

$$\frac{\mathrm{d}V(\xi(t))}{\mathrm{d}t} = \langle \dot{\xi}(t), \Pi_\infty\xi(t)\rangle + \langle \Pi_\infty\xi(t), \dot{\xi}(t)\rangle.$$

We apply the completion of the squares argument and integrate, exactly such as done in the proof of Lemma 5.5.6. It follows that $J'^2(w, \xi_0)$ given by (5.56) can be written as:

$$\begin{aligned} J'(w, \xi_0)^2 = &\lim_{t_e \to \infty} \langle \xi(0), \Pi_\infty\xi(0)\rangle - \lim_{t_e \to \infty} \langle \xi(-t_e), \Pi_\infty\xi(-t_e)\rangle \\ &+ \lim_{t_e \to \infty} \int_{-t_e}^{0} ||(SS^*)^{\frac{1}{2}}w(\tau) + (SS^*)^{-\frac{1}{2}}C\Pi_\infty\xi(\tau)||_2^2 \mathrm{d}\tau. \end{aligned}$$

We assume that $\lim_{t_e \to \infty} \xi(-t_e) = 0$. Since $\langle \xi_0, \Pi_\infty\xi_0\rangle$ is independent of w, it follows that $w(t)$ is the minimizer of $J'(w, \xi_0)^2$ if and only if

$$||(SS^*)^{\frac{1}{2}}w(t) + (SS^*)^{-\frac{1}{2}}C\Pi_\infty\xi(t)||_2 = 0.$$

The closed loop representation of w_{opt} follows analogously as in Lemma 5.5.7. Next we will prove that $\lim_{t_e\to\infty}\xi(-t_e)=0$. We show that $-A^*+C^*(SS^*)^{-1}C\Pi_\infty$ is the infinitesimal generator of the anti-stable evolution operator $\tilde{W}(t)$. We will show that $V(\xi)$ is a Lyapunov function for the system and evaluate $\frac{\mathrm{d}V(\xi)}{\mathrm{d}t}$ along trajectories of the system, i.e. $\xi(t)=\tilde{W}(t)\xi_0$. It follows that:

$$\begin{aligned}\frac{\mathrm{d}V(\xi(t))}{\mathrm{d}t} =&\langle(-A^*+C^*(SS^*)^{-1}C\Pi_\infty)\xi(t),\Pi_\infty\xi(t)\rangle\\ &+\langle\xi(t),\Pi_\infty(-A^*+C^*(SS^*)^{-1}C\Pi_\infty)\xi(t)\rangle\\ =&\langle\xi(t),\Pi_\infty C^*(SS^*)^{-1}C\Pi_\infty\xi(t)\rangle+\langle G^*\xi(t),G^*\xi(t)\rangle\end{aligned}$$

It follows that $\frac{\mathrm{d}V(\xi(t))}{\mathrm{d}t}\geq 0$ and therefore that the $\tilde{W}(t)$ is anti-stable. □

Proof of Theorem 5.7.3. Theorem 5.7.3 can now be proved along the same line as Theorem 5.5.10 and Theorem 5.5.11. Let Π_∞ denote the solution of Riccati equation (5.57). Based on Lemma 5.7.4 it follows that for $n=1$ the criterion $J_{\mathrm{imp}}(M)$ can be written as:

$$J_{\mathrm{imp}}(M)^2=\lim_{t_e\to\infty}\langle h,\Pi_\infty h\rangle+\int_0^{t_e}||-(S^*S)^{\frac{1}{2}}M^*(\tau)+(S^*S)^{-\frac{1}{2}}C\Pi_\infty\xi(\tau)||^2\mathrm{d}\tau$$

Therefore, it follows that for $n=1$ the optimal estimator has the impulse response $M_{opt,LTI}(t)=HU(t)\Pi_\infty C^*(SS^*)^{-1}$ where $U(t):X\to X$ is the semigroup operator with infinitesimal generator $A-\Pi_\infty C^*(S^*S)^{-1}C$. The estimator given by (5.54) implements the input output map:

$$\hat{z}(t)=\int_0^t HU(t-\tau)\Pi_\infty C^*(S^*S)^{-1}y(\tau)\mathrm{d}\tau=\int_0^t M_{opt,LTI}(t-\tau)y(\tau)\mathrm{d}\tau,$$

such that it follows that (5.54) is a realization of an estimator that minimizes the criterion $J_{\mathrm{imp}}(M)=||\Sigma_g\wedge\Sigma_e(M)||_{\mathrm{imp}}$. The extension to the case $n>1$ follows along the same line as presented for the case of the time variant estimator. □

In case that the induced L_2 norm is used as design criterion we have the following result.

Theorem 5.7.5 (Optimal induced L_2 norm LTI estimator design for infinite horizon estimation.)
Consider the estimator design problem with known initial condition. Assume that there exists a positive operator $P_\infty:X\to X$, which is for every $p_1,p_2\in D(A^*)$ a solution of the Riccati equation:

$$\begin{aligned}\langle P_\infty A^*p_1,p_2\rangle+\langle p_1,P_\infty A^*p_2\rangle+\langle G^*p_1,G^*p_2\rangle&\\ -\langle P_\infty(C^*(SS^*)^{-1}C-\gamma^{-2}H^*H)P_\infty p_1,p_2\rangle=0.&\quad(5.58)\end{aligned}$$

and is such that $A-P_\infty(C^*(S^*S)^{-1}C-\gamma^{-2}H^*H)$ is the infinitesimal generator of a exponentially stable semigroup.

Then, the estimator Σ_e, given by:

$$\Sigma_e:\begin{cases}\dot{\xi}=(A-P_\infty C^*(S^*S)^{-1}C)\xi+P_\infty C^*(SS^*)^{-1}y,\quad \textit{with } \xi(0)=0, & (5.59a)\\ \hat{z}=H\xi, & (5.59b)\end{cases}$$

is an estimator for the system Σ_g and is such that $||\Sigma_g\wedge\Sigma_e||_{2,2}\leq\gamma$.

Before we proceed with the proof of Theorem (5.7.5) we introduce the following lemma.

Lemma 5.7.6
Consider the system Σ_g^* given by

$$\Sigma_g^* : \begin{cases} \dot{p}(t) = -A^* p(t) - C^* \tilde{y}(t) - H^* \tilde{e}(t), & \text{(5.60a)} \\ \tilde{d}_1(t) = G^* p(t), & \text{(5.60b)} \\ \tilde{d}_2(t) = S^* \tilde{e}(t), & \text{(5.60c)} \\ \tilde{z}(t) = -\tilde{e}(t) & \text{(5.60d)} \end{cases}$$

with end-point condition $p(0) = p_0$ and $t \in \mathbb{T} = [-t_e, 0]$. The outputs $d_1(t)$ and $d_2(t)$ are uniquely defined for $t \in \mathbb{T}$. Moreover, consider the functional:

$$J_\gamma^\infty(\tilde{y}, \tilde{e}, p_0) = \lim_{t_e \to \infty} \langle p_0, P_\infty p_0 \rangle + \int_{-t_e}^0 ||\tilde{d}_1(t)||_2^2 + ||\tilde{d}_2(t)||_2^2 - \gamma^2 ||\tilde{e}(t)||_2^2 \mathrm{d}t,$$

and assume that there exists a positive operator $P_\infty : X \to X$, which is for every $p_1, p_2 \in D(A^*)$ a solution of the Riccati equation:

$$\begin{aligned} \langle P_\infty A^* p_1, p_2 \rangle + \langle p_1, P_\infty A^* p_2 \rangle + \langle G^* p_1, G^* p_2 \rangle \\ - \langle P_\infty (C^* (SS^*)^{-1} C - \gamma^{-2} H^* H) P_\infty p_1, p_2 \rangle = 0. \end{aligned} \quad \text{(5.61)}$$

and is such that $A - P_\infty (C^*(S^*S)^{-1}C - \gamma^{-2}H^*H)$ is the infinitesimal generator of a exponentially stable semigroup.

Then the strategy $(y_{N,\infty}, e_{N,\infty})$ establishes a Nash equilibrium for the value function J_γ, where:

$$e_{N,\infty}(t) = +\gamma^{-2} H P_\infty p(t), \quad \text{(5.62a)}$$
$$y_{N,\infty}(t) = -(SS^*)^{-1} C P_\infty p(t). \quad \text{(5.62b)}$$

The value of the game under the equilibrium strategy is $J_\gamma(y_{N,\infty}, e_{N,\infty}, p_0) = 0$. Under the Nash equilibrium strategy the closed loop dynamics is given by:

$$\dot{p}_N(t) = (-A^* + (C^*(SS^*)^{-1}C - \gamma^{-2}H^*H)P_\infty) p_N(t), \quad \textit{with} \quad p_N(0) = p_0. \quad \text{(5.63)}$$

Proof. The proof of this lemma follows the same line of reasoning as the proof of Lemma 5.6.5. Analogously as in the proof of Lemma 5.6.4, J_γ can be rewritten to:

$$\begin{aligned} J_\gamma^\infty(\tilde{y}, \tilde{e}, p_0) = \lim_{t_e \to \infty} \int_{-t_e}^0 ||(SS^*)^{\frac{1}{2}} \tilde{y}(t) + (SS^*)^{-\frac{1}{2}} C P_\infty p(t)||_2^2 \\ - ||\gamma \tilde{e}(t) - \gamma^{-1} H P_\infty p(t)||_2^2 \mathrm{d}t \end{aligned} \quad \text{(5.64)}$$

where we have used that $\lim_{t_e \to \infty} p(-t_e) = 0$, due to anti stability of $-A^* + (C^*(SS^*)^{-1}C - \gamma^{-2}H^*H)P_\infty$. When the value function is evaluated at (5.62) the quadratic terms vanish. By convexity of the norms, uniqueness of the Nash equilibrium strategy follows and we have that $J_\gamma^\infty(y_{N,\infty}, e_{N,\infty}, p_0) \leq J_\gamma^\infty(y, e_{N,\infty}, p_0)$ resp. $J_\gamma^\infty(y_{N,\infty}, e, p_0) \leq$

$J_\gamma^\infty(y_{N,\infty}, e_{N,\infty}, p_0)$. Therefore, the following inequality holds for all $y \in L_2(\mathbb{T}, \mathbb{R}^y)$ and $e \in L_2(\mathbb{T}, \mathbb{R}^z)$

$$J_\gamma^\infty(y_N^\infty, e, p_0) \leq J_\gamma^\infty(y_N^\infty, e_N^\infty, p_0) \leq J_\gamma^\infty(y, e_N^\infty, p_0),$$

which shows that (y_N^∞, e_N^∞) establishes a Nash equilibrium. The value at the equilibrium follows by evaluation of $J_\gamma(y_N, e_N, p_0)$. From Equation (5.64) we infer that $J_\gamma(y_N^\infty, e_N^\infty, p_0) = 0$. □

Lemma 5.7.7
Consider the system Σ_g^*, defined by the Equations (5.60)*. The output feedback regulator Σ_c given by the realization:*

$$\Sigma_c : \begin{cases} \dot{p}(t) = (-A^* + C^*(SS^*)^{-1}CP_\infty)p(t) + H^*\tilde{\hat{z}}(t), & \text{with } p(0) = 0, \\ \tilde{y}(t) = -(SS^*)^{-1}CP_\infty p(t). \end{cases}$$

is a regulator for the system Σ_g^* such that $||\Sigma_g^* \wedge \Sigma_c||_{2,2} \leq \gamma$.

Proof. The proof of the lemma follows the same line of reasoning as the proof of Theorem 5.6.7. First we show that the state feedback controller Σ_s

$$\Sigma_s : y_N^\infty(t) = -(SS^*)^{-1}CP_\infty p(t)$$

anti-stabilizes the system Σ_g^*. When the state feedback controller Σ_s is interconnected with Σ_g^* the dynamics of $\Sigma_g^* \wedge \Sigma_s$ are given by:

$$\Sigma_g^* \wedge \Sigma_s : \begin{cases} \dot{p}(t) &= (-A^* + C^*(SS^*)^{-1}CP_\infty)p(t) - H^*\tilde{e}(t), \quad \text{with } p(0) = 0, \\ \tilde{d}_1(t) &= G^*p(t), \\ \tilde{d}_2(t) &= S^*\tilde{e}(t), \\ \tilde{z}(t) &= -\tilde{e}(t) \end{cases} \tag{5.65}$$

We prove that the system $\Sigma_g^* \wedge \Sigma_s$ is anti-stable. To do so, we show that $V(p) := \langle P_\infty p, p\rangle$ is a Lyapunov function for the system $\Sigma_g^* \wedge \Sigma_s$. That is, we differentiate $V(p) := \langle P_\infty p, p\rangle$ and evaluate $\frac{\mathrm{d}V(p(t))}{\mathrm{d}t}$ along trajectories of $\Sigma_g^* \wedge \Sigma_s$:

$$\begin{aligned} \frac{\mathrm{d}V(p(t))}{\mathrm{d}t} &= \langle P_\infty \dot{p}(t), p(t)\rangle + \langle P_\infty p(t), \dot{p}(t)\rangle && (5.66) \\ &= \langle P_\infty(-A^* + C^*(SS^*)^{-1}CP_\infty)p(t), p(t)\rangle \\ &\quad + \langle P_\infty p(t), (-A^* + C^*(SS^*)^{-1}CP_\infty)p(t)\rangle && (5.67) \end{aligned}$$

By substitution of the Riccati equation 5.58 it now follows that:

$$\frac{\mathrm{d}V(p(t))}{\mathrm{d}t} = +\langle G^*p, G^*p\rangle + \langle P_\infty(C^*(SS^*)^{-1}C + \gamma^{-2}H^*H)P_\infty p(t), p(t)\rangle \geq 0 \tag{5.68}$$

Since $\frac{\mathrm{d}V(p(t))}{\mathrm{d}t} \geq 0$ it follows that the system $\Sigma_g^* \wedge \Sigma_s$ is anti-stable. Since the system $\Sigma_g^* \wedge \Sigma_s$ is anti-stable, it follows that $p(t) \in L_2((-t_e, 0], X)$ for all input signals $\tilde{e}(t) \in$

$L_2((-t_e, 0], X)$ and it follows that $\lim_{t_e \to \infty} p(-t_e) = 0$. Therefore, when the controller Σ_s is connected to Σ_g^* the value of the function J_γ^∞ is less than zero, i.e. $J_\gamma^\infty < 0$. This is equivalent to $||\Sigma_g^* \wedge \Sigma_s||_{2,2} < \gamma$. Following the line of reasoning in Theorem 5.6.2 it now follows that the controller Σ_c is a controller such that $||\Sigma_g^* \wedge \Sigma_c|| < \gamma$. □

Proof of Theorem 5.7.5. We are now in the position to prove Theorem 5.7.5. Let Σ_c be as defined in Lemma 5.7.7. Then, simple calculation shows that $\Sigma_c = \Sigma_e^*$. By Lemma 5.7.7 we have that $||\Sigma_g^* \wedge \Sigma_c||_{2,2} < \gamma$. Moreover, we have by Theorem 5.4.10 that $||\Sigma_g \wedge \Sigma_e||_{2,2} = ||\Sigma_g^* \wedge \Sigma_e^*||_{2,2}$, from which it now follows that $||\Sigma_g \wedge \Sigma_e||_{2,2} < \gamma$. □

5.8 Conclusion and Recommendations

In this chapter the design of estimators for infinite dimensional systems has been studied in a deterministic setting.

5.8.1 Conclusions

For the design we have introduced the two distinct error criteria, which are the Hilbert-Schmidt norm and the induced $L2$-norm of the system that represents the transfer between the disturbance inputs and the estimation error. We have defined optimal estimators as the estimators which minimize the Hilbert-Schmidt norm and the induced $L2$-norm of the system that represents the transfer between the disturbance inputs and the estimation error. We distinguish the cases in which the initial condition of the system under consideration is known and in which the initial condition is not known.

In Section 5.4 we have shown that estimator design problems are related to optimal control problems and that the solutions to the optimal estimator design problem can be inferred from the solution of these optimal control problems. The relation between the optimal estimator design problem and optimal control problems is known as duality and it has been shown that this has an interpretation in terms of Hilbert adjoints of operators. In Section 5.4.3 is has been shown how the duality relationship can be established. We have shown that the estimator design problems can be interpreted as optimization problems and we have presented solutions for both problems on a finite time interval.

The solution of the optimal Hilbert-Schmidt norm estimator design problem has been discussed in Section 5.5. In this section it has been shown that the design of a optimal Hilbert-Schmidt output estimator for distributed parameter systems with finite dimensional outputs can be done by optimization of the design criterion over the convolution kernel of the input output map of the estimator to be designed. It has been shown that the estimator design problem is dual to the linear quadratic optimal control problem of an artificial system. Due to the specific structure of the optimal control problem, this problem can be solved elegantly by use of a "'completion of the square"'-argument applied on the cost criterion that is used for optimization in the optimal control problem. It has been shown that the solution of the dual control problem can be used to calculate the convolution kernel of the input/output map of the optimal output estimator. The

solution to the optimal estimator has been presented in terms of the its convolution kernel as well as its state space realization. By use of a completion of the squares argument on the design criterion, it has been shown that the optimal estimators are time invariant estimators for every finite time interval $\mathbb{T} \in [0, t_e]$ with $t_e \in [0, \infty)$.

The solution of the optimal induced $L2$-norm estimator design problem has been discussed and solved in Section 5.6. The method is based on duality theory for distributed parameter systems with finite dimensional input and outputs. It has been shown that there exist a two player differential game problem for which the value function is quadratic in its decision variables. The quadratic structure enables one to apply a completion of the squares argument to obtain the equilibrium strategy for the game. It has been shown that the equilibrium strategy provides a solution to the equivalent optimal L_2-gain regulator design problem and indirectly enables to solve the optimal L_2-gain estimator design problem. Also in this case, by use of the completion a completion of the squares argument on the design criterion has been shown that the optimal estimators are time invariant estimators for every finite time interval $\mathbb{T} \in [0, t_e]$ with $t_e \in [0, \infty)$.

In Section 5.6 it has been shown that for the case of optimal $L2$-norm estimator design, there is a clear interpretation of the initial condition on the Riccati equation involved in the estimator design in terms of the availability of information on the initial condition of the system under consideration.

The design of linear time invariant estimators for problems with infinite time horizon has been studied in Section 5.7. The solution for the optimal Hilbert Schmidt norm estimator design problem and the optimal induced $L2$-norm estimator design problem has been given. The results are based on the analysis of estimator design problems on finite time interval given.

5.8.2 Recommendations

The estimator design problems in the stochastic setting, such as the Kalman Filter, are able to consider the situation where the initial conditions is unknown. The current formulation of Hilbert-Schmidt norm type problem for the situation that the initial condition is unknown is not able to deal with this situation. It would be interesting to be able to deal with unknown initial conditions in the deterministic setting and this might be a topic of future research.

For both the optimal Hilbert-Schmidt norm and the optimal induced $L2$-norm estimator design problems it follows from the analysis that the optimal estimators are infinite dimensional systems. Since, in practical situations, estimators often need to be implemented in simulation environments it is important to study methods to obtain finite dimensional estimators for infinite dimensional systems. In the next chapter, Chapter 6 we will study this problem.

CHAPTER 6

Approximation and implementation of estimators

Abstract

In Chapter 5 it has been shown that optimal impulse response and optimal L_2-gain estimators for distributed parameter systems are infinite dimensional systems. Moreover, the estimator gain of these estimators has been defined in terms of the solution of the operator Riccati equation. Therefore, the optimal estimators cannot directly be implemented and used in practical applications. In this chapter methods for implementation and approximation of the optimal estimators are studied.

6.1 Introduction

In Chapter 5 the design of the optimal impulse response estimator and the optimal L_2-gain estimator for infinite dimensional systems has been studied. There are two severe issues with the designed optimal estimators in Theorem 5.5.11 and Theorem 5.6.8, which hamper the application of this type of estimators to practical situations. These issues are:

- The optimal estimators are infinite dimensional systems. In order to implement such an estimator in a digital computer, a finite dimensional approximation has to be obtained.

- In order to obtain an explicit formulation of the optimal estimators, the estimator gains have to be available in explicit form. For this purpose the Riccati equations with solutions defined as operators on infinite dimensional Hilbert spaces need to be solved. Explicit solutions are only known in very specific cases. For the general case explicit solution methods are not known.

In order to limit the (mathematical) complexity of the estimators, only the approximation of time invariant estimators for estimation problems on infinite time horizon will be considered in this chapter. The desing of time invariant estimators for infinite horizon problems are discussed in Section 5.7.

In this chapter methods to deal with these implementation problems are analyzed. In the remainder of the introduction possible approaches to resolve the mentioned issues will be identified and discussed. In Section 6.2.1 a general approximation framework for systems will be introduced. In Section 6.2.3 the approximation of estimators will be discussed. In Section 6.3 we will discuss convergence of approximations of systems in general. In Section 6.4.1 we will discuss results which are known on the approximation of the solution of Riccati equations in the context of control problems for linear infinite dimensional systems. We will show how these results can be used to analyze convergence of approximations of the optimal impulse response estimator. In Section 6.5 two examples show the applicability of the approximation method to engineering problems.

For completeness the main result on estimator design of Chapter 5 based on the norm of the impulse response ($\mathcal{H}_2$-norm) and the induced L_2-gain of the error system are restated below. Consider the system Σ_p given by:

$$\Sigma_p : \begin{cases} \dot{x} &= Ax + Gd_1 \\ y &= Cx + Sd_2 \\ z &= Hx \end{cases} \tag{6.1}$$

with $A : D(A) \to X$, X a Hilbert space, A the infinitesimal generator of the semigroup $T(t)$, $C : X \to Y$, $H : X \to Z_1$, and $G : D_1 \to X$, $S : Y \to Y$ bounded linear operators with $D_1 = \mathbb{R}^{d_1}$, $Y = \mathbb{R}^m$, $Z_1 = \mathbb{R}^n$. We assume that $T(t)$ is exponentially stable and that the pair (A, C) is detectable.

Both, the optimal impulse response norm and the optimal L_2-gain estimators Σ_e for the system Σ_p, have the realization:

$$\Sigma_e : \begin{cases} \dot{\hat{x}} &= (A - \Pi C^*(SS^*)^{-1}C)\hat{x} + \Pi C^*(SS^*)^{-1}y \\ \hat{z} &= H\hat{x} \end{cases} \tag{6.2}$$

where, in the case of the impulse response norm criterion, $\Pi : X \to X$ is a symmetric operator, which is for all $x_1, x_2 \in D(A^*)$ a solution of the Riccati equation:

$$\langle \Pi A^* x_1, x_2 \rangle + \langle x_1, \Pi A^* x_2 \rangle + \langle G^* x_1, G^* x_2 \rangle - \langle \Pi (C^*(SS^*)^{-1}C)\Pi x_1, x_2 \rangle = 0. \tag{6.3}$$

Similarly, in the case of the L_2 optimal estimator which achieves attenuation level γ, $\Pi : X \to X$ is a symmetric operator, which is for all $x_1, x_2 \in D(A^*)$ a solution of the

Riccati equation:

$$\langle \Pi A^* x_1, x_2\rangle + \langle x_1, \Pi A^* x_2\rangle + \langle G^* x_1, G^* x_2\rangle - \langle \Pi(C^*(SS^*)^{-1}C - \gamma^{-2}H^*H)\Pi x_1, x_2\rangle = 0. \tag{6.4}$$

Since these estimators are not suitable for implementation due to the mentioned reasons, it is interesting and natural to consider the problem of finite dimensional estimator design for infinite dimensional systems. That is:

Problem 6.1 (Estimator design problem)
Let $N > 0$ and $\tilde{\Sigma}(M)$ be an estimator for the system Σ_p. Consider the criterion

$$J(M) = ||\Sigma_p \wedge \tilde{\Sigma}_e(M)||,$$

where $||\cdot||$ is the norm of the impulse response or induced L_2-norm. Find, the time invariant estimator $\tilde{\Sigma}_e(M)$ with M of the form $M(t,\tau) = h(t-\tau)$ with the realization

$$h(t) = \begin{cases} C_e e^{A_e t} B_e & \text{for } t \geq 0 \\ 0 & \text{else} \end{cases}$$

for suitable matrices $A_e \in \mathbb{R}^{N\times N}$, $B_e \in \mathbb{R}^{N\times m}$, $C_e \in \mathbb{R}^{n\times N}$ and N the order *of $\tilde{\Sigma}_e$, such that $J(M) = ||\Sigma_p \wedge \tilde{\Sigma}_e(M)||$ is minimal.*

This problem is hard to solve since the problem amounts to finding estimators with predefined complexity, which has not been solved. Therefore, we consider an alternative approach and study a method to approximate the optimal infinite dimensional estimator by finite dimensional ones.

The optimal estimators have been designed in such a way that they minimize the impulse response norm or the L_2-gain of the error system respectively. It therefore makes sense to address the question to what extent approximations and implementations of the estimators compromise performance as measured in these design criteria. Moreover, it makes sense to address the question whether the approximated estimator Σ_e^N achieves a performance that will converge to the performance of the optimal estimator if the order N of the approximation will be increased.

Problem 6.2 (Estimator approximation problem)
Let Σ_e be an optimal estimator for the system Σ_p. Determine a finite dimensional estimator Σ_e^N of order N that either converges to Σ_e in the sense that:

$$\lim_{N\to\infty} ||\Sigma_e - \Sigma_e^N|| = 0,$$

or that achieves convergence of the estimated (or error) system in the sense that performance converges

$$\lim_{N\to\infty} ||\Sigma_p \wedge \Sigma_e^N - \Sigma_p \wedge \Sigma_e|| = 0.$$

Here, $\Sigma_p \wedge \Sigma_e$ is the system illustrated in Figure 5.3 and $||\cdot||$ is the norm used for optimal estimator design of Σ_e.

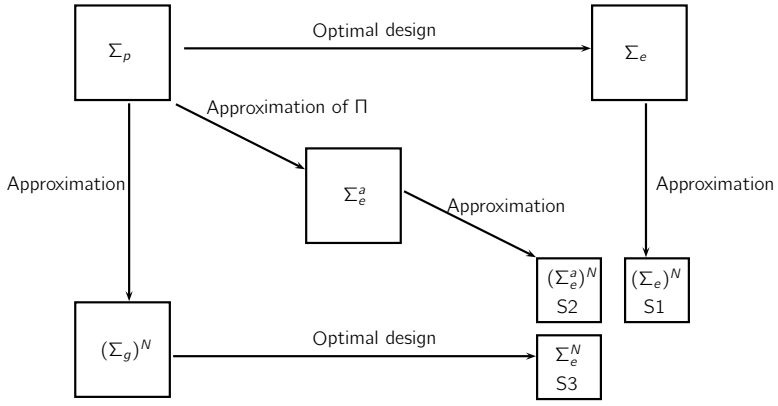

Figure 6.1: Visual representation of possible estimator design and approximation paths.

The idea behind Problem 6.2 is that the performance which could be achieved if Σ_e would be implementable can be approximated arbitrarily close by the implementable estimator Σ_e^N.

Three approaches to obtain finite dimensional approximations of the optimal estimator have been identified and are shown in Figure 6.1. The diagram shows the following three paths:

S1. The system Σ_p is approximated by a finite dimensional linear time invariant system Σ_p^N with state dimension N. An optimal estimator Σ_e^N for the system Σ_p^N is designed that minimizes either of the norms defined in Chapter 5.

S2. The infinite dimensional optimal estimator Σ_e given by (6.2) is approximated by a linear time invariant finite dimensional estimator $(\Sigma_e)^N$ with state dimension N.

S3. The solution $\Pi : X \to X$ of the Riccati Equation (6.3) or (6.4) is approximated by a finite rank solution $\tilde{\Pi} : X \to X$ with $\text{rank}(\tilde{\Pi}) \leq N$ and subsequently substituted for Π in (6.2). This defines the estimator Σ_e^a. Hereafter, the estimator Σ_e^a is approximated by a linear time invariant finite dimensional estimator $(\Sigma_e)^N$ with state dimension N.

It is not a-priori clear which approach is most valuable in practical situations. Clearly, there is a lot of freedom in the scenarios. For instance, there is a choice in the approximation method that will be used. Moreover, we recognize that, it might be possible that other interesting scenarios for approximation exist. In order to identify the most valuable approach we analyze the three scenarios and compare the estimators in this chapter

In the context of approximation of the linear quadratic regulator It has been observed that care has to be taken with the approximation methods and that convergence of system properties and performance is not trivial and inherent. We name a number of cases where problems have been identified:

- Popular methods for finite element discretization [Wesseling, 2001; LeVeque, 2002] for linear convection dominated problems do employ non-linear flux limiters such as the Van Leer or Korens flux limiters [Gunawan et al., 2004; Mesbah et al.,

2009]. In these methods, the linear infinite dimensional system is approximated by a nonlinear finite dimensional system. In [Liu and Sandu, 2008] it has been observed that adjoints of linearization of approximated operators may lose consistency (i.e. do approximate the adjoint of an operator well) especially when approximation schemes with flux limiter methods are employed.

- In [Borggaard et al., 2004] it is conjectured that dual convergence is necessary for strong convergence of the solution of Riccati equations and for the convergence of the gains that need to be calculated in linear quadratic controller design for non-normal distributed parameter systems.
- In [Banks and Fabiano, 1997] an example is given in which the semigroup operator converges but the adjoint semigroup does not converge, and only weak convergence of the Riccati equation is observed.

The topic of approximation of systems, the approximation of controllers and the synthesis of controllers of finite order for systems of infinite dimension is a very wide area that cannot be covered here. In this chapter we will focus on the finite dimensional approximation of estimators for distributed parameter systems by a specific method, the Galerkin projection. We will analyze the convergence of approximations of optimal impulse response norm estimators by use of the results which are known from the context of Linear Quadratic Regulator problems. The analysis of the convergence of approximations of optimal L_2-gain estimators will be left for future research.

The approximation of controllers for infinite dimensional systems has been a topic of research for a very long period of time already. Important results can be found in the survey book Chapter [Morris, 2010].

6.2 Estimator approximation

In this section we will introduce a mathematical framework to formalize the approximation of systems. This framework is found in literature and provides a useful standardization of notation for approximation problems. This will be used to formalize the approximation scenarios S1, S2 and S3, which have been introduced in Section 6.1.

6.2.1 A system approximation framework

In many cases there is a compelling reason to approximate a system by another system, with different properties. For instance, in case the original system is infinite dimensional, approximations of such a system by a finite dimensional one is in general necessary to allow for implementations on computational platforms. In such a case, one is interested in how close (in a well defined measure) the solutions of the approximating system are to the solutions of the original system and whether the approximation error vanishes for approximations of increasing complexity. In general such questions are hard to answer. In this section we describe a framework for approximation of systems. This framework is based on the work described in [Ito and Kappel, 1998] and [Ito and Kappel, 2002, Section 4.1].

We introduce the following situation. Assume that Z is a Banach space with norm $||\cdot||$ and assume that X is a closed linear subspace of Z. In many cases Z equals X, but this is not assumed beforehand. We assume that the operator $A : D(A) \to X$ in (6.1) is the generator of a C_0-semigroup $T(t)$ on X and that the following evolution equation is well posed on X and has a unique solution for any initial condition $x(0) = x_0 \in X$:

$$\dot{x} = Ax. \tag{6.5}$$

This solution is given by $x(t) = T(t)x_0$. Then we introduce the following situation, which we will call situation **A**. Suppose X_N is, for every $N = 1, 2, ...$ a Banach space with norm $||\cdot||_{X_N}$. Moreover we define the following linear mappings between Z and X_N

$$P_N : Z \to X_N,$$
$$E_N : X_N \to Z.$$

In Figure 6.2 a visual representation of the spaces Z, X, X_N and the operators E_N, P_N is given.

We assume that the operator $A_N : D(A_N) \to X_N$ with $D(A_N) \subseteq X_N$ is the generator of a C_0-semigroup $T_N(t)$ on X_N and that the following evolution equation is well posed on X_N and has a unique solution for $x_N(0) = x_{N,0} \in X_N$:

$$\dot{x}_N = A_N x_N. \tag{6.6}$$

This solution is given by $x_N(t) = T_N(t)x_{N,0}$. In order to approximate solutions x to (6.5) with solutions x_N of the system (6.6) we consider the question how close the solutions to (6.5) with initial condition x_0 are to those of (6.6) with initial condition $x_{N,0} = P_N x_0$. For this, we consider the measure

$$||T(t)x_0 - E_N T_N(t) P_N x_0|| \quad \text{for } t \in \mathbb{T}.$$

Moreover, one might be interested to know if the approximation gets better if ones increases the order N of the approximation. It is common to make the following assumptions on the mappings P_N and E_N, following [Ito and Kappel, 1998]:

A1 There exists $M_1, M_2 \in \mathbb{R}$ independent of N, such that $||P_N|| \leq M_1$, $||E_N|| \leq M_2$.

A2 The operator P_N and E_N satisfy the property $\lim_{N\to\infty} ||E_N P_N x - x|| = 0$ for all $x \in X$

A3 The operator P_N and E_N satisfy the property $P_N E_N = I_N$, where I_N is the identity operator on X_N.

In general, (i.e. without special assumptions) there is no relation between the semi groups $T_N(t)$ and $T(t)$. However, we have the following lemma [Ito and Kappel, 2002, Section 4.1]:

Lemma 6.2.1
Assume that the conditions A1, A2 and A3 hold and $T_N(t)$ is defined as above. If the operator T_0, defined by

$$T_0(t)x := \lim_{N\to\infty} E_N T_N(t) P_N x$$

exists for all $x \in X$ and is uniform for all t in bounded intervals with $t \geq 0$, then $T_0(t)$ is a C_0-semigroup.

Proof. For the proof we refer to [Ito and Kappel, 2002, p117]. □

Definition 6.2.1 (Approximation of a system)
We will call the system (6.6) *an approximation of the system* (6.5) *if*

$$||T(t)x - E_N T_N(t) P_N x|| < \infty \quad \textit{for all } t \in [0, \infty) \textit{ and for all } x \in X.$$

Moreover, a convergent approximation is an approximation such that $T(t) = T_0(t)$.

In the same manner as we did for X_N, we can introduce a slightly different setting, which we call setting **B**. We introduce Z_N as follows. Suppose that Z_N is, for every $N = 1, 2, ...$, a subspace of Z with the norm $||\cdot||$, which is the norm on Z.

We introduce the canonical projection π_N and canonical injection i_N.

$$\pi_N : Z \to Z_N$$
$$i_N : Z_N \to Z$$

In Figure 6.2 a visual representation of the spaces Z_N and the operators π_N, i_N is given. We introduce the following assumptions on π_N:

B1 There exists a $\tilde{M} \in \mathbb{R}$ independent of N, such that $||\pi_N|| \leq \tilde{M}$,
B2 The operator π_N satisfy the property $\lim_{N\to\infty} ||\pi_N z - z|| = 0$ for all $z \in X$,

and assume that the operator $\tilde{A}_N : D(\tilde{A}_N) \to Z_N$ with $D(\tilde{A}_N)$ is the generator of a semigroup $\tilde{T}_N(t)$ on Z_N with the evolution equation:

$$\dot{\tilde{x}}_N = \tilde{A}_N \tilde{x}_N. \tag{6.7}$$

In fact the two situations **A** and **B** are identical. Starting from X_N one obtains situation **B** from **A**, i.e. Z_N and π_N by setting $Z_N = range(E_N)$ and $\pi_N = E_N P_N$. The conditions $B1$ and $B2$ are automatically satisfied if P_N and E_N satisfy $A1$, $A2$ and $A3$. Conversely, starting from Z_N one obtains situation **A** from **B**, i.e. X_N, P_N and E_N by setting $X_N = Z_N$, $P_N = \pi_N$ and $E_N = i_N$. The conditions $A1$, $A2$ and $A3$ are automatically satisfied if π_N satisfies $B1$ and $B2$.

For our application, we will be mainly interested in the situation where spaces X_N and Z_N are finite dimensional of dimension N and isomorphic. Then there exists an isomorphic mapping $p_N : Z_N \to X_N$. In this case we have that:

$$P_N x = p_N \pi_N x \quad \text{for } x \in Z_N \tag{6.8}$$
$$E_N x_N = i_N p_N^{-1} x_N \quad \text{for } x_N \in X_N \tag{6.9}$$

The situation **A** is useful in the context of implementation. With X_N finite dimensional the system defined by (6.6) represents a finite system of ordinary differential equations which is suitable for implementation in todays standard software tools such as Matlab. In this case $T_N(t) = exp(A_N t)$.

In Figure 6.2 a visual representation of the spaces Z, X, Z_N and X_N and the operators E_N, P_N, p_N, i_N and π_N is given.

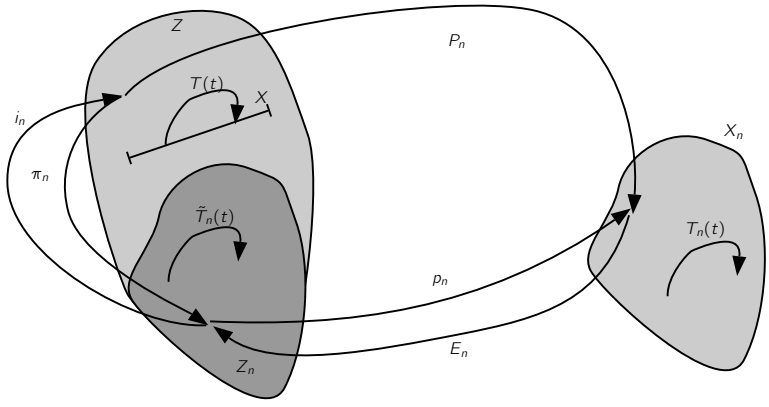

Figure 6.2: Graphical representation of relevant spaces, subspaces, and mappings.

We remark that, until now, we did not specify how to obtain the approximating systems (i.e. either A_N or $T_N(t)$) from the original system (i.e. either A or $T(t)$). The procedure to obtain the approximation, the approximation method, depends from system to system.

The following shows an example of how the spaces Z_N and X_N can be chosen.

Example 6.2.1
Let $Z = X$ be a Hilbert space with norm $||\cdot||$ and with a countable orthonormal basis $\{\phi_i\}_{i=1}^{\infty}$. Let $Z_N = \text{span}\{\phi_i\}_{i=1}^{N}$ and $X_N = \mathbb{R}^N$ with canonical basis $\{e_i\}_{i=1}^{N}$. We define:

$$P_N : Z \to X_N, \qquad E_N : X_N \to Z,$$

as follows:

$$P_N x = \sum_{i=1}^{N} \langle x, \phi_i \rangle e_i,$$
$$E_N x_N = \sum_{i=1}^{N} \langle x_N, e_i \rangle \phi_i.$$

The operators P_N and E_N satisfy the conditions A1, A2, A3. Indeed,

A1 *Boundedness of E_N and P_N follows from Bessel's inequality, for $M_1 = 1$, $M_2 = 1$ we have $||P_N|| \leq M_1$, $||E_N|| \leq M_2$. This follows when we set $x = \sum_{i=1}^{\infty} a_i \phi_i$ and calculate:*

$$||P_N|| = \sup_{x \in Z} \frac{||P_N x||}{||x||} = \sup_{x \in Z} \frac{||a_1, ..., a_N||}{||a||} = 1 \text{ for all } n$$

$$||E_N|| = \sup_{x_N \in X_N} \frac{||E_N x||}{||x||} = 1 \text{ for all } N$$

A2 $||E_N P_N x - x|| \to 0$ *as* $N \to \infty$ *for all* $x \in X$*, which follows from:*

$$||E_N P_N x - x|| = ||\sum_{i=1}^{N} \langle P_N x, e_i \rangle \phi_i - x|| = ||\sum_{i=1}^{N} \langle x, \phi_i \rangle \phi_i - \sum_{i=1}^{\infty} \langle x, \phi_i \rangle \phi_i||$$
$$= ||\sum_{i=N+1}^{\infty} \langle x, \phi_i \rangle \phi_i|| \leq \sum_{i=N+1}^{\infty} |\langle x, \phi_i \rangle|^2$$

A3 $P_N E_N = I_N$*, where* I_N *is the identity operator on* X_N*, which follows from:*

$$P_N E_N x = \sum_{i=1}^{N} \langle \sum_{j=1}^{N} \langle x, e_j \rangle \phi_j, \phi_i \rangle e_i = \sum_{i=1}^{N} \langle x, e_i \rangle e_i = x$$

The operator $\pi_N x = E_N P_N x$ *is now given by* $\pi_N x = \sum_{i=1}^{N} \langle x, \phi_i \rangle \phi_i$*. Moreover, it follows that* $E_N^* = P_N$*:*

$$\langle x_N, E_N^* x \rangle_{X_N} := \langle E_N x_N, x \rangle_{Z_N} \quad \text{for all } x_N \in X_N, x \in Z$$
$$= \langle \sum_{i=1}^{N} \langle x_N, e_i \rangle \phi_i, x \rangle_{Z_N} = \sum_{i=1}^{N} \langle x_N, e_i \rangle \langle \phi_i, x \rangle_{Z_N}$$
$$= \langle x_N, \sum_{i=1}^{N} \langle x, \phi_i \rangle_{Z_N} e_i \rangle = \langle x, P_N x \rangle$$

The latter property will be of use later in the chapter.

6.2.2 System approximation by Galerkin projection

A popular method for system approximation is the Galerkin projection method. In this section we will introduce the Galerkin projection. We will show in two examples how the Galerkin projection can be used to obtain approximations of the convection equation and diffusion equation. Consider the system Σ.

$$\Sigma : \begin{cases} \dot{x} = Ax + Bu, \\ y = Cx, \end{cases}$$

with $x(t) \in X$ and $A : D(A) \to X$, $D(A) \subset X$. Define $E_N : X_N \to X$ and $P_N : X \to X_N$ with the properties that $\pi_N = E_N P_N$ is a projection on X and $E_N^* P_N = I_N$.

The Galerkin projection of the system Σ is defined as follows:

Definition 6.2.2 (Galerkin projection [Antoulas, 2005])
Let P_N *and* E_N *satisfy assumptions* A_1*,* A_2*,* A_3*. The Galerkin projection of the system* Σ*, is defined by* Σ_N

$$\Sigma_N : \begin{cases} \dot{x}_N = A_N x_N + B_N u, \\ y = C_N x_N, \end{cases}$$

with $A_N := P_N A E_N$*,* $C_N := C E_N$ *and* $B_N := P_N B$ *and* $x_{N,0} = P_N x_0$*.*

Note that Σ_N has order N if and only if X_N is N dimensional.

6.2.3 Approximation of estimators

In this section the approximation scenarios $S1$, $S2$ and $S3$ which have been introduced in Section 6.1 will be formalized by use of the framework introduced in Section 6.2.1. In order to do so, it has been assumed that $X_N = \mathbb{R}^N$ and that operators E_N and P_N are as defined in Section 6.1.

Scenario $S1$

In this section the scenario $S1$ is discussed. That is, the system Σ_p is approximated by a finite dimensional linear time invariant system Σ_p^N with state dimension N. This system is represented by:

$$\Sigma_p^N : \begin{cases} \dot{x}_N = & A_N x_N + G_N d_1, \\ y = & C_N x_N + S d_2, \\ z = & H_N x_N, \end{cases}$$

with $x_N(t) \in \mathbb{R}^N$. Subsequently, an optimal estimator Σ_e^N for the system Σ_p^N is designed that minimizes either of the norms defined in Chapter 5. This estimator is given by:

$$\Sigma_e^N : \begin{cases} \dot{\hat{x}} & = (A_N - \Pi_N C_N^* (SS^*)^{-1} C_N)\hat{x} + P_N \Pi_N C_N^* (SS^*)^{-1} y \\ \hat{z} & = H_N \hat{x} \end{cases} \tag{6.10}$$

with $\hat{x}(t) \in \mathbb{R}^N$. In the case of optimal $\mathcal{H}_2$-norm estimator design, Π_N is the solution of the Algebraic Riccati Equation:

$$\Pi_N A_N^* + A_N \Pi_N + G_N G_N^* - \Pi_N (C_N^* (SS^*)^{-1} C_N) \Pi_N = 0, \tag{6.11}$$

In the case of optimal L_2 gain estimator design, Π_N is the solution of the Algebraic Riccati Equation for $x_1, x_2 \in \mathbb{R}^N$:

$$\Pi_N A_N^* + A_N \Pi_N + G_N G_N^* - \Pi_N (C_N^* (SS^*)^{-1} C_N - \gamma^{-2} H_N^* H_N) \Pi_N = 0. \tag{6.12}$$

In practical applications we will consider the interconnection of Σ_p with Σ_e^N, and we will be interested in the system

$$\Sigma_g \wedge \Sigma_e^N : L_2(D_1 \times D_2, \mathbb{T}) \to L_2(\mathbb{T}, Z),$$

where Σ_g is as introduced in Section 5.3.

A representation of $\Sigma_g \wedge \Sigma_e^N$ can be obtained from Equations (5.5) and (5.6) and is given by:

$$(\Sigma_g \wedge \Sigma_e^N \begin{bmatrix} d_1 \\ d_2 \end{bmatrix})(t) = \int_{\mathbb{T}} k_N(t, \tau) \begin{bmatrix} d_1(\tau) \\ d_2(\tau) \end{bmatrix} \mathrm{d}\tau,$$

with

$$k_N(t, \tau) = \begin{bmatrix} HT(t - \tau)G + \int_\tau^t M_N(t, \sigma) C T(\sigma - t) G \mathrm{d}\sigma & M_N(t, \tau) S \end{bmatrix}$$

where $M_N(t,\tau) = h_N(t-\tau)$, with $h_N(t) = H_N S_N(t)\Pi_N C_N^*(SS^*)^{-1}$ where $S_N(t)$ is the semigroup operator with infinitesimal generator $A_N - \Pi_N C_N^*(SS^*)^{-1}C_N$, i.e.

$$S_N(t) = exp((A_N - \Pi_N C_N^*(SS^*)^{-1}C_N)t).$$

We have the following theorems:

Theorem 6.2.2
Consider the systems Σ_g, Σ_e and Σ_e^N. If

$$\lim_{N\to\infty} ||\Sigma_e - \Sigma_e^N||_{imp} = 0 \qquad then \qquad \lim_{N\to\infty} ||\Sigma_p \wedge \Sigma_e - \Sigma_p \wedge \Sigma_e^N||_{imp} = 0.$$

Proof. We recall that:

$$(\Sigma_g \wedge \Sigma_e \begin{bmatrix} d_1 \\ d_2 \end{bmatrix})(t) = \int_{\mathbb{T}} k(t,\tau) \begin{bmatrix} d_1(\tau) \\ d_2(\tau) \end{bmatrix} \mathrm{d}\tau,$$

where k follows from Equation (5.6):

$$k(t,\tau) = \begin{bmatrix} HT(t-\tau)G + \int_\tau^t M(t,\sigma)CT(\sigma - t)G\mathrm{d}\sigma & M(t,\tau)S \end{bmatrix}$$

with $M(t,\tau) = h(t-\tau)$, $h(t) = HS(t)\Pi C^*(SS^*)^{-1}$ and where $S(t)$ is the semigroup operator with infinitesimal generator $A - \Pi C^*(SS^*)^{-1}C$.

By definition of the norm of the impulse response it follows that:

$$\begin{aligned} ||\Sigma_p \wedge \Sigma_e - \Sigma_p \wedge \Sigma_e^N||_{\text{imp}} &= ||k(\cdot,0) - k_N(\cdot,0)||_2 = \\ &|| \begin{bmatrix} \int_0^\cdot (h(\cdot-\sigma) - h_N(\cdot-\sigma))CT(\sigma-\cdot)G\mathrm{d}\sigma & (h(\cdot) - h_N(\cdot))S \end{bmatrix} ||_2 \end{aligned}$$

Using the Cauchy-Schwarz inequality it follows that:

$$\begin{aligned} &||\Sigma_p \wedge \Sigma_e - \Sigma_p \wedge \Sigma_e^N||_{\text{imp}} \\ &\qquad \leq \int_0^\cdot ||h(\cdot-\sigma) - h_N(\cdot-\sigma)||_2 ||CT(\sigma-\cdot)G||_2 \mathrm{d}\sigma + ||h(\cdot) - h_N(\cdot)S||_2 \end{aligned}$$

From definition of the impulse response norm and the assumption that $\lim_{N\to\infty} ||\Sigma_e - \Sigma_e^N||_{\text{imp}}$ it follows:

$$\lim_{N\to\infty} ||h - h_N||_2 = 0,$$

from which it can be concluded that $\lim_{N\to\infty} ||\Sigma_p \wedge \Sigma_e - \Sigma_p \wedge \Sigma_e^N||_{\text{imp}} = 0$. □

The following theorem shows that it is possible to obtain, under some assumptions, convergence in the impulse response norm of the system Σ_e^N to Σ_e.

Theorem 6.2.3
Consider the systems Σ_p, Σ_e and Σ_e^N. Assume that:

$$\begin{aligned} &\lim_{N\to\infty} ||(H - H_N P_N)x|| = 0, && \lim_{N\to\infty} ||(H^* - E_N H_N^*)z|| = 0, \\ &\lim_{N\to\infty} ||(C - C_N P_N)x|| = 0, && \lim_{N\to\infty} ||(C^* - E_N C_N^*)y|| = 0, \\ &\lim_{N\to\infty} ||(S(t) - E_N S_N(t) P_N)x)|| = 0, && \lim_{N\to\infty} ||(S^*(t) - E_N S_N^*(t) P_N)x)|| = 0, \\ &\lim_{N\to\infty} ||(\Pi - \Pi_N P_N)x|| = 0, \end{aligned}$$

for all $t \in \mathbb{T}$, $x \in X$, $y \in Y$ and $z \in Z$ and where Π is the solution of (6.3) *and $S(t)$ is the semigroup operator with infinitesimal generator $A - \Pi C^*(SS^*)^{-1}C$. Then the following holds:*

$$\lim_{N\to\infty} ||\Sigma_e - \Sigma_e^N||_{imp} = 0.$$

Proof. Let $h(t), h_N(t) \in \mathbb{R}^{m\times n}$ be defined by

$$h(t) = HS(t)\Pi C^*(SS^*)^{-1} \text{ and } h_N(t) = H_N S_N(t)\Pi_N C_N^*(SS^*)^{-1}.$$

From the assumptions it follows that:

$$\lim_{N\to\infty} ||(h(t) - h_N(t))y||_Y = 0 \qquad \text{and} \qquad \lim_{N\to\infty} \quad ||(h^*(t) - h_N^*(t))z||_Z = 0, \tag{6.13}$$

for all $t \in \mathbb{T}$, $y \in Y$, $z \in Z$. Let $\{\lambda_{N,i}(t)\}_{i=1}^m$ be the eigenvalues of $(h(t) - h_N(t))^*(h(t) - h_N(t))$. From the Equations (6.13) it follows that for all $t \in \mathbb{T}$, $\lim_{N\to\infty} \lambda_{N,i}(t) = 0$ for $i = 1, ..., m$. Since m is finite it follows from the definition of the trace operator that for all $t \in \mathbb{T}$ $\lim_{N\to\infty} \sum_{i=1}^m \lambda_{N,i}(t) = 0$. Therefore it follows that: $\int_0^\infty \sum_{i=1}^m \lambda_{N,i}(t)\mathrm{d}t = 0$. This proofs the claim, since from the definition of the impulse response norm it now follows that:

$$\begin{aligned}\lim_{N\to\infty} ||\Sigma_e - \Sigma_e^N||_{\text{imp}} &= \lim_{N\to\infty} ||h - h_N||_2 \\ &= \lim_{N\to\infty} \int_0^\infty \operatorname{tr}\,(h(t) - h_N(t))^*(h(t) - h_N(t))\mathrm{d}t \\ &= \lim_{N\to\infty} \int_0^\infty \sum_{i=1}^m \lambda_i(t)\mathrm{d}t = 0\end{aligned}$$

□

Scenario *S2*

In this section we study the scenario *S2*. That is, the infinite dimensional optimal estimator Σ_e given by (6.2) is approximated by a linear time invariant finite dimensional estimator $(\Sigma_e)^N$ with state dimension N. Define $(\Sigma_e)^N$ by:

$$(\Sigma_e)^N : \begin{cases} \dot{\hat{x}} & = P_N(A - \Pi C^*(SS^*)^{-1}C)E_N\hat{x} + P_N\Pi C^*(SS^*)^{-1}y \\ \hat{z} & = HE_N\hat{x} \end{cases} \tag{6.14}$$

with in the case we minimize the impulse response norm, Π is for all $x_1, x_2 \in D(A^*)$ the solution of the Riccati equation:

$$\langle \Pi A^* x_1, x_2\rangle + \langle x_1, \Pi A^* x_2\rangle + \langle G^* x_1, G^* x_2\rangle - \langle \Pi(C^*(SS^*)^{-1}C)\Pi x_1, x_2\rangle = 0, \tag{6.15}$$

and with in the case we minimize the L_2 norm, Π is for all $x_1, x_2 \in D(A^*)$ the solution of the Riccati equation:

$$\langle \Pi A^* x_1, x_2\rangle + \langle x_1, \Pi A^* x_2\rangle + \langle G^* x_1, G^* x_2\rangle - \langle \Pi(C^*(SS^*)^{-1}C - \gamma^{-2}H^*H)\Pi x_1, x_2\rangle = 0. \tag{6.16}$$

Note that this is the Galerkin projection of the optimal estimator Σ_e, given by Equation 6.2. Unfortunately, this scenario is not realistic since the associated implicit Riccati equations need to be solved in this approach. However, for theoretical purposes it might be interesting to study if we have convergence in the sense that:

$$\lim_{N\to\infty} ||\Sigma_e - (\Sigma_e)^N|| = 0.$$

For the optimal impulse response estimators this problem amounts to convergence of the convolution kernels of the system $(\Sigma_e)^N$ and (Σ_e) and might be studied by use of the Kato-Trotter Theorem, which will be introduced in Section 6.3. Unfortunately, convergence results for this problem are not available in this thesis.

Scenario *S*3

In this section we study the scenario *S*3. That is, the solution $\Pi : X \to X$ of the Riccati equation (6.3) or (6.4) is approximated by a finite rank solution $\tilde{\Pi} : X \to X$ with $\text{rank}(\tilde{\Pi}) \leq N$ and subsequently substituted for Π in (6.2). This defines the estimator Σ_e^a. Hereafter, the estimator Σ_e^a is approximated by a linear time invariant finite dimensional estimator $(\Sigma_e)^N$ with state dimension N. This gives

$$(\Sigma_e^a) : \begin{cases} \dot{\hat{x}} &= (A - \tilde{\Pi}C^*(SS^*)^{-1}C)\hat{x} + \tilde{\Pi}C^*(SS^*)^{-1}y \\ \hat{z} &= H\hat{x} \end{cases} \tag{6.17}$$

with $\text{rank}\tilde{\Pi} \leq N$ and the approximate finite dimensional system

$$(\Sigma_e^a)^N : \begin{cases} \dot{\hat{x}} &= P_N(A - \tilde{\Pi}C^*(SS^*)^{-1}C)E_N\hat{x} + P_N\tilde{\Pi}C^*(SS^*)^{-1}y \\ \hat{z} &= HE_N\hat{x} \end{cases} \tag{6.18}$$

In general the properties of $(\Sigma_e^a)^N$ will depend on the choice of the method to compute $\tilde{\Pi}$ and the method to obtain $(\Sigma_e^a)^N$. We remark that (in theory) this setting enables to use methods for computation of $\tilde{\Pi}$ and approximation of the system which are not related. The question, whether or not this freedom is beneficial with respect to performance of the estimator when $(\Sigma_e^a)^N$ interconnected to original plant Σ_p will be left for future research.

Let $\Pi_N \in \mathbb{R}^{N\times N}$ be the solution of either (6.11) or (6.12). We have the following result for the case in which $\tilde{\Pi}$ is obtained from Π_N by setting $\tilde{\Pi} = E_N\Pi_N P_N$.

Theorem 6.2.4
*Consider the situation where P_N and E_N satisfy the conditions A*1*, A*2 *and A*3 *and suppose the estimators Σ_e^N and $(\Sigma_e^a)^N$ are obtained according to scenario's S*1 *and S*3*, where A_N, G_N, C_N and H_N are obtained by the Galerkin projection, i.e.:*

$$A_N = P_N A E_N \qquad G_N = P_N G \qquad C_N = C E_N \qquad H_N = H E_N$$

Moreover assume that $\Pi_N \in \mathbb{R}^{N\times N}$ be the solution of either (6.11) *or* (6.12) *and let $\tilde{\Pi}$ be computed by $\tilde{\Pi} = E_N\Pi_N P_N$.*

In this situation, the estimators $\Sigma_e^N = (\Sigma_e^a)^N$ if $CP_N^* = CE_N$.

Proof. Given that $CP_N^* = CE_N$ and $\tilde{\Pi} = E_N \Pi_N P_N$ it follows that:

$$P_N \tilde{\Pi} C^* (SS^*)^{-1} = \Pi_N (CP_N^*)^* (SS^*)^{-1} = \Pi_N C_N^* (SS^*)^{-1}.$$

Therefore, $(\Sigma_e^a)^N$ can be rewritten to,

$$(\Sigma_e^a)^N : \begin{cases} \dot{\hat{x}} &= (A_N - \Pi_N C_N^* (SS^*)^{-1} C_N)\hat{x} + \Pi_N C_N^* (SS^*)^{-1} y \\ \hat{z} &= H E_N \hat{x} \end{cases} \tag{6.19}$$

and it follows from comparison the latter representation of $(\Sigma_e^a)^N$ with (6.14), that the systems $(\Sigma_e^a)^N$ and Σ_e^N are equal. □

6.3 Convergence of approximations

Approximations of systems can be obtained by the approximation methods described in Section 6.2.1. It is important to know if and eventually at what rate the quality of approximations improves if N increases. This property is called convergence. In this section we provide an introduction to the most imporant convergence results and shown how these results can be used for a special class of systems.

In order to facilitate the discussions we introduce two different types of convergence.

Definition 6.3.1 (Strong convergence)
A series of points x_N in a Hilbert Space H is said to converge strongly, or converge in the norm, if there exist an $x \in H$ such that:

$$\lim_{N \to \infty} ||x_N - x||_H = 0.$$

This type of convergence is also known as convergence in the norm or convergence in the strong topology and is generally denoted by $x_N \to x$.

Definition 6.3.2 (Weak convergence)
A series of points x_N in a Hilbert Space H is said to converge weakly, if there exist an $x \in H$, such that for all $\phi \in H^*$

$$\lim_{N \to \infty} |\langle x_N, \phi \rangle - \langle x, \phi \rangle| = 0.$$

This type of convergence is also known as convergence in the weak topology and denoted by $x_N \overset{w}{\to} x$. Strong convergence implies weak convergence, the converse is in general not true.

We will be interested in the conditions under which the semigroup operators converge stongly, i.e. $T_N(t)x \to T(t)x$ for any $x \in X$. A theorem that establishes a necessary and sufficient condition for strong convergence is the Trotter-Kato Theorem, which can be found (in various formulation) in for instance [Ito and Kappel, 1998] or [Pazy, 1983].

Theorem 6.3.1 (Trotter-Kato theorem in framework of Kappel and Ito.)
Assume that A1, A2, A3 are satisfied. Let A resp. A_N be the generator of a C_0 semigroup $T(t)$ on X resp. $T_N(t)$ on X_N, with $||T_N(t)|| \leq Me^{\omega t}$ and $||T(t)|| \leq Me^{\omega t}$ and M, ω independent of N. Let $\rho(A)$ denote the resolvent set[1] of A. Then the following statements are equivalent

a *There exist a $\lambda_0 \in \rho(A) \cap \bigcap_{N=1}^{\infty} \rho(A_N)$, such that for all $x \in X$*

$$\lim_{N\to\infty} ||E_N(\lambda_0 I_N - A_N)^{-1} P_N x - (\lambda_0 I - A)^{-1} x|| = 0$$

b *For every $x \in X$ and $t \geq 0$*

$$\lim_{N\to\infty} ||E_N T_N(t) P_N x - T(t)x|| = 0$$

uniformly on bounded t-intervals.

Moreover: If (a) or (b) is true, then (a) holds for all λ_0 with $Re(\lambda_0) > \omega$.

For the proof we refer to the proof of Theorem 2.1 in [Ito and Kappel, 1998]. In general, the conditions in the Kato Trotter theorem are hard to verify in practice. The following theorem enables to substitute the condition (a) of the Kato-Trotter theorem, as formulated in [Ito and Kappel, 1998].

Theorem 6.3.2
Let the assumptions made in Theorem 6.3.1 hold. Statement (a) is equivalent to the following conditions:

- **C0** $\lim_{N\to\infty} ||E_N P_N x - x|| = 0$ *for all $x \in X$.*
- **C1** *There exists a $\lambda_0 > \omega$ and a subset $D \subset D(A)$ such that its closure $\bar{D} = X$ and $\overline{(\lambda_0 I - A)D} = X$.*
- **C2** *For all $u \in D$ there exists a sequence $(\bar{u}_N)_{N\in\mathbb{N}}$ with $\bar{u}_N \in \operatorname{dom} A_N$ such that*

$$\lim_{N\to\infty} ||E_N \bar{u}_N - u|| \quad \text{and} \quad \lim_{N\to\infty} ||E_N A_N \bar{u}_N - u||.$$

Proof. For the proof we refer to the proof of Proposition 3.1 in [Ito and Kappel, 1998]. □

A drawback of the Trotter-Kato Theorem is the technicality of the conditions. Therefore, it is useful to search for classes of systems for which convergence can be checked more easily. We will now show a special class of systems, for which convergence can be proved with less technical conditions.

Definition 6.3.3 (Semigroup of contractions, [Curtain and Zwart, 1995, Def 2.2.1])
$T(t)$ is a contraction semigroup if it is a C_0-semigroup that satisfies $||T(t)|| \leq 1$ for all $t \geq 0$.

The following theorem provides a sufficient condition to validate if a linear operator A generates a C_0 semigroup.

[1] The resolvent $R(\lambda, A)$ is defined by $R(\lambda, A) = (\lambda I - A)^{-1}$. The resolvent set $\rho(A)$ is defined as $\rho(A) = \{\lambda \in \mathbb{C} \mid (\lambda I - A)x \neq 0 \text{ for all } x \in D(A)\}$

Lemma 6.3.3 ([Curtain and Zwart, 1995, Corollary 2.2.3])
If A is a densely defined closed operator on a Hilbert Space and

$$Re(\langle Az, z\rangle) \leq \omega||z||^2 \text{ for } z \in D(A)$$
$$Re(\langle A^*z, z\rangle) \leq \omega||z||^2 \text{ for } z \in D(A^*)$$

then A is the infinitesimal generator of a C_0 semigroup with $||T(t)|| \leq e^{\omega t}$.

Note that if $\omega \leq 0$ the semigroup is a semigroup of contractions. The contraction semi groups are closely related to dissipative operators by the Lumer-Phillips theorem. We introduce the definition of a dissipative operator.

Definition 6.3.4 (Dissipative Operator ([Pazy, 1983]))
A linear operator A on a Hilbert space. A is dissipative if for every $x \in D(A)$, $Re\langle Ax, x\rangle \leq 0$.

Therefore, a special case ($\omega \leq 0$) of Lemma 6.3.3 is often found in literature in the context of dissipative operators, which we introduce for completeness.

Corollary 6.3.4 ([Pazy, 1983, Corollary 4.4])
If A is a densely defined closed operator on a Hilbert space and A and A^* are dissipative then, A is the generator of a semigroup of contractions.

The Lumer-Phillips theorem provides a sufficient condition for a linear operator to be the generator of a semigroup of contractions.

Theorem 6.3.5 (Lumer-Phillips ([Pazy, 1983]))
Let A be a linear operator with the dense domain $D(A)$ in X. The following statements are equivalent.

- *A is dissipative and there is an $\lambda_0 > 0$ such that $im(\lambda_0 I + A) = X$.*
- *A is the generator of a C_0 semigroup of contractions.*

Moreover, if A is dissipative and there is an λ_0 such that $im(\lambda_0 I + A) = X$, then $im(\lambda I + A) = X$ for all $\lambda > 0$

By combination of the Lumer-Phillips Theorem 6.3.5 and Lemma 6.3.3 and Theorem 6.4.3 one can derive straight-forward conditions to guarantee convergence of approximations.

Theorem 6.3.6 (Convergence of semigroup generated by dissipative operators)
Let A be a densely defined closed operator on a Hilbert space and be such that:

$$Re(\langle Ax, x\rangle) \leq \gamma||x||^2 \text{ for } x \in D(A),$$
$$Re(\langle A^*x, x\rangle) \leq \gamma||x||^2 \text{ for } x \in D(A^*),$$

with $\gamma \leq 0$.

Let X_N be a finite dimensional Hilbert space of dimension N, $P_N : X \to X_N$ and $E_N : X_N \to X$ be operators for which A1,A2 and A3 hold and assume that $E_N^* = P_N$. Let approximations A_N of A be given by $A_N := P_N A E_N$. Let $T_N(t)$, $T(t)$ be the

semi-groups associated with A_N and A respectively. Then the following holds.

$$\lim_{N\to\infty} ||E_N T_N(t) P_N x - T(t)x|| = 0 \quad \textit{for all } t \geq 0, x \in X$$
$$\lim_{N\to\infty} ||E_N T_N^*(t) P_N x - T^*(t)x|| = 0 \quad \textit{for all } t \geq 0, x \in X$$

Moreover, the semi groups $T_N(t)$ and $T_N^*(t)$ are uniformly exponentially stable, i.e. $||T_N(t)|| \leq e^{\gamma t}$ and $||T_N^*(t)|| \leq e^{\gamma t}$ for all $t \geq 0$.

Proof. We will show that the assumptions in this Theorem imply that the conditions $C0$, $C1$ and $C2$ in Theorem 6.4.3 hold for A to prove convergence of $T_N(t)$ to $T(t)$.
Validation of

- C0: Holds since $C0$ is equal to assumption $A2$.
- C1: By Lemma 6.3.3 it follows that: $||T(t)|| \leq 1$ for all $t \geq 0$. Therefore, A is the generator of a semigroup of contractions. By the Lumer-Phillips Theorem 6.3.5 it follows that $im(\lambda I + A) = X$ for all $\lambda > 0$. Therefore condition C1 holds for $D = D(A)$ and $\lambda > 0$.
- C2: To prove consistency of the approximation of A, we show that condition $C2$ holds. We choose $\bar{x}_N \in X_N$ by $\bar{x}_N = P_N x$ and it follows that:

$$\lim_{N\to\infty} ||E_N \bar{x}_N - x|| = \lim_{N\to\infty} ||E_N \bar{x}_N - x|| = \lim_{N\to\infty} ||(E_N P_N - I)x|| = 0$$
$$\begin{aligned}\lim_{N\to\infty} ||E_N A_N \bar{x}_N - Ax|| &= \lim_{N\to\infty} ||E_N P_N A E_N P_N x - Ax|| \\ &= \lim_{N\to\infty} ||(E_N P_N - I)AE_N P_N x + A(E_N P_N - I)x|| = 0\end{aligned}$$

It follows that $T_N(t)$ convergences to $T(t)$. Moreover, we have that

$$\langle A_N x_N, x_N\rangle = \langle P_N^* A E_N x_N, x_N\rangle = \langle AE_N x_N, P_N^* x_N\rangle \langle AE_N x_N, E_N x_N\rangle \leq \gamma,$$

from which $||T_N(t)|| \leq e^{\gamma t}$ follows by Lemma 6.3.3.

It follows that $A_N^* = (P_N A E_N)^* = E_N^* A^* P_N^*$. We will show that our assumptions imply that the conditions $C0$, $C1$ and $C2$ in Theorem 6.4.3 hold for A^* to prove convergence of $T_N^*(t)$ to $T^*(t)$.
Validation of

- C0: Holds since $C0$ is equal to assumption $A2$.
- C1: By Lemma 6.3.3 it follows that: $||T^*(t)|| \leq 1$ for all $t \geq 0$. Therefore, A^* is the generator of a semigroup of contractions. By Lumer-Phillips theorem it follows that $im(\lambda I + A^*) = X$ for all $\lambda > 0$. Therefore condition C1 holds for $D = D(A^*)$ and $\lambda > 0$.
- C2: To prove consistency of the approximation of A^*, we test condition $C2$. We again choose $\bar{x}_N = P_N x$ and it follows that:

$$\begin{aligned}\lim_{N\to\infty} ||E_N A_N^* \bar{x}_N - A^* x|| &= \lim_{N\to\infty} ||E_N E_N^* A^* P_N^* P_N x - A^* x|| \\ &= \lim_{N\to\infty} ||E_N P_N A^* E_N P_N x - A^* x|| \\ &= \lim_{N\to\infty} ||(E_N P_N - I)A^* E_N P_N x + A^*(E_N P_N - I)x|| \\ &= 0.\end{aligned}$$

Here we have used that $\lim_{N\to\infty} ||(E_N P_N - I)x_N|| = 0$ for all $x_N \in X_N$.

It follows that $T_N^*(t)$ convergences to $T^*(t)$. Moreover, we have that

$$\langle A_N^* x_N, x_N\rangle = \langle E_N^* A^* P_N^* x_N, x_N\rangle = \langle A^* E_N x_N, E_N x_N\rangle \leq \gamma,$$

from which $||T_N^*(t)|| \leq e^{\gamma t}$ follows by Lemma 6.3.3. □

Theorem 6.3.6 is strongly related to the work done in the context of approximation of parabolic systems such as in [Banks and Kunisch, 1984] and systems in which the infinitesimal generators are sectorial operator, such as in [Ito and Kappel, 2002, Section 4.4].

Alternative to the condition $E_N^* = P_N$, we can use a weaker condition to show convergence of the semigroup operators.

Corollary 6.3.7
Consider the assumptions of Theorem 6.3.6. And assume:

$$\lim_{N\to\infty} ||(E_N - P_N^*)x_N||_{x_N} = 0 \text{ for all } x_N \in X_N,$$
$$\lim_{N\to\infty} ||(P_N - E_N^*)x||_x = 0 \text{ for all } x \in X$$

Then the following holds.

$$\lim_{N\to\infty} ||E_N T_N(t) P_N x - T(t)x|| = 0 \quad \text{for all } t \geq 0, x \in X$$
$$\lim_{N\to\infty} ||E_N T_N^*(t) P_N x - T^*(t)x|| = 0 \quad \text{for all } t \geq 0, x \in X$$

Proof. The proof almost identical to the proof of Theorem 6.3.6. In this situation validation of condition $C0$ and $C1$ are equal and validation of $C2$ for A^* follows when we study the convergence of $(A_N)^*$. We have:

$$\lim_{N\to\infty} ||(E_N (A_N)^* P_N - A^*)x|| \leq \lim_{N\to\infty} \sup_{y\in X} \frac{||(E_N (A_N)^* P_N - A^*)y||}{||y||} ||x||$$

We use that for an arbitrary operator $B : X \to X$ we have that $||B|| = ||B^*||$, to obtain:

$$\begin{aligned}
&\lim_{N\to\infty} ||(E_N (A_N)^* P_N - A^*)x|| \\
&\quad \leq \lim_{N\to\infty} \sup_{y\in X} \frac{||(P_N^* A_N E_N^* - A)y||}{||y||} ||x|| \\
&\quad = \lim_{N\to\infty} \sup_{y\in X} \frac{||(E_N A_N P_N - A)y + (E_N - P_N^*)A_N P_N y + P_N^* A_N (P_N - E_N^*)y||}{||y||} ||x||
\end{aligned}$$

Now we use the triangle inequality for the numerator and it follows that $\lim_{N\to\infty} ||(A^* - E_N (A_N)^* P_N)x|| = 0$ for all $x \in X$. The uniform exponential stability of $T_N(t)$ and $T_N^*(t)$ cannot be shown analogously for this case. □

6.4 Approximation of Riccati equations

In this section we will study the approximation of Riccati equations involved in the optimal impulse response estimator design problem. In Theorem 6.2.3 it has been shown that convergence of approximations of the optimal impulse response estimator can be proved under the assumptions which are stated in the theorem. From these assumptions, the following three are influenced by the optimal estimator design procedure:

$$\lim_{N\to\infty} ||(S(t) - E_N S_N(t) P_N)x)|| = 0, \tag{6.20a}$$

$$\lim_{N\to\infty} ||(S^*(t) - E_N S_N^*(t) P_N)x)|| = 0, \tag{6.20b}$$

$$\lim_{N\to\infty} ||(\Pi - E_N \Pi_N P_N)x|| = 0 \tag{6.20c}$$

In this chapter, we will study conditions for which it can be shown that the assumptions given by Equations (6.20a), (6.20b) and (6.20c) hold. In Chapter 5, we have shown that the estimator design problem and the Linear Quadratic Regulator design problem are related by duality. The convergence of approximations of Riccati equations which are used in the context of the Linear Quadratic Regulator (LQR) problem is researched extensively. In this section we will how these results can be used to derive conditions for convergences of the approximations of Riccati equations which are used in the optimal impulse response estimator design problem. In the first part of this section we will review the results known for the Linear Quadratic Regulator problem. In the second part of this section we will show how these results can be applied in the context of the approximations of solutions of Riccati equations used in the design of the optimal impulse response estimator. In this section we will assume that operators E_N and P_N are as introduced in Section 6.2.1 and satisfy the conditions $A1$, $A2$ and $A3$.

6.4.1 Approximation of the LQR problem

In this section we introduce the approximation theory of Banks and Ito. Research on the approximation of the solution to the LQR problem for infinite dimensional systems has a long history. The most well known results on the convergence of algebraic Riccati equations can be found in [Banks and Kunisch, 1984]. The proof of this result is based on the results on approximations of integral Riccati equations in [Gibson, 1979]. An improvement of this result can be found in [Ito, 1987]. Generalization to strongly stabilizable systems can be found in [Oostveen, 2000]. An overview of results on controller design for distributed parameter systems can be found in [Morris, 2010]. We state some key results.

Consider the systems

$$\Sigma : \begin{cases} \dot{x} = Ax + Bu, \\ y = Cx \end{cases} \qquad \Sigma_N : \begin{cases} \dot{x}_N = A_N x_N + B_N u, \\ y_N = C_N x_N \end{cases}$$

with X and X_N Hilbert spaces, Y and U finite dimensional Euclidean spaces, $x(t) \in X$,

$x_N(t) \in X_N$, $y(t) \in Y$,$y_N(t) \in Y$,$u(t) \in U$, and

$$A : X \to X, \qquad A_N : X_N \to X_N,$$
$$B : U \to X, \qquad B_N : U \to X_N,$$
$$C : X \to Y, \qquad C_N : X_N \to Y.$$

Let $T_N(t) : X_N \to X_N$ and $T(t) : X \to X$ be semigroup operators with generators A_N and A respectively. We assume that the system Σ is exponentially stabilizable.

Moreover, we introduce $Q : X \to X$ and $Q_N : X_N \to X_N$ with $Q > 0$ and $Q_N > 0$ and we introduce the following two Algebraic Riccati Equations, associated with the systems Σ and Σ_N respectively:

$$A_N^* \Psi_N + \Psi_N A_N - \Psi_N B_N^* Q_N^{-1} B_N \Psi_N + C_N^* C_N = 0, \tag{6.21}$$
$$\langle A^* \Psi x_1, x_2 \rangle + \langle \Psi A x_1, x_2 \rangle - \langle \Psi B^* Q^{-1} B \Psi x_1, x_2 \rangle + \langle C^* C x_1, x_2 \rangle = 0, \tag{6.22}$$

for $x_1, x_2 \in D(A)$.

The Riccati equations (6.22) and (6.21) play an important role in the Linear Quadratic Regulator design problem for the system Σ and Σ_N. We will be interested in the convergence of the solutions of the Riccati equations (6.22) and (6.21), i.e.

$$\lim_{N \to \infty} ||E_N \Psi_N P_N - \Psi|| = 0.$$

We will introduce two theorems which are well known in the literature, that can used to prove convergence of Ψ_N to Ψ. First, we introduce the assumptions $H1$, $H2$ and $H3$, which will be used in the following theorems.

H1 - Converge of semigroup and dual semigroup:

1. For each $x \in X$, $\lim_{N \to \infty} ||T(t)x - E_N T_N(t) P_N x|| = 0$ for all $t \geq 0$.
2. For each $x \in X$, $\lim_{N \to \infty} ||T^*(t)x - E_N T_N^*(t) P_N x|| = 0$ for all $t \geq 0$.

H2 - Convergence of input and output operators:

1. For each $u \in U$, $\lim_{N \to \infty} ||Bu - E_N B_N u|| = 0$.
   For each $x \in X$, $\lim_{N \to \infty} ||B^* x - B_N^* P_N x|| = 0$.
2. For each $x \in X$, $\lim_{N \to \infty} ||Cx - C_N P_N x|| = 0$.
   For each $y \in Y$, $\lim_{N \to \infty} ||C^* y - E_N C_N^* y|| = 0$.

H3 - Uniform Stabilizability and Uniform Detectability:

1. The family of pairs (A_N, B_N) is uniformly stabilizable. That is, there exist numbers $M_1 \geq 1$ and $\omega_1 > 0$ and a sequence of operators $K_N : X_N \to U$, with $||K_N|| < \infty$ such that:
$$||e^{(A_N - B_N K_N)t} P_N x|| \leq M_1 e^{-\omega_1 t} ||x|| \quad \text{for } t \geq 0 \quad \text{and } x \in X.$$
2. The family of pairs (A_N, C_N) is uniformly detectable. That is, there exists numbers $M_2 \geq 1$ and $\omega_2 > 0$ and a sequence of operators $L_N : Y \to X_N$, with $||L_N|| < \infty$ such that:
$$||e^{(A_N - L_N C_N)t} P_N x|| \leq M_2 e^{-\omega_2 t} ||x|| \quad \text{for } t \geq 0 \quad \text{and } x \in X.$$

The following theorem is well known [Banks and Kunisch, 1984, Theorem 2.2] and can be used to analyze the convergence of the solution of Riccati equations (6.22) and (6.21).

Theorem 6.4.1 (Convergence of solutions Riccati equations.)
Suppose that the assumptions H_1 and H_2 hold and let $Q : X \to X$ be such that $Q > 0$. Let Ψ_N denote the non negative self adjoint solution of the finite dimensional Algebraic Riccati Equation (6.21). *Assume that Ψ is the non-negative self adjoint solution of the infinite dimensional Algebraic Riccati Equation* (6.22). *Let $S(t)$ and $S_N(t)$ be closed loop semigroup operators with generators $A - BQ^{-1}B^*\Psi$ and $A_N - B_N Q^{-1} B_N^* \Psi_N$ and assume there are positive constants M_S, M_Ψ and ω independent of N satisfying:*

$$||S_N(t)||_{X_N} \leq M_S e^{-\omega t} \quad \text{for all } t \geq 0, \text{ for all } N \tag{6.23}$$

$$||\Psi_N||_{X_N} \leq M_\Psi \quad \text{for all } N. \tag{6.24}$$

Then the following holds:

1. *The solutions of the Riccati equations converge in strong sense:*

$$\lim_{N\to\infty} ||E_N \Psi_N P_N x - \Psi x|| = 0 \quad \text{for every } x \in X. \tag{6.25}$$

2. *The closed loop semigroup operators $S_N(t)$ and $S(t)$ converge in strong sense:*

$$\lim_{N\to\infty} ||E_N S_N(t) P_N x - S(t)x|| \quad \text{for every } x \in X, \tag{6.26}$$

3. *The closed loop semigroup $S(t)$ is exponentially bounded:*

$$||S(t)|| \leq M_S e^{-\omega t} \quad \text{for } t \geq 0. \tag{6.27}$$

For the proof of this theorem we refer to [Banks and Kunisch, 1984].

Moreover, we have the following corollary:

Corollary 6.4.2
From strong convergence of Ψ_N to Ψ it follows that:

$$||\Psi|| \leq M_\Psi.$$

Proof. From Equation (6.25) states that $\Psi x = \lim_{N\to\infty} E_N \Psi_N P_N x$. It follows that $||\Psi|| = \lim_{N\to\infty} ||E_N \Psi_N P_N x|| \leq M_\Psi ||x||$. □

A big hurdle for the application of Theorem 6.4.1 to practical situations is the condition given by Equation (6.23), which is difficult to check in practice. The following theorem enables to replace the condition on Ψ_N given by Equation (6.23) by a slightly more practical condition.

Theorem 6.4.3 (Theorem 2.1 in [Ito, 1987])
Suppose H_1, H_2 and H_3 are satisfied and let $S_N(t) := e^{(A_N - B_N Q_N^{-1} B_N^* \Psi_N)t}$. Then for each N the Riccati equation

$$A_N^* \Psi_N + \Psi_N A_N - \Psi_N B_N Q_N^{-1} B_N^* \Psi_N + C_N^* C_N = 0$$

admits a unique non negative solution Ψ_N. *Moreover, there exists a positive constant* M_4 *such that*

$$||\Psi_N|| \leq M_4 < \infty$$

and there exists positive constants $M_3 \geq 1$, *and* $\omega_3 > 0$ *(independent of N) such that for all* $x \in X$*:*

$$||E_N S_N(t) P_N x|| \leq M_3 e^{-\omega_3 t} ||x|| \quad \text{for } t \geq 0.$$

Proof. A correction to the original proof in[Ito, 1987] is given in Appendix D.1. □

We obtain the following corollary which follows from the combination of the Theorems 6.4.3 and 6.4.1.

Corollary 6.4.4
Suppose that the pair (A, B) *is exponentially stabilizable and the pair* (A, C) *is exponentially detectable and that the conditions H1, H2, H3 hold. Let* M_3 *and* M_4 *be constants and defined as in Theorem 6.4.3. Then* $||\Psi|| \leq M_4$ *and*

1. *The solutions of the Riccati equations* (6.21) *and* (6.22) *converge in strong sense:*

$$\lim_{N\to\infty} ||E_N \Psi_N P_N x - \Psi x|| = 0 \quad \text{for every } x \in X.$$

2. *The closed loop semi groups operators* $S_N(t)$ *and* $S(t)$ *converge in strong sense:*

$$\lim_{N\to\infty} ||E_N S_N(t) P_N x - S(t) x|| \quad \text{for every } x \in X,$$

3. *The closed loop semi groups* $S(t)$ *is exponentially bounded:*

$$||S(t)|| \leq M_3 e^{-\omega t} \quad \text{for } t \geq 0.$$

We also show that the dual of $S_N(t)$ converges to the dual semigroup of $S(t)$. First we introduce a technical Theorem.

Theorem 6.4.5
Let the operator $A : D(A) \to X$ *be the generator of semigroup* $T(t)$ *and let* $W : X \to X$ *be bounded operator and let* $A + W$ *be the generator of semigroup* $S(t)$. *Let* $A_N : X_N \to X_N$ *be the generator of semigroup* $T_N(t)$ *and let* $W_N : X_N \to X_N$ *be a bounded operator. Moreover, let* $A_N + W_N$ *be the generator of semigroup* $S_N(t)$ *and assume that* $\lim_{N\to\infty} ||(E_N P_N - I)x||_= 0$ *for all* $x \in X$. *If the following holds:*

$$\lim_{N\to\infty} ||T_N(t)x - T(t)x|| = 0 \quad \text{for all } x \in X \text{ and } t \geq 0, \tag{6.28}$$

$$\lim_{N\to\infty} ||W_N x - W x|| = 0 \quad \text{for all } x \in X, \tag{6.29}$$

then the following holds:

$$\lim_{N\to\infty} ||S_N(t)x - S(t)x|| = 0.$$

Before we proceed with the proof, we will introduce an additional Lemma.

Lemma 6.4.6 (Variation of parameters equation)
Let A be the generator of semigroup $T(t)$ and let $W : X \to X$ be bounded operator. Then $A + W$ is the generator of semigroup $S(t)$ which satisfies:

$$S(t)x = T(t)x + \int_0^t T(t-\tau)WS(\tau)x\mathrm{d}\tau.$$

For the proof we refer to [Engel and Nagel, 2000, Corollary 1.7].

By use of Lemma 6.4.6 we can now proof Theorem 6.4.5.

Proof of Theorem 6.4.5. It follows from Lemma 6.4.6 that $[S_N(t) - S(t)]x$ can be represented as:

$$\begin{aligned}[S_N(t) - S(t)]x =& [T_N(t) - T(t)]x + \int_0^t [T_N(t-\tau) - T(t-\tau)]WS(\tau)x \\ &+ T_N(t-\tau)[W_N - W]S(\tau)x + T_N(t-\tau)W_N[S_N(\tau) - S(\tau)]x\mathrm{d}\tau.\end{aligned}$$

We calculate $\lim_{N\to\infty} ||S_N(t)x - S(t)x||$ and find:

$$\lim_{N\to\infty} ||S_N(t)x - S(t)x|| = \lim_{N\to\infty} \int_0^t T_N(t-\tau)B_N[S_N(\tau) - S(\tau)]x\mathrm{d}\tau.$$

Since $S_N(0) = I$ and $S(0) = I$, we have that $\lim_{N\to\infty} ||[E_N S_N(0)P_N - S(0)]x|| = 0$ and it follows that $\lim_{N\to\infty} ||[S_N(t) - S(t)]x|| = 0$ for all $t > 0$. □

The convergence of the adjoint of $S_N(t)$ to adjoint of $S(t)$ follows directly from Theorem 6.4.5.

Corollary 6.4.7
Suppose that the pair (A, B) is exponentially stabilizable and the pair (A, C) is exponentially detectable and that the conditions $H1$, $H2$, $H3$ hold. Let M_3 and M_4 be constants and defined as in Theorem 6.4.3. Let $S(t)$ and $S_N(t)$ be the semigroup operators with infinitesimal generators $A - BQ^{-1}B^*\Psi$ and $A_N - B_N Q_N^{-1}B_N^*\Psi_N$ and let $S^*(t)$ and $S_N^*(t)$ be the adjoint of $S^*(t)$ and $S_N^*(t)$ respectively. The following holds:

$$\lim_{N\to\infty} ||E_N S_N^*(t)P_N x - S^*(t)x|| \quad \textit{for every } x \in X,$$

Proof. It is well known that the semigroup operators $S^*(t)$ and $S_N^*(t)$ have the infinitesimal generators $A^* - \Psi B^* Q^{-1}B$ and $A_N^* - \Psi_n B_N^* Q_N^{-1}B_N$. We will use Theorem 6.4.5 to prove convergence, were we will set $W = -\Psi B^* Q^{-1}B$ and $W_N = -\Psi_N B_N^* Q_N^{-1}B_N$. From application of Theorem 6.4.4 it follows that $||\Psi_N|| \leq M_4$ and $||\Psi|| \leq M_4$ and therefore boundedness of W and W_N follows. From assumption $H1.2$ and by application of Theorem 6.4.5 the result follows. □

6.4.2 Approximation of optimal impulse response estimators

In this section we will use the results from Section 6.4.1 to derive sufficient conditions such that it can be shown that the assumptions (6.20a), (6.20b), (6.20c) hold and

thus can be used for Theorem 6.2.3. In essence we will reformulate the result on the convergence for Linear Quadratic estimator design by use of the duality results derived in Chapter 5. Consider the systems

$$\Sigma_p : \begin{cases} \dot{x} = Ax + Gd_1, \\ y = Cx + Sd_2, \\ z = Hx \end{cases} \qquad \Sigma_{p,N} : \begin{cases} \dot{x}_N = A_N x_N + G_N d_1, \\ y_N = C_N x_N + S d_2, \\ z_N = H_N x_N \end{cases}$$

with X and X_N Hilbert spaces and the operators defined by:

$$\begin{aligned} A &: X \to X, & A_N &: X_N \to X_N, \\ G &: D_1 \to X, & G_N &: D_1 \to X_N, \\ C &: X \to Y, & C_N &: X_N \to Y, \\ H &: X \to Z, & H_N &: X_N \to Z, \\ S &: D_2 \to Y. \end{aligned}$$

Let $T_N(t) : X_N \to X_N$ and $T(t) : X \to X$ be semigroup operators with generators A_N and A respectively. We assume that the system Σ is exponentially detectable.

Moreover, we introduce the following two Algebraic Riccati Equations, associated with the estimation problem for the systems Σ_p and $\Sigma_{p,N}$ respectively:

$$A_N\Pi_N + \Pi_N A_N^* - \Pi_N C_N^*(SS^*)^{-1}C_N\Pi_N + G_N^* G_N = 0, \tag{6.30}$$

$$\langle A\Pi x_1, x_2\rangle + \langle \Pi A^* x_1, x_2\rangle - \langle \Pi C^*(SS^*)^{-1}C\Pi x_1, x_2\rangle + \langle G^* G x_1, x_2\rangle = 0, \tag{6.31}$$

for $x_1, x_2 \in D(A^*)$.

We will be interested in the convergence of the solutions of the Riccati equations (6.31) and (6.30), i.e. $\lim_{N\to\infty} ||E_N\Pi_N P_N x - \Pi x||$ for all $x \in X$. We will introduce a theorem that can be used to prove convergence. First,we introduce the following assumptions:

E1 - Converge of semigroup and dual semigroup:

1. For each $x \in X$, $\lim_{N\to\infty} ||T(t)x - E_N T_N(t) P_N x|| = 0$ for all $t \geq 0$.
2. For each $x \in X$, $\lim_{N\to\infty} ||T^*(t)x - E_N T_N^*(t) P_N x|| = 0$ for all $t \geq 0$.

E2 - Convergence of input and output operators:

1. For each $d \in D_1$, $\lim_{N\to\infty} ||Gd_1 - E_N G_N d_1|| = 0$.
   For each $x \in X$, $\lim_{N\to\infty} ||G^* x - G_N^* P_N x|| = 0$.
2. For each $x \in X$, $\lim_{N\to\infty} ||Cx - C_N P_N x|| = 0$.
   For each $y \in Y$, $\lim_{N\to\infty} ||C^* y - E_N C_N^* y|| = 0$.
3. For each $x \in X$, $\lim_{N\to\infty} ||Hx - H_N P_N x|| = 0$.
   For each $z \in Z$, $\lim_{N\to\infty} ||H^* z - E_N H_N^* z|| = 0$.

E3 - Uniform Stabilizability and Uniform Detectability:

1. The family of pairs (A_N, G_N) is uniformly stabilizable. That is, there exist numbers $M_1 \geq 1$ and $\omega_1 > 0$ and a sequence of operators $K_N : X_N \to D_1$, with $||K_N|| < \infty$ such that:

$$||e^{(A_N - G_N K_N)t} P_N x|| \leq M_1 e^{-\omega_1 t}||x|| \quad \text{for } t \geq 0 \quad \text{and } x \in X.$$

2. The family of pairs (A_N, C_N) is uniformly detectable. That is, there exists numbers $M_2 \geq 1$ and $\omega_2 > 0$ and a sequence of operators $L_N : Y \to X_N$, with $||L_N|| < \infty$ such that:

$$||e^{(A_N - L_N C_N)t} P_N x|| \leq M_2 e^{-\omega_2 t} ||x|| \quad \text{for } t \geq 0 \quad \text{and } x \in X.$$

The following theorem is analogous to Theorem 6.4.1, but now for the Riccati equations (6.30) and (6.31).

Theorem 6.4.8 (Convergence of solutions of estimator Riccati equations)
Suppose that the assumptions E1 and E2 hold. Let Π_N denote the non-negative self-adjoint solution of the finite dimensional Algebraic Riccati Equation (6.30). *Assume that Π is the non-negative selfadjoint solution of the infinite dimensional Algebraic Riccati Equation* (6.31). *Let $S(t)$ and $S_N(t)$ be closed loop semigroup operators with generators $A - \Pi C^*(SS^*)^{-1}C$ and $A_N - \Pi_N C_N^*(SS^*)^{-1}C_N$ and assume there are positive constants M_T, M_Π independent of N and ω independent of N satisfying:*

$$||S_N(t)||_{X_N} \leq M_T e^{-\omega t} \quad \textit{for all} t \geq 0, \tag{6.32}$$

$$\tag{6.33}$$

$$||\Pi_N||_{X_N} \leq M_\Pi \quad \textit{for all } N. \tag{6.34}$$

Then the following holds:

1. *The solutions of the Riccati equations converge in strong sense:*

$$\lim_{N\to\infty} ||E_N \Pi_N P_N x - \Pi x|| = 0 \quad \textit{for every } x \in X.$$

2. *The closed loop semigroup operators $S_N(t)$ and $S(t)$ converge in strong sense:*

$$\lim_{N\to\infty} ||E_N S_N(t) P_N x - S(t)x|| \quad \textit{for every } x \in X,$$

3. *The closed loop semigroup $S(t)$ is exponentially bounded:*

$$||S(t)|| \leq M_T e^{-\omega t} \quad \textit{for } t \geq 0.$$

Proof. By use of the duality results derived in Chapter 5, it follows that the optimal linear time invariant optimal estimator design problem based on the impulse response of the error system, for the plant Σ_p (c.q. Σ_p^N) is related to the Linear Quadratic controller design problem. We introduce the systems $\tilde{\Sigma}_p$ and $\tilde{\Sigma}_{p,N}$:

$$\tilde{\Sigma}_p : \begin{cases} \dot{\xi} = A^*\xi + C^*\tilde{y}, \\ \tilde{d}_1 = G^*\tilde{\xi}, \\ \tilde{d}_2 = S^*\tilde{y}, \end{cases} \qquad \tilde{\Sigma}_{p,N} : \begin{cases} \dot{\xi}_N = A_N^*\xi_N + C_N^*\tilde{y}, \\ \tilde{d}_1 = G_N^*\tilde{\xi}, \\ \tilde{d}_2 = S^*\tilde{y}, \end{cases}$$

with initial conditions $\xi(0) = \xi_0$ and $\xi_N(0) = \xi_{N,0}$. It follows that the Riccati equations (6.30) and (6.31) correspond to the Riccati equations involved in the Linear Quadratic Regulator design problem for the systems $\tilde{\Sigma}_p$ and $\tilde{\Sigma}_{p,N}$. We will show that the assumptions $E1$, $E2$ on the systems Σ_p and $\Sigma_{p,N}$ imply that the conditions $H1$, $H2$ and $H3$ for the systems $\tilde{\Sigma}_p$ and $\tilde{\Sigma}_{p,N}$ hold.

Assumption $E1$ implies that assumption $H1$ holds, since $E1.1 = H1.2$ and $E1.2 = H1.1$. By comparison of $\tilde{\Sigma}_p$ with Σ it follows that and assumption $E2$ implies that assumption $H2$ holds. Moreover, from $||S_N^*(t)|| = ||S_N^*(t)||$ it follows that:

$$||S_N^*(t)||_{X_N} \leq M_T e^{-\omega t} \quad \text{for all} t \geq 0.$$

Now, we can analyse the convergence of the solution of Equations (6.30) and (6.31) in the context of the LQR problem for the plants $\tilde{\Sigma}_{p,N}$ and $\tilde{\Sigma}_p$. Since the assumption that $H1$, $H2$ hold and the assumptions (6.24) and (6.23), strong convergence of Π_N to Π follows by direct application of Theorem 6.4.1. That is, it follows that:

$$\lim_{N\to\infty} ||E_N \Pi_N P_N x - \Pi x|| = 0.$$

Moreover it follows as a result of Theorem 6.4.1 that the semigroup operators $S^*(t)$ with infinitesimal generator $A^* - C(S^*S)^{-1}C^*\Pi$ is exponentially bounded, i.e.:

$$||S^*(t)|| \leq M_T e^{-\omega t} \quad \text{for } t \geq 0.$$

Since $||S(t)|| = ||S^*(t)||$, we have that $||S(t)|| \leq M_T e^{-\omega t}$ for $t \geq 0$. By application of Theorem 6.4.5 in combination with assumption $H1$ and $H2$ and the fact that Π_N and Π are bounded operators it follows that the semigroup $S_N(t)$ converges strongly the semigroup $S(t)$, i.e:

$$\lim_{N\to\infty} ||E_N S_N(t) P_N x - S(t)x|| \quad \text{for every } x \in X,$$

□

Analogously as for the approximation of the solution of Riccati equations in the LQR-problem, the assumption $E3$ can be used to replace the conditions (6.33) and (6.34). That is, equivalent to Theorem 6.4.3, we have:

Theorem 6.4.9
Suppose E_1, E_2 and E_3 are satisfied and let $S_N(t) := e^{(A_N - \Pi_N C_N^*(SS^*)^{-1}C_N)t}$. Then for each N the Riccati equation

$$A_N\Pi_N + \Pi_N A_N^* - \Pi_N C_N^*(SS^*)^{-1}C_N\Pi_N + G_N^*G_N = 0, \tag{6.35}$$

admits a unique non negative solution Π_N. Moreover, there exists a positive constant M_6 such that

$$||\Pi_N|| \leq M_6 < \infty$$

and there exists positive constants $M_5 \geq 1$, and $\omega_4 > 0$ (independent of N) such that for all $x \in X$:

$$||E_N S_N(t) P_N x|| \leq M_5 e^{-\omega_4 t}||x|| \quad \text{for } t \geq 0.$$

Proof. We interpret Theorem 6.4.3 in the context of the systems $\tilde{\Sigma}_p$ and $\tilde{\Sigma}_{p,N}$. In Theorem 6.4.8 is has been shown that $E1$ implies $H1$ and that $E2$ implies $H2$. From

assumption $E3.1$ it follows that the pair A_N^*, G_N^* is uniformly exponentially detectable as follows. $E3.1$ assumes that there is a sequence K_N with $||K_N|| < \infty$ such that:

$$||e^{(A_N - G_N K_N)t} P_N x|| \leq M_1 e^{-\omega_1 t} ||x|| \quad \text{for } t \geq 0 \quad \text{and } x \in X.$$

Therefore it follows that:

$$||e^{(A_N^* - K_N^* G_N^*)t} P_N x|| \leq M_1 e^{-\omega_1 t} ||x|| \quad \text{for } t \geq 0 \quad \text{and } x \in X,$$

such that the sequence K_N^* shows that A_N^*, G_N^* is uniformly exponentially detectable. From assumption $E3.2$ it follows that family of pairs (A_N^*, C_N^*) is uniformly exponentially stabilizable as follows. $E3.2$ assumes that there is a sequence L_N with $||L_N|| < \infty$ such that:

$$||e^{(A_N - L_N C_N)t} P_N x|| \leq M_2 e^{-\omega_2 t} ||x|| \quad \text{for } t \geq 0 \quad \text{and } x \in X.$$

Therefore it follows that:

$$||e^{(A_N^* - C_N^* L_N^*)t} P_N x|| \leq M_2 e^{-\omega_2 t} ||x|| \quad \text{for } t \geq 0 \quad \text{and } x \in X.$$

such that the sequence L_N^* shows that A_N^*, C_N^* is uniformly exponentially stabilizable. Therefore, from assumption $E3$ uniform exponential detectability and uniform exponentially stabilizability for the system $\tilde{\Sigma}_{p,N}$ follows, i.e. assumption $H3$ for the system $\tilde{\Sigma}_{p,N}$ holds. Therefore, the proof follows from application of Theorem 6.4.3 on the systems $\tilde{\Sigma}_p$ and $\tilde{\Sigma}_{p,N}$. □

Finally, by combination of Theorem (6.4.8) and Theorem (6.4.9), convergence of the solution of the Riccati equations (6.30) and (6.31) follows from the assumptions $E1$, $E2$ and $E3$. This is reflected by the following corollary.

Corollary 6.4.10
Suppose that the pair (A, G) is exponentially stabilizable and the pair (A, C) is exponentially detectable and that the conditions $E1$, $E2$, $E3$ hold. Let M_5 and M_6 be constants and defined as in Theorem 6.4.9. Let $S_N(t) := e^{(A_N - \Pi_N C_N^* (SS^*)^{-1} C_N)t}$ and let $S(t)$ be the semigroup operator with infinitesimal generator $A - \Pi C^* (SS^*)^{-1} C$. Then $||\Psi|| \leq M_6$ and

1. *The solutions of the Riccati equations* (6.30) *and* (6.31) *converge in strong sense:*

$$\lim_{N \to \infty} ||E_N \Pi_N P_N x - \Pi x|| = 0 \quad \textit{for every } x \in X.$$

2. *The closed loop semi groups operators $S_N(t)$ and $S(t)$ converge in strong sense:*

$$\lim_{N \to \infty} ||E_N S_N(t) P_N x - S(t) x|| \quad \textit{for every } x \in X,$$

3. *The closed loop semi groups $S(t)$ is exponentially bounded:*

$$||S(t)|| \leq M_5 e^{-\omega t} \quad \textit{for } t \geq 0.$$

In this section it has been shown that the convergence approximation of the Riccati equation involved in the optimal impulse response norm estimator design can be analyzed on the basis of the result which are known for the convergence approximation of the Riccati equation in linear quadratic regulator design. We have reformulated the results in Theorem 6.4.9 and Theorem 6.4.8, such that the results can be used in the context of optimal optimal impulse response estimator design problems. In the next section we will introduce to examples of estimation problems and we will analyze the convergence of the optimal estimators.

6.5 Examples on estimator design

In this section we will show the implementation of estimators for two systems via scenario $S1$. We study a system with diffusion on the interval $\mathbb{L} = [0, 1]$ and a system with convection on $\mathbb{L} = [0, 1]$, denoted by Σ_d and Σ_c respectively. For both systems a finite dimensional approximation will be obtained by Galerkin projection.

For both systems we have $X = L_2(\mathbb{L})$ and we will assume that $D_1 = \mathbb{R}^2$ and $Y = \mathbb{R}^3$. That is, we have two disturbance sources and three measurements. For both cases, we will use the following disturbance operator $G : D_1 \to X$ and measurement operators $C : X \to Y$, $H : X \to Z$:

$$\begin{aligned} Gd_1 &= \sum_{i=1}^{2} g_i \langle e_i, d_1 \rangle, \\ Cx &= \sum_{j=1}^{3} \langle c_j, x \rangle e_j, \\ Hx &= x, \end{aligned}$$

with $g_i \in X$, $c_j \in X$ and $\{e_i\}_{i=1,n}$ the canonical basis in $\mathbb{R}^n$.

We choose disturbance sources and sensors which are centered around the points $\ell_{g,i} \in \mathbb{L}$ and $\ell_{c,j} \in \mathbb{L}$ respectively and that can be represented by:

$$g_i(\ell) = w(\ell - \ell_{g,i}), \quad i = 1, 2 \tag{6.36}$$

$$c_j(\ell) = w(\ell - \ell_{c,j}), \quad j = 1, 2, 3 \tag{6.37}$$

where we use the weight function:

$$w(\ell) = \frac{1}{\sqrt{2\pi\sigma_w^2}} e^{-\frac{\ell}{\sigma_w^2}}.$$

We will make the choice $\Sigma_w = 1 \cdot 10^{-2}$, $\{\ell_{g,1}, \ell_{g,2}\} = \{0.15, 0.5\}$ and $\{\ell_{c,1}, \ell_{c,2}, \ell_{c,3}\} = \{0.25, 0.65, 0.8\}$, which results in a sensors and disturbance source configuration as shown in Figure 6.3.

We will assume that the noise in the three measurements is uncorrelated, such that $S = \text{diag}(\sigma_{d_{2,1}}, \sigma_{d_{2,2}}, \sigma_{d_{2,3}})$. We will use the same approximation method for both examples

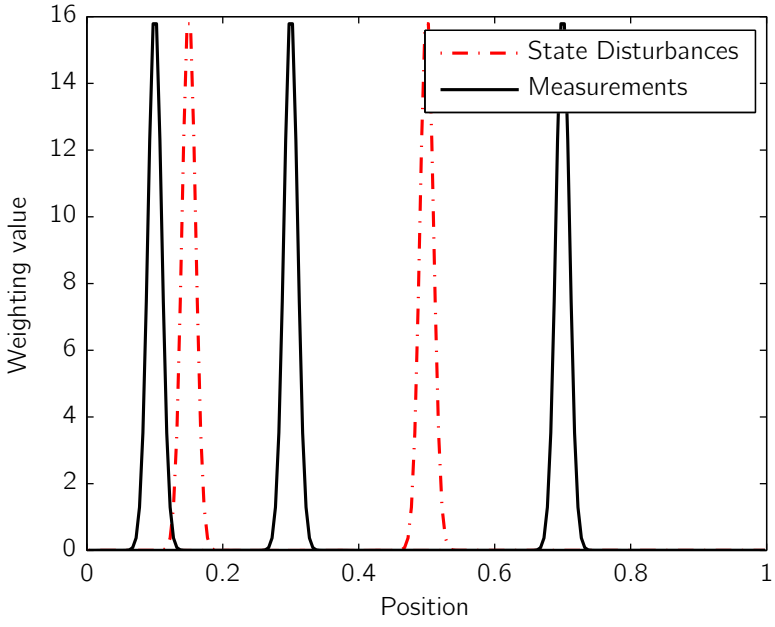

Figure 6.3: Position of sensors and disturbance sources

systems. We will introduce the approximation space Z_N and X_N together with the operators E_N and P_N as described in Section 6.2.1.

We will assume that a basis for Z is given by $\{\phi_i\}_1^\infty$. Moreover, we define the subspace Z_N by $Z_N := \text{span}\{\phi_i\}_{i=1}^N$ and define the Euclidean space $X_N = \mathbb{R}^N$ and use $\{e_i\}_{i=1}^N$ to denote the canonical basis for $\mathbb{R}^N$. Note that both Z_N and X_N have dimension N. In this section we define the operator $E_N : X_N \to Z$ and $P_N : Z \to X_N$ as in Example (6.2.1) with:

$$E_N x_N = \sum_{i=1}^N \langle x_N, e_i \rangle \phi_i \qquad P_N x = \sum_{i=1}^N \langle x, \phi_i \rangle e_i \tag{6.38}$$

In example 6.2.1 it has been shown that E_N and P_N satisfy the conditions $A1$, $A2$ and $A3$ of the approximation framework, and that E_N and P_N satisfy $E_N = P_N^*$.

6.5.1 Approximation of an estimator for a heat diffusion system

In this example, we consider the system Σ_d, which is a system with diffusion. An example of such a system is given in Example 5.1.2. For the system Σ_d, we will discuss the design

and approximation of an estimator via the scenario $S1$. The system Σ_d is given by:

$$\Sigma_d : \begin{cases} \frac{\partial x}{\partial t} = Ax + Gd_1 \\ y = Cx + Sd_2 \\ z = Hx \end{cases} \tag{6.39}$$

with $x \in L_2(\mathbb{L}, \mathbb{R})$, $\ell \in \mathbb{L} = [0, 1]$, boundary conditions $\frac{\partial x}{\partial \ell}(0, t) = 0$, $\frac{\partial x}{\partial \ell}(1, t) = 0$, initial condition $x(\ell, 0) = x_0(\ell)$ and with

$$Ax = \frac{\partial^2 x}{\partial \ell^2} - \gamma x$$

with $\gamma > 0$ and $D(A) = \{x \in L_2(0, 1) | \frac{\partial x}{\partial \ell}$ absolutely continuous, $\frac{\partial^2 x}{\partial \ell^2} \in L_2(0, 1)$.

Following scenario $S1$ we will first obtain an finite dimensional approximation Σ_d^N for the system Σ_d and subsequently calculate a finite dimensional optimal impulse response norm estimator for Σ_d^N. By the method of Galerkin projection, described in Section 6.2.2, the system has been approximated. The approximation of the system Σ_d is given by:

$$\Sigma_d^N : \begin{cases} \dot{x}_N = A_N x_N + G_N d_1 \\ y_N = C_N x_N + S d_2 \\ z_N = H_N x_N \end{cases},$$

with: $A_N = P_N A E_N$, $G_N = P_N G$, $C_N = C E_N$, $H_N = H E_N$. In this example we will use $\phi_1(\ell) = 1$ and $\phi_i(\ell) = \sqrt{2}\cos(2\pi i \ell)$ for $i \geq 2$.

Let $\Sigma_{d,e}$ and $\Sigma_{d,e}^N$ denote the optimal impulse response estimators for the systems Σ_d and Σ_d^N. We will show that for this approximation scheme the estimator $\Sigma_{d,e}^N$ will converge to $\Sigma_{d,e}$.

Proposition 6.5.1

Consider the approximation scheme presented in this example. In this setting, the estimators $\Sigma_{d,e}^N$ converges to $\Sigma_{d,e}$ in the impulse response norm, i.e.:

$$\lim_{N \to \infty} ||\Sigma_{d,e} - \Sigma_{d,e}^N||_{imp} = 0.$$

Before we give the proof of this proposition, we introduce a Lemma.

Lemma 6.5.2

Let the operator A be as defined. The operator A satisfies:

$$Re(\langle Ax, x \rangle) \leq -\gamma ||x||^2 \text{ for } x \in D(A),$$
$$Re(\langle A^* x, x \rangle) \leq -\gamma ||x||^2 \text{ for } x \in D(A^*).$$

Proof. We calculate for ϕ_1 and ϕ_i, $i > 1$:

$$Re(\langle A\phi_1, \phi_1 \rangle) = Re(\langle \frac{\partial^2 \phi_1}{\partial x^2} - \gamma \phi_1, \phi_1 \rangle) \leq -\gamma ||\phi_1||^2 \tag{6.40}$$

$$Re(\langle A\phi_i, \phi_i \rangle) = Re(\langle \frac{\partial^2 \phi_i}{\partial x^2} - \gamma \phi_i, \phi_i \rangle) = -(k^2\pi^2 + \gamma) Re(\langle \phi_i, \phi_i \rangle) \leq -\gamma ||\phi_i||^2. \tag{6.41}$$

Therefore it follows that $Re(\langle Ax, x\rangle) \leq -\gamma||x||^2$ for $x \in D(A)$. Since the operator A is self adjoint, $Re(\langle A^*x, x\rangle) \leq -\gamma||x||^2$ immediately follows from $Re(\langle Ax, x\rangle) \leq -\gamma||x||^2$. □

Proof of Proposition 6.5.1. We will show that the combination of the system and the approximation scheme satisfies the conditions $E1, E2$ and $E3$ used in Corollary 6.4.10. Therefore, it will follow by, Corollary 6.4.10, that optimal impulse response estimators $\Sigma_{d,e}^N$ for the system Σ_d^N will arbitrarily close approximate the optimal estimator $\Sigma_{d,e}$ for the system Σ_d if the order N increases. We validate the assumptions as follows:

Validation E1: By Lemma 6.5.2 it follows that the operators A and A^* satisfy the condition stated in Theorem 6.3.6. Therefore the semigroups $T_N(t)$ converge to $T(t)$ and the semigroups $T_N^*(t)$ converge to $T^*(t)$.

Validation E2: Since it is assumed that the operators G, C and H are compact the assumption holds.

Validation E3: By Lemma 6.5.2 it follows that the operators A and A^* satisfy the condition stated in Theorem 6.3.6, therefore the semi groups $T_N(t)$ and $T^*N(t)$ are uniformly exponentially stable. Uniform exponential stabilizability and exponential detectability both follow from uniform exponential stability of the system.

By Corollary 6.4.10 we conclude that the solutions of the Riccati equations involved in the optimal impulse response norm estimator design for the systems Σ_d and Σ_d^N converge, i.e. we have that:

$$\lim_{N\to\infty} ||E_N\Pi_N P_N x - \Pi x|| = 0.$$

From Theorem 6.2.3 the convergence of the estimators follows. □

An simulation with the plant Σ_d^N and estimator $\Sigma_{d,e}^N$ has been implemented in Matlab 2011*b*. In the simulation we have set $\gamma = 1 \cdot 10^{-5}$ and $\sigma_w = 1 \cdot 10^{-2}$. In order to get an impression of the convergence of Π_N, the distance between Π_N and Π_{150} has been calculated. The distance has been measured in the spectral norm for $N = \{1, .., 149\}$. A graph of the distance is shown in Figure 6.4. The figure shows an exponential decrease of the distance. Note that the decrease of the distance is not monotone, which also might not be expected by the theoretical results.

In order to investigate the performance of the estimator we interconnect the estimator $\Sigma_{d,e}^N$ with the plant Σ_d^N. The disturbance signals $d_1(t)$ and $d_2(t)$ have been generated by a zero mean normally distributed white noise generator with variances $\sigma_{d_1}^2 = 1$ and $\sigma_{d_2}^2 = 1$. In the simulation a 50-th order approximation has been used. Figure 6.5a shows the state x_N of the system Σ_d. Measurement by the sensors y_1, y_2 and y_3 are shown in Figure 6.5d. The state of the estimator is shown in Figure 6.5b, the difference between the state of the plant and state of the estimator, i.e. the estimation error, is shown in Figure 6.5c. The figure shows that the estimation error is largest at the position of the error source and decays in the direction of the sensors. Moreover, the error around disturbance source $d_{1,2}(t)$ is larger than the error around disturbance source $d_{1,1}(t)$, which can be explained since the distance between disturbance source $d_{1,2}(t)$ and the sensors is larger than the distance between the sensors and disturbance sources $d_{1,1}(t)$.

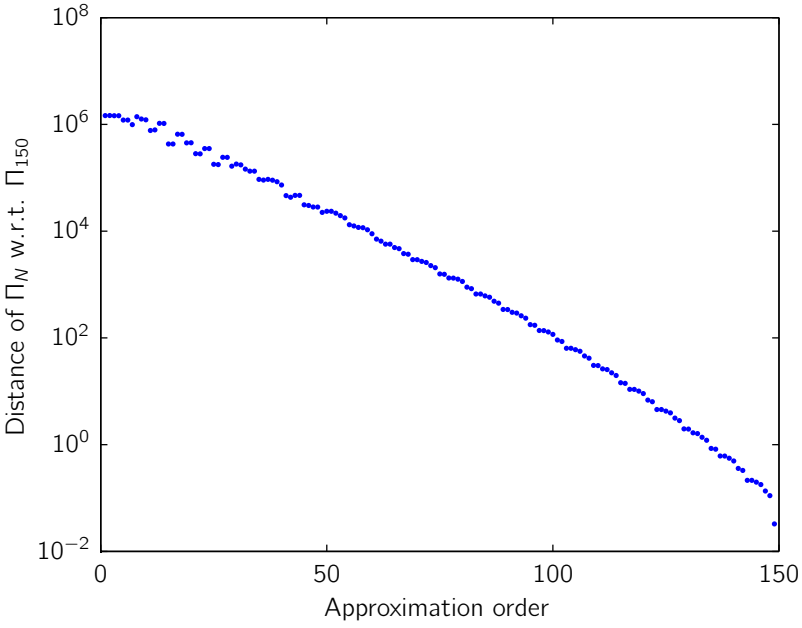

Figure 6.4: Distance between Π_N and Π_{150} for plant Σ_d, measured in $||\Pi_N - \Pi_{150}||_2$.

6.5.2 Approximation of an estimator for a system with convection

In this example we will discuss the design and approximation of an estimator for a system that models convection in a one dimensional fluid flow. We will follow Scenario 1 the design and implementation of an estimator via the scenario $S1$. The example shows large similarities with the previous example. The system Σ_c is given by

$$\Sigma_c : \begin{cases} \frac{\partial x}{\partial t} = Ax + Gd_1 \\ y = Cx + Sd_2 \\ z = Hx \end{cases} \tag{6.42}$$

with $x \in L_2$, $\ell \in \mathbb{L} = [0, 1]$, $Ax = -\frac{\partial x}{\partial \ell}$, initial condition $x(\ell, 0) \in X$, boundary condition $x(0, t) = 0$ and:

$$Ax = -\frac{\partial x}{\partial \xi} - \gamma x, \quad \text{with } \gamma > 0$$

and:

$$D(A) = \{x \in L_2(0,1) |\ Ax \in L_2(0,1),\ x(0) = 0,\ \text{and } x \text{ is absolutely continuous}\}.$$

Following scenario $S1$ we will first obtain an finite dimensional approximation Σ_c^N for the system Σ_c and subsequently calculate a finite dimensional optimal impulse response

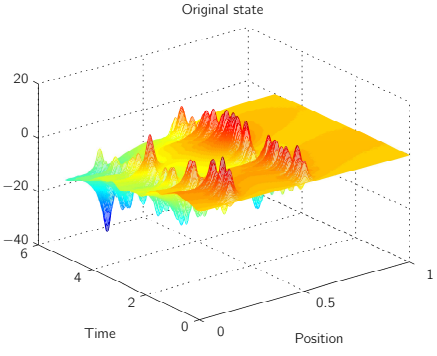

(a) Real Temperature on slab

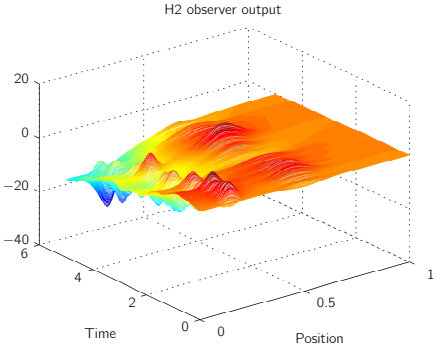

(b) Estimated

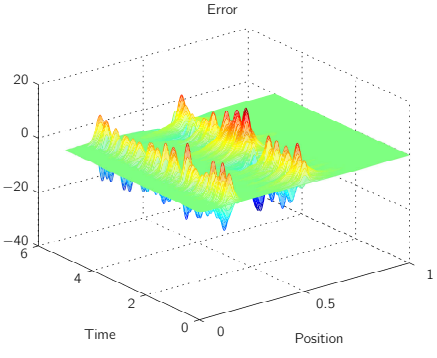

(c) Estimation Error

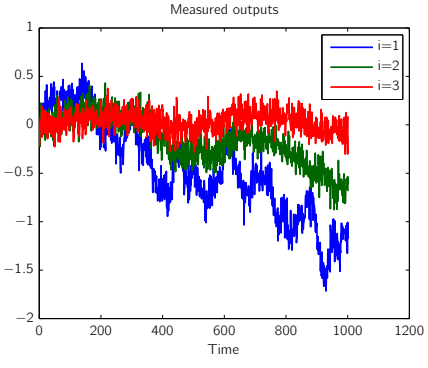

(d) Measured temperature by sensors c_1, c_2 and c_3.

Figure 6.5: Simulation results of plant Σ_d^{50} interconnected with estimator $\Sigma_{d,e}^{50}$.

estimator $\Sigma_{c,e}^N$ for Σ_c^N. By the method of Galerkin projection, described in 6.2.2 we obtain Σ_c^N:

$$\Sigma_c^N : \begin{cases} \dot{x}_N = A_N x_N + G_N d_1 \\ y_N = C_N x_N + S d_2 \\ z_N = H_N x_N \end{cases},$$

with: $A_N = P_N A E_N$, $G_N = P_N G$, $C_N = C E_N$, $H_N = H E_N$. In this example we will use $\phi_1(\ell) = 1$ and $\phi_i(\ell) = \sqrt{2}\cos(\pi(i-1)\ell)$ for $i \geq 2$, which is a basis for $L_2(0,1)$, as shown in for instance [Curtain and Zwart, 1995, Example A.2.33].

Let $\Sigma_{c,e}$ and $\Sigma_{c,e}^N$ denote the optimal impulse response estimators for the systems Σ_c and Σ_c^N. We will show that for this approximation scheme the estimator $\Sigma_{c,e}^N$ will converge to $\Sigma_{c,e}$.

Proposition 6.5.3
Consider the approximation scheme presented in this example. In this setting, the estimators $\Sigma_{c,e}^N$ converges to $\Sigma_{c,e}$ in the impulse response norm, i.e.:

$$\lim_{N\to\infty} ||\Sigma_{c,e} - \Sigma_{c,e}^N||_{imp} = 0.$$

Before we give the proof of this proposition, we introduce a Lemma.

Lemma 6.5.4
Let the operator A be as defined. The operator A satisfies:

$$Re(\langle Ax, x\rangle) \leq -\gamma||x||^2 \; for x \in D(A)$$
$$Re(\langle A^*x, x\rangle) \leq -\gamma||x||^2 \; for x \in D(A^*)$$

Proof. From [Curtain and Zwart, 1995, example 2.2.4] is follows that the operator A^*, the adjoint operator of A is given by $A^*x = \frac{\partial x}{\partial \ell} - \gamma x$ and that the domain of A^* is given by:

$$D(A^*) = \{x \in L_2(0,1) |\; A^*x \in L_2(0,1),\; x(1) = 0, \text{ and } x \text{ is absolutely continuous}\}.$$

By calculation it follows that:

$$Re(\langle Ax, x\rangle) = Re(\int_0^1 -\frac{\partial x}{\partial \ell}(\ell,t)x(\ell,t)\mathrm{d}\ell - \gamma||x||^2) \tag{6.43}$$
$$= Re(-[x^2(\ell,t)]_0^1 - \int_0^1 -x\frac{\partial x}{\partial \ell}\mathrm{d}\ell) - \gamma||x||^2 \leq -\gamma||x||^2, \tag{6.44}$$

and therefore we conclude that A is dissipative. Similarly, the operator A^* is dissipative, since it follows by calculation of $Re(\langle A^*x, x\rangle)$ that :

$$Re(\langle A^*x, x\rangle) = -\tfrac{1}{2}[x^2(0)] - \gamma||x||^2 \leq -\gamma||x||^2.$$

□

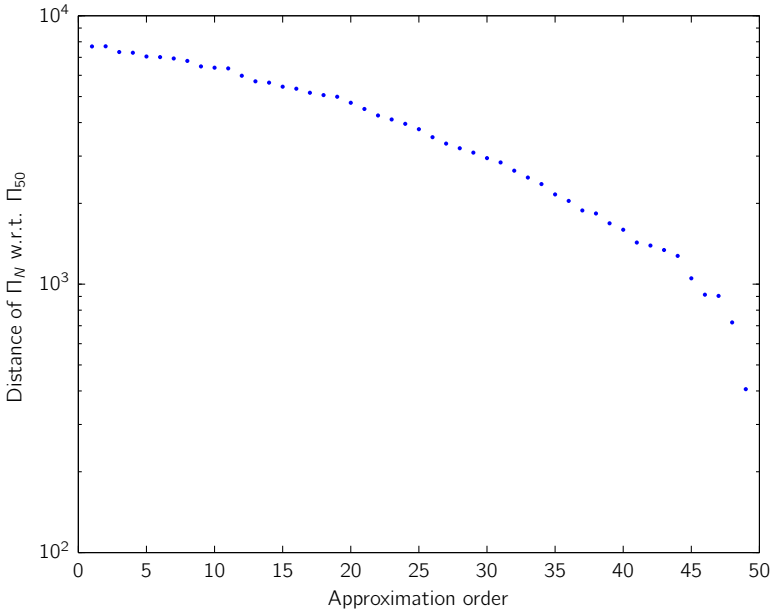

Figure 6.6: Distance between Π_N and Π_{50} for Σ_c, measured in $||\Pi_N - \Pi_{50}||_2$.

Proof of Proposition 6.5.3 . The proof is almost identical to the proof of Proposition 6.5.1. Validation of the conditions $E1$, $E2$ and $E3$ used in Corollary 6.4.10 follows in exactly the same way as in Proposition 6.5.1, where we now use Lemma 6.5.4 in stead of Lemma 6.5.2. By Corollary 6.4.10 we conclude that the solutions of the Riccati equations involved in the optimal impulse response norm estimator design for the systems Σ_c and Σ_c^N converge, i.e. we have that:

$$\lim_{N\to\infty} ||E_N \Pi_N P_N x - \Pi x|| = 0.$$

Moreover, it follows that the semigroup operators $S_N(t)$ and $S(t)$ with infinitesimal generators $A_N \Pi_N C_N^* (SS^*)^1 C_N$ and $A\Pi C^* (SS^*)^1 C$ converge. From Theorem 6.2.3 the convergence of the estimators follows. □

A simulation with the plant Σ_c^N and estimator $\Sigma_{c,e}^N$ has been implemented in Matlab. In the simulation we have set $\gamma = 1 \cdot 10^{-5}$ and $\sigma_w = 1 \cdot 10^{-2}$. In order to get an impression of the convergence of Π_N, the distance between Π_N and Π_{50} has been calculated. The distance has been measured in the spectral norm for $N = \{1, .., 50\}$. A graph of the distance is shown in Figure 6.6. The figure show a slower decrease for the convergence of Π than in the case of the diffusion example. The reason for this is not known, but it is expected to be related to the difference between the system properties of both systems. Note that the decrease of the distance is not monotone, which, indeed, cannot be expected from the theoretical results.

In order to investigate the performance of the estimator we interconnect the estimator

$\Sigma_{c,e}^N$ with the plant Σ_c^N. The disturbance signals $d_1(t)$ and $d_2(t)$ have been generated by a zero mean normally distributed white noise generator with standard deviation $(\sigma_{d_{1,1}}, \sigma_{d_{1,2}}) = (0.1, 0.1)$ and $(\sigma_{d_{2,1}}, \sigma_{d_{2,2}}, \sigma_{d_{2,3}}) = (0.1, 1.0, 0.1)$. Note that measurement 2 contains more noise than measurements 1 and 3. In the simulation a 50-th order approximation of the system Σ_c has been used. Figure 6.7a shows the state x_N of the system Σ_c^N. In this figure the transport mechanism can be clearly observed from the straight lines in the figure along which the wave is transported. Measurements by the sensors y_1, y_2 and y_3 are shown in Figure 6.7d. The state of the estimator $\Sigma_{c,e}^N$is shown in Figure 6.7b, the difference between the state of the plant and state of the estimator, i.e. the estimation error, is shown in Figure 6.7c. The figure shows that the estimation error is large in the area at the left hand side between disturbance sources and the sensors. This is expected behavior, since it might be expected that a sensor cannot infer information about the state before the wave is transported to the sensor. Moreover, the error around sensor y_2 is larger than around the other sensors. This is also expected behavior since $\sigma_{d_{2,2}}$ is much larger than $\sigma_{d_{2,1}}$ and $\sigma_{d_{2,3}}$.

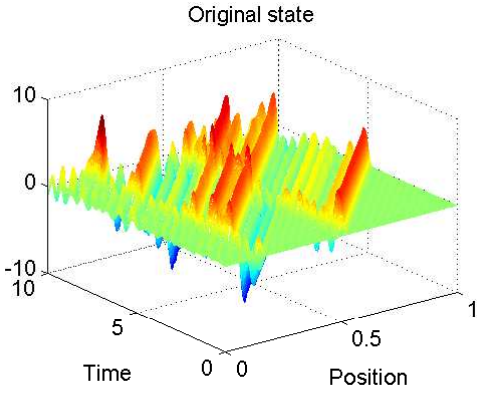

(a) Real state of the system

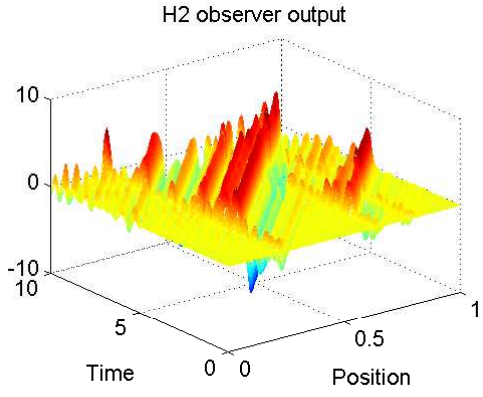

(b) Estimated state of the system

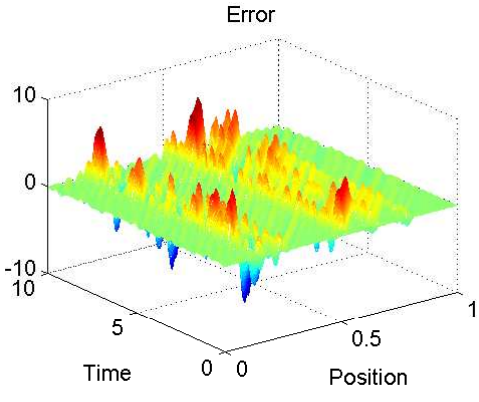

(c) Estimation Error

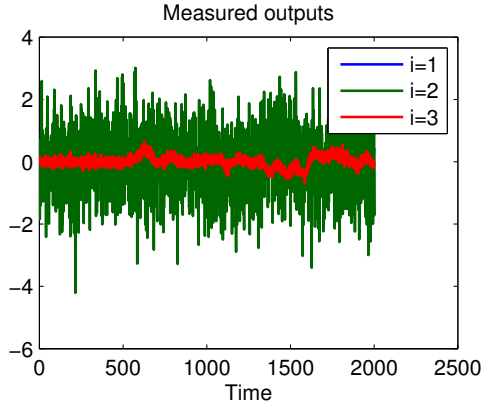

(d) Measured value by sensors c_1, c_2 and c_3.

Figure 6.7: Simulation results of plant Σ_c^{50} interconnected with estimator $\Sigma_{c,e}^{50}$.

6.6 Conclusions and Recommendations

In this chapter we have studied methods for the approximation and implementation of optimal estimators for infinite dimensional systems. The analysis is necessary, since the optimal estimators developed in Chapter 5 cannot be implemented directly.

6.6.1 Conclusions

We have proposed three different scenarios to analyze the performance and convergence of approximations of the optimal estimators for a system with a finite number of disturbances and measurements. With use of the framework of Ito and Kappel for system approximation we have shown that under very specific conditions the finite dimensional approximate estimators converge to the optimal estimator measured in strong sense measured in the impulse response norm. Convergence of the approximation of the estimators to the optimal estimator measured in the L_2-norm has not been studied. We have shown two examples in which we approximate optimal estimators for a system that models $1D$ diffusion and for a system that models $1D$ convection. We prove the convergence of the approximations to the optimal estimators in the impulse response norm. Simulation examples show that the approximate estimators can be implemented in a software environment.

6.6.2 Recommendations

In this chapter it has been shown that under very specific conditions finite dimensional estimators converge to the optimal estimators for systems with a finite number of disturbances and measurements measured in the impulse response norm. The simulation examples show that with the specific choice of system and approximation method, the convergence of the solution of the Algebraic Riccati equation is not uniform in the approximation order. It would be interesting to study the existence of schemes that guarantee uniform convergence and to study the rate of convergence. The convergence of approximations in the L_2 norm has not been studied. Also, the convergence of approximations of estimators to the optimal estimators for systems with infinite dimensional input and output operators has not been studied and might be of interest for future research.

The conditions that we stated in Section 6.2.3 to show convergence are very stringent and technical. This certainly limits the scope of the results an causes the results to be difficult to apply or verify in engineering applications. In order to be of value to engineers working with dynamical systems in applications, it is import that users of the theory do not have to be an expert, but can rely on general, easy verifiable conditions. One of the problems with the approximation methods is that the conditions to be verified depend on the combination of the approximation scheme as well as the system under consideration and on how both of these conditions interact. Therefore, it is important to classify the systems for which conditions are easy verifiable and to develop approximation methods and schemes for which convergence properties are guaranteed. Moreover, it is important

to study how the approximation schemes, especially the operators P_N and E_N, should be constructed and what the influence on the convergence properties is.

In this chapter we have only studied the approximation of estimators which are linear time invariant. It would also be interesting to study the approximation of time variant estimators, for instance for implementation of the estimators that have been obtained in Chapter 5 for the finite time horizon estimator design problems.

CHAPTER 7

Estimator design and implementation for crystallization

Abstract

In this chapter an estimator for batch cooling crystallization processes will be developed and implemented. The results on estimator design as obtained in the Chapter 5 and Chapter 6 will be used and will be applied to a model which is representative for a batch cooling crystallization process that could be encountered in a practical application. Special attention will be paid to the linearization of the process model and the implementation of the estimator in the simulation environment Matlab. Simulations are carried out to validate the performance of the estimator.

7.1 Estimator design for batch crystallizers

In this chapter an estimator for batch crystallization processes equipped with a specific measurement of the population balance and the temperature has been developed. It is assumed that the process can be modeled as introduced in Chapter 2, especially by Equation (2.15). The modeling of the population balance measurement and the analysis of observability properties of the process in this configuration have been discussed in

Section 3.2.2. The model that will be used for estimator design is the following:

$$\Sigma_{nlin}: \begin{cases} \dfrac{\partial n}{\partial t} = -\dfrac{\partial G(c,T)n}{\partial \ell}, & (7.1a) \\ \dfrac{\mathrm{d}T}{\mathrm{d}t} = \alpha(T_j - T), & (7.1b) \\ y = \begin{bmatrix} Fn \\ T \end{bmatrix} + \begin{bmatrix} \sigma_F I_k & 0 \\ 0 & \sigma_T \end{bmatrix} \begin{bmatrix} d_{2,n} \\ d_{2,T} \end{bmatrix} & (7.1c) \end{cases}$$

Here, $n(\cdot, t) \in L_2(0, \infty)$ is the population balance, $T(t) \in \mathbb{R}$ the reactor temperature, c is the concentration, $T_j(t) \in \mathbb{R}$ the jacket temperature, $y(t) \in \mathbb{R}^k$ the measured signal. The growth rate G is assumed to be size independent and dependent on concentration and temperature, i.e. $G := G(c, T)$. In Chapter 2, a detailed explanation of this model is given. The input signals $d_{2,n}$ and $d_{2,T}$ represent the measurement noise in the particle size measurement and the temperature measurement, respectively. In the analysis only operation of the process in regimes of concentration and temperature pairs (c, T) such that $G > 0$ is considered. Therefore, the population balance Equation (7.1a) remains well defined for all $t \geq 0$, as explained in Chapter 2. Additional to the population balance equation it has been assumed that the boundary condition $n(0, t) = 0$ holds. The initial state $(n(\ell, 0), T(0))$ is assumed to be given by $(n_0(\ell), T_0)$, where $n_0 \in L_2(0, \infty)$ and $T_0 \in \mathbb{R}$.

The measurement of the particle population is modeled by the measurement operator F which acts on the particle population n and is given by:

$$Fn = \begin{bmatrix} f_1 \\ \vdots \\ f_k \end{bmatrix} n \quad \text{with} \quad f_i n = \int_0^\infty w_i(\ell) n(\ell) \mathrm{d}\ell, \quad i = 1, \ldots, k, \tag{7.2}$$

where w_i is a weight function corresponding to particles of class i. That is $w_i : [0, \infty) \to \mathbb{R}$ has compact support in the interval $\mathbb{L}_i = [\ell_i^-, \ell_i^+]$ where $\mathbb{L}_i$ represent the particle size class i. We assume that k disjoint particle classes are measured, that is $\mathbb{L}_i \cap \mathbb{L}_j = \emptyset$ for $i \neq j$. Together with the temperature measurement this gives:

$$y(t) = \begin{bmatrix} Fn(\cdot, t) \\ T(t) \end{bmatrix} + \begin{bmatrix} \sigma_F I_k & 0 \\ 0 & \sigma_T \end{bmatrix} \begin{bmatrix} d_{2,n}(t) \\ d_{2,T}(t) \end{bmatrix}, \tag{7.3}$$

as measurement, where σ_f and σ_T are the standard deviation of the measurement noise in the particle size and temperature measurement and $d_{2,n} \in L_2(\mathbb{T}, \mathbb{R}^k)$ and $d_{2,T} \in L_2(\mathbb{T}, \mathbb{R})$ represent the noise signals present in the measurements.

It is assumed that the system is closed with respect to the mass balance. Therefore, (as described in Section 2.2.4), the concentration of material in the liquid phase and the mass of the particles in the solid phase are related via an algebraic relation due to the mass balance. This means that the concentration can be expressed as function of the population balance. By use of Equation (2.2), one obtains that the concentration $c(t)$ at time t is given by:

$$c(t) = c_0 - V(n - n_0)(t) = c_0 + V(n_0) - [V(n)](t),$$

where c_0 is the initial concentration, n_0 is the population balance at time $t = 0$, $n(\cdot, t)$ is the population balance at time t, and $V : L_2([0, \infty), \mathbb{R}) \to \mathbb{R}$ is the volume function that assigns $n \mapsto V(n)$, the volume of all particles corresponding to the distribution n. We assume that the volume of the particles linearly depends on the population $n(\ell, t)$, i.e. V is a linear functional of n, as described by Equation (2.2). The model (7.1) can be written in the form:

$$\Sigma : \begin{cases} \dot{x} = f(x, u, d), & \text{(7.4a)} \\ y = h(x, u, d), & \text{(7.4b)} \end{cases}$$

with the state $x(t) = \mathrm{col}(n(\cdot, t), T(t)) \in L_2(0, \infty) \times \mathbb{R}$, the output $y(t) \in \mathbb{R}^{k+1}$ and the known input $u(t) = T_j(t) \in U = \mathbb{R}$ and the unknown disturbance $d(t) = \mathrm{col}(d_{2,n}(t), d_{2,T}(t)) \in D = \mathbb{R}^{k+1}$. The functions $f(x, u, d)$ and $h(x, u, d)$ are given by:

$$f(x, u, d) = \begin{bmatrix} -\frac{\partial G(c,T)n}{\partial \ell} \\ \alpha(T_j - T) \end{bmatrix}, \qquad h(x, u, d) = \begin{bmatrix} Fn + \sigma_F I_k d_{2,n} \\ T + \sigma_T d_{2,T} \end{bmatrix}. \tag{7.5}$$

The model is augmented with the equation for the to-be-estimated variable z:

$$z = g(x), \tag{7.4c}$$

In this chapter we will assume one is interested in estimation of a finite dimensional projection of the crystal size distribution and the temperature of the reactor. This means that $g(x) = [Mn, T]^\top$, where M is a projection operator $M : X \to X_N$ and X_N is a subspace of X.

As stated in Chapter 2, the model for batch crystallization is nonlinear and infinite dimensional. Therefore the results on estimator design and implementation obtained in Chapter 5 and Chapter 6 are not directly applicable to this model. For that reason, linear approximations of the model will be derived by linearization in an operating point. Thereafter, a linear optimal impulse response estimator for the linearized (but still infinite dimensional) model will be derived. The estimator will be a linear infinite dimensional system itself and will be approximated and implemented by the method described in Chapter 6. Since the estimator obtained in this way can (only) be expected to function properly in a limited region around the operating point, the procedure of successive linearization, finite dimensional approximation and estimator design is repeated after a fixed time period. That is, for the system Σ given by Equation (7.4) Algorithm 7.1 has been obtained. A graphical representation of the algorithm is shown in Figure 7.1.

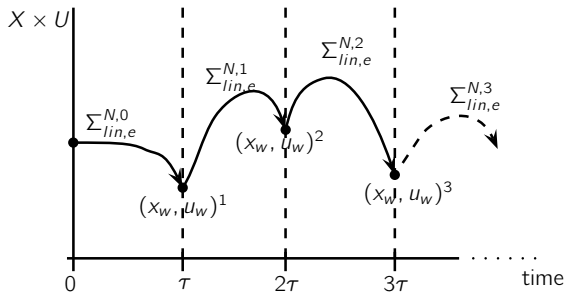

Figure 7.1: Graphical representation of estimation algorithm described in Algorithm 7.1.

Algorithm 7.1 (Time scheduled linear estimator)

[Initialize] *Set $k = 1$ and choose a linearization interval $\tau > 0$. Define $(x_w, u_w)^1 \in X \times U$ as initial operating points for the state and input. Define the order of approximation $N \in \mathbb{N}^+$, the Euclidean space X_N and the operators $E_N : X_N \to X$ and $P_N X \to X_N$ such that they satisfy the assumptions A1, A2 and A3 given in Section 6.2.1.*

[Step 1] *Linearize Σ at $(x_w, u_w)^k$ to obtain the linear system Σ^k_{lin}.*

[Step 2] *Approximate Σ^k_{lin} by the N-th order system $\Sigma^{N,k}_{lin}$ via Galerkin projection, conform Definition 6.2.2.*

[Step 3] *Calculate for $\Sigma^{N,k}_{lin}$ the L_2 or H_2 optimal estimator $\Sigma^{N,k}_{lin,e}$.*

[Step 4] *Define the time interval $\mathbb{T}^k = ((k-1)\tau, k\tau]$. Let $\hat{x}^k$ denote the state of the estimator $\Sigma^{N,k}_{lin,e}$. Initialize the estimator $\Sigma^{N,k}_{lin,e}$ with initial condition $\hat{x}^k = P_N(x_w)^k$. Obtain for $t \in \mathbb{T}^k$ the estimate $\hat{z}_k(t)$ as for $z(t)$, where $\hat{z}_k(t)$ is the output of the estimator $\Sigma^{N,k}_{lin,e}$.*

[Step 5] *Set $x_{w,k+1} = E_N \hat{x}^k(k\tau)$. Set $u_{w,k+1} = u(k\tau)$ where $u(k\tau)$ is the value of the input u at time $k\tau$. Set $k = k + 1$ and go to step 1.*

The estimator obtained in this way shows large similarities with the continuous time extended Kalman filter. This approach has been chosen since the complexity of the approach followed in Algorithm 7.1 is limited and therefore it is possible to analyze the method. It is possible to generalize the algorithm to the continuous time extended Kalman filter. Since the presented approach is based on linearization of the process model around the estimated state, the method is expected to have only a limited region of validity in which the error dynamics will converge. This property is inherent to all methods based on subsequent or scheduled linearization.

In the remainder of this chapter, the derivation and implementation of an estimator for the batch cooling crystallization process will be described. In Section 7.2, the method of linearization for infinite dimensional systems will be introduced and applied to the population balance model given by the Equations (7.4). In Section 7.3 an estimator for the the linearized infinite dimensional model will be designed. The implementation of the estimator and the estimation algorithm in the simulation environment Matlab will be discussed in Section 7.4. Simulation results will be presented in Section 7.5.

7.2 Linearization of population balance model

The batch cooling crystallization process is described by a nonlinear infinite dimensional system, as given in (7.1). The procedure for linearization of finite dimensional systems is well known, however the state space of the system under condiseration is of infinite dimension. A generalization of the Jacobian and the Taylor expansion of a mapping, suitable for operators on Hilbert spaces, will be introduced. Then, the linearization of a nonlinear infinite dimensional system will be derived. A linearization of the model for batch cooling crystallization will be derived subsequently.

7.2.1 Linearization of infinite dimensional systems

The linearization of a infinite dimensional systems will be introduced for the following system:

$$\begin{cases} \dot{x} = f(x, u, d) & \text{(7.6a)} \\ y = h(x, u, d) & \text{(7.6b)} \end{cases}$$

where $x(t) \in X$, $u(t) \in U$, $d(t) \in D$, and X, U and D are Hilbert spaces. A linear approximation to the model (7.6) can be obtained by linearization of the dynamics in an operating point $(x_w, u_w, d_w) \in X \times U \times D$. That is, one neglects nonlinear contributions in $f(x, u, d)$ and $h(x, u, d)$ due to changes in x, u or d with respect to the nominal value $(x_w, u_w, d_w) \in X \times U \times D$.

The following provides a definition of the Fréchet derivative.

Definition 7.2.1 (Fréchet derivative [Zeidler, 1995], p.228.)
Let $f : V \subset X \to Y$ be an operator defined on a neighborhood of the point $v \in V$, and let X and Y be Hilbert spaces. The differential $df(v)$ of f at point v exists if there is a linear bounded operator denoted by $df(v) : X \to Y$ such that

$$\lim_{||h|| \to 0} \frac{||f(v+h) - f(v) - df(v)h||_Y}{||h||_X} = 0$$

holds for all $h \in X$ in some open neighborhood of $h = 0$ in X. The operator $df(v)$ is also denoted by $f'(v)$ and known as the Fréchet derivative of f at v.

The operator $df(v)$ is, if it exists, uniquely determined by:

$$df(v)h = \lim_{t \to 0} \frac{f(v+th) - f(v)}{t}.$$

Remark 7.2.1. The Fréchet derivative is a generalization of the directional derivative. Therefore, the Fréchet derivative may not exist, depending on the properties of the operator under consideration.

If the Fréchet derivative of f exists at every $v \in V$, and the mapping $v \to f'(v) = df(v)$ is continuous at v_0, then f is called continuously Fréchet differentiable at v_0. If f is continuously Fréchet differentiable for every $v_0 \in V$, then f is called is continuously Fréchet differentiable on V.

The Frechet derivative of df at the point $v \in V \subset X$ is again a linear map in $\mathcal{L}(X, Y)$, denoted by df^2. The object df^2 therefore defines, by ranging over V, a mapping $V \to \mathcal{L}(X, \mathcal{L}(X, Y))$, where we identify the latter object with $\mathcal{L}(X \times X, Y)$. Likewise, $df^k : V \to L(X^k, Y)$ and we denote $df^{(k)}(h, \ldots, h)$ by $df^{(k)}h^k$.

With use of the Fréchet derivative, the generalized Taylor expansion can be defined.

Definition 7.2.2 (Generalized Taylor Expansion [Zeidler, 1995], p.243.)
Let the map $f : V \subset X \to Y$ be defined on the open convex set V and let X and Y be Hilbert spaces, such that $f^{(k)}(v)$ exists for $k = 1, .., n-1$. The generalized Taylor expansion of order n at the point $v \in V$ reads as:

$$f(v+h) = f(v) + \sum_{k=1}^{n-1} \frac{1}{k!} f^{(k)}(v)h^k + R_n(v, h),$$

where $n = 1, 2, \ldots$ and R_n denotes the residual. The residual R_n can be characterized as follows:

$$R_n(v, h) := \int_0^1 \frac{(1-\tau)^{n-1}}{(n-1)!} f^{(n)}(v + \tau h)h^n \mathrm{d}\tau.$$

Likewise in the finite dimensional case, the partial Fréchet derivative can be defined as follows.

Definition 7.2.3 (Partial Fréchet derivative [Zeidler, 1995], p.232.)
Let the map $f : V(v, w) \subset X \times Y \to Z$ be defined on the open neighborhood of the point (v, w), where X, Y and Z are Hilbert spaces. Let w be fixed and set $g(v) := f(v, w)$. If g has a Fréchet derivative at the point v, then we define the Partial Fréchet derivative of f with respect to v, say $f_v(v, w)$, through

$$f_v(v, w) := g'(v) = dg(v).$$

We are now in the position to define linearization of dynamical systems. The linearization of (7.6) around $(x_w, u_w, d_w) \in X \times U \times D$ is defined as follows:

Definition 7.2.4 (Linearization around (x_w, u_w, d_w).)
Define $\delta x \in X$, $\delta u \in U$, $\delta d \in D$ and assume that and the partial Fréchet derivatives $f_x(x_w, u_w, d_w)$, $f_u(x_w, u_w, d_w)$, $f_d(x_w, u_w, d_w)$, $h_x(x_w, u_w, d_w)$, $h_u(x_u, u_w, d_w)$, $h_d(x_u, u_w, d_w)$ exist. The linearization of (7.6) around (x_w, u_w, d_w) is given by:

$$\begin{cases} \dot{\delta x} = f(x_w, u_w, d_w) + f_x(x_w, u_w, d_w)\delta x + f_u(x_w, u_w, d_w)\delta u + f_d(x_w, u_w, d_w)\delta d, \\ y = h(x_w, u_w, d_w) + h_x(x_w, u_w, d_w)\delta x + h_u(x_w, u_w, d_w)\delta u + h_d(x_w, u_w, d_w)\delta d. \end{cases}$$

The point (x_w, u_w, d_w) is known as the operating point, linearization point or working point.

Remark 7.2.2. Note that we do not assume that $f(x_w, u_w, d_w) = 0$, i.e. the operating point (x_w, u_w, d_w) is not necessarily an equilibrium point [1] of the system.

[1] The operating point (x_w, u_w, d_w) is an a equilibrium point of the differential equation $\dot{x} = f(x, u, d)$ if $f(x_w, u_w, d_w) = 0$.

Remark 7.2.3. Note that for the system under consideration the linearization also depends on the unknown disturbance d_w. In practical applications it is often assumed that $d_w = 0$.

In general, it is interesting to know if there exists a preferable order to perform linearization and approximation respectively. That is, if there is difference between a procedure in which *linearization* is followed by *approximation* and a procedure in which *approximation* is followed by *linearization*. We consider the situation where approximations are made by Galerkin projection and introduce the following theorem.

Theorem 7.2.1
Consider the nonlinear system

$$\Sigma : \dot{x} = f(x),$$

with $x \in X$, where X is a Hilbert Space. Define the operating points $x_w \in X$, $x_{w,N} \in X_N$ and let the Galerkin projection be defined according to Definition 6.2.2 with $P_N : X \to X_N$ and $E_N : X_N \to X$.

Let the system $\Sigma_{l,p}$ be obtained by applying a Galerkin projection to a linearization of Σ at operating point x_w and let $\Sigma_{l,p}$ be given by:

$$\Sigma_{l,p} : \dot{x}_N = A_{l,p}x_N + R_{l,p} \quad \text{with } A_{l,p} : X_N \to X_N \text{ and } x_N(0) \in X_N.$$

Let the system $\Sigma_{p,l}$ be obtained by applying a linearization at the operating point $x_{w,N}$ of a Galerkin projection of Σ and let $\Sigma_{p,l}$ be given by:

$$\Sigma_{p,l} : \dot{x}_N = A_{p,l}x_N + R_{p,l} \quad \text{with } A_{p,l} : X_N \to X_N \text{ and } x_N(0) \in X_N.$$

Then $\Sigma_{l,p} = \Sigma_{p,l}$ if and only if the following two conditions hold:

$$P_N\left(\frac{\partial f}{\partial x}\Big|_{x_w} - \frac{\partial f}{\partial x}\Big|_{E_N P_N x_w}\right)E_N = 0, \tag{7.7}$$

$$P_N(f(x_w) - f(E_N x_{w,N})) = 0. \tag{7.8}$$

Proof. The proof follows from straightforward computation of $A_{l,p}$, $A_{p,l}$, $R_{l,p}$ and $R_{p,l}$. Define $f_N : X_N \to X_N$ by the Galerkin projection of f, i.e. $f_N(x_N) := P_N f(E_N x_N)$ for $x_N \in X_N$. It follows that $A_{l,p}$ and $A_{p,l}$ are given by:

$$A_{l,p} = P_N \frac{\partial f}{\partial x}\Big|_{x_w} E_N \qquad A_{p,l} = \frac{\partial f_N}{\partial x_N}\Big|_{x_{w,N}} \tag{7.9}$$

The operator $A_{p,l}$ can be rewritten with use of the chain-rule for differentiation as follows:

$$A_{p,l} = \frac{\partial P_N f(E_N x_N)}{\partial x_N}\Big|_{x_{w,N}} = P_N \frac{\partial f(E_N x_N)}{\partial x_N}\Big|_{x_{w,N}} = P_N \frac{\partial f}{\partial x}\Big|_{E_N x_{w,N}} E_N$$

Comparison of the expressions for $A_{l,p}$ and $A_{p,l}$ shows that $A_{l,p}$ and $A_{p,l}$ are equal if and only if

$$P_N \frac{\partial f}{\partial x}\Big|_{x_w} E_N = P_N \frac{\partial f}{\partial x}\Big|_{E_N x_{w,N}} E_N.$$

Moreover, it follows that $R_{l,p} = P_N f(x_w)$ and $R_{p,l} = P_N f(E_N x_{w,N})$, such that $R_{l,p} = R_{p,l}$ if and only if $P_N(f(x_w) - f(E_N x_{w,N})) = 0$. □

We have the following corollary:

Corollary 7.2.2
Let the linearization points be chosen such that $x_{w,N} = P_N x_w$ and $x_w = E_N P_N x_w$. Then, the conditions (7.7) and (7.8) in Theorem 7.2.1 are satisfied and the order of linearization and approximation are not of influence on the resulting approximate linear model.

Proof. The corollary follows from the observation that under the assumed conditions the following is true:

$$R_{p,l} = P_N f(E_N x_{w,N}) = P_N f(x_w) = R_{l,p}, \quad \text{and} \quad f(E_N x_{w,N}) = f(x_w).$$

□

Next, we will continue with the linearization of the model for batch cooling crystallization processes.

7.2.2 Linearization of population balance model.

In this section the linearization of the population balance model will be presented. Introduce the operating point $(x_w, u_w, d_w) \in L_2(\mathbb{L}, \mathbb{R}) \times U \times D$, the perturbation on the known input $\delta u = \delta T_j \in L_2(\mathbb{T}, \mathbb{R})$, the perturbation on the unknown input $\delta d \in L_2(\mathbb{T}, \mathbb{R}^{k+1})$ and the state $\delta x \in L_2(\mathbb{T} \times \mathbb{L}, \mathbb{R}) \times L_2(\mathbb{T}, \mathbb{R})$ as follows:

$$(x_w, u_w, d_w) = \left(\begin{bmatrix} n_w \\ T_w \end{bmatrix}, T_{j,w}, \begin{bmatrix} d_{2,n,w} \\ d_{2,T,w} \end{bmatrix} \right), \qquad \delta x = \begin{bmatrix} \delta n \\ \delta T \end{bmatrix}. \tag{7.10}$$

The operating point also defines the concentration (at the operating point), which we denote by $c_w = c_0 + V(n_0) - V(n_w)$. We define the set X_w as follows:

$$X_w = \left\{ \begin{bmatrix} n_w \\ T_w \end{bmatrix} \mid \begin{bmatrix} n_w \\ T_w \end{bmatrix} \in X \text{ and } \frac{\partial n_w}{\partial \ell} \in L_2 \right\},$$

and we will assume that $x_w \in X_w$. The differentiability condition on n_w will be necessary to define the linearization of the system. Moreover, we assume that (x_w, u_w, d_w) is a valid operating condition of the system (7.1) in the sense that $G(c_w, T_w) > 0$.

We linearize the system (7.4) following Definition 7.2.4 and obtain:

$$\dot{\delta x} = f(x_w, u_w, d_w) + f_u(x_w, u_w, d_w)\delta u + f_x(x_w, u_w, d_w)\delta x, \tag{7.11a}$$
$$y = h(x_w, u_w, d_w) + h_x(x_w, u_w, d_w)\delta x + h_d(x_w, u_w, d_w)\delta d, \tag{7.11b}$$
$$z = g(x_w) + g_x(x_w)\delta_x, \tag{7.11c}$$

with:

$$f(x_w, u_w, d_w) = \begin{bmatrix} -G(c_w, T_w)\frac{\partial n_w}{\partial \ell} \\ \alpha(T_{j,w} - T_w) \end{bmatrix}, \qquad f_u(x_w, u_w, d_w)\delta u = \begin{bmatrix} 0 \\ \alpha \delta T_j \end{bmatrix},$$

$$f_x(x_w, u_w, d_w)\delta x = \begin{bmatrix} -G(c_w, T_w)\frac{\partial \delta n}{\partial \ell} + G_c(c_w, T_w)\frac{\partial n_w}{\partial \ell} V(\delta n) - G_T(c_w, T_w)\frac{\partial n_w}{\partial \ell}\delta T \\ -\alpha \delta T \end{bmatrix},$$

$$h(x_w, u_w, d_w) = \begin{bmatrix} F n_w + \sigma_F I_k d_{2,n,w} \\ T_w + \sigma_T d_{2,T,w} \end{bmatrix}, \quad h_x(x_w, u_w, d_w)\delta x = \begin{bmatrix} F\delta n \\ \delta T \end{bmatrix},$$

$$h_d(x_w, u_w, d_w)\delta d = \begin{bmatrix} \sigma_F I_k \delta d_{2,n} \\ \sigma_T I_k \delta d_{2,T} \end{bmatrix}, \quad g(x_w) = \begin{bmatrix} M n_w \\ T_w \end{bmatrix}, \quad g_x(x_w)\delta_x = \begin{bmatrix} M & 0 \\ 0 & 1 \end{bmatrix} \begin{bmatrix} \delta n \\ \delta T \end{bmatrix}$$

where V is the volume function and G_c and G_T denote the derivatives of G with respect to c and T respectively. It follows that for the model under consideration $f_d(x_w, u_w, d_w) = 0$ and $h_u(x_w, u_w, d_w) = 0$. Clearly, f and f_x are only well defined if n_w is differentiable, which it is by assumption on X_w.

In the remainder of this chapter we will denote the linearization of Σ_{nlin} by Σ_{lin} and use the following notation:

$$\Sigma_{lin} : \begin{cases} \dot{\delta x} = A\delta x + B\delta u + R, & \text{(7.12a)} \\ \delta y = C\delta x + S\delta d, & \text{(7.12b)} \\ \delta z = H\delta x & \text{(7.12c)} \end{cases}$$

where $\delta y = y - h(x_w)$, $\delta z = z - g(x_w)$ and $A : X \to X$, $B : U \to X$, $C : X \to Y$, $H : X \to Z$ $S : D \to Y$ and $R \in X$, are such that:

$$\begin{aligned} A &= f_x(x_w, u_w, d_w) & B &= f_u(x_w, u_w, d_w), & R &= f(x_w, u_w, d_w), \\ C &= h_x(x_w, u_w, d_w), & S &= h_d(x_w, u_w, d_w), & H &= g_x(x_w) \end{aligned}$$

The system Σ_{lin} can be interpreted as a linear infinite dimensional system with input $B\delta u + R$, initial condition $\delta x_0 = \mathrm{col}(\delta n_0, \delta T_0)$ for $\delta x(t) = 0$ at time $t = 0$, and boundary condition $\delta n(0, t) = n(0, t) - n_w(0, t) = 0$ for all $t \geq 0$. It is important to study if the equations obtained after linearization still make sense and whether they define a system of equations for which unique solutions do exist. That is, it is important to study if the system Σ_{lin} is a well posed linear system and if solutions do exist.

First we introduce the following lemma.

Lemma 7.2.3 (Perturbation by bounded linear operators, [Pazy, 1983, Theorem 3.1.1]) *Let X be a Hilbert space and A be the infinitesimal generator of a C_0-semigroup $T(t)$, satisfying $||T(t)|| \leq Me^{\omega t}$ with $M > 0$ and $\omega \in \mathbb{R}$. If B is a bounded linear operator on X then $A + B$ is the infinitesimal generator of a C_0-semigroup $S(t)$, with $||S(t)|| \leq Me^{(\omega + M||B||)t}$.*

Proof. For the proof we refer to [Pazy, 1983]. □

The operator A is the generator of a C_0-semigroup, which is shown in the following theorem.

Theorem 7.2.4
Consider the system Σ_{lin} defined by (7.12). Assume that $G(c,T)$ is continuously differentiable with respect to c and T, that $\frac{\partial n_w}{\partial \ell} \in L_2$. The operator A is the infinitesimal generator of a C_0-semigroup on X.

Proof. Consider the operator $A_0 : D(A_0) \to X$:

$$A_0 \begin{bmatrix} \delta n \\ \delta T \end{bmatrix} = \begin{bmatrix} -G(c_w, T_w)\frac{\partial}{\partial \ell} & 0 \\ 0 & -\alpha \end{bmatrix} \begin{bmatrix} \delta n \\ \delta T \end{bmatrix} \tag{7.13}$$

The operator A_0 is a diagonal operator. It is well known [Curtain and Zwart, 1995] that the operator $-G(c_w, T_w)\frac{\partial}{\partial \ell}$ is the infinitesimal generator of the right shift C_0-semigroup, which we denote by $\mathcal{T}_n(t) : L_2([0,\infty),\mathbb{R}) \to \mathbb{R}$:

$$\mathcal{T}_n(t)\delta n = \begin{cases} \delta n(\ell - G(c_w, T_w)t) & \text{for } G(c_w, T_w)t < \ell, \\ 0 & \text{else.} \end{cases}$$

Therefore A_0 is the infinitesimal generator of the C_0-semigroup $\mathcal{T}_0(t) : X \to X$:

$$\mathcal{T}_0(t) \begin{bmatrix} \delta n \\ \delta T \end{bmatrix} = \begin{bmatrix} \mathcal{T}_n(t)\delta n & 0 \\ 0 & e^{-\alpha t}\delta T \end{bmatrix}$$

The operator A in (7.12) can be interpreted as a perturbed version of A_0, i.e

$$A \begin{bmatrix} \delta n \\ \delta T \end{bmatrix} = (A_0 + \Delta A) \begin{bmatrix} \delta n \\ \delta T \end{bmatrix},$$

with:

$$\Delta A \begin{bmatrix} \delta n \\ \delta T \end{bmatrix} = \begin{bmatrix} G_c(c_w, T_w)\frac{\partial n_w}{\partial \ell} V(\delta n) - G_T(c_w, T_w)\frac{\partial n_w}{\partial \ell}\delta T \\ 0 \end{bmatrix}. \tag{7.14}$$

Since $\frac{\partial n_w}{\partial \ell} \in L_2$ and from continuous differentiability of G it follows that $G_c(c_w, T_w) < \infty$, $G_T(c_w, T_w) < \infty$, we conclude that the operator ΔA is a bounded operator. Moreover, based on physical limitations it can be assumed that $V(\delta n) < \infty$. It therefore follows from Lemma 7.2.3 that A is the generator of a C_0-semigroup $\mathcal{T}(t) : X \to X$. □

Since the system is well posed and the operator (t) is a c_0 semigroup, it followed from the standard results on the abstract Cauchy problem, for instance see
[Curtain and Zwart, 1995, Theorem 3.1.3], we have that for an input $\delta T_j \in C^1(\mathbb{T};\mathbb{R})$ and initial condition δx_0, the unique classical solution of Σ_{lin} is given by:

$$\delta x(t) = \mathcal{T}(t)\delta x_0 + \int_0^t \mathcal{T}(t-\tau)(B\delta T_j(\tau) + R)\mathrm{d}\tau.$$

In the next section we will derive a finite dimensional approximation Σ_{lin}^N for Σ_{lin} and an estimator for Σ_{lin}^N .

7.3 Estimator design for linearized models

In this section we will design an estimator for the linearized model of the Batch Cooling Crystallization process, given by Σ_{lin} in Equation (7.12) obtained by linearization in the operating point (x_w, u_w, d_w). Ideally, one would like to apply the estimator design method as described in Chapter 5 to obtain the optimal estimator $\Sigma_{lin,e}$ for the system Σ_{lin}. However, as described in Chapter 6, the optimal estimator obtained by this approach is not implementable since it is infinite dimensional and in order to obtain an explicit realization of the optimal estimator, one needs to solve the implicit Riccati equation involved in the design procedure. As alternative, we will obtain an estimator for the system Σ_{lin} by Scenario $S1$, which is introduced in Section 6.2.3. That is, first we will derive a finite dimensional approximation Σ_{lin}^N of the linearized infinite dimensional system Σ_{lin}. Subsequently we will design an optimal estimator $\Sigma_{lin,e}^N$ for the system Σ_{lin}^N.

We will use the approximation framework introduced in Chapter 6 where the Galerkin projection is used. The Galerkin projection is defined in Section 6.2.2 to obtain the finite dimensional approximations of Σ_{lin}. First, we truncate the domain of the particle size from $[0, \infty)$ to $[0, \bar{\ell}]$, which is possible since we have assumed that there is a maximum size that the particles can obtain. That is we choose $\bar{\ell}$ larger this maximum particle size. We will define $Z = X = L_2(0, \bar{\ell}) \times \mathbb{R}$, and let $X_N = \mathbb{R}^N$ with canonical basis $\{e_i\}_{i=1}^N$. We introduce for any $N > 1$ the following orthonormal basis $\{\phi_i\}_{i=1}^N$ of a subspace of Z:

$$\phi_1 = \begin{bmatrix} 1 \\ 0 \end{bmatrix}, \quad \phi_i = \begin{bmatrix} \sqrt{\frac{2}{\bar{\ell}}} \cos\left(\frac{\pi}{\bar{\ell}}(i-1)\ell\right) \\ 0 \end{bmatrix} \text{ for } i \in \{2, \ldots N-1\} \quad \phi_N = \begin{bmatrix} 0 \\ 1 \end{bmatrix}. \tag{7.15a,b,c}$$

We will define operators P_N and E_N as in Example 6.2.1, that is $P_N : Z \to X_N$ and $E_N : X_N \to Z$, given by:

$$P_N x = \sum_{i=1}^{N} \langle x, \phi_i \rangle e_i, \qquad E_N x_N = \sum_{i=1}^{N} \langle x, e_i \rangle \phi_i.$$

By use of Galerkin projection, we obtain the system Σ_{lin}^N from the linear system Σ_{lin}, which is given by:

$$\Sigma_{lin}^N : \begin{cases} \dot{\delta x}_N &= A_N \delta x_N + B_N \delta u + G_N \delta d_1 + R_N, \\ \delta y &= C_N \delta x_N + S_N \delta d_2, \\ \delta z &= H_N \delta x_N, \end{cases} \tag{7.16}$$

with $A_N \in \mathbb{R}^{N \times N}$, $B_N \in \mathbb{R}^{N \times \dim(U)}$, $R_N \in \mathbb{R}^{N \times 1}$, $C_N \in \mathbb{R}^{N \times (k+1)}$ and $H_N \in \mathbb{R}^{N \times N}$ given by

$$A_N := P_N A E_N, \qquad B_N := P_N B, \qquad R_N := P_N R, \tag{7.17a}$$

$$C_N := C E_N, \qquad H_N := H E_N, \qquad S_N := S. \tag{7.17b}$$

The operator G_N represents the influence of the external disturbances on the evolution of the state δx_N. Note that, in general state disturbances are not modeled in first principle models and that there is also no state disturbance considered in the process model (7.1). Therefore, there is also no state disturbance present in the linearized model Σ_{lin}. We have introduced, somewhat artificially, the operator G_N and unknown disturbance signal d_1 to represent the influences of the linearization and approximation error on the state evolution. It will (again somewhat artificially) be assumed that the disturbance signal is uncorrelated with x_N.

Note that the approximation is finite dimensional of order N. It reflects a projection on the first $N-1$ harmonics of the spatially distributed population balances in $L_2([0,\bar{\ell}])$.

For the system Σ_{lin}^N we would like to obtain an optimal impulse response estimator by use of the estimator design method given in Chapter 5. However, the system Σ_{lin}^N contains the known input signal $\delta u = \delta T_j$ and the drift vector R_N, which are not considered in the estimator design problems discussed in Chapter 5. By linearity it follows that the design method of Chapter 5 can be used with a minor modification as follows. Consider the systems $\Sigma_{lin,d}^N$ and $\Sigma_{lin,u}^N$, given by:

$$\Sigma_{lin,d}^N : \begin{cases} \delta\dot{x}_d &= A_N\delta x_d + G_N\delta d_1, \\ \delta y_d &= C_N\delta x_d + S_N\delta d_2, \\ \delta z_d &= H_N\delta x_d, \end{cases} \quad \Sigma_{lin,u}^N : \begin{cases} \delta\dot{x}_u &= A_N\delta x_u + B_N\delta u + R_N, \\ \delta y_u &= C_N\delta x_u, \\ \delta z_u &= H_N\delta x_u, \end{cases}$$

where $\delta x_u \in X_N$, $\delta x_d \in X_N$. We set the initial conditions to $x_d(0) = 0$ and $x_u(0) = x_N(0)$ and the matrices A_N, G_N, R_N, C_N, S_N and H_N are as defined by (7.17a) and (7.17b). The systems are constructed such that state δx_u denotes the contribution in δx due to input $\delta u = \delta T_j$ and the drift vector R_N. Moreover, $\delta x_d \in X_N$ denotes the contribution in δx_N due to disturbance δd_1. By linearity it follows that $\delta x_N = \delta x_u + \delta x_d$, $\delta y = \delta y_u + \delta y_d$ and $\delta z = \delta z_u + \delta z_d$.

Since it is assumed that δu and R_N are known, the outputs δy_u and δz_u are exactly known and hence not part of the estimation problem. Following the same line of reasoning as in Remark 5.2.2, in which we consider the case with a known initial condition, an estimator for the system Σ_{lin}^N can be constructed by use of the estimator design method given in Chapter 5. That is, we obtain an optimal impulse response estimator for the system Σ_{lin}^N considering the estimator design problem for the system $\Sigma_{lin,d}^N$, with which we estimate $\delta\hat{z}_d$ of δz_d based on $\delta y_d = y - \delta y_u$. The estimate $\delta\hat{z}$ of δz is now obtained by $\delta\hat{z} = \delta\hat{z}_d + \delta z_u$. Concluding, the optimal impulse response estimator $\Sigma_{lin,e}^N$ for the system Σ_{lin}^N is given by:

$$\Sigma_{lin,e}^N : \begin{cases} \dot{\hat{x}} &= (A_N - \Pi_N C_N^*(SS^*)^{-1}C_N)\hat{x} + P_N\Pi_N C_N^*(SS^*)^{-1}\delta y + B_N\delta u + R_N \\ \delta\hat{z} &= H_N\hat{x} \end{cases} \tag{7.18}$$

with $\hat{x}(t) \in \mathbb{R}^N$ and where we will use $\delta u = u - u_w$ and $\delta y = y - h(x_w, u_w, d_w)$. In the case of optimal impulse response estimator design, Π_N is the solution of the Algebraic Riccati Equation:

$$\Pi_N A_N^* + A_N\Pi_N + G_N G_N^* - \Pi_N(C_N^*(SS^*)^{-1}C_N)\Pi_N = 0. \tag{7.19}$$

To obtain an estimate for z, we will use that $\hat{z} = g(x_w) + \delta\hat{z}$.

Of course, it is important to validate if the estimator $\Sigma^N_{lin,e}$ converges to the estimator $\Sigma_{lin,e}$ when the order of N increases. Unfortunately we have not been able to prove convergence by use of the method presented in Section 6.4.2. Especially the condition $E3$ is hard to validate. The convergence of the semigroup operators $\mathcal{T}_N(t) : X_N \to X_N$ and $\mathcal{T}(t) : X \to X$, with infinitesimal generator by A and A_N (stated in condition $E1$) can be shown as follows.

Theorem 7.3.1
Consider the operators A and A_N as defined for the systems (7.12) *and* (7.16). *Let $\mathcal{T}_N(t) : X_N \to X_N$ and $\mathcal{T}(t) : X \to X$ be the semigroup operators with infinitesimal generators A and A_N. Then:*

$$\lim_{N\to\infty} ||E_N\mathcal{T}_N(t)P_Nx - \mathcal{T}(t)x|| = 0 \quad \textit{for all } x \in X.$$

Proof. Let A_0 and ΔA be as defined in the Equations (7.13) and (7.14). Then, as in Theorem 7.2.4, it follows that that A can be obtained by a bounded perturbation of the generator A_0, i.e. $A = A_0 + \Delta A$. Equivalently, A_N can be expressed by $A_N = P_NA_0E_N + P_N\Delta AE_N$. Let $\mathcal{T}_0(t) : X \to X$ and $\mathcal{T}_{N,0}(t) : X_N \to X_N$ be the semigroup operators with generators $P_NA_0E_N$ and A_0. Convergence of $\mathcal{T}_0(t) : X \to X$ and $\mathcal{T}_{N,0}(t) : X_N \to X_N$ follows use of Theorem 6.3.2 and is equivalent to the proof in the Example with convection in Section 6.5.2. By use of Theorem 6.4.5, convergence of the semigroup operators $\mathcal{T}_N(t) : X_N \to X_N$ and $\mathcal{T}(t) : X \to X$ follows. □

7.4 Implementation and simulation of the estimation algorithm

For the experimental validation and testing of the estimators when used for batch cooling crystallization processes, an estimator based on Algorithm 7.1 has been implemented in a simulation environment. We will test the estimator for a batch cooling crystallization process that is described by the model (7.1), which is equipped with the temperature and particle size distribution sensors that can be represented by Equation (7.3). The simulation has been performed with model parameters as given in Table 7.1. The model parameters do not correspond to a specific industrial process bt are chosen such they are representative. The solubility data corresponds to the solubility data of $KNO3$ and is obtained from [Matthews et al., 1996]. The data on the crystal growth kinetics is fictional by lack of reliable kinetic data and is chosen such that the batch time is representative for practical situations.

It is assumed that particle population sensor F is a sensor with ideal classification as described in Section 3.2.2 and that the sensor performs classification in 10 equally sized classes which cover the complete domain $[0, \bar{\ell}]$. $\bar{\ell}$ represent the largest particle size that can exist. The measurement disturbances, are modeled by zero mean Gaussian white noise, with a standard deviation σ_T and σ_F. It has been assumed that the noise of the measurement channels is uncorrelated. Moreover it has been assumed that the state

Table 7.1: Model parameters

Parameter	Interpretation	Value	Unit
ρ_c	Specific density	2000	$[J/^\circ\mathrm{C}kg]$
α	Thermal time constant	1500	$[1/s]$
V_r	Reactor volume	1	$[m^3]$
$c_s(T)$	Solubility	$A0 + A1T + A2T^2$	$[g/g]$
$S_r(c,T)$	Relative super saturation	$(c - c_s(T))/c_s(T)$	$[-]$
$G(c,T)$	Growth rate	$k_g S_r(c,T)^g$	$[m/s]$
$V(n)$	Volume function	$\int_0^{\bar{\ell}} \ell^3 n(\ell)\mathrm{d}\ell$	$[m^3/kg]$
$A0$	Coefficient solubility polynomial	0.127	$[g/g]$
$A1$	Coefficient solubility polynomial	$5.88 \cdot 10^{-3}$	$[g/g^\circ\mathrm{C}]$
$A2$	Coefficient solubility polynomial	$1.72 \cdot 10^{-4}$	$[g/g^\circ\mathrm{C}^2]$
k_g	growth rate factor	$1 \cdot 10^5$	$[m/s]$
g	growth rate exponent	1	$[-]$
σ_F	Standard deviation on measurement noise $d_{2,F}$	$5 \cdot 10^{11}$	$[1/m^3]$
σ_T	Standard deviation on measurement noise $d_{2,T}$	$1 \cdot 10^{-1}$	$[^\circ\mathrm{C}]$
σ_{Gn}	Standard deviation on state noise $d_{1,n}$	$1 \cdot 10^5$	$[1/m^3]$
σ_{GT}	Standard deviation on state noise $d_{1,T}$	$1 \cdot 10^{-1}$	$[^\circ\mathrm{C}]$

noise $d_1(t)$ acts uncorrelated on the states of the projected model. Also the state noise $d_1 = [d_{1,n}, d_{1,T}]^\top$ has been modeled by zero mean Gaussian white noise, such that G_N is diagonal and has the representation:

$$G_N = \begin{bmatrix} \sigma_{Gn} I_{N-1} & 0 \\ 0 & \sigma_{GT} \end{bmatrix}.$$

We assume that the states of the population balance are disturbed by noise with variance σ_{Gn}^2 and that the state of the reactor temperature is disturbed by noise with variance σ_{GT}^2. It is assumed that one is interested in estimation of a projection of the state x on the subspace X_N of X, such that we assume that $H = E_N P_N$.

Algorithm 7.1 has been implemented for estimation of the state of the batch cooling crystallizer. In the Algorithm we use the method for linearization described in Section 7.2 and the methods for approximation and estimator design described in Section 7.3. For completeness, we state Algorithm 7.1 again, now with specific references to previous sections.

Algorithm 7.2 (Linearized estimator for Batch Cooling Crystallization)

[Initialize] *Set $k = 1$ and choose a linearization interval $\tau > 0$. Define $(x_w, u_w)^1 \in X \times U$ as initial operating points for the state and input. Define the order of approximation $N \in \mathbb{N}^+$. Moreover define $Z_N = \text{span}\{\phi_i\}_{i=1}^N$ and the operators E_N and P_N by:*

$$P_N x = \sum_{i=1}^{N} \langle x, \phi_i \rangle e_i, \qquad E_N x_N = \sum_{i=1}^{N} \langle x, e_i \rangle \phi_i,$$

where, for $i \in \{2, \ldots N-1\}$:

$$\phi_1 = \begin{bmatrix} 1 \\ 0 \end{bmatrix}, \quad \phi_i = \begin{bmatrix} \sqrt{\frac{2}{\bar{\ell}}} \cos\left(\frac{\pi}{\bar{\ell}}(i-1)\ell\right) \\ 0 \end{bmatrix}, \quad \phi_N = \begin{bmatrix} 0 \\ 1 \end{bmatrix}.$$

[Step 1] *Linearize Σ_{nlin} at $(x_w, u_w)^k$ to obtain the linear system Σ_{lin}^k, following Equation (7.12), i.e:*

$$\Sigma_{lin}^k : \begin{cases} \dot{\delta x}^k = A^k \delta x^k + B^k \delta u + R^k, \\ \delta y^k = C^k \delta x + S^k \delta d, \\ \delta z^k = H_N^k \delta x. \end{cases}$$

[Step 2] *Approximate Σ_{lin}^k by the N-th order system $\Sigma_{lin}^{N,k}$ via Galerkin projection, conform Definition 6.2.2. The system $\Sigma_{lin}^{N,k}$ following (7.16), i.e.*

$$\Sigma_{lin}^k : \begin{cases} \dot{\delta x}_N^k = A_N^k \delta x_N^k + B_N^k \delta u + R_N^k, \\ \delta y_N^k = C_N^k \delta x + S \delta d, \\ \delta z_N^k = H_N^k \delta x. \end{cases}$$

[Step 3] *Calculate for $\Sigma_{lin}^{N,k}$ the optimal impulse response estimator $\Sigma_{lin,e}^{N,k}$, following the Equations (7.18), i.e.*

$$\Sigma_{lin,e}^{N,k} : \begin{cases} \dot{\hat{x}}^k = (A_N^K - \Pi_N^k C_N^{k*} (SS^*)^{-1} C_N^k) \hat{x}^k + \Pi_N^k C_N^{k*} (SS^*)^{-1} y + B_N^k \delta u + R_N^k, \\ \hat{z} = H_N^k \hat{x}, \end{cases}$$

with $\hat{x}(t) \in \mathbb{R}^N$ and where Π_N^K is the solution of the algebraic Riccati equation $\Pi_N^k A_N^{k*} + A_N^k \Pi_N^k + G_N^k G_N^{k*} - \Pi_N^k (C_N^{k*} (SS^*)^{-1} C_N^k) \Pi_N^k = 0$.

[Step 4] *Define the time interval $\mathbb{T}^k = ((k-1)\tau, k\tau]$. Initialize the estimator $\Sigma_{lin,e}^{N,k}$ with initial condition $\hat{x}_N^k = P_N(x_w)^k$. Obtain for $t \in \mathbb{T}^k$ the estimate $\hat{z}_k(t)$ as for $z(t)$, where $\hat{z}_k(t)$ is the output of the estimator $\Sigma_{lin,e}^{N,k}$.*

[Step 5] *Set $x_{w,k+1} = E_N \hat{x}_N^k(k\tau)$. Set $u_{w,k+1} = u(k\tau)$ where $u(k\tau)$ is the value of the input u at time $k\tau$. Set $k = k+1$ and go to step 1.*

The estimation algorithm has been implemented in Matlab and computations have been performed on an Intel core I5, 540 M processor at a clock frequency of 2.53 GHz with 4Gb of RAM on a Windows 7 Enterprise SP1 32bit installation. The order of the approximations is $N = 31$ and is chosen as a tradeoff between computational complexity and satisfactory performance of the approximations of the open loop of the system Σ_{nlin}, given by equation (7.1) (compared to a simulation with $N = 100$). The range of the crystal size distribution has been set to $\ell = [0, \bar{\ell}] = [0, 1 \cdot 10^{-3}]$, and this domain has been been divided into 200 equally spaced bins. In order to obtain numerically reliable results, all inner products involved in the Galerkin projection of the system Σ_{lin} have been calculated symbolically by use of the Matlab Symbolic Toolbox. Also, integration involved in the computation of the volume function V has been implemented analytically to avoid numerical instabilities in the integration. By calculation with Mathematica it

Table 7.2: Simulation parameters

Parameter	Interpretation	Value	Unit
N_ℓ	Discretization point computational domain	200	$[-]$
$\bar{\ell}$	Domain boundary	$1.^{10-3}$	$[m]$
N	Approximation order	31	$[-]$
τ	Linearization interval	150	$[s]$
Ts	Sample time	15	$[s]$
c_0	Initial concentration	0.86	$[g/g]$
n_0	Initial distribution	$\frac{5\cdot 10^{12}}{\sqrt{2\pi}} e^{-\frac{(\ell - n_{0,\mu}).^2}{n_{0,\sigma}^2}}$	$[-]$
$n_{0,\mu}$	Initial distribution mean	$3 \cdot 10^{-4}$	$[m]$
$n_{0,\sigma}$	Initial distribution standard variation	$7 \cdot 10^{-5}$	$[m]$
T_0	Initial reactor temperature	50	$[^\circ\mathrm{C}]$
n_w^0	Operating point	$0.8 \cdot n_0$	$[-]$
T_w^0	Operating point	49.9	$[^\circ\mathrm{C}]$
$T_{j,w}^0$	Operating point	50	$[^\circ\mathrm{C}]$
$d_{2,n,w}$	Operating point	0	$[m^{-3}]$
$d_{2,T,w}$	Operating point	0	$[^\circ\mathrm{C}]$

has be found that:

$$\int \ell^3 \cos(a\ell)\mathrm{d}\ell = \frac{-6 + 3a^2\ell^2}{a^4} \cos(a\ell) + \frac{-6\ell + a^2\ell^3}{a^3} \sin(a\ell) \tag{7.20}$$

where, we use $a = \frac{\pi i}{\bar{\ell}}$ in the computation of the projections.

The simulation has been carried out with simulation parameters as given in Table 7.2. The time interval τ between two linearization steps has been chosen $\tau = 150s$. This choice is a tradeoff between the computational complexity complexity and performance off the estimator. It has been observed that the demand of the value for τ, depend on the way the process is operated. In the simulations that when dynamics of the process change rapidly, i.e. when growth rates are large and vary fast, the value of τ needs to be smaller than in the situation of more modest operation of the process, which is as expected.

7.5 Simulation results

In this section we present simulation results in which the model of the batch crystallization process has been interconnected with the estimator. In these simulations, we study the scenario where the crystallizer is cooled using a predefined temperature trajectory in the reactor jacket. The predefined temperature trajectory in jacket and the resulting reactor temperature are shown in Figure 7.2a. The evolution of the particles size distribution as function of time is shown Figure 7.3a. The measurement of the particle numbers by the particle size sensor is shown in Figure 7.2b. With use of the estimator, the particles size distribution and the reactor temperate are estimated. The estimates

are shown in Figure 7.2a and Figure 7.3b. Visually, the figures 7.3a and 7.3b show a reasonable agreement of the particle size distributions. From comparison of the figures one can conclude that the dominant growth behavior of the particles in the process is captured in the estimate. In the Figure 7.3b one can see the periodic behavior of the basis functions $\phi_i(\ell)$ along the ℓ-axis appearing in the estimate of the population. This might be due to the approximation error in the system approximation. In order to obtain a quantification of the error, we define the 2-norm of the estimation error as function of time by

$$e(t) = ||n(\cdot, t) - \hat{n}(\cdot, t)||_2.$$

The estimation error, as function of time, is shown in Figures 7.2c and 7.2d. This figure shows the effect of the switching between the estimators.

The simulations with the implemented algorithm show that the estimation algorithm indeed does only perform reasonable when the initial operating point used for the linearization in the design of the initial estimator, is close to the real state of the process. That means that the initial estimation error is small. Moreover, simulations have shown that with the current type of algorithms one cannot guarantee that the state of the estimator remains in the domain of validity of the process model. As a result, it might happen that at the moment when the estimator is updated, the process model cannot be linearized at $\hat{x}(k\tau)$. Simulations have also shown that in the case when cooling is very slow and the crystal growth rate is very low, problems with the solvability of the Algebraic Riccati Equation occur. This might be due to numerical reasons. One has also to take into account that when the growth rate is small, i.e. $G(c, T) \approx 0$, the measurements of the population balance are almost constant. This indicates that the observability properties of the process might change here and the process might loose the observability properties.

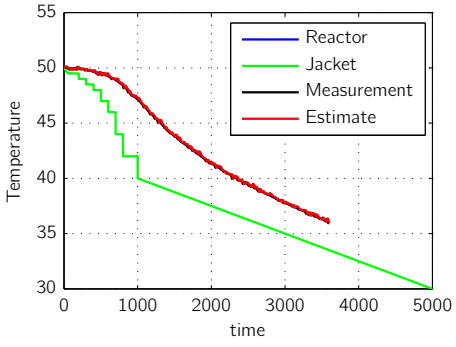

(a) Trajectory of the reactor temperature and the jacket temperature, the temperature measurement and estimated reactor temperature.

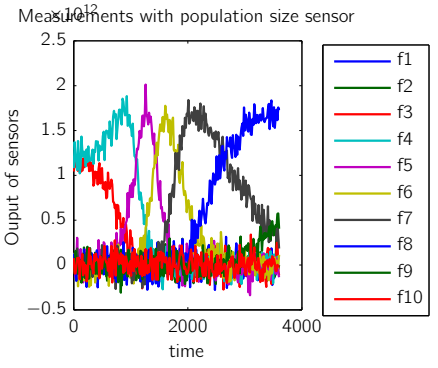

(b) Output of the particle size sensor with 10 size classes.

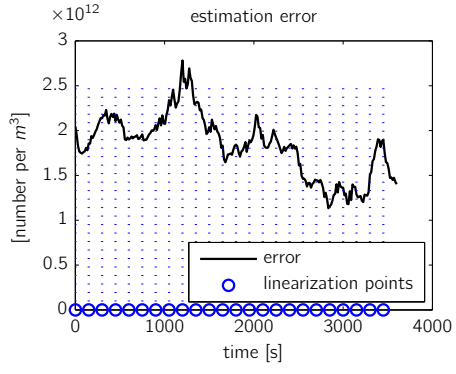

(c) Absolute estimation error

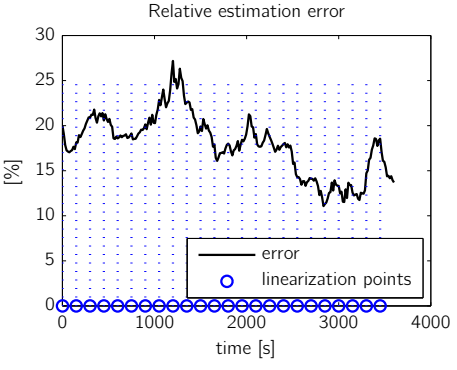

(d) Relative estimation error

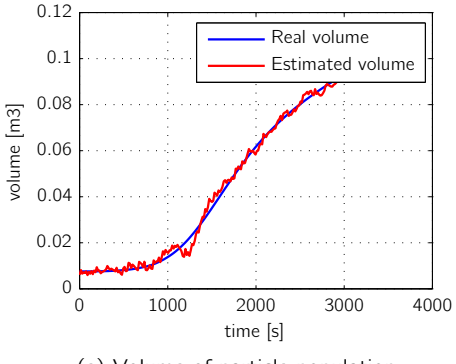

(e) Volume of particle population

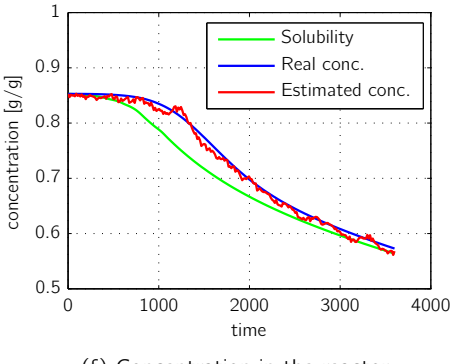

(f) Concentration in the reactor

Figure 7.2: Simulation results with population distribution measurement and temperature measurement.

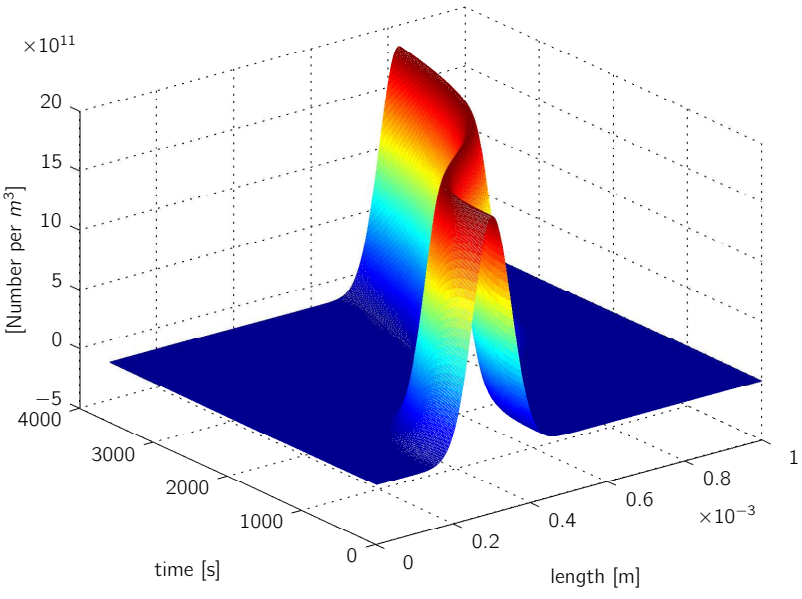

(a) Real particle population

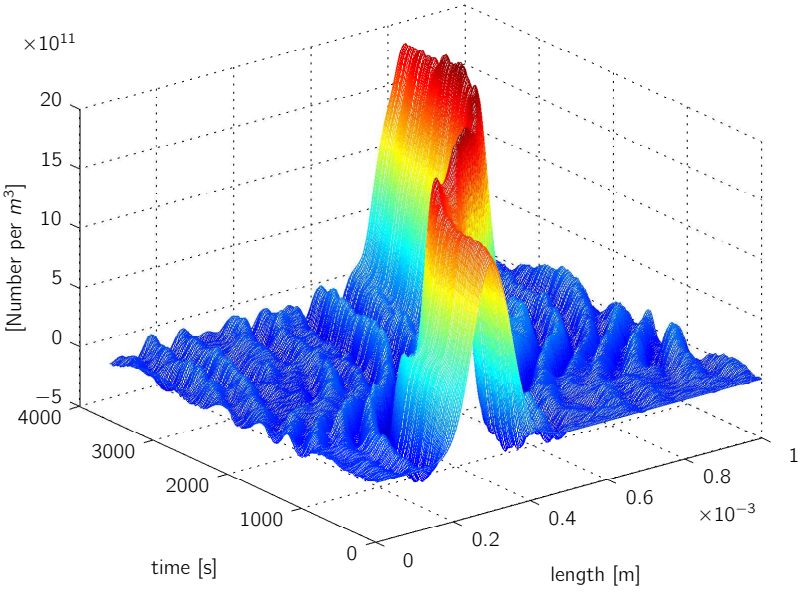

(b) Estimate of particle population

Figure 7.3: Real particle population and estimated particle population.

7.6 Conclusions and recommendations

7.6.1 Conclusions

In this chapter the design and implementation of an estimator for a Batch Cooling Crystallization process has been discussed. Since the process model is nonlinear we have introduced an algorithm in which linear estimators are used for estimation. Linear approximations of the model have been derived by linearization, and with use of the methods discussed in Chapter 6 an estimator for the linearized model has been implemented. The convergence of approximations of the optimal estimators for the linearized models has not been proved. The problem here is that we cannot show that the linearized models are uniform exponentially stabilizable and detectable. A simulation has been implemented to test the performance of the estimation algorithm. Simulations show that, under the assumption that the initial guess of the state of the process is close the real state of the process, the estimators perform reasonable and can be used to estimate the dominant behavior of the batch crystallization process.

7.6.2 Recommendations

In this study, simulations with the optimal induced 2-norm estimator have not been performed due to time limitations. It would be interesting to compare the performance of the optimal impulse response norm estimator and the optimal induced 2-norm estimator. Moreover, it is interesting to develop the algorithm further to obtain an equivalent to the extended Kalman filter for distributed parameter processes.

It is also an interesting option to investigate the possibility to design estimators based on techniques for nonlinear system such is proposed by invariant estimators [Bonnabel et al., 2008] and nonlinear observer design by coordinate transformations as described in [Kravaris et al., 2007] and [Krener and Xiao, 2002]. These techniques have the advantage to have a large domain of convergence, but are known for their computational complexity. Since the dynamics of the nonlinear batch crystallization process seems to contain a lot of structure, it is interesting to study if this structure in the model can be exploited for estimator design.

CHAPTER 8

Conclusions and Recommendations

In this thesis we have developed methods which contribute to the goal to operate batch cooling crystallization processes in such a way that the quality parameters are reproducible and predictable. This chapter gives an overview of the conclusions which have been obtained in the chapters in this thesis. The implications of the results for industrial batch crystallization processes are explained. Moreover, recommendations on how to proceed with research in these directions are provided. Finally, general conclusions on the basis of the research are given.

8.1 Overview

The research documented in this thesis has the goal to develop methods which, given the available models, knowledge of crystallization, state of the art industrial equipment and measurement technology, enable to analyze the possibility to operate the current batch cooling crystallization processes in such a way that the quality parameters become reproducible and predictable. Control and estimation methods that contribute to achieve this goal have been developed. An overview of the conclusions presented in this thesis will be given.

In the first chapter an introduction to batch crystallization processes was given. The introduction has an industrial perspective and focuses on the aspects of crystallization processes which are of importance in industrial environments. Special attention has been paid to specify the quality parameters of crystallization processes and to identity the issues which are commonly encountered in industry with respect to those quality parameters.

The second chapter was devoted to the introduction of a first principle model for the batch cooling crystallization processes. The model serves as a basis for analysis and the model based controller and estimator design in the rest of the thesis.

In Chapter 3 an analysis of the observability and controllability of the batch cooling crystallization process was presented. The analysis of observability shows what the possibilities are on the inference of information on the process states from measurements of crystallization process. The observability properties of a general batch cooling crystallization process equipped with a concentration sensor has been analyzed for the situation that the process is modeled by a population balance model and for the case that the process is modeled by a moment model. Also the observability properties of a general batch cooling crystallization process equipped with a particle size sensor has been analyzed. In the same chapter the analysis the controllability of the model of the batch cooling crystallizer is presented.

In Chapter 4 a method for control of the level of supersaturation in batch cooling crystallization processes was introduced. The control method has been based on state feedback linearization. In an experiment in an industrial environment an approximation of the control law has been tested. The experiment shows that with the (approximate) feedback linearization method, supersaturation control is possible when the rate of the consumption of material due to crystal growth is small.

In the Chapters 5, 6 and 7 we have considered the design and implementation of estimators for batch crystallization processes. The motivation stems from the fact that in batch cooling crystallization processes only a limited subset of the relevant process variables can be measured. The estimation problem deals with estimation of non-measured variables from measured ones in a causal manner. Therefore, estimators can contribute to infer more reliable, reproducible and predictable information on the process.

In Chapter 5 the design of optimal estimators for linear infinite dimensional parameters systems with finite dimensional inputs and outputs has been studied. In this chapter it has been shown how the design of estimators and controllers are related by duality. On the basis of this duality relation it has been shown how estimators can be obtained which minimize either the Hilbert-Schmidt norm or the induced $L2$ norm of the system that defines how the disturbance signals are related to the estimation error.

In Chapter 6 the problem of computation and implementation of the optimal estimators which are obtained by the design procedure in Chapter 5 has been considered. In Chapter 5 is has been shown that optimal estimators for infinite dimensional system are infinite dimensional system themselves. Moreover, the estimators cannot be computed explicitly for most systems. In Chapter 6 methods for approximation of the solutions for the linear quadratic optimal control problem are summarized and these methods have been applied in the context of the approximation and implementation of estimators. In two examples it has shown that for the test problems the convergence of approximation of estimators to the optimal estimator can be shown.

In Chapter 7 we have applied the results which were obtained in Chapter 5 and Chapter 6 to derive an estimator for the batch cooling crystallization process. Special attention has been paid to the implementation of the estimator in a simulation environment. In a

simulation-example is has been shown that this estimator can be used to obtain estimates of the temperature and population balance in the crystallization process.

8.2 Contributions and recommendation for future work

Chapter 2 - Modeling of batch cooling crystallization processes

In Chapter 2 a model that is representative for most of the batch cooling crystallization processes with closed mass balance has bee introduced. The model is based on the use of population balance models and in order the focus on the dominant dynamic behavior and characteristic of the process, the model contains only the dominant mechanisms of the crystallization process. That is, the structure of the model is independent of the exact growth rate and birth rate kinetics of the crystallization process. Since the model of the process is a hybrid nonlinear distributed parameter model, three scenarios of operation has been proposed to reduce the complexity of the analysis. In two scenarios, the growth scenario and the dissolution scenario, it is assumed that the model does not switch between the modes such that the process model does not exposes its hybrid character. Therefore, the behavior of the process in these two modes can be analyzed without the hybrid character has to be taken in to account. In the third scenario, the hybrid character of the process is exposed and analysis of the process behavior is more complicated.

Chapter 3 - Observability and controllability of crystallization processes

In Chapter 3 we have analyzed the observability and controllability of the batch cooling crystallization process. Although the concept of observability is well known, we have returned to the definitions of observability since our process is not described by a linear finite dimensional model. Starting from the definition we have analyzed the observability of process model for batch cooling crystallization. The observability properties of a general batch cooling crystallization process equipped with a concentration sensor have been analyzed for the situation that the process is modeled by a population balance model and for the case that the process is modeled by a moment model. The analysis has shown that from concentration measurements, only information about the first three moments can be obtained. The observability properties of a general batch cooling crystallization process equipped with a particle size measurement has been analyzed. In order to do so we have proposed a model for the crystal size sensors. We have analyzed the observability for the case where the population sensors performs ideal classification and the crystal growth rate is constant with respect to time. It follows that in this situation, the process is approximately observable. The situation in which the crystal growth rate is not constant, no results have been derived. This situation is left open for future research.

In the second part of Chapter 3 we have analyzed the controllability of batch cooling crystallization processes. We have started from our definition of controllability and we have shown that when the process is operated in either the growth mode or the dissolution mode the process is not controllable. With our notion of controllability and

with temperature as actuation mechanism, this means that it is not possible to steer the system towards an arbitrary particle size distribution in finite time. For the scenario that the process switches between growth and dissolution mode no analysis has been given. This is due to the lack of analysis methods and the complexity the controllability problem for such processes. On the other hand, we indicate that it is very likely that, in case the process would be controllable by use of this operation sceneario, the development of a control methodology that is able to cope with the hybrid characteristics of the process is a very complex task.

It is recommended to analyze if there are possibilities to improve the controllability properties of the batch cooling crystallization process. One possibility is to investigate if one can find more principles of actuation for the state of the population balance. It is recommended to pay extra attention to actuation principles that enable to apply corrective action in the direction of the desired state. Examples are the design of systems in which undesired particles can be dissolved, a lack of particles can be compensated by controlled nucleation and seeding or systems in which small particles can achieve a higher growth rate than particles with the desired size.

Secondly, in our definition of controllability we have discussed the situation in which we desire to steer the process from an arbitrary state to an arbitrary different state in finite time. This definition might be over restrictive. From an industrial point of view, a large set of states might be not interesting or not relevant of physical ground. It might be interesting to investigate alternatives for the definition of controllability and to study if it is possible to connect the concept of controllability more directly with control of the quality parameters of the process.

Chapter 4 - Control of batch cooling crystallization by feedback linearization

Chapter 4 we have developed a method that enables the control of the super saturation in a batch crystallization process. The method for supersaturation control enables to control the driving force for crystal growth and nucleation. The method is based on an application of the theory of feedback linearization. Extensive attention has been paid to the theoretical analysis of the method. The application of the feedback linearization method enables to control the supersaturation in the process by use of a linear controller. The situation in the presence of parametric uncertainties in the model has been analyzed. It has been shown that an uncertainty description of suitable for robust controller design can be obtained and can be used for robust controller design. We proved that this method results in controllers that stabilize the nonlinear process in a robust way. This is very much in contrast to earlier results in which feedback linearization methods are known to be non-robust. As such, the method enables to operate crystallization processes such that the supersaturation trajectory is reproducible. The performance of the controlled system and the influence of measurement noise has been analyzed in a simulation study. An approximation of the method of feedback linearization has been tested in an industrially representative case.

The experimental results show the method can be applied successfully in an industrial environment. The approach offers an efficacious method for the control the super-saturation level and the controller enables proper control of the supersaturation in a

crystallization process for situations where material consumption is small. A nice feature is the limited complexity and the limited need of kinetic information.

Chapter 5 - Estimation for distributed parameter systems

In Chapter 5 the design of optimal estimators for infinite dimensional systems has been analyzed. We have defined two criteria for estimator design. In both the criteria we have defined a norm of the system that represents the transfer from the disturbance sources to the estimation error. We have considered the Hilbert-Schmidt norm of the error system and the induced L_2 norm of the error system as design criterion. We have shown how the designs of estimators and controllers are related by duality. On the basis of this duality relation, we have shown how estimators can be obtained which minimize either the Hilbert-Schmidt norm or the induced L_2 norm of the error system. We have presented a very complete solution to the optimal estimator design problem for both cases in the setting of estimation over finite time horizon. Both optimal the Hilbert-Schmidt optimal and optimal L_2 induced gain estimators prove to be infinite dimensional time-variant and causal systems. We have provided explicit representations of the estimators both in kernel as well as in state space form. In the situation of minimization of the induced L_2 norm we have analyzed the situation with known and unknown initial condition. Moreover, we have presented a solution to the design problem for time invariant estimators for estimation problems over infinite time horizon.

Chapter 6 - Approximation and implementation of estimators

In Chapter 6 the implementation of estimators for linear distributed parameter systems has been studied. We have introduced a fairly general mathematical framework for the approximation of infinite dimensional systems with the purpose to implement estimators for infinite dimensional systems. We have analyzed the approximation of optimal impulse response estimators and introduced a condition for which the performance of the approximations converges to the optimal estimator. Using the theory that relates estimation and control problems, developed in Chapter 5 we have shown how existing results on approximations in the context of the linear quadratic regulator can be applied in the context of estimation problems. We have applied the theoretical results in two examples. In the examples we analyzed and implemented the approximation of estimators for a system with diffusion and for a system with convection. We have not studied the approximation of optimal L_2 estimators, which is left for future research. In two examples we have shown that the approximations of estimators can be implemented in a suitable application.

In the approximation framework introduced in Chapter 6, there are some choices that have to be made, especially in the subspaces and projection operators used for approximation. We have not discussed on how the choices in system approximation should be made, but this is an interesting topic of future research to study if one can find preferred projections for the approximation of estimators. It would be interesting to study if there exist preferable choices that are generally suitable for typical classes of systems.

Chapter 7 - Estimators design and implementation for crystallization

Chapter 7 is devoted to the application of the results which have been developed in

Chapter 5 and Chapter 6 to a model of batch cooling crystallization process. Since the results obtained in the Chapter 5 and Chapter 6 are only valid for linear systems, we have proposed an estimation algorithm based on linear approximations of the model of the batch cooling crystallization process. Since the linear approximations have a limited region of validity, we proposed a method of scheduled re-linearization, estimators synthesis and switching of estimators.

We have introduced the method of linearization for distributed parameter systems. In the analysis we have studied whether there exists a preferred order in linearization and finite dimensional approximation of the nonlinear system. Moreover, we have identified conditions on the operating point and approximation scheme for which the order is not of relevance.

In the design and implementation of the estimator for the crystallization process we have taken a different approach than what is common in engineering applications. That is, we have not relied on numerical approximation tools to obtain a high dimensional finite dimensional approximation of the system from the start of the implementation phase, but we have postponed the system approximation. Idea behind this approach is that we prefer to treat the approximated system not as complete black box.

The estimation algorithm has been implemented in the simulation environment Matlab. In the simulation we estimate the states of a simulator of the batch cooling crystallization process. The simulation shows that the estimator is able to estimate the state of the process. We have identified some issues that arise due to the linearization approach that we have chosen. The estimator which has been developed has been based on estimation for linear systems and is not able to incorporate constraints on states or the estimated variables. The incorporation of constraints in estimation methods is an interesting research topic for future research. Moreover, it should be noted that the estimator is not optimal for the system and that it might be interesting to compare the performance of the algorithm with estimation algorithms such as the Ensemble Kalman Filter and or a Particle Filter.

Future research is possible in the direction of the robustness of the estimators with respect to parameter variations and structural variations in the process model. Also, since the estimators are based on linear approximations of the nonlinear process model, convergence of the estimation error cannot be expected when the initial estimation error is large. Possibilities for the improvement of the convergence region might be a subject of study.

8.3 General conclusions

The work presented in this thesis has been motivated by the goal to develop methods which enable to operate the current batch cooling crystallization processes in such a way that the quality parameters become reproducible and predictable. Although there are still a large number of open questions, the methods for supersaturation control and methods to design and implement estimators contribute to this goal.

With the development and analysis of estimators for distributed parameter systems we have shown that it is possible to develop estimators for population balance systems. In this way, we have provided an alternative to moment model based estimators, that is able to estimate particle size distributions. The methods for estimator design and implementation are not restricted to crystallization processes, but can also be used for different systems and engineering applications.

It is important to note that the methods developed are based on models of the process. Therefore, we rely on the validity of these models. Especially in crystallization processes accurate predictive dynamic models often do not exist and it is known that the solubility, and growth and birth rate kinetics are sensitive to impurities. The development of methods to learn this type of information from online experiments or even during the batch is recommended.

The methods developed do not provide a methodology which strictly guarantees that the quality parameters of crystallization are reproducible and predictable. The analysis of the controllability of the process has shown that the controllability of the process, especially of the particle size distribution, is limited. Therefore, the possibilities to steer the system from undesired states to more desired states are rather limited. The development of actuation methods and other methods to improve the controllability of the process have to be encouraged.

General recommendations

During the research some interesting topics have been encountered which are worth to be considered as topic for further investigation.

- In the process industry it is common practice to classify processes in batch and continuous process. Is has been generally accepted by process engineers and control engineers that batch processes suffer from "limited actuation" and are "more difficult to control" compared to continuous processes [Bonvin, 1998, 2006]. It would be a very interesting challenge to study what the fundamental difference between the two classes of processes is from a system theoretic point of view and what the implications are for the identification, optimization, robustness analysis, and controller and estimator synthesis for batch processes.
- The complex step differentiation [Squire and Trapp, 1998; Martins et al., 2003] method has been analyzed and has shown extraordinary results in the numerical approximation of derivatives of functions. The method is an interesting alternative for standard finite difference methods and can be useful for the development of algorithms where numerical differentiation of functions is used, such as the extended Kalman estimator.
- During a study on methods for numerical approximation and simulation of the population balance equations the CE/SE method has shown to be interesting. The method has can be found in [Chang, 1995; Chang et al., 2000] and originates from research in computational fluid dynamics. The method has been applied to population balance systems in [Motz et al., 2002].

APPENDIX A

Mathematical Notation

A.1 Lie derivative

The Lie-derivative evaluates the change of a vector field or scalar function with respect to the flow of another vector field. In this section, the Lie-derivative of the scalar function h with respect to the vector field f will be introduced. For an in-depth introduction we refer to [Nijmeijer and Van der Schaft, 1990]. Let f be a continuously differentiable vector field defined on $\mathbb{R}^n$ and let $h(x)$ be a continuously differentiable function $h : \mathbb{R}^n \mapsto \mathbb{R}$. The Lie derivative of h with respect to f, is a mapping $L_f h(x) : \mathbb{R}^n \to \mathbb{R}$ and is defined as,

$$L_f h(x) := \langle d_x h, f \rangle (x) \in \mathbb{R}, \tag{A.1}$$

where $d_x = \frac{\partial}{\partial x}$ and $\langle \cdot, \cdot \rangle$ denotes the Euclidean inner product.

Higher order Lie derivatives are defined as follows,

$$L_f^k h(x) := L_f[L_f^{k-1} h(x)] = \left\langle d_x L_f^{k-1} h, f \right\rangle (x), \;\; k = 2, 3, \ldots . \tag{A.2}$$

For $f(x) = [f_1(x), \cdots, f_n(x)]^\top$ and $x = [x_1, x_2, \ldots, x_n]^\top$ the Lie-derivative $L_f h(x)$ can be computed as follows:

$$L_f h(x) = \langle d_x h, f \rangle = \frac{\partial h}{\partial x_1}(x) f_1(x) + \cdots + \frac{\partial h}{\partial x_n}(x) f_n(x).$$

APPENDIX B

Appendix to Chapter 3

B.1 Construction of indistinguishable distributions

In Section 3.2.1 the observability of a batch cooling crystallization process with concentration measurements has been analyzed. For the analysis the process has been modeled by the model (3.4) and the sensors has been modeled by Equation (3.7). It has been shown in theorem 3.2.1 that for a sensor which measures moments of the distribution up to the order k (c.f. Equation (3.7)), the kernel of the observability can be characterized by distributions $n \in L_2(\mathbb{L}, \mathbb{R})$ for which the moments $0, 1, ...k$ are zero. As such, distributions of which the moments $0, 1, ...k$ are zero are indistinguishable from each other. It is interesting to know if indistinguishable distrubutions have physical relevance.

In this section we consider an method to construct distributions which are indistinguishable by concentration measurements, as introduced in Section 3.2.1. That is, we show that it is possible to construct a non zero function $n(\ell) \neq 0$ such that the first k moments are zero. The following theorem allows to characterized the moments of a special class of functions as a matrix equation in the coefficients. With use of Theorem B.1.1 one can construct states which indistinguishable at the output of system (3.8). As illustration we will construct a function which is unobservable for a sensor with $k = 3$.

Theorem B.1.1
Consider functions $h(\ell)$ in the class:

$$\mathcal{H} := \{h : \mathbb{R} \to \mathbb{R} = h(\ell) = \sum_{i=1}^{m} a_i e^{p_i \ell}, m < \infty a_i \in \mathbb{R}, p_i < 0, p_i \neq p_j\}$$

Let $\alpha_0, ..., \alpha_m \in \mathbb{R}^m$ be the set of moments of h defined by $\alpha_i = \int_0^\infty \ell^i h(\ell) \mathrm{d}\ell$ for

$i = \{0, ..., m\}$. *Then the the moments of* $h(\ell)$ *and the coefficients* a_i, p_i *for* $i \in \{0, ..., m\}$ *are related by the matrix equation:*

$$Ma = b$$

$$\begin{bmatrix} p_1^{-1} & p_2^{-1} & \cdots & \cdots & p_{m-1}^{-1} & p_m^{-1} \\ \vdots & \vdots & \vdots & \vdots & \vdots & \vdots \\ (-1)^m m! p_1^{-1-m} & (-1)^m m! p_2^{-1-m} & \cdots & \cdots & (-1)^m m! p_{m-1}^{-1-m} & (-1)^m m! p_m^{-1-m} \end{bmatrix} \begin{bmatrix} a_1 \\ \vdots \\ a_m \end{bmatrix} = \begin{bmatrix} \alpha_0 \\ \vdots \\ \alpha_m \end{bmatrix} \tag{B.1}$$

Proof. We introduce the Laplace transforms $H(s)$ of the function $h(\ell)$, which is given by:

$$H(S) = \sum_{i=1}^{m} a_i (s + p_i)^{-1},$$

with region of conversion $s < min(Re(p_i))$. Then use the following property, which can be found in [Antoulas, 2005, p345]

$$\alpha_k = \int_0^\infty \ell^k h(\ell) \mathrm{d}\ell = (-1)^k \frac{\mathrm{d}^k H}{\mathrm{d}s^k}\Big|_{s=0}. \tag{B.2}$$

For the class of functions under consideration $\frac{\mathrm{d}^k H}{\mathrm{d}s^k}$ is given by:

$$\frac{\mathrm{d}^k H}{\mathrm{d}s^k} = \sum_{i=1}^{m} a_i (-1)^k k! (s + p_i)^{-1-k}. \tag{B.3}$$

Therefore, it follows from substitution of (B.3) into (B.2) that the moment α_k is given by:

$$\alpha_k = \frac{\mathrm{d}^k H}{\mathrm{d}s^k}\Big|_{s=0} = \sum_{i=1}^{m} a_i (-1)^k k! p_i^{-1-k}. \tag{B.4}$$

The Matrix-equation (B.1) is a matrix representation of (B.4) for $k \in \{0, 1, ..., m\}$ □

The theorem now enables to construct a function $h(\ell)$ which has the first k moments equal to zeros. We will show this in the following example.

Example B.1.1

In this example we construct a nonzero function $n(\ell)$ *which is indistinguishable from* $n_0(\ell) = 0$ *for a sensor defined by Equation* (3.7) *with* $k = 3$. *From Theorem B.1.1 it follows that this can be done by choosing* $m > k$. *In addition to the constraints on the first three moments, we demand* $n(0) = 0$ *to be compatible with the boundary condition of* (3.8). *This results in the following system of equations,*

$$Ma = b \tag{B.5}$$

$$\begin{bmatrix} 1 & 1 & 1 & 1 & 1 & 1 \\ p_1^{-1} & p_2^{-1} & p_3^{-1} & p_4^{-1} & p_5^{-1} & p_6^{-1} \\ -p_1^{-2} & -p_2^{-2} & -p_3^{-2} & -p_4^{-2} & -p_5^{-2} & -p_6^{-2} \\ 2p_1^{-3} & 2p_2^{-3} & 2p_3^{-3} & 2p_4^{-3} & 2p_5^{-3} & 2p_6^{-3} \\ -6p_1^{-4} & -6p_2^{-4} & -6p_3^{-4} & -6p_4^{-4} & -6p_5^{-4} & -6p_6^{-4} \\ 24p_1^{-5} & 24p_2^{-5} & 24p_3^{-5} & 24p_4^{-5} & 24p_5^{-5} & 24p_6^{-5} \end{bmatrix} \begin{bmatrix} a_1 \\ a_2 \\ a_3 \\ a_4 \\ a_5 \\ a_6 \end{bmatrix} = \begin{bmatrix} n(0) \\ \alpha_0 \\ \alpha_1 \\ \alpha_2 \\ \alpha_3 \\ \alpha_4 \end{bmatrix}, \tag{B.6}$$

where the first row of M is due to the boundary condition n at $\ell = 0$. We choose $n(0) = 0$, and $\alpha_0 = \alpha_1 = \alpha_2 = \alpha_3 = 0$. The coefficients due to $k!$ in Equation (B.4) can be divided out of the equations and we observe that the matrix M is the transpose of a Vandermonde matrix and is invertable for all $p_i \leq 0$. We have the following result on the regarding determinant of M:

Lemma B.1.2
The determinant of M is given by:

$$\det M = \prod_{1 \leq i < j \leq 6} (p_j - p_i)$$

A proof can be found in [Golub and Van Loan, 1996].

Therefore, we conclude that $\det(M) \neq 0$ *if and only if $p_j \neq p_i$ for $i \neq j$. Equivalently, the inverse of M exists if we chose the poles p_i distinct. To test the algorithm, we choose the poles such that $p_i = i$ and $\alpha_6 = 1/24$ and we obtain the function shown in Figure 3.1.*

B.2 Observability co-distribution for moment models

In this appendix we show the calculation of the observability co-distribution that has been used in the analysis of the observability of the moment model (3.30a) with concentration measurements, which is presented in Section 3.2.2. For the analysis, we only consider states in which crystals do grow, i.e. states $x \in X^G$, with X^G defined by the set(3.31). For the system Σ_{mon} we calculate the observability algebra and observability co-distribution.

B.3 Observability Algebra of moment model

We use the Lie-derivative of $h : X \to \mathbb{R}$ along f:

$$L_f(h) = \langle dh, f \rangle$$

First we calculate the one forms dh_1 and dh_2:

$$dh_1 = \begin{bmatrix} 0, 0, 0, -1, 0 \end{bmatrix}^\top, \qquad dh_2 = \begin{bmatrix} 0, 0, 0, 0, 1 \end{bmatrix}^\top.$$

Then we calculate the first order Lie derivatives:

$$\begin{aligned} L_f h_1 &= \langle dh_1, f \rangle = -3G\mu_2, & L_f h_2 &= \langle dh_2, f \rangle = -\alpha T, \\ L_g h_1 &= \langle dh_1, g \rangle = 0, & L_g h_2 &= \langle dh_2, g \rangle = 1. \end{aligned}$$

From the first order Lie derivatives the following one forms are calculated:

$$\begin{aligned} dL_f h_1 &= \begin{bmatrix} 0, 0, -3G, 0, -3G_c\mu_2, -3G_T\mu_2 \end{bmatrix}^\top, \\ dL_f h_2 &= \begin{bmatrix} 0, 0, 0, 0, 0, -1 \end{bmatrix}^\top, \\ dL_g h_1 &= dL_g h_2 = 0. \end{aligned}$$

Then we calculate the second order Lie derivatives, which are given by:

$$\begin{aligned}
L_f L_f h_1 =& \langle dL_f h_1, f\rangle = -2G^2\mu_1 + 9GG_c\mu_2^2 - 3G_T\mu_2(T_0 - T),\\
L_g L_f h_1 =& \langle dL_f h_1, g\rangle = -3G_T\mu_2,\\
L_f L_f h_2 =& \langle dL_f h_2, f\rangle = -\alpha T,\\
L_g L_f h_2 =& \langle dL_f h_2, g\rangle = -1.
\end{aligned}$$

The second order Lie derivatives $L_f L_g h_1$,$L_g L_g h_1$,$L_f L_g h_2$,$L_g L_g h_2$ are zero. Moreover we have that$L_f L_f h_2 = L_f h_2$, from which we deduce that $(L_f)^i h_2 = L_f h_2$ for $i \in \mathbb{Z}$. It follows that $L_g(L_f)^i h_2 = L_g L_f h_2 = -1$ for $i \in \mathbb{Z}$ and that $L_f L_g(L_f)^i h_2 = L_g L_g(L_f)^i h_2 = 0$ for $i \in \mathbb{Z}$.

From the second order Lie derivatives we calculate the one forms $dL_f L_f h_1$, $dL_g L_f h_1$, $dL_f L_f h_2$,$dL_g L_f h_2$:

$$dL_f L_f h_1 = \begin{bmatrix} 0 \\ -2G^2 \\ 18GG_c\mu_2 \\ 0 \\ -4GG_c\mu_1 + 9(G_cG_c + GG_{cc})\mu_2^2, -3G_c\mu_2 \\ -4G_TG\mu_1 + 9(G_TG_c + GG_{cT})\mu_2^2 - 3(G_{TT}(T_0 - T) - G_T)\mu_2 \end{bmatrix} \qquad dL_g L_f h_1 = \begin{bmatrix} 0 \\ 0 \\ -3G_T \\ 0 \\ -3G_{Tc}\mu_2 \\ -3G_{TT}\mu_2 \end{bmatrix}$$

Then we calculate the third order Lie derivatives, which are given by:

$$\begin{aligned}
L_f L_f L_f h_1 =& \langle dL_f L_f h_1, f\rangle\\
=& -2G^3\mu_0 + 36G^2G_c\mu_1\mu_2 - 3(-4GG_c\mu_1 + 9(G_cG_c + GG_{cc})\mu_2^2, -3G_c\mu_2)G\mu_2\\
& - (-4G_TG\mu_1 + 9(G_TG_c + GG_{cT})\mu_2^2 - 3(G_{TT}(T_0 - T) - G_T)\mu_2)(T_0 - T)\\
L_g L_f L_f h_1 =& \langle dL_f L_f h_1, g\rangle = -6G_T u_1 - 9G_{Tc}G\mu_2^2 - 3G_{TT}\mu_2(T_0 - T)
\end{aligned}$$

From the second order Lie derivatives we calculate the one forms $dL_f L_f L_f h_1$ and $dL_g L_f L_f h_1$:

$$dL_f L_f L_f h_1 = \begin{bmatrix} -2G^3 \\ * \\ * \\ * \\ * \end{bmatrix} \qquad dL_g L_f L_f h_1 = \begin{bmatrix} 0 \\ -6G_T \\ -18G_{Tc}G(c(t), T(t))\mu_2 - 3G_{TT}(T_0 - T) \\ * \\ * \end{bmatrix},$$

We construct the space $d\mathcal{O}'$, which is a subspace $d\mathcal{O}$:

$$\begin{aligned}
d\mathcal{O}' =& span\{dh_1, dh_2, dL_f h_1, dL_f L_f h_1, dL_g L_f h_1 dL_f L_f L_f h_1\}\\
=& span\{ \begin{bmatrix} 0 \\ 0 \\ 0 \\ 1 \\ 0 \end{bmatrix}, \begin{bmatrix} 0 \\ 0 \\ 0 \\ 0 \\ 1 \end{bmatrix}, \begin{bmatrix} 0 \\ 0 \\ -3G \\ -3G_c\mu_2 \\ -3G_T\mu_2 \end{bmatrix}, \begin{bmatrix} 0 \\ -2G^2 \\ 18GG_c\mu_2 \\ * \\ * \end{bmatrix} \begin{bmatrix} 0 \\ 0 \\ -3G_T \\ -3G_{Tc}\mu_2 \\ -3G_{TT}\mu_2 \end{bmatrix}, \begin{bmatrix} -2G^3 \\ * \\ * \\ * \\ * \end{bmatrix} \}.
\end{aligned}$$

APPENDIX C

Lagrangian formulation of optimal LQ control

In this appendix we document the solution to the linear quadratic optimal control problem with exogenous input and linear and quadratic final stage cost based on the Lagrangian method of optimization.

Consider the problem of optimal control in the presence of an exogenous input w.

$$\min_{u,x} \frac{1}{2} \int_{t_0}^{t_f} x^\top Q x + u^\top R u + x^\top S u \, dt + x^\top(t_f) E x(t_f) + h^\top x(t_f)$$
$$\text{subject to } \dot{x} = Ax + Bu + Dw,\ x(0) = 0$$

Recognizing the standard formulation of a optimization problem with equality constraints:

$$\min_{u,x} \int_{t_0}^{t_f} F(x,u)\mathrm{d}t + \Phi(x(t_f)),$$
$$\text{subject to } Ax + Bu + Dw - \dot{x} = 0,\ x(0) = 0$$
$$\text{with: } \Phi(x(t_f)) = x^\top(t_f) E x(t_f) + h^\top x(t_f),$$
$$F(x,u) = \frac{1}{2}(x^\top Q x + u^\top R u + x^\top S u).$$

With use of Lagrange multipliers we define the Lagrangian $L(x,u,\lambda)$ for this problem as follows

$$L(x,u,\lambda) = \int_{t_0}^{t_f} F(x,u) + \lambda^\top [Ax + Bu + Dw - \dot{x}]\mathrm{d}t + \Phi(x(t_f)).$$

By use of integration by parts, we rewrite this to:

$$\begin{aligned}
L(x,u,\lambda) =& \int_{t_0}^{t_f} F(x,u) + \lambda^\top [Ax + Bu + Dw - \dot{x}]\,\mathrm{d}t + x^\top(t_f)Ex(t_f) + h^\top x(t_f) \\
=& \int_{t_0}^{t_f} F(x,u) + \lambda^\top [Ax + Bu + Dw]\,\mathrm{d}t - [\lambda^\top x]_{t_0}^{t_f} + \\
& \int_{t_0}^{t_f} \dot{\lambda}^\top x\,\mathrm{d}t + x^\top(t_f)Ex(t_f) + h^\top x(t_f) \\
=& \int_{t_0}^{t_f} H(x,u,\lambda) + \dot{\lambda}^\top x\,\mathrm{d}t - [\lambda^\top(t_f)x(t_f) - \lambda^\top(t_0)x(t_0)] + x^\top(t_f)Ex(t_f) + h^\top x(t_f)
\end{aligned}$$

with $H(x,u,\lambda) = F(x,u) + \lambda^\top[Ax + Bu + Dw]$

The minimum of the Lagrangian with respect to (x,u), defines the cost function for the dual optimization problem, denoted by $l(\lambda)$:

$$l(\lambda) = \min_{u,x} L(x,u,\lambda).$$

The dual (unconstrained) optimization problem is given by:

$$\max_{\lambda} l(\lambda)$$

In the remainder of this section we will solve the dual optimization problem.

Using the first order optimality conditions state that the optimum is located at the saddle point of $L(x,u,\lambda)$, given certain necessary conditions hold. At the optimum (x^*,u^*,λ^*) the following condition holds:

$$\nabla L(x^*,u^*,\lambda^*) = 0$$

This provides the conditions that at the optimum:

$$\frac{\partial L}{\partial \lambda}(x^*,u^*,\lambda^*) = 0,\ \frac{\partial L}{\partial x}(x^*,u^*,\lambda^*) = 0,\ \frac{\partial L}{\partial u}(x^*,u^*,\lambda^*) = 0$$

We calculate the partial derivatives:

$$\begin{aligned}
\frac{\partial L}{\partial \lambda} &= \frac{\partial H}{\partial \lambda} = Ax + Bu + Dw - \dot{x} \\
\frac{\partial L}{\partial x} &= \frac{\partial H}{\partial x} + \dot{\lambda} = Qx + Su + \lambda^\top A + \dot{\lambda} \\
\frac{\partial L}{\partial u} &= \frac{\partial H}{\partial u} = Ru + S^\top x + B^\top \lambda
\end{aligned}$$

Therefore, it follows from the condition $\nabla L(x^*,u^*,\lambda^*) = 0$ that at the optimimum:

$$u = -R^{-1}(B^\top \lambda + S^\top x) \tag{C.1}$$

$$\dot{\lambda} = -Qx - Su - \lambda^\top A, \tag{C.2}$$

$$\dot{x} = Ax + Bu + Dw \tag{C.3}$$

and we deduce that at the optimum the following relations hold:

$$\begin{bmatrix} \dot{x} \\ \dot{\lambda} \end{bmatrix} = \begin{bmatrix} A - BR^{-1}S^\top & -BR^{-1}B^\top \\ -Q + SR^{-1}S^\top & -A^\top + SR^{-\top}B^\top \end{bmatrix} \begin{bmatrix} x \\ \lambda \end{bmatrix} + \begin{bmatrix} D \\ 0 \end{bmatrix} w \tag{C.4}$$

with the boundary values $x(0) = x_0$ and $\lambda(t_f) = Ex(t_f) + h$.

Next we will introduce the following coordinates $\begin{bmatrix} x(t) \\ \sigma(t) \end{bmatrix}$ with $\sigma(t) = \lambda(t) - P(t)x(t)$ and time dependent operator P. The time index of P has been omitted for brevity. This is described by the coordinate transformation $T = \begin{bmatrix} I & 0 \\ P & I \end{bmatrix}$ and $T^{-1} = \begin{bmatrix} I & 0 \\ -P & I \end{bmatrix}$ and it follows that $\begin{bmatrix} x \\ \lambda \end{bmatrix} = T \begin{bmatrix} x \\ \sigma \end{bmatrix}$. This gives $\begin{bmatrix} \dot{x} \\ \dot{\lambda} \end{bmatrix} = T \begin{bmatrix} \dot{x} \\ \dot{\sigma} \end{bmatrix} + \dot{T} \begin{bmatrix} x \\ \sigma \end{bmatrix}$, such that we conclude that:

$$\begin{bmatrix} \dot{x} \\ \dot{\sigma} \end{bmatrix} = T^{-1}(\begin{bmatrix} \dot{x} \\ \dot{\lambda} \end{bmatrix} - \dot{T} \begin{bmatrix} x \\ \sigma \end{bmatrix}).$$

The system (C.4) in new coordinates is given by:

$$\begin{bmatrix} \dot{x} \\ \dot{\sigma} \end{bmatrix} = \begin{bmatrix} A - BR^{-1}S^\top - BR^{-1}B^\top P & -BR^{-1}B^\top \\ \chi & -A^\top + SR^{-\top}B^\top + PBR^{-1}B^\top \end{bmatrix} \begin{bmatrix} x \\ \sigma \end{bmatrix} + \begin{bmatrix} D \\ -PD \end{bmatrix} w$$

with: $\chi = -\dot{P} - Q + SR^{-1}S^\top - (A^\top - SR^{-\top}B^\top)P - P(A - BR^{-1}S^\top) + PBR^{-1}B^\top P$

Then it follows the state $\sigma(t)$ is independent of $x(t)$ if $\chi(t) = 0$ for all t This implies that for decoupling of σ and x, P has to the Riccati differential equation:

$$-\dot{P} = (A^\top - SR^{-\top}B^\top)P + P(A - BR^{-1}S^\top) - PBR^{-1}B^\top P + (Q - SR^{-1}S^\top) \tag{C.5}$$

The initial condition of the Riccati differential equation follow from the boundary values of x and σ. From the problem description if follows that $x(0) = x_0$. Therefore:

$$\begin{aligned} \sigma(t_f) &= \lambda(t_f) - P(t_f)x(t_f) \\ &= Ex(t_f) + h - P(t_f)x(t_f) \end{aligned}$$

Choosing $P(t_f) = E(t_f)$ yields $\sigma(t_f) = h$. Alternatively, the Riccati equationC.5can be rewritten into the following form:

$$-\dot{P} = A^\top P + PA + Q - (PB - S)R^{-1}(B^\top P - S^\top)$$

When $\chi = 0$, σ statisfies the following differenctial equation

$$\dot{\sigma} = (-A^\top + SR^{-\top}B^\top + PBR^{-1}B^\top)\sigma - PDw, \quad \text{with } \sigma(t_f) = h. \tag{C.6}$$

It follows from (C.1) that the optimal input is given by:

$$u^* = -R^{-1}((B^\top P + S^\top)x + B^\top \sigma),$$

where σ satisfies (C.6).

It follows that the optimal input u depends on x but also on σ. The system σ represents a differential equation in reversed time with end-point condition and dependent on w. Therefore the input u depends noncausal on the disturbance w and anticipates on distrurbances in future. When we set $h = 0$ and $w = 0$ the solution to the linear quadratic regulator problem is obtained. In this case we have $\sigma(t) = 0$ for all t, which follows since it can be shown that $V(x) = xPx$ is a Lyaponov function and that $A - BR^{-1}S^{\top} - BR^{-1}B^{\top}P$ is exponentially stable. It is interesting to observe that if $w = 0$, $h \neq 0$, the solution remains non causal.

APPENDIX D

Proofs

D.1 Adapted proof for Theorem 6.4.3

An incorrect step in the original proof of Theorem 2.1 in [Ito, 1987], which can be found in this thesis as Theorem 6.4.3, has been observed. First the setting of the theorem will be defined. Secondly the Theorem will be stated and then the point of concern will be indicated. Finally, an alternative to correct the proof will be presented.

Assume that X, U and Y are Hilbert spaces, that X_N is a finite dimensional subspace of X and that $P_N : X \to X_N$ is a projection operator. Let $A : D(A) \to X$ and $A : X_N \to X_N$ be the generators of c_0 semigroups $T(t) : X \to X$ and $T_N(t) : X_N \to X_N$ respectively. Consider the systems Σ and Σ_N, given by:

$$\Sigma : \begin{cases} \dot{x} = Ax + Bu \\ y = Cx \end{cases} \qquad \Sigma_N : \begin{cases} \dot{x}_N = A_N x_N + B_N u \\ y_N = C_N x_N \end{cases}$$

with initial conditions $x(0) = x_0$ $x_N(0) = x_{N,0}$ and the operators B, B_N, C, C_N be bounded and defined such that $B \in \mathcal{L}(U, X)$,$B_N \in \mathcal{L}(U, X_N)$, $C \in \mathcal{L}(X, Y)$ and $C_N \in \mathcal{L}(X_N, Y)$.

Associated to the system Σ we consider the problem of minimization of the following functional

$$J(u, x_0) = \int_0^\infty ||y(t)||_2^2 + ||u(t)||_2^2 \mathrm{d}t.$$

It is well known that if (A, B) is stabilizable and (A, C) is detectable that the optimal solution is $u_{opt}(t) = -B^* \Pi T(t) x_0$, where Π is the non negative solution of the Riccati

equation:

$$A^*\Pi + \Pi A - \Pi BB^*\Pi + C^*C = 0. \tag{D.1}$$

Moreover it is known that the minimum value of $J(u, x_0)$ is given by $J(u_{opt}, x_0) = \langle \Pi x_0, x_0 \rangle$. Likewise, associated to the system Σ_N we consider the problem of minimization of the following functional

$$J_N(u, x_{N,0}) = \int_0^\infty ||y_N(t)||_2^2 + ||u(t)||_2^2 \mathrm{d}t.$$

It is well known that if (A_N, B_N) is stabilizable and (A_N, C_N) is detectable that the optimal solution is $u_{N,opt}(t) = -B_N^*\Pi_N T_N(t)x_{N,0}$, where Π_N is the non negative solution of the Riccati equation:

$$A_N^*\Pi_N + \Pi_N A_N - \Pi_N B_N B_N^*\Pi_N + C_N^*C_N = 0. \tag{D.2}$$

Moreover it is known that the minimum value of $J_N(u, x_0)$ is given by $J_N(u_{N,opt}, x_{N,0}) = \langle \Pi_N x_{N,0}, x_{N,0} \rangle$.

We introduce the following assumptions:

H1 For each $x \in X_N$ we have that
1. $\lim_{N\to\infty} ||T_N(t)P_N x - T(t)x|| = 0$,
2. $\lim_{N\to\infty} ||T_N^*(t)P_N x - T^*(t)x|| = 0$,

uniform in t on bounded subsets of $[0, \infty)$.

H2
1. For each $u \in U$, $\lim_{N\to\infty} ||B_N u - Bu|| = 0$.
   For each $x \in X$, $\lim_{N\to\infty} ||B_N^* P_N x - B^* x|| = 0$.
2. For each $x \in X$, $\lim_{N\to\infty} ||C_N P_N x - Cx|| = 0$.
   For each $y \in Y$, $\lim_{N\to\infty} ||C_N^* y - C^* y|| = 0$.

H3
1. The family of pairs (A_N, B_N) is uniformly stabilizable: i.e. there exists a sequence of operators $K_N \in \mathcal{L}(X_N, U)$, with $\sup_N ||K_N|| < \infty$ such that

$$||e^{(A_N - B_N K_N)t} P_N|| \leq M_1 e^{-\omega_1 t}, \text{for } t \geq 0 \tag{D.3}$$

   for some constants $M_1 \geq 1$ and $\omega_1 > 0$.
2. The family of pairs (A_N, C_N) is uniformly detectable: i.e. there exists a sequence of operators $G_N \in \mathcal{L}(Y, X_N)$, with $\sup_N ||G_N|| < \infty$ such that

$$||e^{(A_N - G_N C_N)t} P_N|| \leq M_2 e^{-\omega_2 t}, \text{for } t \geq 0 \tag{D.4}$$

   for some constants $M_2 \geq 1$ and $\omega_2 > 0$.

The theorem under consideration is the following:

Theorem D.1.1
Suppose that H1, H2 and H3 are satisfied. Then for each N the Riccati Equation D.2 admits a unique, non-negative solution Π_N *with* $\sup_N ||\Pi_N|| < \infty$ *and there exist constants* $M_3 \geq 1$ *and* ω_3 *such that*

$$||e^{(A_N - B_N B_N^* \Pi_N)t} P_N|| \leq M_3 e^{-\omega_3 t} \quad \textit{for } t \geq 0.$$

In the original proof it is suggested that by use Datko's lemma [Salamon, 1985, Theorem 6.2.] and [Gibson, 1979, Theorem 2.2] one can conclude that from:

$$\lim_{t\to\infty}\int_0^t ||x_N(t)||\mathrm{d}t < \infty \text{ for all } N$$

it follows that there exists a uniform exponential bound on $x_N(t)$, i.e. the existence of an M independen of N and $\gamma \leq 0$, such that:

$$||x_N(t)|| \leq Me^{\gamma t} \quad \text{for all } N \text{ and for all } t \geq 0$$

This is not true, since in M might still depend on N.

The theorem can be repaired on compact time intervals.

Proof. Existence and uniqueness of Π_N follows from standard finite dimensional LQR theory. We show that $\sup_N ||\Pi_N|| < \infty$ first. From the setting it follows that Π_N provides the optimal solution to the optimal control problem with cost $J_N(u(\dot{)}; z)$. Since the solution is unique, it follows that when the feedback $u = K_N x_N$ is applied, the value of J_N is such that

$$\langle \Pi_N x_{N,0}, P_N x_{N,0}\rangle \leq J_N(-K_N z_N(\cdot); x_{N,0}) \quad \text{for any initial condition } x_{N,0} \in X_N$$

The cost under the feedback $u_N = -K_N z_N$, i.e. $J_N(u_N; x_{N,0}) = J_N(-K_N x_N(\cdot); x_{N,0})$, can be calculated as follows:

$$J_N(-K_N x_N(\cdot); x_{N,0}) = \int_0^\infty ||C_N e^{(A_N - B_N K_N)t} x_{N,0}||^2 + ||K_N e^{(A_N - B_N K_N)t} x_{N,0}||^2 \mathrm{d}t$$

Since C_N, K_N are bounded operators and $||e^{(A_N - B_N K_N)t} x_{N,0}|| \leq M_2 e^{-\omega_2 t}||x_{N,0}||$, it follows that

$$J_N(-K_N x_N(\cdot); x_{N,0}) \leq \int_0^\infty (||C_N||^2 + ||K_N||^2) M_2^2 e^{-2\omega_2 t}||x_{N,0}||^2 \mathrm{d}t.$$

Define $\beta_N := \int_0^\infty (||C_N||^2 + ||K_N||^2) M_2^2 e^{-2\omega_2 t}\mathrm{d}t$. Then $J_N(-K_N x_N(\cdot); x_{N,0}) \leq \beta_N ||x_{N,0}||^2$. Since C_N, K_N are bounded operators and M_2, ω_2 are independent of N it follows that there exists a $\bar{\beta}$ independent of N such that $\bar{\beta} = \sup_N \beta_N < \infty$. Therefore it follows that $J_N(-K_N x_N(\cdot); x_{N,0}) \leq \bar{\beta}||x_{N,0}||^2$. This implies that $\langle \Pi_N P_N x_{N,0}, x_{N,0}\rangle \leq \bar{\beta}||x_{N,0}||^2$, from which it follows that $\Pi_N \leq \bar{\beta}$.

We now proof uniform exponential boundedness. Introduce the identity:

$$e^{(A_N - B_N B_N^* \Pi_n)t} = e^{(A_N - G_N C_N^*)t} + \int_0^t e^{(A_N - G_N C_N^*)(t-s)}(G_N C_N - B_N B_N^* \Pi_N) e^{(A_N - B_N B_N^* \Pi_N)t}\mathrm{d}s.$$

From the identity we infer that

$$\begin{aligned} ||e^{(A_N - B_N B_N^* \Pi_N)t} x_{N,0}|| \leq\ & ||e^{(A_N - G_N C_N^*)t} x_{N,0}|| \\ & + ||\int_0^t e^{(A_N - G_N C_N^*)(t-s)}(G_N C_N - B_N B_N^* \Pi_N) e^{(A_N - B_N B_N^* \Pi_N)s} x_{N,0}\mathrm{d}s||. \end{aligned}$$

We apply the triangular inequality and Cauchy Schwartz to obtain

$$||e^{(A_N - B_N B_N^* \Pi_N)t} x_{N,0}|| \leq ||e^{(A_N - G_N C_N^*)t} x_{N,0}|| + \int_0^t ||e^{(A_N - G_N C_N^*)(t-s)}|| ||(G_N C_N - B_N B_N^* \Pi_N)|| ||e^{(A_N - B_N B_N^* \Pi_N)t} x_{N,0}|| \mathrm{d}s.$$

We will set $x_{N,0} = P_N x_0$. Then we will use Equation (D.4) and apply Cauchy Schwartz again,

$$||e^{(A_N - B_N B_N^* \Pi_N)t} P_N x_0|| \leq M_2 ||P_N x_0|| + M_2 ||(G_N C_N - B_N B_N^* \Pi_N)|| \sqrt{t} \sqrt{\int_0^t ||e^{(A_N - B_N B_N^* \Pi_N)t} P_N x_0||^2 \mathrm{d}s}.$$

Because the optimal controlled cost is bounded independent of N, the contribution of

$$\int_0^t ||e^{(A_N - B_N B_N^* \Pi_N)t} P_N x_0||^2 \mathrm{d}s$$

is bounded independent of N. Moreover $||(G_N C_N - B_N B_N^* \Pi_N)||$ is bounded independent of N by assumption. From $H1$ it follows that $\lim_{N \to \infty} ||P_N x - x|| = 0$. Therefore, we conclude that for $t \in [0, \infty)$, $||e^{(A_N - B_N B_N^* \Pi_N)t} P_N x_0||$ is bounded independent of N. □

APPENDIX E

Physical properties KNO3

The following parameters where used for the simulations in Chapter 4. The data is adopted from [Matthews et al., 1996].

Process parameters	Symbol	Value	Unit
growth exponent	g	1.32	-
growth coefficient	k_g	$6.97 \cdot 10^{-3}$	$\frac{m}{min}$
nucleation exponent	b	1.78	-
nucleation coefficient	k_b	$3.47 \cdot 10^{13}$	$\frac{1}{m^3 min}$
crystal density	ρ_c	$2.11 \cdot 10^{6}$	$\frac{g}{m^3}$
solvent density	ρ	$1 \cdot 10^{6}$	$\frac{g}{m^3}$
Volume shape factor	k_v	1	-
Conversion factor	h	$1.5062 \cdot 10^{-6}$	$\frac{m^3(slurry)}{g(H_2O)}$
Saturation parameters of KNO3	A_0	0.1286	$\frac{g(KNO_3)}{g(H_2O)}$
	A_1	$5.88 \cdot 10^{-3}$	$\frac{g(KNO_3)}{g(H_2O)^\circ\mathrm{C}}$
	A_2	$1.721 \cdot 10^{-4}$	$\frac{g(KNO_3)}{g(H_2O)^\circ\mathrm{C}^2}$
Crystallization heat parameters	B_0	-358.78	$\frac{J}{g(KNO_3)}$
	B_1	388.36	$\frac{J}{g^2(KNO_3)}$
	B_2	-418.27	$\frac{J}{g^3(KNO_3)}$
Heat capacity parameters	C_0	4.172	$\frac{J}{g_{solution}{}^\circ\mathrm{C}}$
	C_1	-4.435	$\frac{J}{g_{solution}{}^\circ\mathrm{C}}$
	C_2	4.213	$\frac{J}{g_{solution}{}^\circ\mathrm{C}}$

Table E.1: Physical properties $KNO3$.

Bibliography

Alatalo, H. (2010). *Supersaturation-controlled crystallization*. PhD thesis, Lappeenranta University of Technology.

Antoulas, A. (2005). *Approximation of Large-Scale Dynamical Systems*. Society for Industrial & Applied Mathematics.

Banks, H. and Fabiano, R. (1997). Approximation issues for applications in optimal control and parameter estimation. *Modelling and computation for applications in mathematics, science, and engineering (Evanston, IL, 1996)*, pages 141–165.

Banks, H. and Kunisch, K. (1984). The linear regulator problem for parabolic systems. *SIAM journal on control and optimization*, 22:684.

Bensoussan, A. and Bernhard, P. (1992). On the standard problem of h_∞-optimal control for infinite dimensional systems,. *Identification and control in systems governed by partial differential equations*.

Bonnabel, S., Martin, P., and Rouchon, P. (2008). Symmetry-preserving observers. *Automatic Control, IEEE Transactions on*, 53(11):2514–2526.

Bonvin, D. (1998). Optimal operation of batch reactors–a personal view. *Journal of process control*, 8(5-6):355–368.

Bonvin, D. (2006). Control and optimization of batch processes. *Control Systems Magazine, IEEE*, 26(6):34–45.

Borggaard, J., Burns, J., Vugrin, E., and Zietsman, L. (2004). On strong convergence of feedback operators for non-normal distributed parameter systems. In *Decision and Control, 2004. CDC. 43rd IEEE Conference on*, volume 2, pages 1526–1531. IEEE.

Braatz, R. (2002). Advanced control of crystallization processes. *annual reviews in control*, 26(1):87–99.

Chang, S. (1995). The method of space-time conservation element and solution elementa new approach for solving the navier-stokes and euler equations. *Journal of computational Physics*, 119(2):295–324.

Chang, S., Wang, X., and To, W. (2000). Application of the space–time conservation element and solution element method to one-dimensional convection–diffusion problems. *Journal of Computational Physics*, 165(1):189–215.

Corrioua, J. and Rohani, S. (2002). Nonlinear control of a batch crystallizer. *Chemical Engineering Communications*.

Curtain, R. and Pritchard, A. (1978). *Infinite dimensional linear systems theory*, volume 8. Springer-Verlag New York.

Curtain, R. and Zwart, H. (1995). *An introduction to infinite-dimensional linear systems theory*, volume 21. Springer.

Deng, J., Becerra, V. M., and Stobart, R. (2009). Input Constraints Handling in an MPC/Feedback Linearization Scheme. *International Journal of Applied Mathematics and Computer Science*, 19(2):219–232.

Eek, R. and Bosgra, O. (2000). Controllability of particulate processes in relation to the sensor characteristics. *Powder technology*, 108(2):137–146.

EFPIA (2011). *The Pharmaceutical Industry in Figures 2011*. The European Federation of Pharmaceutical Industries and Associations (EFPIA), Leopold Plaza Building, Rue du Trne 108 - B-1050 Brussels - Belgium.

Engel, K. and Nagel, R. (2000). *One-parameter semigroups for linear evolution equations*, volume 194. Springer Verlag.

Filippov, A. (1961). On the distribution of the sizes of particles which undergo splitting. *Theory of Probability and its Applications*, 6:275.

Gibson, J. (1979). The riccati integral equations for optimal control problems on hilbert spaces. *SIAM Journal on Control and Optimization*, 17:537.

Golub, G. and Van Loan, C. (1996). *Matrix computations*, volume 3. The Johns Hopkins University Press.

Gunawan, R., Fusman, I., and Braatz, R. (2004). High resolution algorithms for multidimensional population balance equations. *AIChE journal*, 50(11):2738–2749.

Hang, K., Nadri, M., Xu, C., Uccheddu, B., and G., F. (2010). Control of crystal size distribution in batch crystallization processes with size-dependent growth using reachability analysis. In *Decision and Control (CDC), 2010 49th IEEE Conference on*, pages 3295–3300. IEEE.

Henson, M. (2003). Distribution control of particulate systems based on population balance equation models. In *American Control Conference, 2003. Proceedings of the 2003*, volume 5, pages 3967–3972. IEEE.

Henson, M. and Seborg, D. (1997). Feedback linearizing control. *Nonlinear process control*, pages 149–231.

Hulburt, H. and Katz, S. (1964). Some problems in particle technology. A statistical mechanical formulation. *Chemical Engineering Science*, 19(8):555.

Ito, K. (1987). Strong convergence and convergence rates of approximating solutions for algebraic riccati equations in hilbert spaces. *Distributed Parameter Systems*, pages 153–166.

Ito, K. and Kappel, F. (1998). The trotter-kato theorem and approximation of pdes. *Mathematics of computation*, 67(221):21–44.

Ito, K. and Kappel, F. (2002). *Evolution equations and approximations*, volume 61. World Scientific Pub Co Inc.

Jansen, P. (2011). State feedback linearization of a seeded batch cooling crystallizer for supersaturation control. In *Eindhoven University of Technology - Graduation papers*.

John, V., Angelov, I., Oncul, A., and Thévenin, D. (2007). Techniques for the reconstruction of a distribution from a finite number of its moments. *Chemical engineering science*, 62(11):2890–2904.

Kadam, S. (2012). *Monitoring and Characterization of Crystal Nucleation and Growth during Batch Crystallization*. PhD thesis, Delft University of Technology.

Kailath, T. (1980). *Linear systems*, volume 1. Prentice-Hall Englewood Cliffs, NJ.

Kailath, T., Sayed, A., and Hassibi, B. (2000). Linear estimation. *Upper Saddle River, NJ*.

Kalbasenka, A., Huesman, A., Kramer, H., and Bosgra, O. (2005). Controllability analysis of industrial crystallizers. In *Proceedings of the 12th International Workshop on Industrial Crystallization, Halle (Saale), Germany*, pages 157–164.

Khalil, H. (1992). *Nonlinear systems*, volume 3. Prentice Hall.

Khan, S., Ma, C., Mahmud, T., Penchev, R., Roberts, K., Morris, J., Ozkan, L., White, G., Grieve, B., and Hall, A. (2011). In-process monitoring and control of supersaturation in seeded batch cooling crystallisation of l-glutamic acid: From laboratory to industrial pilot plant. *Organic Process Research & Development*.

Kravaris, C. and Chung, C.-b. (1987). Nonlinear state feedback synthesis by global input/output linearization. *AIChE Journal*, 33(4):592–603.

Kravaris, C., Sotiropoulos, V., Georgiou, C., Kazantzis, N., Xiao, M., and Krener, A. (2007). Nonlinear observer design for state and disturbance estimation. *Systems & Control Letters*, 56(11-12):730–735.

Krener, A. and Xiao, M. (2002). Nonlinear observer design in the siegel domain. *SIAM journal on control and optimization*, 41(3):932–953.

Kreyszig, E. (1989). *Introductory functional analysis with applications*, volume 21. wiley.

Kwakernaak, H. and Sivan, R. (1972). *Linear optimal control systems*, volume 172. Wiley-Interscience New York.

Larsen, P., Patience, D., and Rawlings, J. (2006). Industrial crystallization process control. *Control Systems Magazine, IEEE*, 26(4):70–80.

LeVeque, R. (2002). *Finite volume methods for hyperbolic problems*, volume 31. Cambridge Univ Pr.

Liu, Z. and Sandu, A. (2008). On the properties of discrete adjoints of numerical methods for the advection equation. *International journal for numerical methods in fluids*, 56(7):769–803.

Martins, J., Sturdza, P., and Alonso, J. (2003). The complex-step derivative approximation. *ACM Transactions on Mathematical Software (TOMS)*, 29(3):245–262.

Matthews, H., Miller, S., and Rawlings, J. (1996). Model identification for crystallization: Theory and experimental verification. *Powder Technology*, 88(3):227–235.

Mersmann, A. (2001). *Crystallization Technology Handbook*. CRC Press.

Mesbah, A. (2010). *Optimal Operation of Industrial Batch Crystallizers*. PhD thesis, TU Delft.

Mesbah, A., Kramer, H., Huesman, A., and Van den Hof, P. (2009). A control oriented study on the numerical solution of the population balance equation for crystallization processes. *Chemical Engineering Science*, 64(20):4262–4277.

Miller, S. M. (1993). *Modelling and Quality Control Strategies for Batch Cooling Crystallizers*. PhD thesis, The University of Texas at Austin.

Morris, K. (2010). *The Control Systems Handbook, Second Edition*, chapter Control of Systems Governed by Partial Differential Equations, pages 67–167–37. CRC Press.

Motz, S., Mitrovic, A., and Gilles, E. (2002). Comparison of numerical methods for the simulation of dispersed phase systems. *Chemical Engineering Science*, 57(20):4329–4344.

Mullin, J. (2001). *Crystallization*. Butterworth-Heinemann.

Mutsaers, M. and Weiland, S. (2009). Reduced-order observer design using a lagrangian method. In *Proceedings of the Conference on Decision and Control*, Cancun, Mexico.

Myerson, A. (2002). *Handbook of industrial crystallization*. Butterworth-Heinemann.

Nagy, Z. and Braatz, R. (2003). Robust nonlinear model predictive control of batch processes. *AIChE Journal*, 49(7):1776–1786.

Nijmeijer, H. and Van der Schaft, A. (1990). *Nonlinear dynamical control systems*. Springer.

Oostveen, J. (2000). *Strongly stabilizable distributed parameter systems*, volume 20. Society for Industrial Mathematics.

Oxford (2010). *Oxford Dictionaries*. Oxford University Press.

Pazy, A. (1983). *Semigroups of linear operators and applications to partial differential equations*, volume 44. Springer.

Peterson, T., Scotto, M., and Sarofim, A. (1985). Comparison of comminution data with analytical solutions of the fragmentation equation. *Powder technology*, 45(1):87–93.

Polderman, J. and Willems, J. (1998). *Introduction to mathematical systems theory: a behavioral approach*, volume 26. Springer Verlag.

Ramkrishna, D. (2000). *Population balances: theory and applications to particulate systems in engineering*. Academic Press San Diego.

Randolph, A. and Larson, M. (1971). *Theory of Particulate Processes: Analysis and Techniques of Continuous Crystallization*. Academic Press.

Salamon, D. (1985). Structure and stability of finite dimensional approximations for functional differential equations. *SIAM journal on control and optimization*, 23:928.

Sampath, V., Palanki, S., Cockburn, J., and Corriou, J. (2002). Robust controller design for temperature tracking problems in jacketed batch reactors. *Journal of Process Control*, 12(1):27–38.

Sastry, S. (1999). *Nonlinear systems: analysis, stability, and control*, volume 10. Springer Verlag.

Semino, D. and Ray, W. (1995). Control of systems described by population balance equations–i. controllability analysis. *Chemical Engineering Science*, 50(11):1805–1824.

Squire, W. and Trapp, G. (1998). Using complex variables to estimate derivatives of real functions. *Siam Review*, pages 110–112.

Talenti, G. (1987). Recovering a function from a finite number of moments. *Inverse Problems*, 3:501.

Valentas, K. and Amundson, N. (1966). Breakage and Coalescence in Dispersed Phase Systems. *Industrial & Engineering Chemistry Fundamentals*, 5(4):533–542.

van den Boom, T. and Stoorvogel, A. (2010). DISC Lecture notes on Model Predictive Control.

Van der Schaft, A. (1990). Duality for linear systems: External and state space characterizations of the adjoint system. In *In Analysis of controlled dynamical systems: proceedings of a conference held in Lyon, France, July 1990, Volume 8 van Progress in systems and control theory, P 393-403*.

Van Keulen, B. (1993). *H_∞-control for distributed parameter systems: a state space approach*. Birkhauser.

Vissers, J., Forgione, M., Kadam, S., Daudey, P., Backx, A., Huesman, A., Kramer, H., and van den Hof, P. (2011a). Novel control of supersaturation on an industrial scale pharmaceutical batch cooling crystallizer. In *Proceedings of the 18th International Symposium on Industrial Crystallization (ISIC18)*, Zurich, Switzerland.

Vissers, J., Jansen, P., and Weiland, S. (2011b). Control of supersaturation in batch cooling crystallization by robust state feedback linearization. In *9th IEEE International Conference on Control and Automation (ICCA)*, pages 1114 –1120, Santiago, Chile.

Vissers, J. and Weiland, S. (2010). Design of optimal deterministic output estimators for distributed parameter systems,. In *Proceeding of Conference on Mathmatical Theory of Networks and Systems*, Budapest, Hungary.

Vollmer, U. (2004). *Control of Crystallization Processes Based on Population Balances*. PhD thesis, Universitat Magdeburg.

Wang, Y. and Doyle III, F. (2004). Reachability of particle size distribution in semibatch emulsion polymerization. *AIChE journal*, 50(12):3049–3059.

Webb, G. (1985). Dynamics of populations structured by internal variables. *Mathematische Zeitschrift*, 189(3):319–335.

Weidmann, J. (1980). *Linear operators in Hilbert spaces*. Springer-Verlag New York.

Wesseling, P. (2001). *Principles of computational fluid dynamics*, volume 29. Springer Verlag.

Xie, W., Rohani, S., and Phoenix, A. (2002). Extended kalman filter based nonlinear geometric control of a seeded batch cooling crystallizer. *The Canadian Journal of Chemical Engineering*, 80(1):167–172.

Zeidler, E. (1995). Applied functional analysis, vol. 109 of. *Applied Mathematical Sciences*.

Zhang, G. (2003). On-line optimal control of a seeded batch cooling crystallizer. *Chemical Engineering Science*, 58(9):1887–1896.

Zhang, K., Nadri, M., and Xu, C. (2010). Reachability analysis and control of crystal size distribution in batch crystallization processes. In *Decision and Control (CDC), 2010 49th IEEE Conference on*, pages 3295–3300. IEEE.

Acknowledgments

I would like to express my gratitude to my first promoter professor Ton Backx. I'm very thankful for all the thing I have learned from you, as well as on the topic of process control as on the softer skills necessary in daily life. I would like to thank my second promoter professor Siep Weiland. I'm thankful for the weekly discussions on the project and the patience you had in teaching me control theory and mathematics. You have played an important role as daily supervisor, as source of inspiration, as critical and fair reviewer and in the finalization of the thesis.

I would like to thank the committee members prof.dr.ir. O.H. Bosgra, dr. ir P.J. Daudey, prof.dr.ir. P.M.J. Van den Hof, dr.ir. H.J Kramer and prof.dr.H.J. Zwart for their participation in the committee and the valuable feedback I received on the manuscript.

This project has been supported by the Institute for Sustainable Process Technology (ISPT). I would like to thank the people from ISPT for their support. Moreover, I would like to thank my colleagues from the project and the companies Frieslandfoods, Albemarle, DSM, IPCOS and Perdix and their representatives for their support. I would like to thank Peter Daudey for leading the project and the intensive discussions on crystallization processes. Somnath Kadam and Marco Forgione, thanks you for being my project mates, especially during the experimental campaign at MSD Apeldoorn. I would like to express my thanks to Rob Geertman, Ramon Harting and Edwin Stokkingreef for their organizational efforts with respect to this campaign.

Pieter and Juan, I would thank you for your contributions to my research. I have learned a lot from you projects and I enjoyed our cooperation.

I would like to express my gratitude to my roommates Satya and Koen. Satya, I thank you for your friendliness as roommate and for the insights you gave me in your, the Indian, culture. Koen, I enjoyed having a roommate again after a roommate-less period of almost a year.

I would like to express my gratitude to all my colleagues of the Control Systems group.

Mark, Jaron, Jasper and Patrick, I would like to express special thanks to you for your willingness to discuss on any topics on modeling and control at any moment. The discussions and your openness have been very useful for me.

Finally, I would like to thank my parents Jan and Ria for their generous support. I'm very thankful for the education which you gave to me, the common sense which you have taught to me and the never ending support I receive from you both. Finally, I would like to thank my sister Babette and my girlfriend Femke both for being part of my life.

Curriculum Vitae

Jochem Vissers was born at 18 November 1982 in Bergen op Zoom, The Netherlands. He completed secondary school at the Cambreur College in Dongen, The Netherlands in 2001. In the same year he started working towards a master's degree in the study Electrical Engineering at the Eindhoven University of Technology. As part of the master's program he carried out an internship at BASF Ludwigshafen, Germany. In November 2007 he received the received the Master's degree in Electrical Engineering, for which he specialized towards the analysis and control of dynamic systems. The title of his master thesis is "Perspectives on the control of heterogeneous catalytic chemical reactions by non-uniform heating". The work was supervised by Professor A.C.P.M. Backx.

Jochem's research interests focus on the development and implementation of automated and model-based control methods for industrial production processes. In 2008, Jochem started his PhD-project under supervision of Professor A.C.P.M. Backx and Professor S. Weiland. He successfully completed the post graduate course program of the Dutch Institute for Systems and Control (DISC). In August 2012 he started working as Associate Scientist at DSM Limburg B.V. in Sittard, The Netherlands.